University of Minnesota
St. Anthony Falls Hydraulic Laboratory

Project Report 193

WATER TEMPERATURE DYNAMICS IN EXPERIMENTAL FIELD CHANNELS: ANALYSIS AND MODELING

by

Heinz G. Stefan,
John Gulliver
Michael G. Hahn
and
Alec Y. Fu

Prepared under

Grant Nos. R 80368601 and R 80473601

Project Officer

Kenneth E. Hokanson
Monticello Ecological Research Station,
Box 500, Monticello, Minnesota 55362

for

ENVIRONMENTAL RESEARCH LABORATORY - DULUTH
OFFICE OF RESEARCH AND DEVELOPMENT
U. S. ENVIRONMENTAL PROTECTION AGENCY
Duluth, Minnesota 55804

June, 1980
Minneapolis, Minnesota

DISCLAIMER

This report has been reviewed by the Environmental Research Laboratory-Duluth, U. S. Environmental Protection Agency, and approved for publication. Approval does not signify that the contents necessarily reflect the views and policies of the U. S. Environmental Protection Agency, nor does mention of trade names or commercial products constitute endorsement or recommendation for use.

PREFACE

Shortly after the Monticello Ecological Research Station (MERS), a field laboratory of the USEPA Environmental Research Laboratory - Duluth, went into operation in August 1973 a research program on the effects of elevated water temperatures, resulting from waste heat discharges on fish and other aquatic organisms, was initiated by the USEPA staff. The purpose of these studies was (a) to validate water quality criteria data produced in the laboratory under semi-natural field (mesoscale) conditions and (b) to identify significant response by aquatic organisms under field monitoring conditions. The field channels in which the experimental studies were conducted were supplied with water, heated artificially by waste heat, from Northern States Power Company's Monticello Generating Plant.

To provide assistance in these ecological studies, it was necessary to document, analyze, and predict water temperature characteristics in the field channels. The study described herein fulfilled that purpose. The study of water temperature characteristics in the 520 m (1700 ft) long field channels required investigation of several components such as surface heat exchange processes , longitudinal dispersion, stratification, and heat transfer to the channel bed. A summary of these studies is provided in this report. Additional details on the substudies can be found in the following memoranda and theses.

1. Physical Characteristics of the Experimental Field Channels at the USEPA Ecological Research Station in Monticello, Minnesota, by Michael G. Hahn, John S. Gulliver, and H. Stefan, Memorandum No. 156. St. Anthony Falls Hydraulic Laboratory, University of Minnesota, April, 1978.

2. Operational Water Temperature Characteristics in Channel No. 1 of the USEPA Monticello Ecological Research Station, by Michael Hahn, John Gulliver, and H. Stefan, Memorandum No. 151, St. Anthony Falls Hydraulic Laboratory, University of Minnesota, January, 1978.

3. User's Manual for Operational Water Temperature Statistics Computer Programs WTEMP1 and WTEMP2, by Alec Y. Fu and H. Stefan, Memorandum No. 162, St. Anthony Falls Hydraulic Laboratory, University of Minnesota, July, 1979.

4. Water Temperature Data Processing for the Experimental Field Channels at the USEPA Ecological Research Station in Monticello, Minnesota, by Alec Y. Fu and H. Stefan, Memorandum No. 167, St. Anthony Falls Hydraulic Laboratory, University of Minnesota, April, 1979.

5. Soil Thermal Conductivity and Temperature Prediction in the Bed of the Experimental Field Channels at the USEPA Ecological Research Station in Monticello, Minnesota, by J. S. Gulliver and H. Stefan, Memorandum No. 165, St. Anthony Falls Hydraulic Laboratory, University of Minnesota, January, 1980.

6. Pore Water Temperatures and Heat Transfer in a Riffle (Rock) Section of the Experimental Field Channels at the USEPA Ecological Research Station at Monticello, Minnesota, by H. Stefan and J. S. Gulliver, Memorandum No. 166, St. Anthony Falls Hydraulic Laboratory, University of Minnesota, April, 1980.

7. Analysis of Surface Heat Exchange and Longitudinal Dispersion in a Narrow Open Field Channel with Application to Water Temperature Prediction, by John S. Gulliver, M.S. thesis, University of Minnesota, August, 1977.

8. Experimental Studies of Vertical Mixing in Temperature Stratified Waters, by Michael G. Hahn, M.S. thesis, University of Minnesota, March, 1978.

9. Stochastic Water Temperature Characteristics in an Outdoor Experimental Channel, by Alexander C. Demetracopoulos, Plan B paper for M.S. degree, University of Minnesota, November, 1976.

The overall geometrical, hydraulic, and soil thermal characteristics of the Monticello field channels have been described in Item No. 1 above. A first summary of operational water temperature characteristics in the field channels was given in Item 2. The surface heat exchange and the longitudinal dispersion in the artificially heated channels subjected to real (unsteady) weather conditions were described in Item 7. The water temperature stratification in the "pools" of the field channels was described and analyzed in Item 8. A computer program was developed for the statistical analysis of 3-hour water temperatures recorded at several stations in four of the eight field channels. A user's manual was prepared and made available to the MERS staff (Item 3). Water temperature data processing was described in Item 4. Water temperature statistics were computed for the four channels equipped with water temperature instrumentation for the periods from December 1975 to September 1977. The tabular computer printout covers many pages and copies

are available for purchase. Earlier statistical analysis of some partial records led to an unpublished, but fairly extensive, progress report by H. Stefan, C. Gutschik, A. Demetracopoulos and J. Gulliver entitled "Water Temperature Data Retrieval and Statistical Analysis for the Experimental Channels at the USEPA Monticello Field Station," September, 1976, 53 pp. A spectral analysis of some water temperature records is given in Item 9. Finally, the heating and cooling of the channel bed by the water above has been analyzed and a computer program for soil temperature prediction was described in Item 5. Pore water temperatures in the riffles are described in Item 6.

The work performed for the USEPA Monticello Ecological Research Station (MERS) under this grant had two basically different purposes. One was to provide background material and general information in support of the biological work conducted by the MERS field station staff. The second purpose was to investigate surface heat transfer, longitudinal dispersion, and water temperature predictions in streams under field conditions. The second purpose is basic and includes verification of the applicability of relationships developed for larger water bodies to smaller streams.

This report has been divided into sections which address the two above purposes separately. Section 4 - Hydraulic and Thermal Characteristics of the MERS Field Channels provide general background information, Section 5, Longitudinal Dispersion, Section 6 - Heat Budget, and Section 7 - Water Temperature Prediction, give results of basic experimental and analytical studies.

ABSTRACT

This report summarizes some of the morphological, hydraulic, thermal and meteorological characteristics of the experimental field channels at the USEPA Monticello Ecological Research Station. It contains an overview of measurements and parameters which characterized the physical operation conditions of the channels from December 1975 through December 1977.

Reported herein are measured values of hydraulic channel roughness, permeability and porosity of rock sections, and thermal diffusivity of bed materials. Recorded water temperatures have been statistically analyzed to give local diel, longitudinal,and vertical water temperature variations. A data bank of 3-hour water temperature data was established. Mean, standard deviation, skewness, and water temperature values at 5 per cent and 95 per cent probability of occurrence have been calculated on sliding, weekly samples of these 3-hour data.

Various aspects of the water temperature regime of the experimental field channels of the USEPA Monticello Ecological Research Station (MERS) were studied theoretically. Longitudinal dispersion and heat transfer relationships which were included in a dynamic water temperature model had to be established. Water temperatures at various channel locations and meteorological parameters were continuously recorded. A convective water surface heat transfer relationship (wind function) was determined from the recorded longitudinal temperature profile and meteorological parameters during quasi-steady state periods. Progressive heat fronts were used with tracer theory to determine longitudinal dispersion coefficients for the field channels.

The wind function and the longitudinal dispersion coefficient were incorporated in an implicit finite difference computer model, MNSTREM, for the highly dynamic water temperature prediction in the very shallow field channels. The water temperature model results were verified against 3-hour water temperature measurements over four time periods of up to one month.

Development of a model for diel water temperature variations at a one to three hour time scale goes beyond conventional stream water temperature modeling. The value and necessity of 3-hour to 6-hour weather data in making accurate predictions has been demonstrated. A standard error of $0.24^{o}C$ between predictions and measurements could be achieved.

TABLE OF CONTENTS

LIST OF FIGURES

LIST OF TABLES

ABBREVIATIONS AND SYMBOLS

A = cross sectional area (L^2)

$\bar{A}$ = mean cross sectional area over entire reach

B = surface width (L)

$\bar{B}$ = mean channel width over entire reach

C = concentration (ML^{-3})

C_c = fraction cloud cover (-)

C_r = cloudiness ratio

c_p = specific heat of water ($EM^{-1}\ {}^{o}C^{-1}$)

a,b,c = coefficients

D = thermal diffusivity (L^2T^{-1})

$\bar{D}$ = $2D_L/U$

D^* = $D_L\ BQ^{-1}$

D^*_B = $D_L\ \bar{A}\ \bar{B}\ Q^{-1}\ A^{-1}$

D_L = longitudinal dispersion coefficient ($L^2\ T^{-1}$)

e_a = actual air pressure (mb)

e_{a2} = saturation vapor pressure at dewpoint (mb)

e_{sw} = saturated vapor pressure (mb)

f_b = bottom friction factor

h = mean channel depth (L)

$\bar{h}$ = mean channel depth over entire reach

H_c = convective heat loss ($EL^{-2}\ T^{-1}$)

H_e = evaporative heat loss ($EL^{-2}\ T^{-1}$)

H_ℓ = net long wave radiation ($EL^{-2}\ T^{-1}$)

H_s = net short wave solar radiation ($EL^{-2}\ T^{-1}$)

H_{si} = incoming solar radiation ($EL^{-2}\ T^{-1}$)

H_{sr} = reflected solar radiation ($EL^{-2}\ T^{-1}$)

i = distance node

j_n = time node

k = Darcy permeability coefficient (LT^{-1})

$\bar{K}$ = $2m/U = 2\ K_s\ \rho^{-1}\ c_p^{-1}\ h^{-1}\ U^{-1}$

K_s = bulk surface heat transfer coefficient

L = latent heat of vaporization (EM^{-1})

$m = K_s \rho^{-1} c_p^{-1} h^{-1}$

M = mass of tracer injection (M)

n = Mannings roughness coefficient

NS = $\partial T/\partial t$

P = wetted perimeter (L)

p_a = atmospheric pressure (mb)

Q = flow rate ($L^3 T^{-1}$)

r = reflectivity or albedo of water surface

R = hydraulic radius (L)

RH = relative humidity (-)

S = rate of surface heat input ($EL^{-1} T^{-1}$)

S_E = slope of energy grade line (-)

SS = $Q B^{-1} h^{-1} \partial T/\partial x$

t = time (T)

T = water temperature (^oC)

T_a = air temperature (^oC or ^oK)

T_d = dew point temperature (^oC)

T_E = equilibrium temperature (^oC)

T_o = T(x=0)

T_s = surface water temperature (^oC or ^oK)

U = mean channel flow velocity (LT^{-1})

$\bar{U}$ = mean channel flow velocity over entire reach

u_* = shear velocity (LT^{-1})

$(Wftu)_z$ = wind speed function

W_z = wind velocity at elevation z above ground (LT^{-1})

x = distance along channel (L)

α = solar angle (degrees)

$\Delta\theta_v$ = virtual temperature difference (^oC)

ε = porosity of bed material (-)

ε_a = emissivity of atmosphere ($E\ ^oK^{-4}\ L^{-2}$)

ε_w = emissivity of water ($E\ L^{-2}\ ^oK^{-4}$)

Θ = dimensionless water temperature = $[T(t)-T(0)/\ T(\infty)-T(0)]$

θ = dimensionless temperature = $[T(x)-T_E]/(T_o-T_E)$

ρ = water density (ML^{-3})

σ = Stefan-Boltzman constant

τ_o = bed shear stress (FL^{-2})

ACKNOWLEDGEMENTS

The very understanding cooperation and planning by the Project Officer, Dr. Kenneth E. Hokanson is gratefully acknowledged. The planning and performance of many of the field experiments required some involvement and help from the permanent staff of the field station (MERS), expecially Mr. Thomas P. Henry and Mr. Jack Arthur, Acting Chief of MERS. The cooperation of Mr. Charles F. Kleiner in providing and maintaining some of the required instrumentation deserved particular recognition and gratitude.

Funding for this study was provided through grants from the U. S. Environmental Protection Agency, Environmental Research Laboratory - Duluth, Minnesota 55362.

Reviews of a draft copy of the report by Professor John A. Hoopes, University of Wisconsin, Madison, Wisconsin, and Professor Frank H. Verhoff, West Virginia University, Morgantown, West Virginia, are gratefully acknowledged.

SECTION 1

INTRODUCTION

The Monticello Ecological Research Station (MERS) is a Branch of the U.S. Environmental Protection Agency's Environmental Research Laboratory in Duluth, Minnesota. The MERS is located approximately 40 miles northwest of Minneapolis, near Monticello, Minnesota, on 34 acres adjacent to a Nuclear Power Generating Plant owned and operated by Northern States Power Company. An aerial photograph of the Monticello Field Station is given in Fig. 1.1. The MERS has eight soil bottom experimental open channels of approximately 520 m (1700 ft) length each. The Mississippi River serves as the main source of water for the channels which operate in a once-through mode. Heat exchangers using waste heat from the power plant can be used to artificially heat the water in any of the channels. The channels are in an elevated area above the Mississippi River and not normally subjected to flooding.

Flow rates in each of the channels as well as water stages can be controlled. The discharge from the channels is returned to the Mississippi River without any provision for treatment.

Heated cooling water effluents from power facilities create artificially high temperatures in natural waters. These thermal additions also intensify the dynamic character of natural water temperatures. Analysis of the higher, more variable water temperatures is needed to aid in determining effects upon the ecology of natural waters. Such studies are conducted at the MERS.

Artificially heated water in a river, lake, pond, estuary, or coastal area is cooled primarily through heat transfer with the air. Such heat transfer has been thoroughly studied for large water surface areas but the relationships developed may not apply well to shallow and narrow open channels. The quantitative effect of wind velocity, which enhances heat transfer, is different for narrow channels and wide surface areas.

Fig. 1.1. Aerial photograph of the Monticello Station experimental channels (center). Right - Northern States Power Company Monticello Power Plant. Bottom - Mississippi River.

Water temperatures in small open channels are highly dynamic due to the time dependent character of the controlling processes: advective transport, wind and flow induced mixing, and heat exchange with the air and the channel bed. In the MERS field channels the unsteady character of water temperature is especially acute since neither the mixing characteristics nor the effect of advective transport are negligible in the channels. The channels are exposed to a wide range of air temperatures, humidities, wind velocities, and solar radiation. The corresponding heat transfer with the environment is significant: a difference in temperature between the upper and lower end as high as $15^{o}C$ has been recorded and diurnal variations above $5^{o}C$ have been observed at the downstream end. The experimental channels provide an excellent medium for the study of unsteady water temperatures in open channel flow and their relationship to meteorological parameters.

The energy transport equation applied to an open channel of constant cross section takes the following form:

$$\frac{\partial T}{\partial t} = - U \frac{\partial T}{\partial x} + D_L \frac{\partial^2 T}{\partial x^2} + \frac{S}{\rho c_p h} \qquad (1\text{-}1)$$

D_L is a dispersion coefficient in the direction of flow (x-direction), S is a source or sink term which includes heat transfer with the surrounding environment, t is time, U is mean channel velocity, h is mean depth, ρ is the density of water, and c_p is the heat capacity of water. The potential importance of the dispersion mechanism and of heat exchange with the air is evident in Eq. 1-1.

Continuous water temperature records and meteorological data were gathered and used to determine longitudinal dispersion and adapt known air-water heat transfer relationships to narrow open channels with well defined non-uniform cross sections (crenelations). The effect of wind upon longitudinal dispersion in the channels was studied. This information was needed to develop a dynamic model of channel water temperatures. It was intended that the model should be able to predict the diurnal water temperature variations on a time-scale of 1 to 3 hours, as well as the longitudinal gradients. The longitudinal gradients were induced by adding artificially heated water to the channels and by the diurnal heating and cooling cycle at the channel surface.

A time scale of 3 hours was found adequate to simulate the observed diurnal variations.

The model simulation had to pay attention to several factors not usually considered in stream temperature modeling: (a) the particularly complex geometry of the channels caused by the alternation of riffles and pools, (b) the presence of weeds and intermittent stratification and (c) the unusually short time scale required. This led to a water temperature model which is more dynamic than any other model known to the authors.

This study of the physical environment in the MERS field channels was intended to provide some background for several biological studies at the Research Station, including one on the effects of artificially high water temperatures on fish and invertebrate populations. An analysis of the temperature measurement problem, channel temperature regime, microhabitat conditions, and temporal and spatial dynamics was essential for such investigations. The planning of future channel experiments may be facilitated by the results of this study. In a broader sense, this study also contains material applicable to the study of temperature dynamics in thermally polluted streams, to the design of irrigation canals for cooling water disposal, and to the natural water temperature regime of small streams.

SECTION 2

CONCLUSIONS

1. The field channels at the Monticello Ecological Research Station represent a meso-scale ecosystem whose temperature regime and hydraulic characteristics have been measured. The water temperature regime has also been simulated in a dynamic numerical model using channel morphological and hydraulic parameters as an input and air/water heat exchange as a water temperature forcing function.

2. Development and operation of instrumentation for continuous monitoring of flow rates and water temperatures in the channels from 1975 to 1977 was in the hands of MERS staff, in particular Charles F. Kleiner. The investigators participated in the selection of the temperature sampling sites shown in Fig. 4.13. The investigators also collected intermittently data on flow velocity profiles, water temperature stratification, surface water surface slope and flow cross sections. These data have been used to describe the temperature regime of the channels, derive a number of relevant physical parameters, and verify techniques for the analysis of temperature dynamics as described below.

3. The hydraulic characteristics include:

Mannings roughness:	$n = 0.06$ in the clear channels
	$n = 0.3$ with weed growth
Mean flow velocities:	$U \simeq 0.1$ m/s in riffles
	$U \simeq 0.02$ m/s in pools

depending on flow rate and downstream channel control. Velocity profiles are strongly affected by growth of filamentous algae in the rock sections and macrophytes in the pools.

Darcy permeability coefficient of rock $k = 0.18$ m/s

Rock porosity $\varepsilon = 0.42$.

4. The soil profile below pool bends is composed of four layers: a highly organic surface layer, water saturated sandy loam, water saturated bentonite clay layer, and a dry sandy loam, in order, from surface downward. The depth of the highly organic surface layer is variable and increases with time. The thermal diffusivity of each layer was determined by fitting soil temperature prediction to temperature measurements.

$D = 0.0017\ cm^2/s$ in the organic surface layer
$D = 0.013\ cm^2/s$ in the wet sandy loam below
$D = 0.0013\ cm^2/s$ in the dry sandy loam below the bentonite seal

The thermal diffusivity of the riffle was estimated to be $D = 0.0031\ cm^2/s$ in the rock/water system without natural convection.

5. Vertical stratification of the pool sections was studied in the artificially heated channel 1 and was found to occur most frequently in August. The temperature gradient was found to occur primarily in the lowermost 20 cm of the pool below a 60 cm isothermal layer; the temperature difference was up to 5^oC strong. Analysis of some 1975/76 data in pools 6 and 12 showed that a temperature differential of more than 1^oC developed during 33 per cent of all hours in August and less frequently during other months. The more downstream pool showed a stronger tendency toward stratification, presumably because the cumulative effect of atmospheric heating of the water in it is stronger.

6. A dynamic soil temperature model for the pool sections was developed, primarily to assist in invertebrate studies. The model solves the unsteady heat conduction equation and predicts the soil temperature profile for a specified time variation of the water temperature at the soil/water interface. It was verified (Fig. 4.11) that soil temperatures may be accurately predicted with this model.

7. Three-hour water temperature measurements in four of eight field channels have been recorded, processed and statistically analyzed for a period from December 1975 through September 1977. A computer program and User's Manual were provided to EPA.

8. Longitudinal dispersion in the MERS field channels was studied separately using temperature fronts. The longitudinal dispersion coefficient was found to be best approximated by

$$D_L = 7.47 * \frac{Q}{B} ,$$

where Q is flow rate and B is mean surface width. The effects of pool/riffle interaction appeared to be minor and longitudinal dispersion was similar to that in a channel of uniform cross section. In the range of very low mean flow velocities investigated (0.04 m^3/s discharge and $U \simeq 0.02$ m/s in pool to 0.1 m/s in riffle), the typical wind and vegetation effects could not be distinguished separately. A typical value of D_L was 0.1 m^2/s, with more detail provided in Tables 5.1 and 5.2.

9. Evaporative and convective surface heat exchange were found to be dependent on wind speeds and natural convection potential. A wind speed function

$$Wftn = 0.0096 \ (\Delta\theta_v)^{1/3} + 0.0083 \ W_2$$

was found to fit the experimental field data well. $\Delta\theta_v$ represents a virtual temperature differential defined by Eq. 6-30 and W_2 is the wind speed at 2 meters above the ground in m/s. The windspeed function is used to calculate evaporative surface heat transfer in accordance with Eq. 6-22 and convective surface heat transfer according to Eq. 6-26.

10. The water temperature regime was found to be highly dynamic for several reasons:

    (a) the shallow mean depth of the channels (< 1 m)
    (b) the residence time of several hours in the channels
    (c) the open cycle mode of operation whereby water from the Mississippi River is fed (heated or unheated through the MERS channels in a once-through mode)

    Since the hydraulic conditions on thermal responses in the Mississippi River and in the MERS field channels are very different, channel water temperatures are usually in transient conditions with both strong longitudinal gradients (several degrees C) and significant diurnal variations (several degrees C) at the downstream end. Table 4.4 provides specific figures. Upstream conditions were more stable because the inlet water came from the Mississipi River, a deeper water body than the channels.

11. A finite difference, implicit computer model MNSTREM for the simulation of the very dynamic channel water temperature regime was developed. It was shown capable of simulating 1 hr, 3 hr or 6 hr water temperatures over periods up to one month with standard errors of 0.2 to 0.3^{o}C between measurements and predictions. Weather data, specifically solar radiation, air temperature, dewpoint and wind velocity are required as input at least every six hours. Three hour input data are standard for the model. If intervals of more than six hours are used, the accuracy of the prediction suffers (Table 7.1). MNSTREM has unusually high time resolution meaning that it can predict rapid water temperature changes in very shallow water.

SECTION 3

RECOMMENDATIONS

Water temperature variations in time and space are a characteristic of any aquatic environment and especially the MERS field channels. Standard methods for the characterization of water temperature dynamics and incorporation of these characterizations into water temperature criteria for pollution control are needed. The MERS field channels lend themselves to studies of dynamics very well. They should be used for continued studies of fate and effect of various pollutants in an ecosystem at the meso-scale.

The focus of this study was on water temperature as a water quality parameter. For the model formulation, a dispersion parameter and surface exchange relationship adequate for water temperature modeling were derived.

Studies of pollutant (mass) transport in the MERS channels require more refined and detailed information on the flow and dispersion in a bed of macrophytes since uptake and precipitation are added factors (not present in the temperature model).

If further ecosystem studies in the MERS channels are conducted, detailed investigations of the hydrodynamics and transport dynamics of a pool and of a riffle, including the effects of vegetation must be conducted. For example, the effect of vegetation on longitudinal dispersion needs investigation. Flow effects must be sorted out from the field observations to derive the true biological and chemical kinetics of the system.

The 3-hour water temperature data base derived from continuous recordings should be analyzed further by time series (spectral, correlation) analysis. In addition, weather data and flow data should be digitized.

Continuously recording flow metering and channel stage recording devices at each end of a channel should be installed in the MERS channels. Flow rates were recorded manually once a day and stages only intermittently.

SECTION 4

HYDRAULIC AND THERMAL CHARACTERISTICS OF THE MERS FIELD CHANNELS

4.1. CHANNEL GEOMETRY

Each of the eight experimental channels at the MERS is approximately 520 m (1700 ft) long, with alternating "pool" and "riffle" sections of approximately 30.5 m(100 ft) length each and one 90 degree bend from an east-west to north-south alignment. There are nine pools and eight riffles in each channel. The approximate geometry of the pool sections is 3.5 m (12 ft) surface width and 0.8 m (3 ft) maximum depth. The pool cross section is approximately parabolic. The riffle sections are contracted areas to increase flow velocity. They are trapezoidal in shape and formed by 38 mm (1.5 inch) gravel placed in the channel. The riffle width at the water surface is approximately 2.5 m (8 ft). Riffles are very shallow, e.g. 0.3 m (12 inches). As the water stage can be controlled by a bulkhead at the end of each channel, the exact water depths and surface widths can also be changed.

The channels are arranged in pairs, separated by a high berm. There is a gravel road between channel pairs. Figure 4.1 shows one pair of channels.

Locations in the channels are numbered, with the number 1 assigned to the inlet, number 2 to the first pool, number 3 to the first riffle, etc., up to the outlet which is numbered 19. In addition, each channel was given a number from 1 to 8. Figure 4.2 gives measured average riffle and pool cross sections in Channel 1 (northernmost channel). Cross sections are not uniform in all cases. One example of a non-uniform riffle cross section is given in Fig. 4.3.

Fig. 4.1. MERS channels showing the transition from pool (foreground) to riffle to pool. The channel on the left is flowing full, while the channel on the right is partially drained, exposing the gravel sides and bottom of the riffle section.

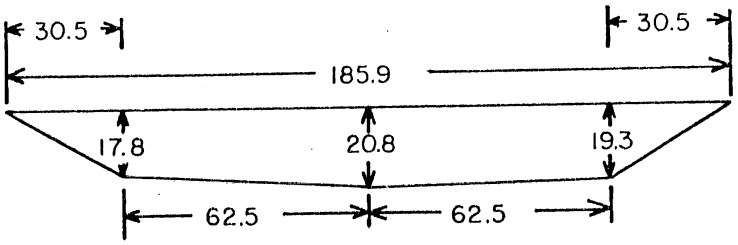

Average riffle cross section for Channel 1 on April 6, 1977.

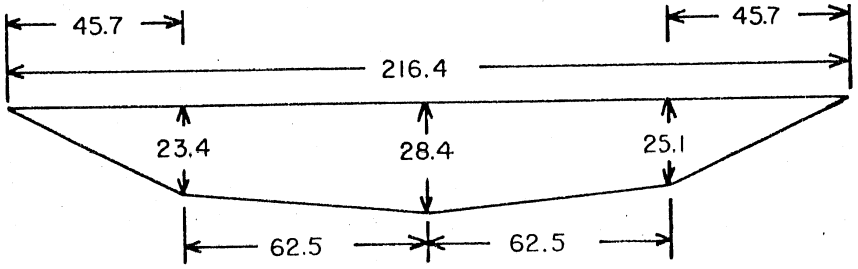

Average riffle cross section for Channel 1 on June 15, 1977.

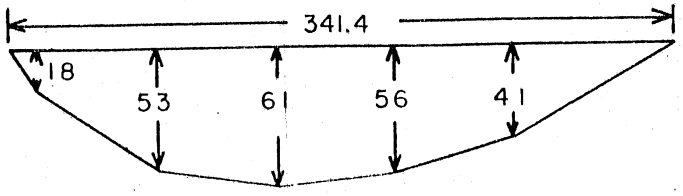

Average pool cross section for Channel 1 calculated from measurments made from July 13, 1977 through July 19, 1977.

Fig. 4.2. Channel cross sections. (dimensions in centimeters)

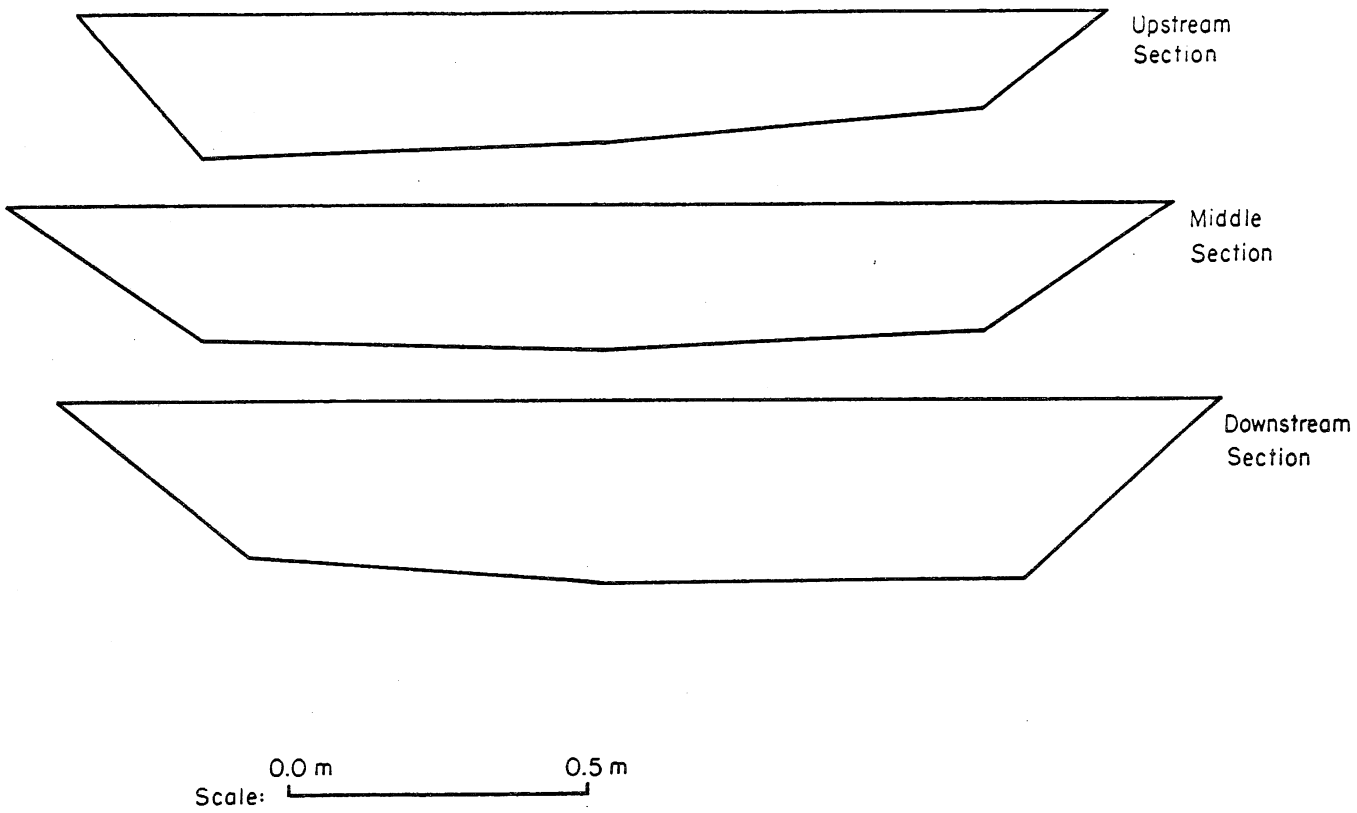

Fig. 4.3. Cross sections of riffle 5, channel 1 on April 6, 1977.

4.2. CHANNEL HYDRAULICS

Flow Rates and Residence Times

Flow rates in each channel are controlled and metered in the control room of the office building. V-notch weirs are installed at the head (inlet) of each channel and are available for installation at the end of each channel. Maximum design flow for a channel is on the order of 37.9 ℓ/s (600 gpm). Actual flow rates have been as high as 39.1 ℓ/s (620 gpm). In its first year of operation the flow rate in Channel 1 was approximately 18.9 ℓ/s (300 gpm), and the total hydraulic residence time of the water in the channel on the order of 12 hours. In the second year, beginning in August 1976, the flow rate was approximately 28.4 ℓ/s (450 gpm) to 37.9 ℓ/s (600 gpm), with residence time on the order of 4 hours. A lower stage was used with the higher flow.

Roughness and Water Surface Slope

The hydraulic roughness was determined in Channel 1 on three different occasions. Water surface slopes were measured in Channel 1, enabling calculation of roughness coefficients, wall shear stresses on the wetted perimeter, and shear velocities. Two sets of values are presented in Tables 4.1 and 4.2 where the station numbers refer to pool and riffle locations. (Counting in a downstream direction, the odd-numbered stations are riffles and the even-numbered stations are pools.) Computations were made for three different flow rates and for clear and weed choked conditions in the channel.

On April 18, 1977 the channel was relatively free from weeds and obstructions. On June 15, 1977 heavy macrophyte growth in both the riffles and pools had raised the water surface level substantially from the April level.

Manning's roughness coefficient 'n' is defined by the Manning equation (see e.g. Olson, 1973 or Barnes, 1967 or Limerinos, 1970).

$$Q = \frac{1}{n} A R^{2/3} S_E^{1/2} \qquad (4\text{-}1)$$

where Q = flow rate in m^3/s,

A = cross sectional area of the channel in m^2,

R = hydraulic radius (m) of the channel cross section, defined as the cross section area A divided by the wetted perimeter P, and

S_E = slope of energy grade line

TABLE 4.1. WATER SURFACE SLOPES (S), CROSS SECTIONAL AREAS (A), WETTED PERIMETERS (P), MANNING'S ROUGHNESS COEFFICIENTS (n), SHEAR VELOCITIES (u_*), and SHEAR STRESSES ON THE BOTTOM OF CHANNEL 1, τ_o, ON APRIL 18, 1977. (Flow rate = 0.0320 m^3/s)*

Section	S	A (m^2)	P (m)	n	u_* (m/s)	τ_o (N/m^2)
3	0.000537	.316	2.13	0.064	0.028	0.78
4	0					
5	0.000263	.372	2.04	0.061	0.022	0.48
6	0.000104					
7	0.000208	.372	2.16	0.052	0.019	0.36
8	0.000116					
9	0.000436	.307	2.04	0.057	0.025	0.63
10	0.000053					
11	0.000312	.297	1.92	0.047	0.022	0.48
12	0					
13	0.000573	.279	1.89	0.058	0.029	0.84
14	0					
15	0.000260	.297	1.92	0.043	0.020	0.40
16	0.000104					
17	0.000210	.214	1.71	0.024	0.016	0.26

* After Hahn et al, 1978b.

TABLE 4.2. WATER SURFACE SLOPES (S), CROSS SECTIONAL AREAS (A), WETTED PERIMETERS (P), MANNING'S ROUGHNESS COEFFICIENTS (n), SHEAR VELOCITIES (u_*), AND SHEAR STRESSES ON THE BOTTOM OF CHANNEL 1, τ_o, ON JUNE 15, 1977. (Flow rate = 0.0379 m^3/s)*

Section	S	A (m^2)	P (m)	n	u_* (m/s)	τ_o (N/m^2)
3	0.000773	0.576	2.77	.148	.0396	1.57
4	0.001020	1.77	3.93	.881	.0671	4.50
5	0.000505	0.520	2.50	.109	.0320	1.02
6	0.000333	1.81	3.96	.518	.0387	1.50
7	0.000250	0.548	2.62	.081	.0226	0.51
8	0.000185	1.79	4.02	.376	.0283	0.80
9	0.000908	0.465	2.19	.131	.0433	1.87
10	0	1.64	3.81	0	0	0
11	0.000467	0.465	2.26	.093	.0308	0.95
12	0.000330	1.70	3.87	.472	.0378	1.43
13	0.001417	0.353	2.10	.107	.0485	2.35
14	0.000168	1.65	3.93	.318	.0262	0.69
15		0.399	2.19			
16		1.56	3.69			
17	0.001010	0.242	1.71	.055	.0375	1.41

*After Hahn et al, 1978b.

The transitions between pools and riffles appeared to produce an insignificant loss compared to the roughness of the riffle sections.

It is noteworthy that in the clear channels (without growth) the hydraulic headloss occurs predominantly in the riffle sections. With heavy weed growth the contributions of pools and riffles may, however, be equal.

The average values of Manning's roughness coefficient were $n = 0.056$ on April 18, 1977, and $n = 0.29$ on June 15, 1977. The associated measured headlosses along the channel were 0.097 m (3.8 in.) on April 18, 1977, and 0.21 m (8.3 in.) on June 15, 1977. The measurements excluded the first and the last pool.

It should be noted that the roughness coefficients calculated for the channel with heavy weed growth account not only for the additional resistance to flow caused by the weeds, but also implicitly include the effects of the weeds in altering the channel cross section and length of flow. The overall pool and riffle cross sections with no area reduction were used in computing the 'n' values. In parts of the weedy sections the flow may have been apportioned between several subsections, thus producing a divided flow with several cross sections and hydraulic radii.

Flow Velocities

Mean flow velocities in riffles and pools vary, of course, with flow rate and stage. Mean values applicable to conditions observed on April 18, 1977 with a flow of .033 m^3/s (508 gpm) were:

Riffles: .108 m/s (.335 ft/s)

Pools: .019 m/s (.062 ft/s)

Velocity distributions as a function of depth were measured on several occasions with the aid of a micro currentmeter. Sample results are shown in Figs. 4.4 through 4.6. The effect of the attached filamentous algae growth on the velocity distribution is very apparent.

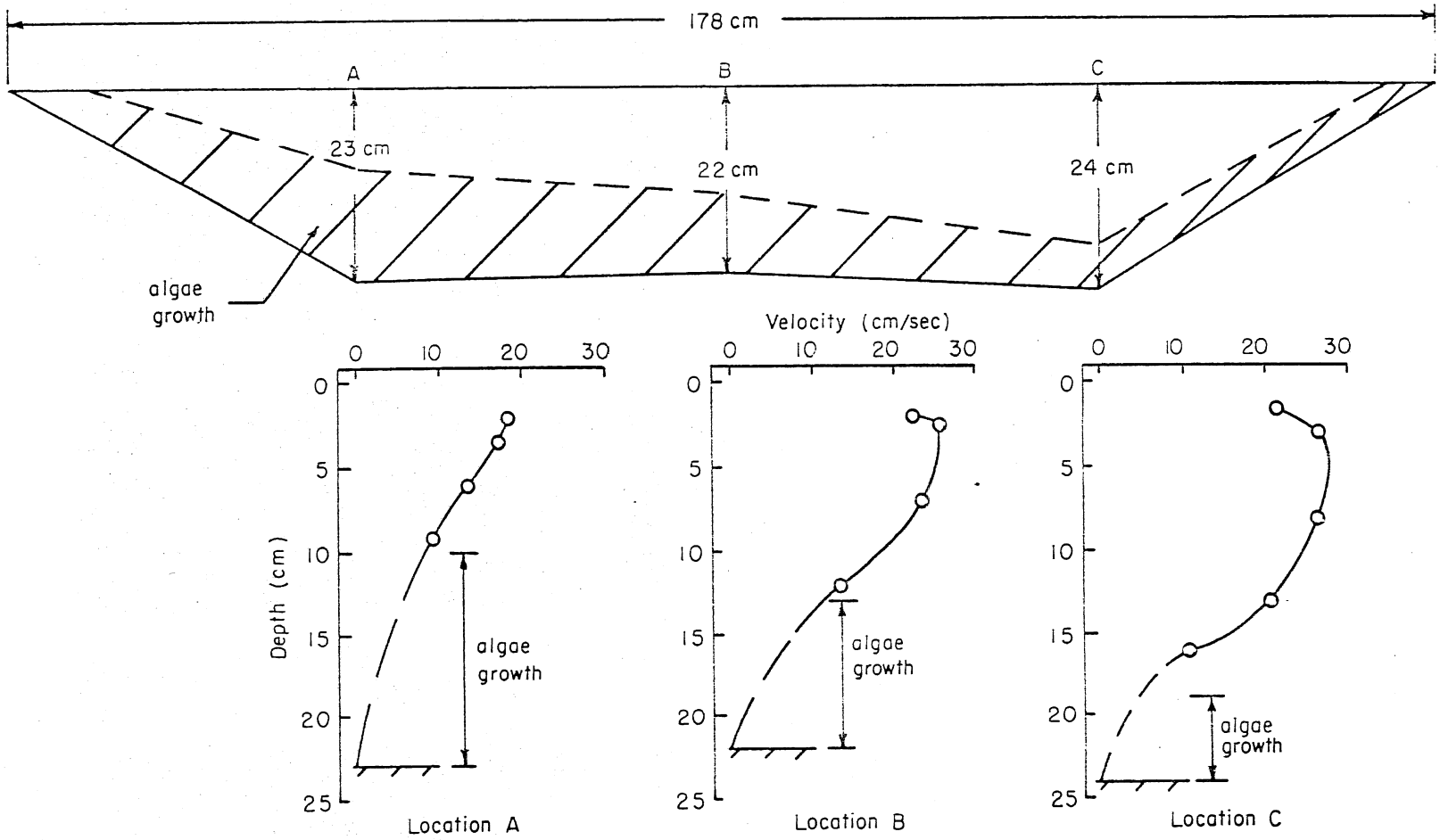

Fig. 4.4. Velocity profiles in Channel 1, riffle 5, looking downstream. Measured October 30, 1976.

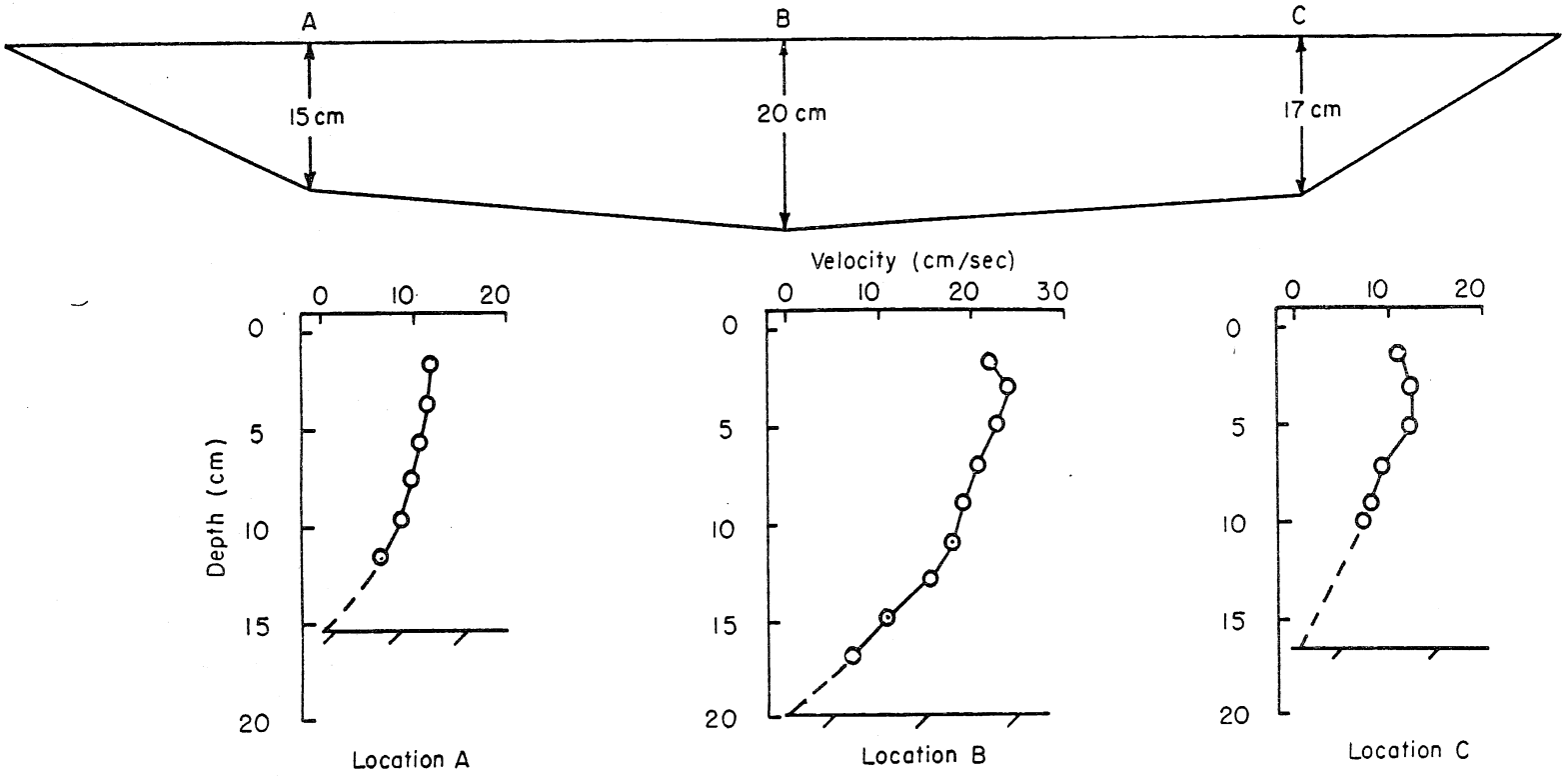

Fig. 4.5. Velocity profiles in Channel 4, riffle 11, looking downstream, with bottom free of weeds. Measured May 9, 1977.

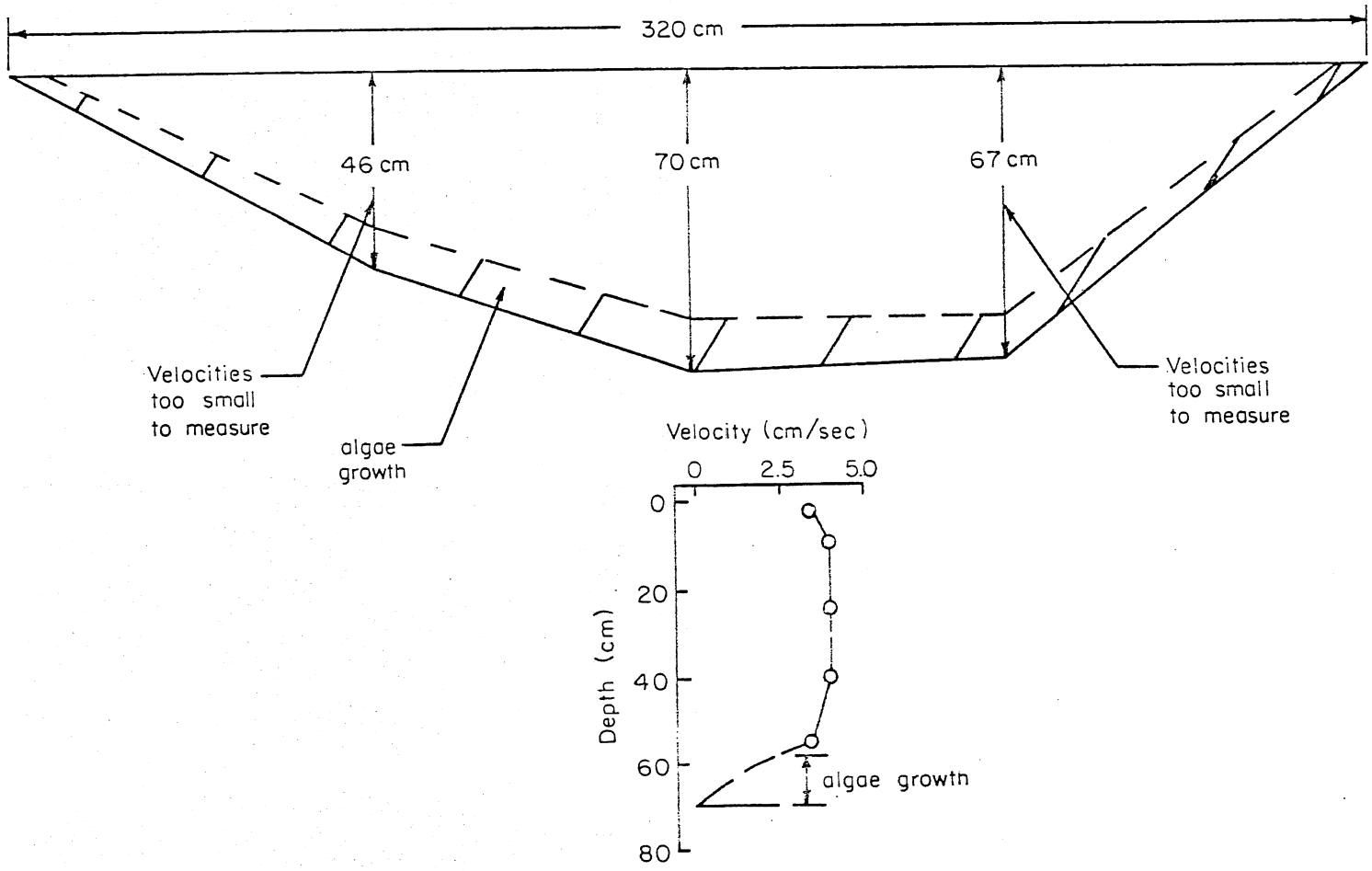

Fig. 4.6. Velocity profile in Channel 5, Pool 14, looking downstream. Measured October 30, 1976.

4.3. SOIL AND ROCK CHARACTERISTICS

Grain Size Distribution

Size distributions of the pool and riffle bed materials and of the sediment deposited within the first riffle section of Channel 1 were measured.

The rock size distribution for the riffles was made on a random 325 N (73 lb) sample of the gravel collected from the sides of all riffles in Channel 1. Two in. (50.8 mm), 1.5 in. (38.1 mm), 1.0 in. (25.4 mm), and 0.75 in. (19.0 mm) sieves were used. The results are plotted in Fig. 4.7.

A visual inspection of the rock material in the first (farthest upstream) riffle of Channel 1 indicated that it contained a considerable amount of fine sediment in the form of a mud or slurry. No such sediment was observed in the last (farthest downstream) riffle of Channel 1. Permeability measurements made in the two riffles indicated a lower permeability of the first riffle compared to the last, as would be expected if there were sediment deposition upstream. The origin of the sediment accumulation is presumably the Mississippi River water. The first pool of each channel acts as a settling basin for suspended sediment carried by the river. The sediment removal in the first pool is, however, not complete and some sediment is apparently deposited in the rock of the first riffle.

A sample of the sediment in the first riffle was obtained by digging a hole into the gravel cross section and collecting samples of the gravel and the slurry from throughout the vertical cross section. The sediment adhering to the rocks was later collected by washing the rocks.

The mechanical analysis of the sediment was performed according to the standard method (AASHO Designation: T88-57) described in the *Soils Manual for Design of Asphalt Pavement Structures* published by the Asphalt Institute. The resulting sediment size distribution is shown in Fig. 4.7.

The size distribution data for the pool bottoms in Channel 1 obtained in 1975 and available at MERS were also plotted in Fig. 4.7. The bed material was previously sampled in each pool and a size distribution was determined for each individual sample. The *per cents finer than* in each category were averaged for the nine pools and the resulting size distribution curve was plotted. Also, the *per cent finer than* in each category was determined for

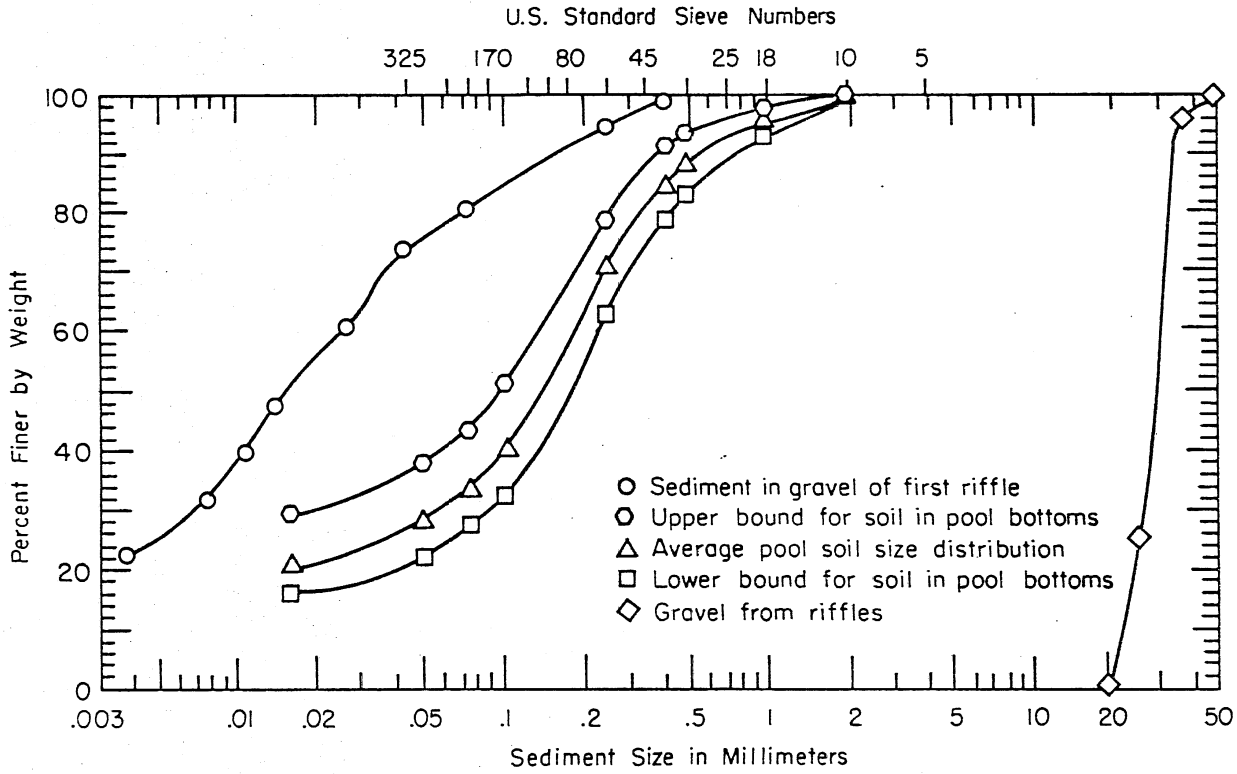

Fig. 4.7. Size distributions for material in Channel 1 in MERS.

each pool, and the highest and lowest per cents among all the pools in each size category were plotted as upper and lower bounds for the sediment sizes.

Permeability of Riffle Rock Sections

The hydraulic (Darcy) permeability of the rock was determined by separate experiments for the downstream part of the last riffle in Channel 1 and for both the upstream and the downstream part of the first riffle in Channel 1.

In the case of the last riffle, the water level in the pool immediately downstream was lowered so that all flow was only through the rocks and piezometric elevations were measured to determine the water table profile along the riffle section as a function of location and of time. Experiments were continued for several hours. For the downstream riffle a quasi-steady state condition was reached. The Darcy permeability coefficient of the rock was found to be 18 cm/s. With a channel flow on the order of 0.0315 m^3/s (500 gpm), the mean flow velocity through the pores of the rock was calculated to be approximately 0.02 cm/sec with a rock porosity on the order of 0.42.

Porosity of the rock was found by measuring void space in a container of 19.6 liters total volume. Average porosity from several samples was 0.44.

Soil Thermal Diffusivity and Soil Temperature in Pool Sections

A study of soil thermal diffusivity and temperatures below the bed of the pools was made for two reasons. One reason was to determine if the heat exchange between the pool water and the bed had an important influence on the water temperature regime in the channels. The influence was found to be negligible. The second reason was that aquatic biologists studying benthic organisms desired to know something about the temperature regime in the mud. The soil temperature regime was studied by heat transfer analysis (unsteady and one-dimensional).

The soil temperature profile as a function of depth and time was predicted for known water temperature in the pool above the soil/water interface. A numerical finite difference model of the unsteady, one-dimensional heat conduction equation was developed (Gulliver and Stefan, 1980). Measurements of soil temperature profiles were obtained from thermistor arrays placed in the bed of pools 6 and 12 in Channel 1.

Analysis of soil composition and of measured soil temperature profiles led to the conclusion that a four-layered system had to be used: the first layer of the pool bed was a highly organic layer of variable depth (0-15 cm). It appeared that this layer had developed since the channels went into operation and that the organic material was the residue of several growth seasons. The second layer (below) was a water saturated sandy loam of 38 cm (15 in.) thickness. This second layer was backfill material which rested on a 5 cm (2 in.) bentonite layer which had been installed to prevent the channels from leaking. The fourth layer below was a dry sandy loam. Figures 4.8 and 4.9 give cross sections.

Several heat wave experiments were performed. The soil surface was suddenly exposed to heated water, after a cold period, and the penetration of the warm front into the soil with time was recorded by the thermistor arrays. An example of a record is given in Fig. 4.10. Analysis of several such fronts made it possible to refine initial estimates of soil thermal diffusivities.

Although there were three thermal diffusivities and one layer depth to be determined, the heat wave experiment encompassed two unsteady and two quasi-steady periods and the problems of fitting four parameters could be solved. The surface layer thermal diffusivity and surface layer depth were highly interacting, but the use of unsteady periods helped resolve the problem to a reasonable degree of accuracy. The following soil properties were determined by fitting predictions of the numerical finite difference model to soil temperature measurements:

Highly organic (surface) layer depth = 12.5 cm (5 in.)

Thermal diffusivities:

Highly organic surface layer	$D = 1.7 \times 10^{-3}$ cm^2/sec
Water saturated sandy loam and bentonite layer	$D = 1.3 \times 10^{-2}$ cm^2/sec
Dry sandy loam (lowest layer)	$D = 1.3 \times 10^{-3}$ cm^2/sec

The above thermal diffusivities were used to predict soil temperatures in pool 12 during other heat wave tests. A set of predicted soil temperatures is compared with thermistor soil temperature measurements in Fig. 4.11. A

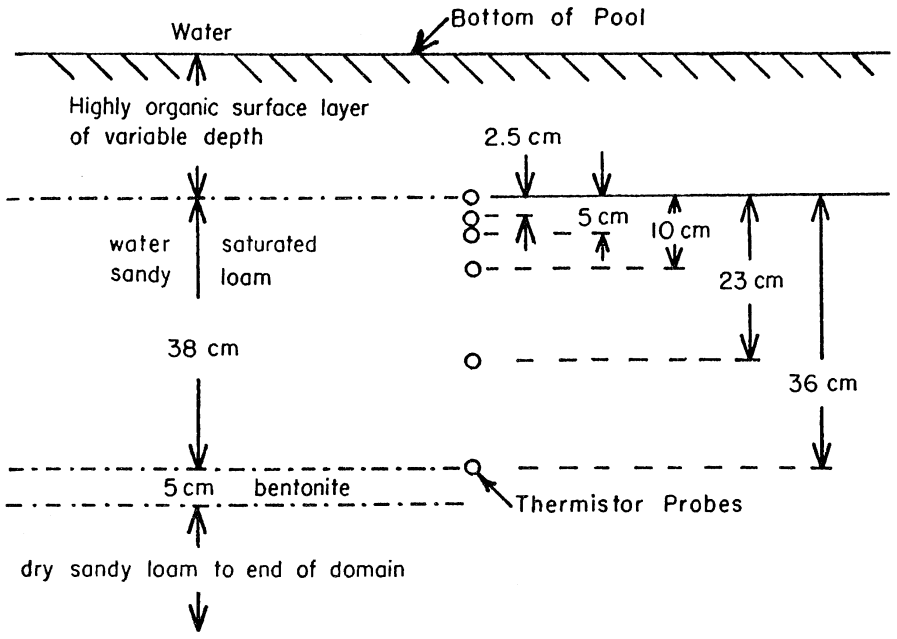

Fig. 4.8. Soil profile below pool and location of thermistor probes.

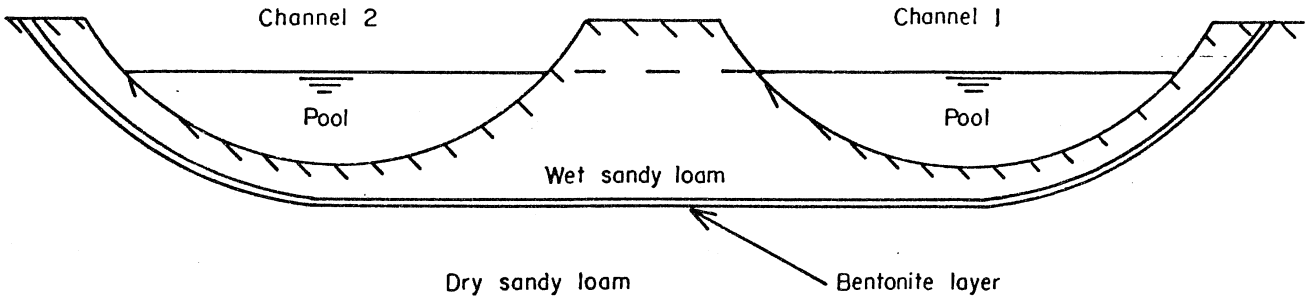

Fig. 4.9. Schematic cross section of one channel pair drawn to approximate scale.

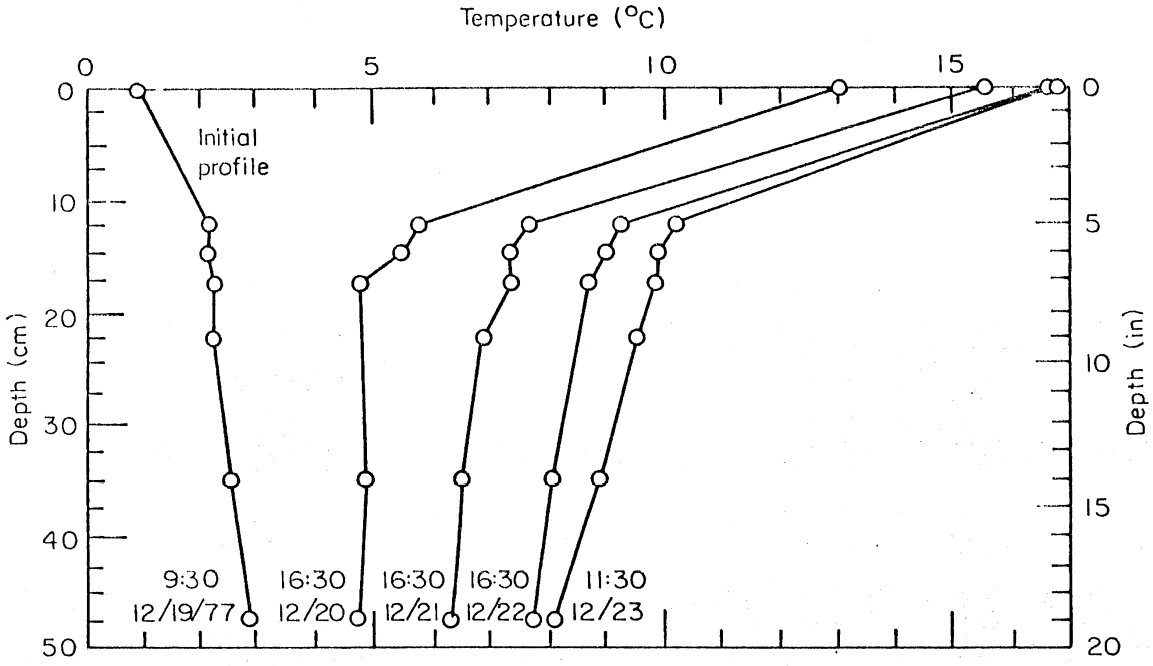

Fig. 4.10. Measured soil temperature profiles in pool 6 during heat wave test: warming period.

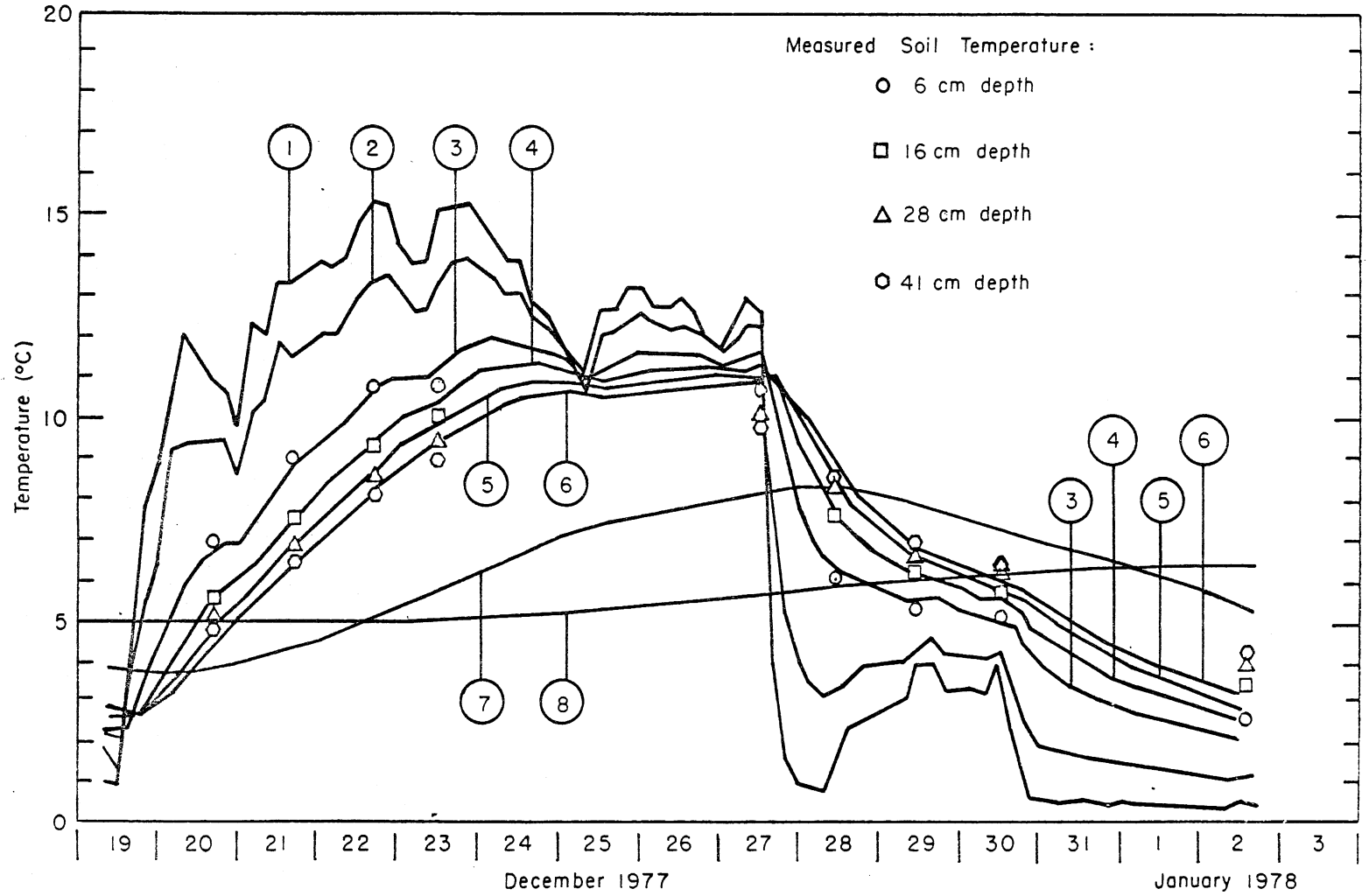

Fig. 4.11. Comparison of measured and predicted (solid lines) soil temperatures in Pool 12 during heat wave test. Notation for depth of predicted soil temperatures: (1) soil surface, (2) 2.5 cm, (3) 6 cm, (4) 16 cm, (5) 28 cm, (6) 41 cm, (7) 60 cm, (8) 1 m.

surface organic layer of 6.25 cm (2.5 in.) was assumed. The standard error of the predicted soil temperatures in the example is 0.48°C.

More information on the soil temperature investigations conducted at the MERS is given in Gulliver and Stefan, 1980.

Rock/Water Thermal Diffusivity and Temperatures in Riffle Sections

Water temperatures in the voids of the rocks forming the riffle section were studied for the same reasons as the soil temperature profile in the pool. It may be recalled that the rocks are of 30 mm average size and form a system of high hydraulic permeability.

The transfer of heat from the water flowing over the riffle into the water and rock below is potentially by the following processes.

(a) Horizontal flow of water through the pores of the rock. The hydraulic permeability was determined previously to be 18 cm/sec and the effective pore flow velocity on the order of $0.4 * 10^{-4}$ to $2.5 * 10^{-3}$ cm/sec, assuming a porosity of 0.44.

(b) Vertical conduction through the water and the rock mass. Estimates of thermal diffusivity of the water and the rock as found in the literature are 5.9×10^{-3} cm^2/sec for dry gravel and 1.4×10^{-3} cm^2/sec for water.

(c) Vertical forced convection through the voids of the rock system. This could also be looked at as a downward hydrodynamic diffusion process.

(d) Vertical natural convection through the voids of the rock system, when unstable water temperature stratification occurs.

The penetration of a heat wave from the bed surface into the rock of riffle 17 was studied experimentally from December 19, 1977, through January 2, 1978 (Stefan and Gulliver, 1980).

A vertical array of six thermocouples at 2.5, 7.6, 15, 25, 38, and 51 cm below the rock surface was installed in the center of riffle section 17 in Channel 1. The location is approximately 15 m from the upstream end of the riffle. The lowermost thermocouple is in the sandy loam below the rock.

Temperatures at the six sensor locations were read once daily during each working day following an artificially imposed surface water temperature rise. The rock temperature profiles indicated by the sensors are shown in Fig. 4.12.

The temperature response in the upper 15 cm (6 in.) appears to be with a time lag on the order of only a few hours. This rapid response as well as the shape of the temperature distributions with depth suggests that a very effective vertical mixing mechanism in the upper 15 cm of the rock exists. This mechanism could be a hydrodynamic diffusion or forced convection process induced by the bed shear stress of the free surface flow in the riffle section.

Below 15 cm depth the temperature response is delayed but still quite rapid. It is noteworthy that between December 20 and 22 and over a 48 hour period the temperatures in the rock rose by the same amount as the surface water temperature, namely $2^{o}C$ per 24 hours. This observation would suggest that the rate of downward heat flow during that time period was constant and that the sandy loam (below the rock) was the main heat sink.

The observed rapid changes in rock temperature profiles cannot be explained by horizontal flow through the rock. The horizontal advance of a temperature front based on uniform horizontal flow and measured permeability would be about 5 m/day in terms of real pore flow velocity.

Density stratification of the water in the rock mass is associated with vertical temperature gradients. Stratification may be responsible for the steeper temperature gradient below 15 cm than above. It reflects a smaller vertical thermal diffusivity than above 15 cm depth.

During the cooling phase the vertical temperature profiles are more uniform than during the heating. This reflects the effect of natural vertical convection induced by density instability.

An analysis of the data described by Stefan and Gulliver (1980), gave a thermal diffusivity of $3.1*10^{-3}$ cm^2/s for the rock/water system at depths between 15 cm and 38 cm below the riffle bed. This value is applicable when the water temperature in the rock section provides a stable density stratification (channel water lighter than pore water in the rocks).

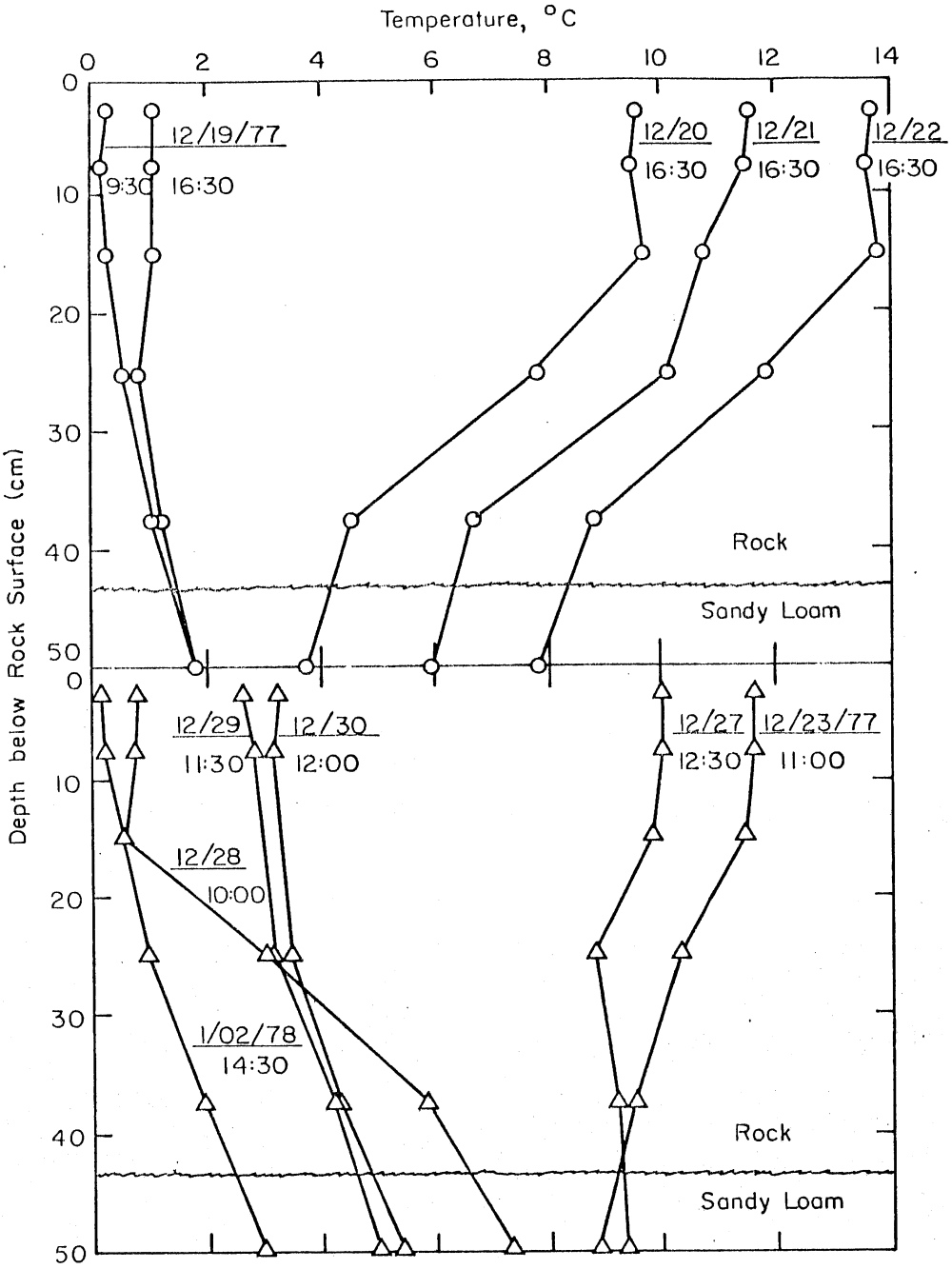

Fig. 4.12. Vertical temperature profiles in Riffle 17 during period of rock temperature study.

In the upper 15 cm of the riffle bed a mixed layer appears to exist. Water temperature in that layer is very nearly the same as the channel water temperature.

Under unstable conditions (pore water lighter than channel water) natural convection takes place and thermal diffusivity is much increased.

4.4. OBSERVED OPERATIONAL WATER TEMPERATURE REGIME

Water Temperature Instrumentation

Temperature sensors (thermocouples) were installed at the upstream and downstream ends and in the center pools and riffles of each of experimental channels 1, 4, 5, and 8. The sensors provided continuous water temperature information which was recorded on four strip charts for the four channels. Three stations per channel were not sufficient, however, for the analysis of stratification, surface heat transfer and mixing. Channel 1 was selected for in-depth study of temperature regimes, and 21 continuous recording sensors were installed in Channel 1 (schematic in Fig. 4.13). Ten of the sensors measured water temperature 12.5 cm (5 in.) to 25 cm (10 in.) below the water surface. There were two vertical arrays of four sensors each installed in Pools 6 and 12 which provided information on water temperature stratification and soil temperature. Three sensors were within 12.5 cm (5 in.) from the bottom of pools 4, 10, and 18, and one sensor 2 to 5 cm (1 to 2 in.) in the rocks of riffle 17. All temperature sensors were connected to Leads-Northrup multi-channel color-coded temperature chart recorders. Temperatures were recorded from November 1975 through December 1977.

Water Temperature Data Processing

Elements

The water temperature data processing described herein is for water temperatures measured at several stations in channels 1, 4, 5, and 8 of the MERS. The data processing had the following elements.

- Extraction from strip charts
- Review and estimation of missing or faulty data
- Calibration
- Storage

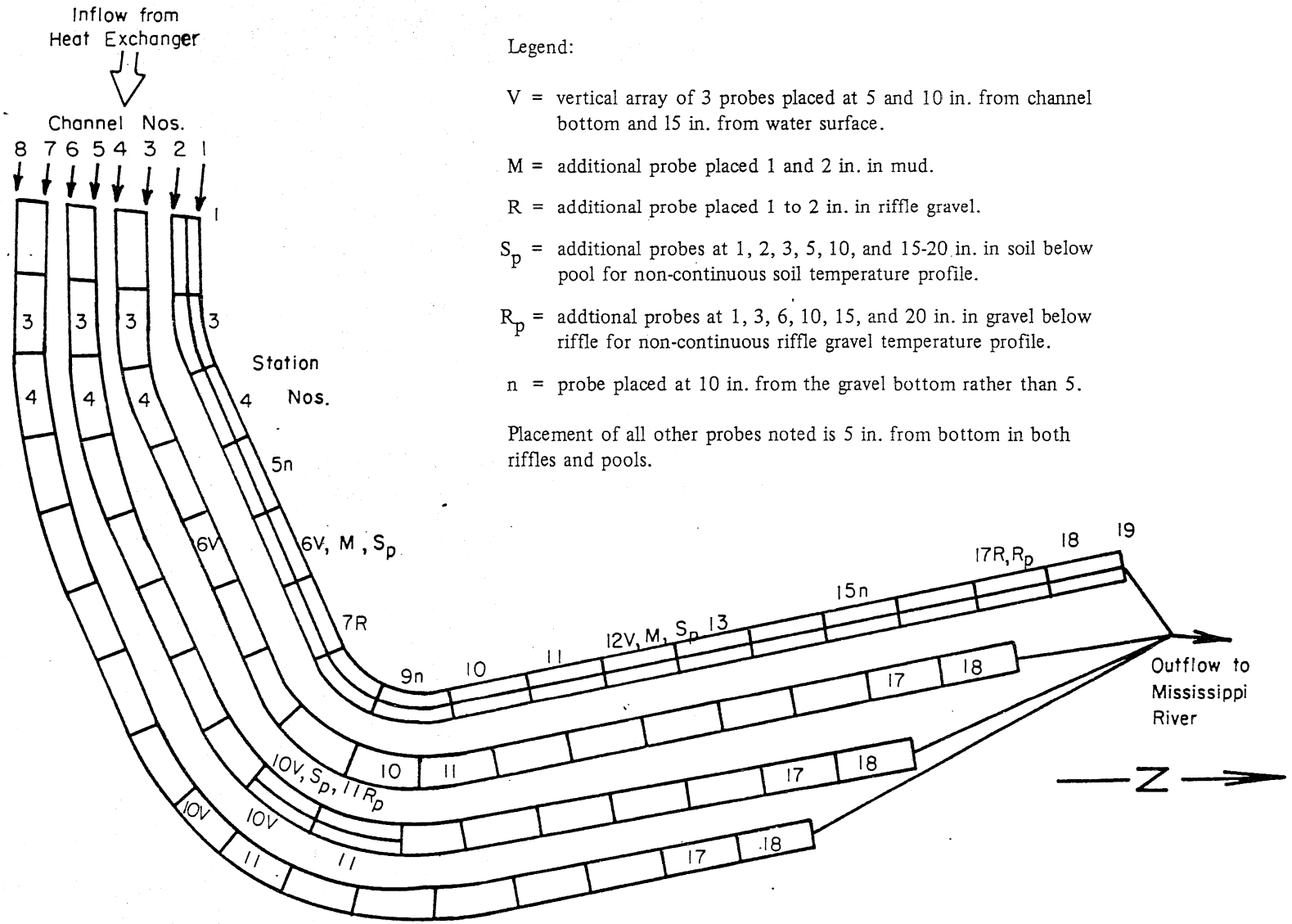

Legend:

V = vertical array of 3 probes placed at 5 and 10 in. from channel bottom and 15 in. from water surface.

M = additional probe placed 1 and 2 in. in mud.

R = additional probe placed 1 to 2 in. in riffle gravel.

S_p = additional probes at 1, 2, 3, 5, 10, and 15-20 in. in soil below pool for non-continuous soil temperature profile.

R_p = addtional probes at 1, 3, 6, 10, 15, and 20 in. in gravel below riffle for non-continuous riffle gravel temperature profile.

n = probe placed at 10 in. from the gravel bottom rather than 5.

Placement of all other probes noted is 5 in. from bottom in both riffles and pools.

Fig. 4.13. Thermal probe placement in MERS experimental channels (four channel pairs).

These elements will be described in sequence.

Extraction of data

Water temperature data were extracted for four channels including two *hot* channels, with up to 15°C above the Mississippi River temperature, one *warm* channel, with up to 8°C above river temperature, and one *ambient* channel which has no heat addition above river temperature.

For the statistical analysis, stations 2, 3, 9, 10, 17, and 18 of channels 4, 5, and 8, as well as stations 3, 4, 6, 12, 17, and 18 of Channel 1 were selected. For each station, 3-hour water temperatures beginning at midnight of each day were read off the strip charts and hand recorded on data sheets (eight values per day).

Estimation of data

For periods during which no temperatures were recorded, estimation of water temperature became necessary. This was done by one of the four following procedures.

(a) Linear interpolation between water temperatures at upstream and downstream stations.

(b) When the period of missing data was only a few hours, and when no water temperatures were recorded for all stations, linear interpolation between the last water temperature before the gap and the first water temperature after the gap was used.

(c) When a temperature record was not available for the first station (or the last station), linear extrapolation using temperatures from the two immediate downstream (or upstream) stations was used.

(d) When no temperature record was available for all stations and for a long duration, temperatures from another channel multiplied by a coefficient were substituted (linear intra-channel transfer).

Details on the periods of missing data, their causes, and the procedures used in estimating the data were documented by Fu and Stefan (1979b).

Erroneous data were also found in the records. Some water temperatures recorded on the strip charts were not representative for several reasons: (a) sensor might be in the air due to low flow, (b) sensor might be buried in the sediment, and (c) sensor might not be recording the true water temperature values. Owing to these reasons, estimation of corrected water temperature data was also necessary. The procedure is explained in Fu and Stefan (1979b). Periods during which estimates had to be made are also identified by Fu and Stefan (1979b)

Calibration

From January 1976 through June 1976, one complete calibration and numerous *spot checks* of the recorded temperatures in Channel 1 were made. After July 1976, temperature calibrations were made approximately every month. Channels 4, 5, and 8 were included.

The corrections obtained from these calibrations were tabulated by Fu and Stefan (1979b). Between the dates when calibrations were made, strip charts were examined to identify discontinuities in the records. Calibrations were considered valid only up to these points. Operational records and abbreviated remarks on the strip charts were also consulted for this purpose.

Corrections of less than $\pm$ 0.2^{o}C were ignored. Corrections $\geq |0.2|$ were added to the hand recorded water temperatures. The entire water temperature records for Channels 1, 4, 5, and 8 were stored on a magnetic tape. No calibrations were applied to the estimated water temperatures.

Water temperature data storage

All calibrated water temperatures were stored on a nine track magnetic tape. The length of the temperature record of each station is listed in Table 4.3. The magnetic tape is divided into four files (multi-file tape). Each file contains a temperature record of a single channel. Within each file, temperature records are stored in the order listed in Table 4.3. The first file contains temperature records of Channel 1, the second file those of Channel 4, the third file those of Channel 5, and the fourth file those of Channel 8. A computer program was used to read the raw data (without calibration), to apply the calibration and to write the calibrated water temperatures on the magnetic tape. More detailed information on the data tape can be found in Fu and Stefan, (1979a).

TABLE 4.3. SUMMARY OF WATER TEMPERATURE INFORMATION STORED ON MAGNETIC TAPE (Cont'd)

File Sequence No. QN	Set Identifier SI	Set Identifier FI	Channel No.	Station No. in Order of Storage	Period	No. of Days	No. of 3-hour Temperatures
1	PFILED	CHANNEL 1	1	3	12/4/75 - 9/19/77	656	5,248
				4	12/4/75 - 9/19/77	656	5,248
				6	12/4/75 - 9/19/77	656	5,248
				12	12/4/75 - 9/19/77	656	5,248
				17	12/4/75 - 9/19/77	656	5,248
				18	12/4/75 - 9/19/77	656	5,248
					TOTAL	3,936	31,488
2	PFILED	CHANNEL 4	4	2	10/20/76 - 9/19/77	335	2,680
				3	11/26/75 - 9/19/77	664	5,312
				11	11/26/75 - 10/18/76	328	2,624
				9	10/19/76 - 9/19/77	336	2,688
				10	10/10/76 - 9/19/77	335	2,680
				17	11/26/75 - 9/19/77	664	5,312
				18	10/20/76 - 9/19/77	335	2,680
					TOTAL	2,997	23,976
3	PFILED	CHANNEL 5	5	2	10/19/76 - 9/14/77	331	2,648
				3	11/24/75 - 9/14/77	661	5,288
				11	11/24/75 - 10/17/76	329	2,632
				9	10/18/76 - 9/14/77	332	2,656
				10	10/19/76 - 9/14/77	331	2,648
				17	11/24/75 - 9/14/77	661	5,288
				18	10/19/76 - 9/14/77	331	2,648
					TOTAL	2,976	23,808

TABLE 4.3 (Cont'd). SUMMARY OF WATER TEMPERATURE INFORMATION STORED ON MAGNETIC TAPE

File Sequence No. QN	Set Identifier SI	Set Identifier FI	Channel No.	Station No. in Order of Storage	Period	No. of Days	No. of 3-hour Temperatures
4	PFILED	CHANNEL 8	8	2	10/15/76 - 9/13/77	334	2,672
				3	11/24/75 - 9/13/77	660	5,280
				11	11/24/75 - 10/13/76	325	2,600
				9	10/14/76 - 9/13/77	335	2,680
				10	10/15/76 - 9/13/77	334	2,672
				17	11/24/75 - 9/13/77	660	5,280
				18	10/15/76 - 9/13/77	334	2,672
					TOTAL	2,982	23,856
					GRAND TOTAL	12,891	103,128

Water Temperature Data Analysis and Results

Elements

The water temperature data analysis as described herein included

- Development of a statistical analysis package
- Computation of a number of statistical parameters from 3-hour data
- Determination of the seasonal cycle
- Determination of the diurnal cycle
- Analysis of longitudinal gradients
- Analysis of water temperature stratification in the pools

These elements will be described in sequence.

Development of a statistical analysis package

A computer program WTEMP1, described in detail by Fu and Stefan (1979a), to extract from the 3-hour water temperature data statistical information was developed including:

- Water temperatures at three probabilities of occurrence specified by the user
- Maximum and minimum water temperatures in the period analyzed
- Mean, standard deviation and dimensionless skewness coefficient of the water temperature

WTEMP1 can handle a series containing up to 19,200 individual water temperatures, equivalent to 400 days of data from six stations in a single channel. WTEMP1 can also handle sliding statistic calculations for sample periods of up to 7 days. The output is in tabular form.

A second interactive program WTEMP2 for computing statistics on specified data time intervals, composite station locations etc. from daily statistics was also developed (Fu and Stefan, 1979a).

Computations

Computations have been carried out for individual stations and channel composite using weekly sliding samples. The tabular output format from WTEMP1 is shown in Appendix H. The complete output comprises 151 pages for Channel 1 and 126 pages each for Channels 4, 5, and 8.

Seasonal water temperature cycle

A graphical presentation of the statistical computer output is shown in Figs. 4.14 and 4.15. The weekly mean, maximum and minimum water temperatures have been plotted for two channels and several stations. Channel 1 was artificially heated, and Channel 5 was not. The seasonal water temperature cycle can be easily seen. The seasonal amplitude is on the order of $\pm$ 15°C. The annual mean differed by channel and station depending on the artificial heating.

Water temperature fluctuations superimposed on the seasonal cycle are either due to irregularities in the artificial heating of the inflowing water or due to weather. Those due to heating are smoothed out along the channel.

Diurnal water temperature cycles

Diurnal water temperature cycles are shown in Figs. 4.16 and 4.17. Because the inflowing water is taken from the Mississippi River, upstream stations in the field channels reflect conditions found in the river, modified (or not) by artificial heating. Because the field channels are shallower than the river, diurnal water temperature amplitudes at the downstream end of the channels are larger than upstream. Amplitudes of diurnal water temperature cycles also vary strongly with season as seen in Fig. 4.16. Winter values have been on the order of 1°C upstream and 2 to 3°C downstream. In the summer 2°C diurnal amplitude upstream and 5°C amplitude downstream are not uncommon.

Longitudinal water temperature gradients

Water temperature differentials between the upstream and the downstream ends of a channel are of interest for fish studies in the field channels. Such longitudinal water temperature gradients are dependent on several other hydrothermal parameters as will be shown by theoretical analysis in a later section. It may suffice here to indicate that the longitudinal ΔT can be expected to rise with the addition of artificial heat. A greater flow rate will decrease the longitudinal ΔT. Since the geometry of the MERS channels is fixed in terms of length and width, the two most important controllable parameters are flow rate and heat input. Actual values of longitudinal ΔT's will then depend on the amount of heat rejected to the atmosphere, which is a weather dependent process.

The daily minimum and maximum temperature difference between the inflow and outflow of the artificially heated Channel 1 was recorded over a one-year

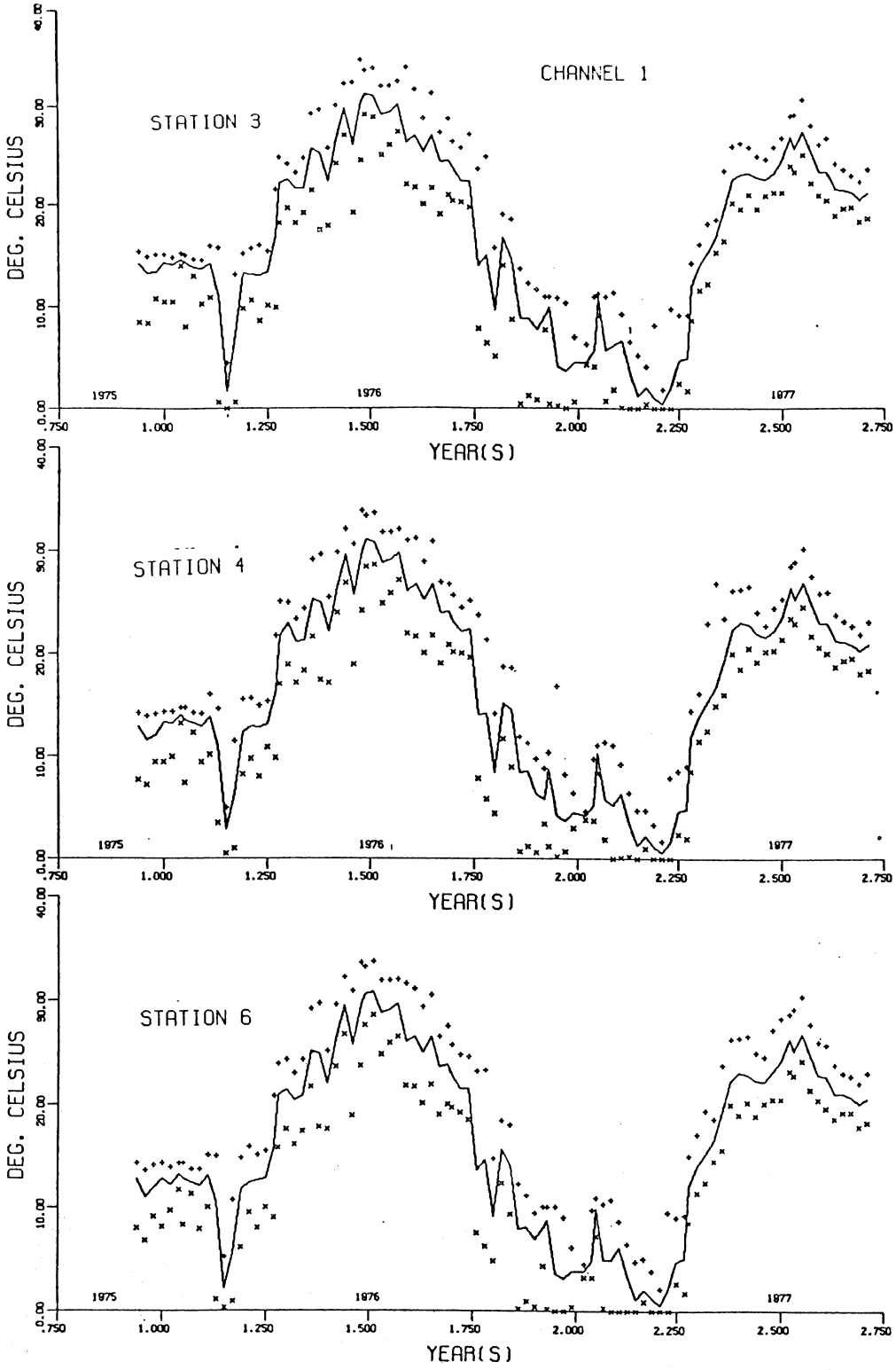

Fig. 4.14. Seasonal water temperature plots of Channel 1. (Cont'd)

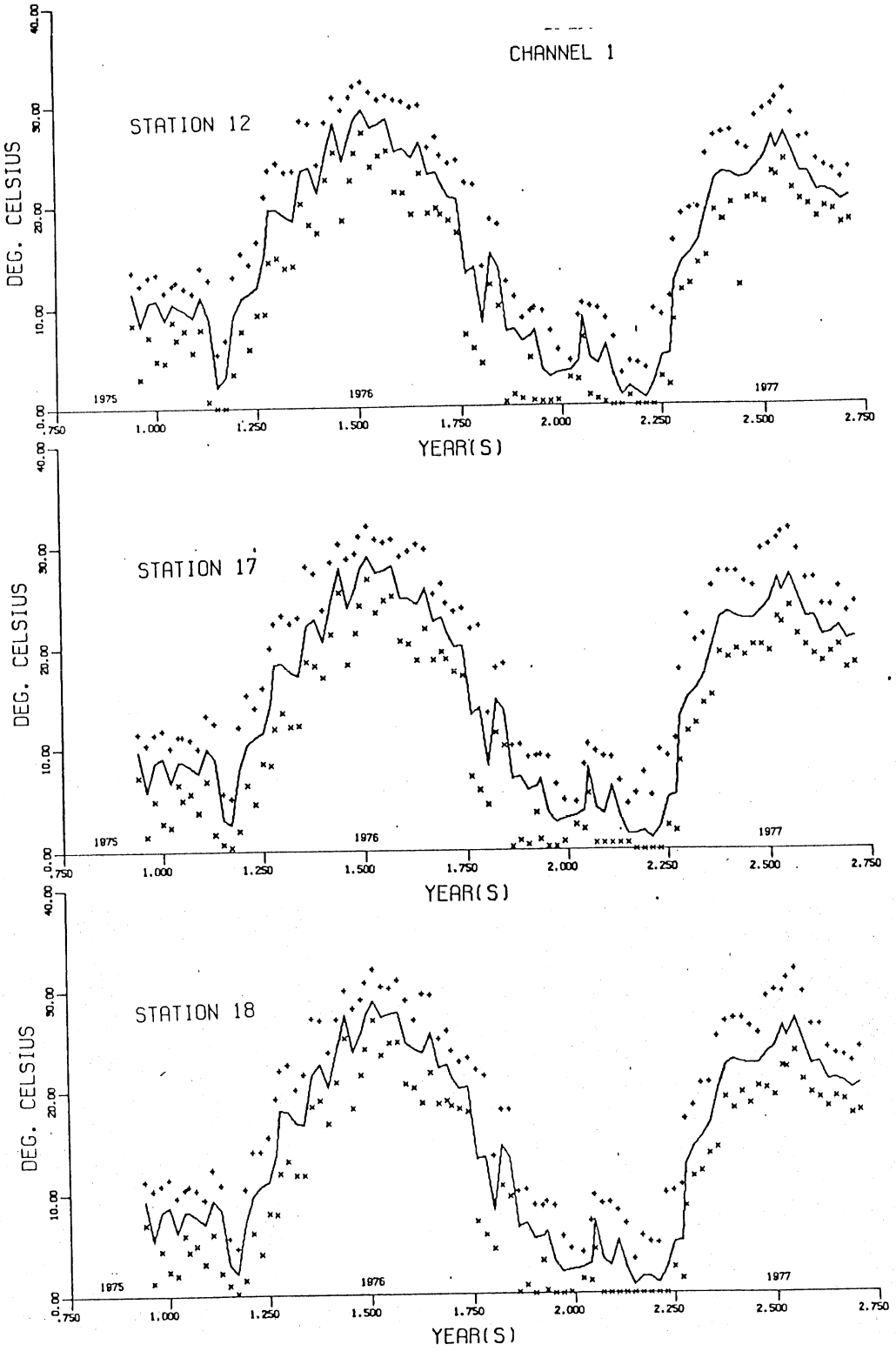

Fig. 4.14. (Cont'd). Seasonal water temperature plots of Channel 1.

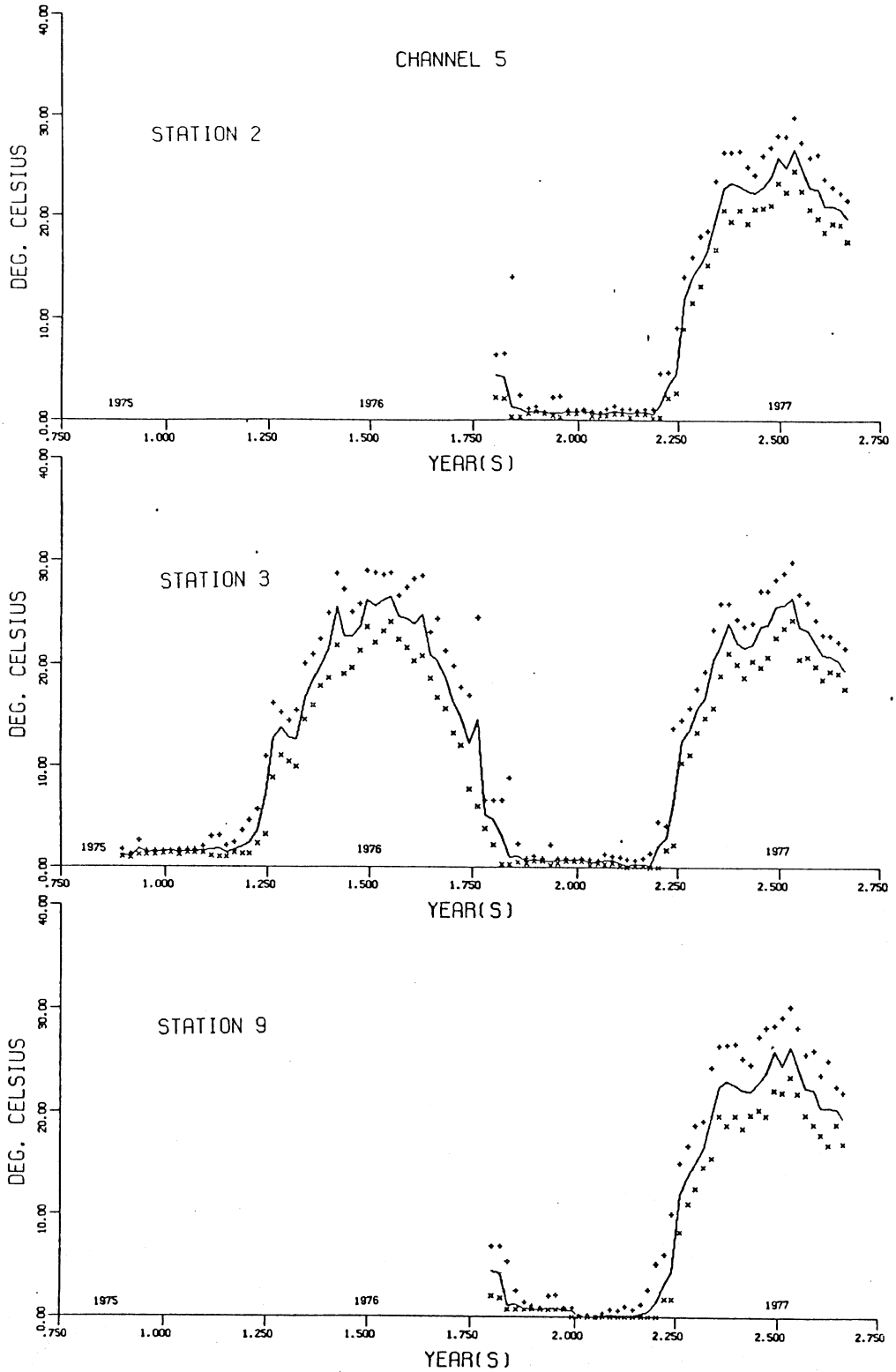

Fig. 4.15. Seasonal water temperature plots of Channel 5. (Cont'd)

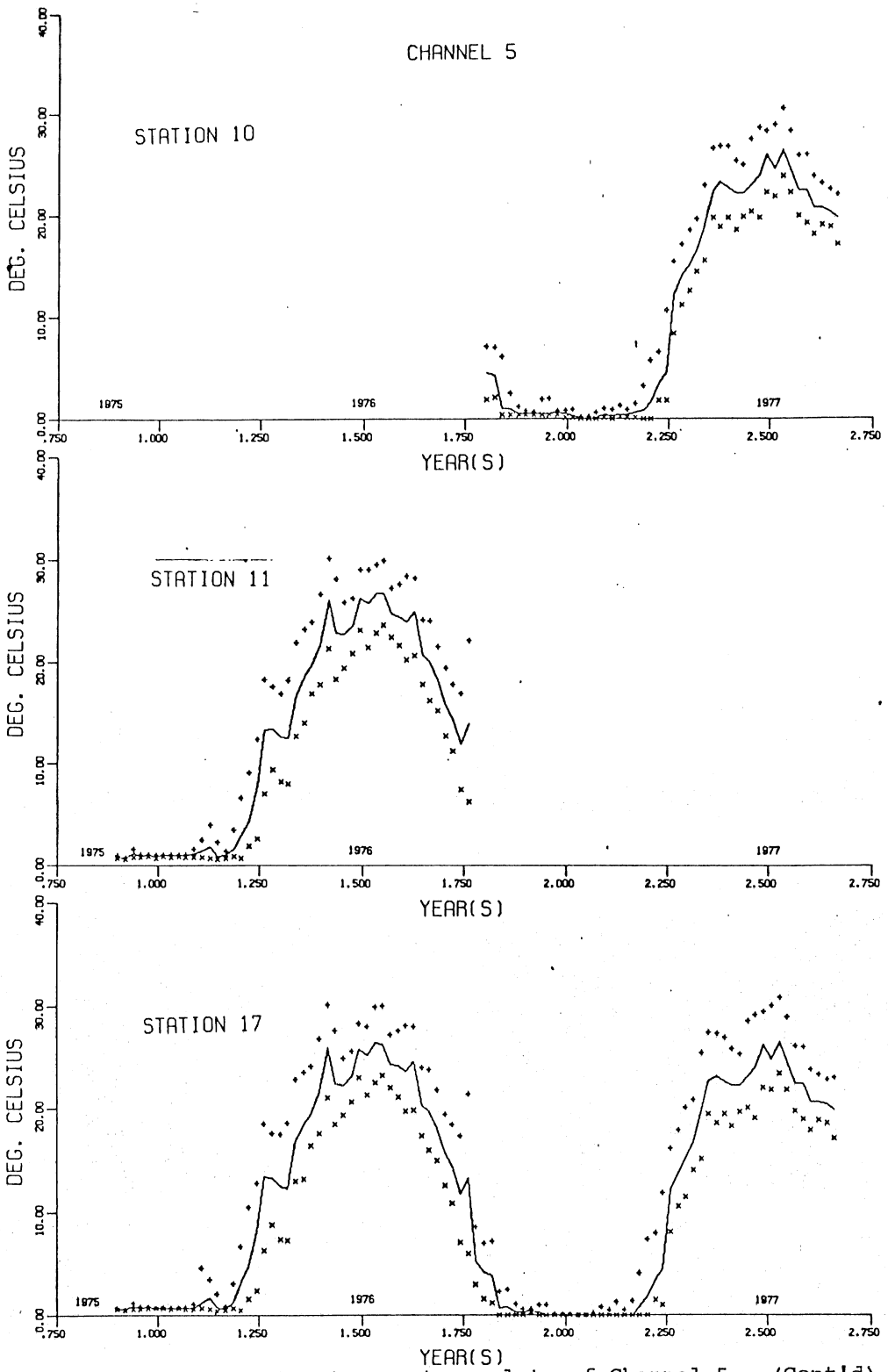

Fig. 4.15. Seasonal water temperature plots of Channel 5. (Cont'd)

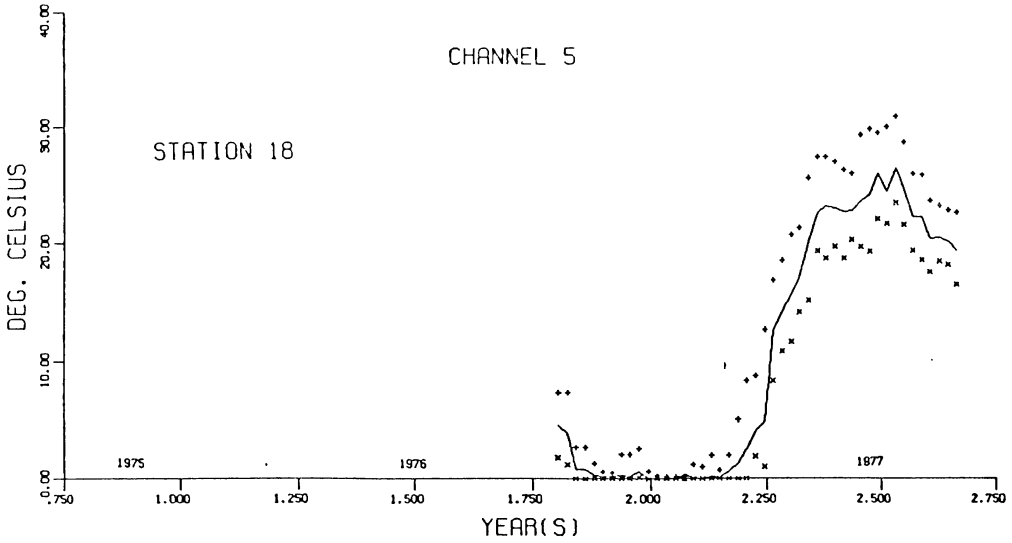

Fig. 4.15. (Cont'd). Seasonal water temperature plots of Channel 5.

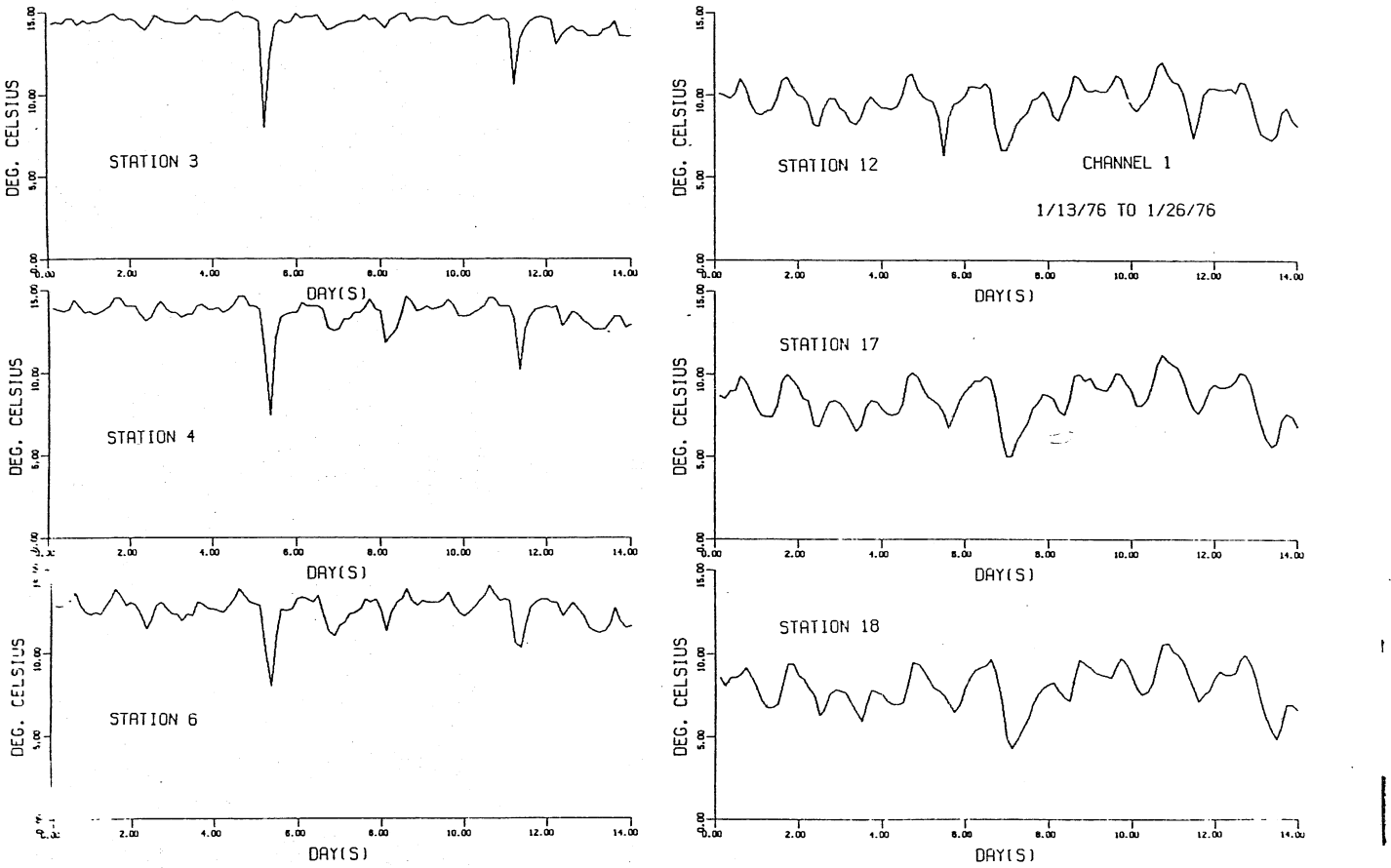

Fig. 4.16. Diurnal water temperature plots of Channel 1.(Cont'd)
1/13/76 to 1/26/76

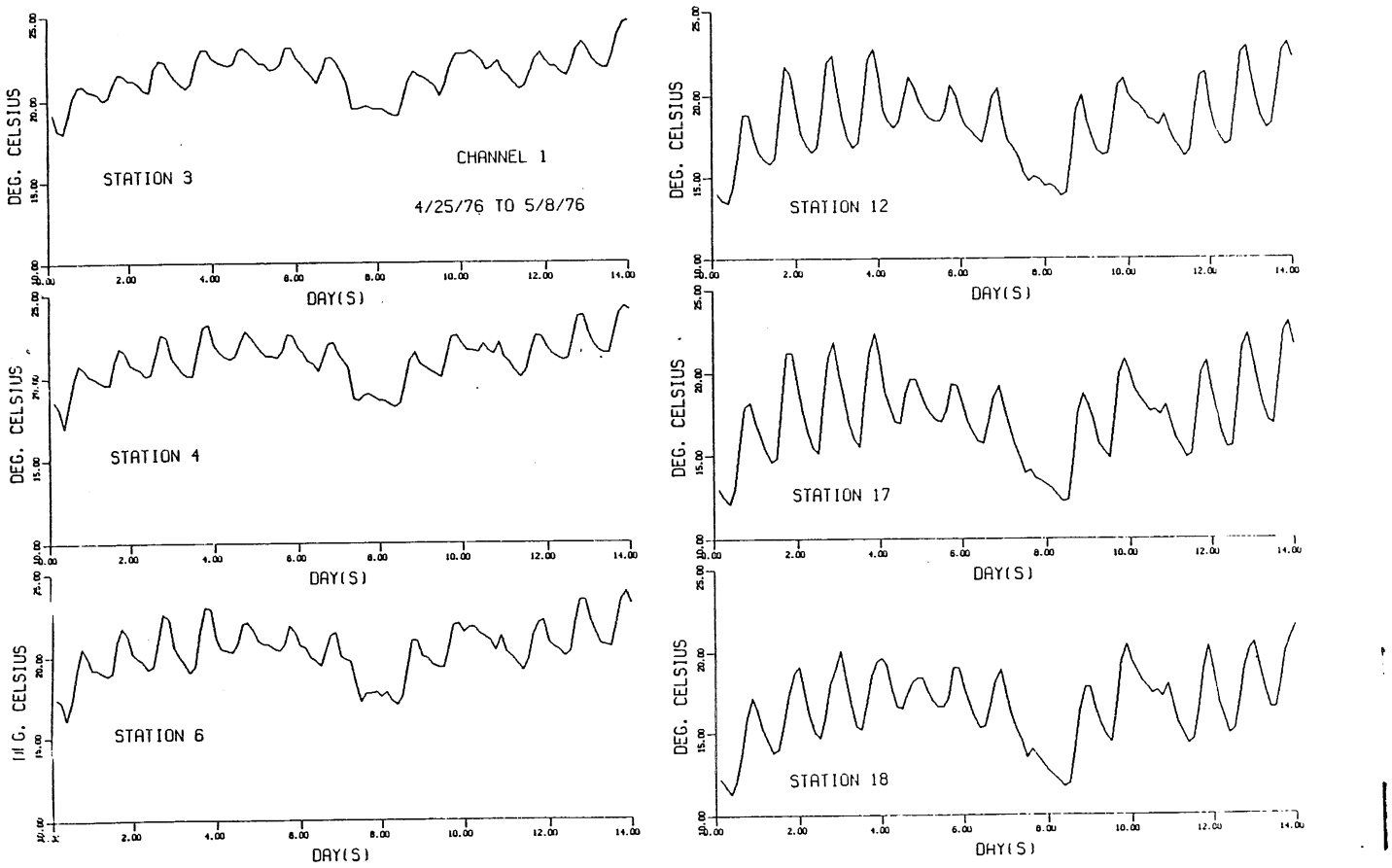

Fig. 4.16. Diurnal water temperature plots of Channel 1. (Cont'd)
4/25/76 to 5/8/76

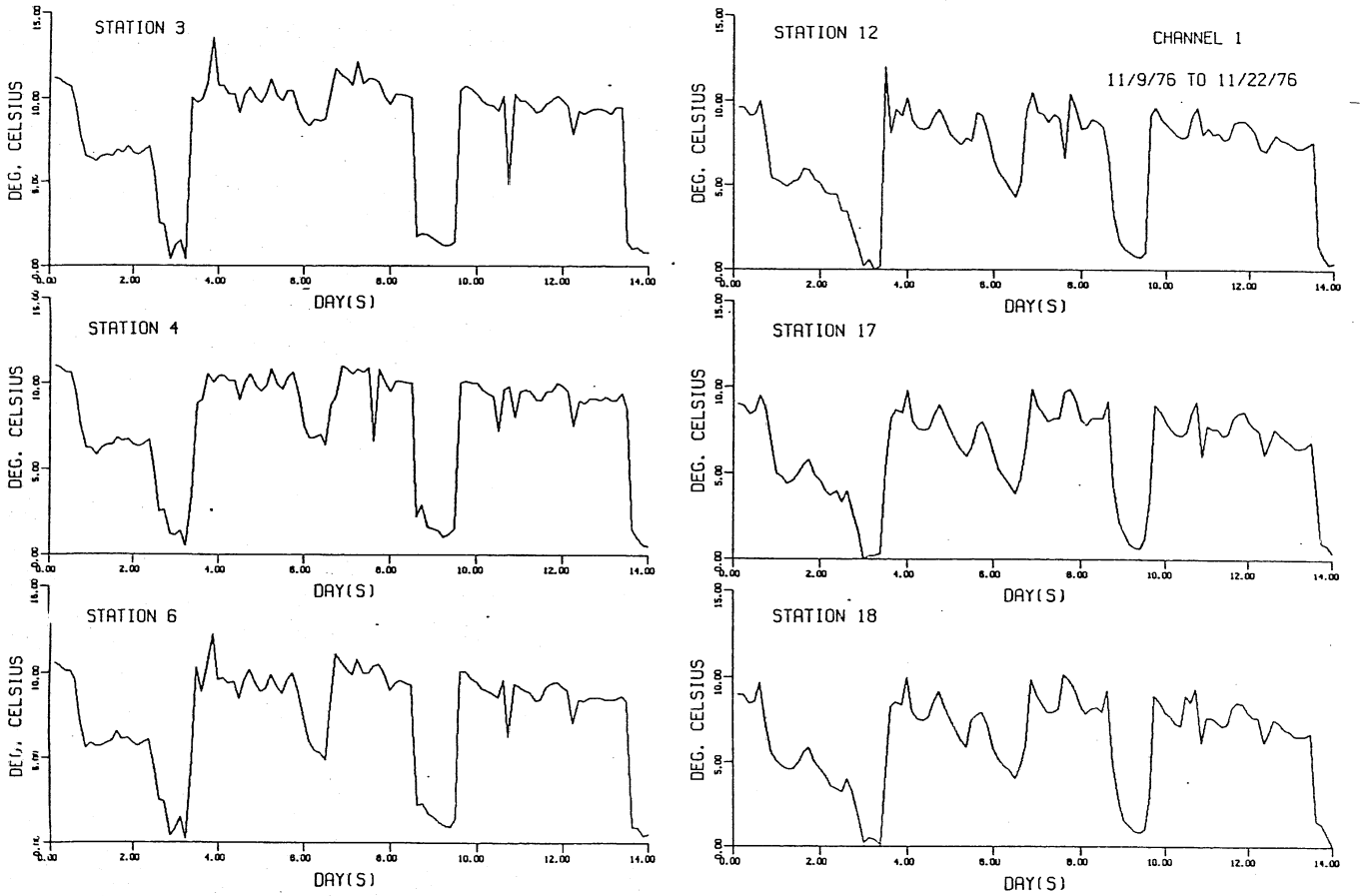

Fig. 4.16. Diurnal water temperature plots of Channel 1. (Cont'd) 11/9/76 to 11/22/76

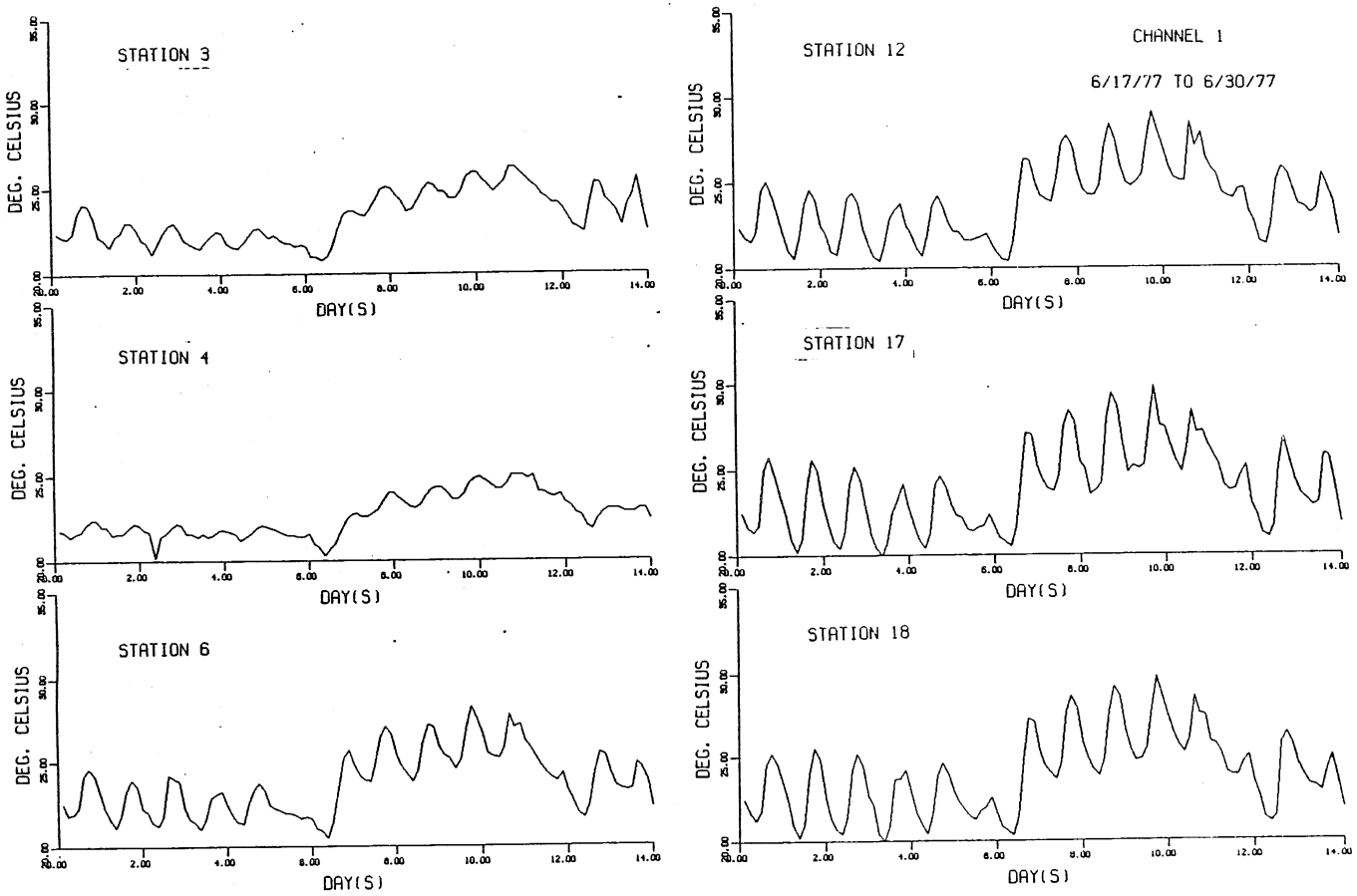

Fig. 4.16 (Cont'd). Diurnal water temperature plots of Channel 1. 6/17/77 to 6/30/77

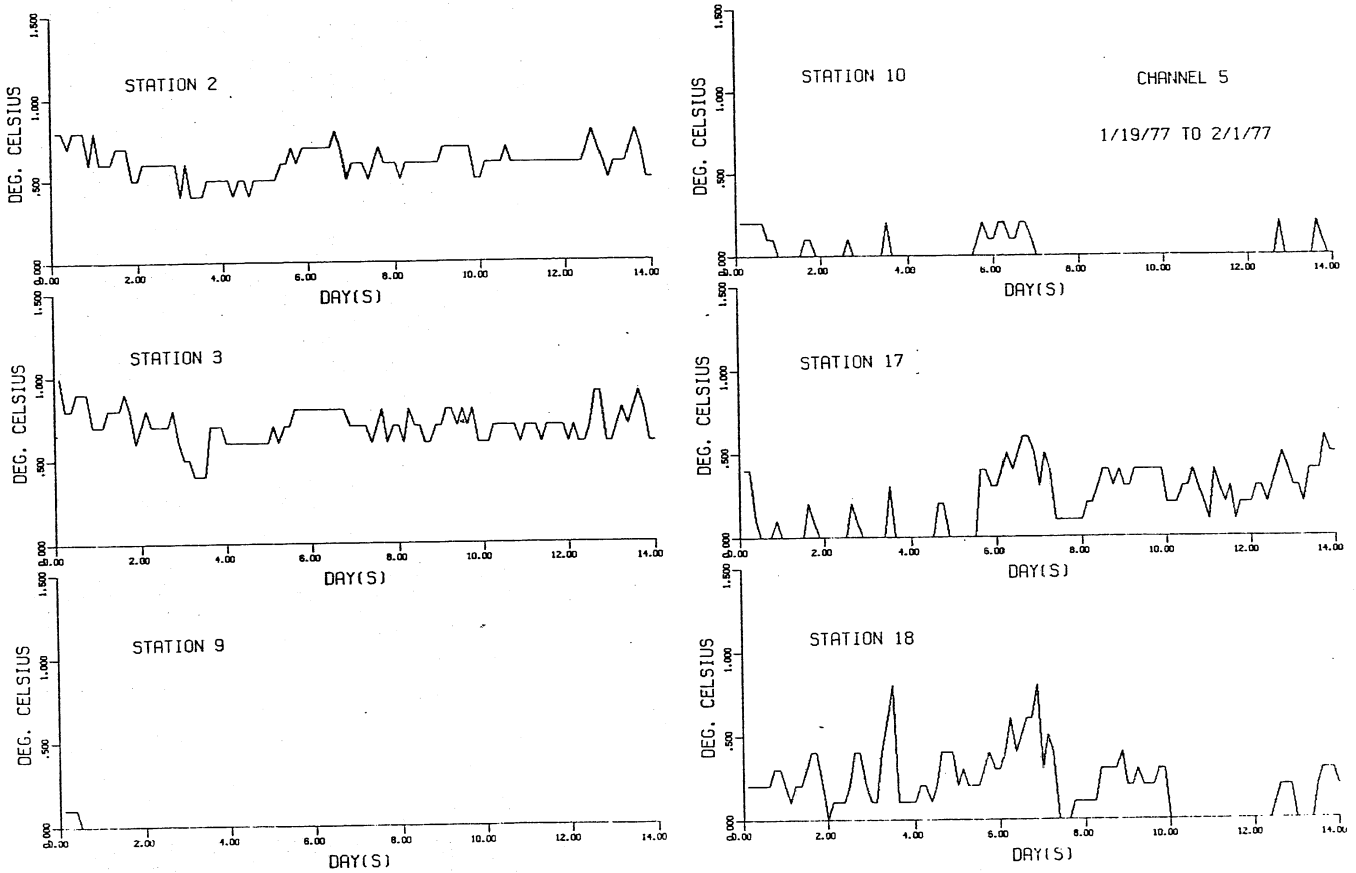

Fig. 4.17. Diurnal water temperature plots of Channel 5. (Cont'd)
1/19/77 to 2/1/77

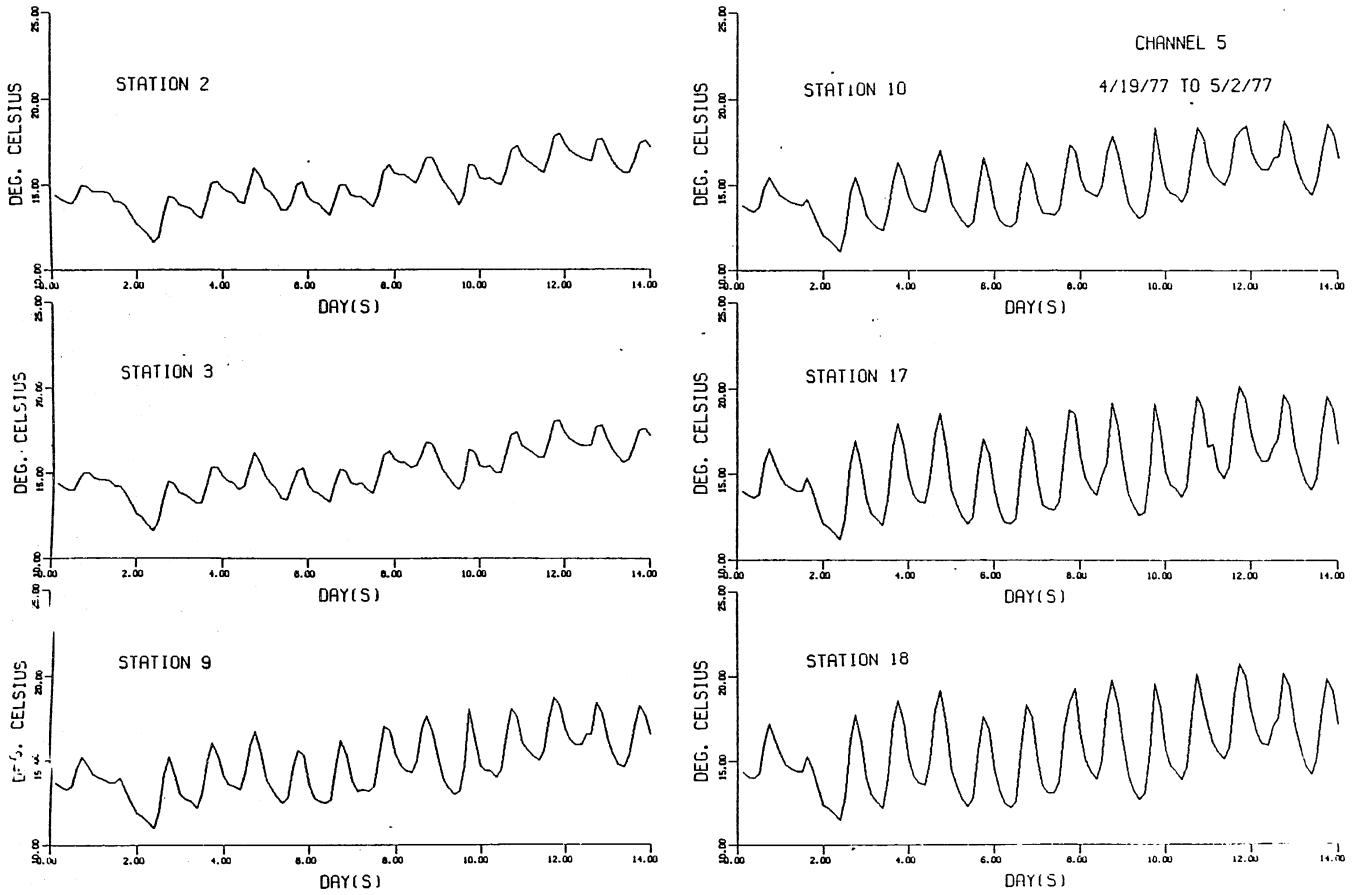

Fig. 4.17. Diurnal water temperature plots of Channel 5. (Cont'd)
4/19/77 to 5/2/77

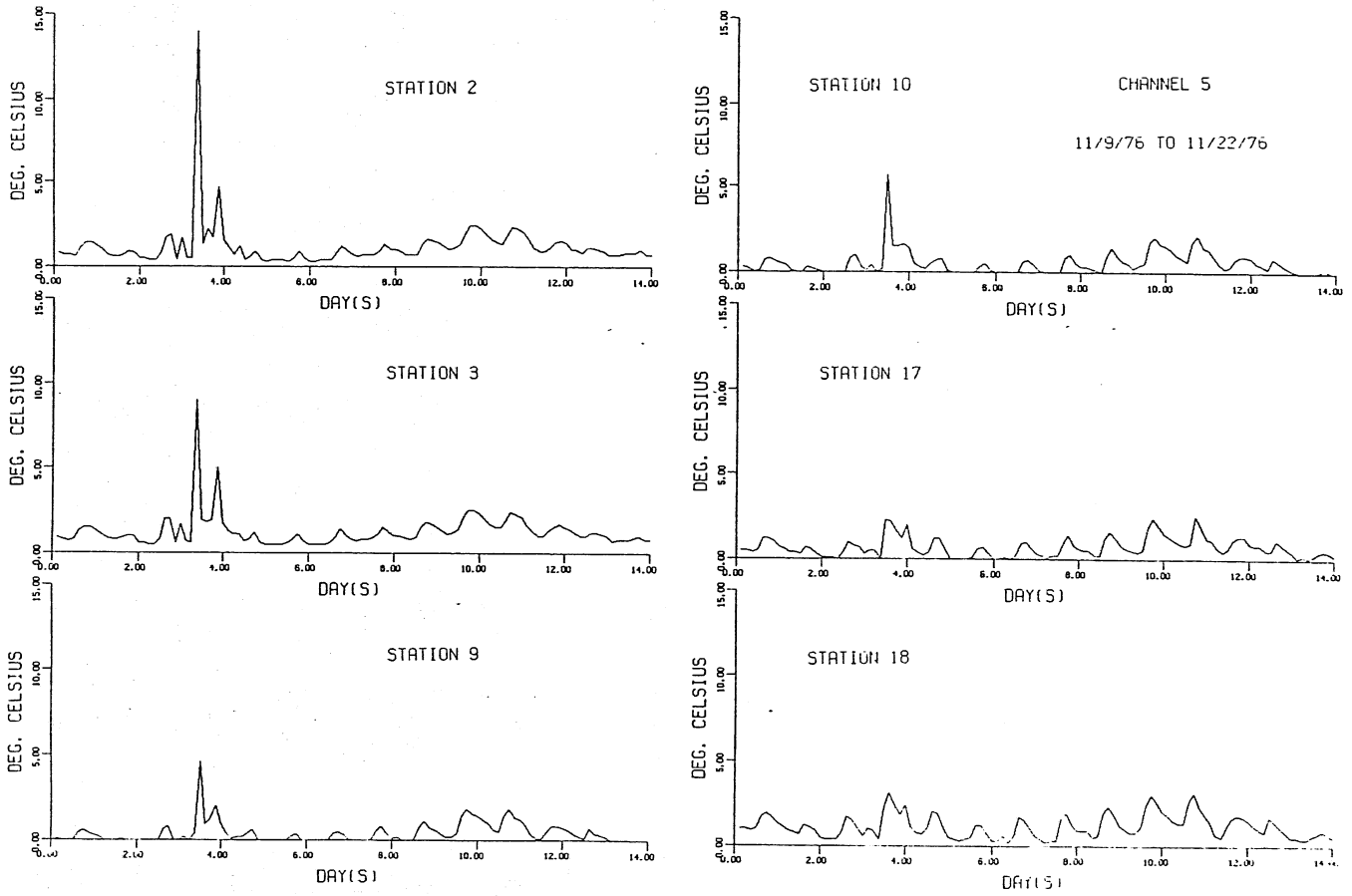

Fig. 4.17. Diurnal water temperature plots of Channel 5. (Cont'd)
11/9/76 to 11/22/76

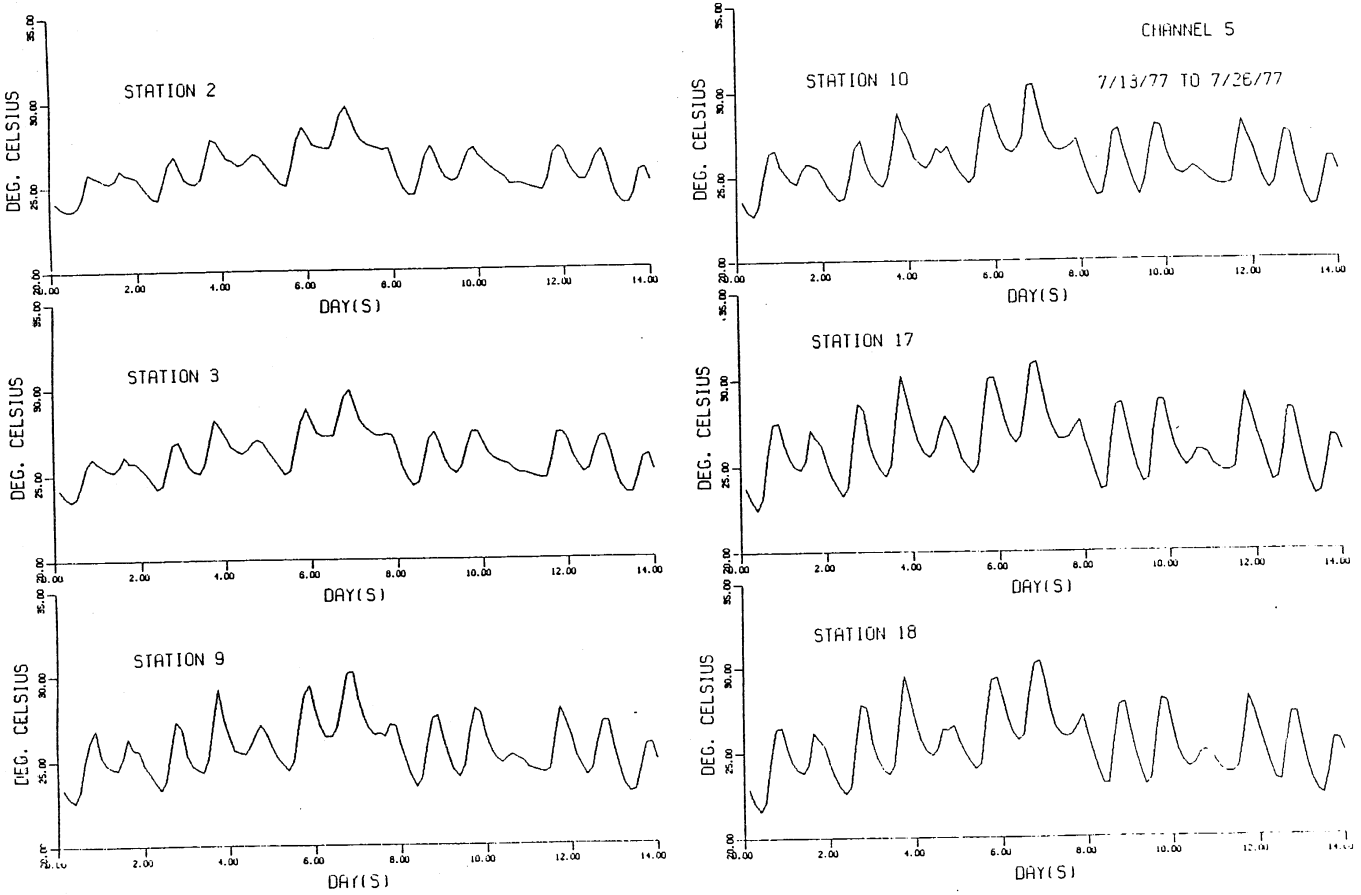

Fig. 4.17 (Cont'd). Diurnal water temperature plots of Channel 5. 7/13/77 to 7/26/77

period. Complete results are given in Hahn et al, 1978a. Table 4.4 summarizes the monthly mean and standard deviation of the longitudinal temperature differences.

Daily diurnal water temperature variations at the outflow of Channel 1 were also recorded over a one-year period (Hahn et al, 1978a). The monthly mean and standard deviation of these values are also given in Table 4.4. It should be emphasized that Table 4.4 gives the characteristics of a heated channel, meaning that inflow temperatures were increased up to 15^{o}C above the temperature of the Mississippi River water. Longitudinal temperature gradients and diurnal variations are not as large in a channel with ambient unheated inflow.

Water temperature stratification in pools

It was found that the pool sections would frequently become thermally stratified. Spot measurements of vertical water temperature stratification in Channels 1, 5, and 8 were made using six thermistors attached vertically to a point gauge and connected to a telethermometer. The point gauge was attached to a cross bar which spanned the width of the channel. Vertical adjustment of the point gauge enabled measurement of a complete temperature profile. An example of the vertical stratification measurements is shown in Fig. 4.18. Typically a thermocline would form at about 60 to 70 cm from the surface. The lowermost 15 to 20 cm would have strong temperature gradients. Additional measured water temperature profiles can be found in Appendix B of Hahn, 1978.

A frequency analysis of temperature stratification in pools 6 and 12 of Channel 1 was made for the calendar year 1976. The continuous temperature records of a vertical array of thermocouples were analyzed on a day by day basis. Daily tabulations of the number of hours of stratification in the ranges $0.5^{o}C < \Delta T \leq 1.0^{o}C$, $1.0^{o} \leq \Delta T \leq 2.0^{o}C$, and $\Delta T \geq 2.0^{o}C$ were made. ΔT is the vertical temperature differential. The magnitude of ΔT was determined from the temperatures measured by the top and bottom thermocouples in each pool. If stratification occurred for one hour or more in a given pool, the day was classified as a day with stratification. If the total number of hours of stratification in a particular range was less than one, zero hours were recorded. Stratification was observed somewhat more frequently in the downstream pools than the upstream ones. Water reaching the downstream pools has had a longer exposure to solar radiation than water in the upstream ones. An annual summary frequency analysis of the stratification data is given in Table 4.5. A breakdown by months is shown in Figs. 4.19 and 4.20.

TABLE 4.4. MONTHLY MEAN AND STANDARD DEVIATION (σ) OF DAILY MINIMUM AND DAILY MAXIMUM LONGITUDINAL (SPATIAL) TEMPERATURE DIFFERENCE, AND OF DIURNAL (TEMPORAL) TEMPERATURE DIFFERENCE AT THE OUTFLOW FOR A HEATED CHANNEL 1, DECEMBER 1975 - NOVEMBER 1976

Month	Minimum Longitudinal ΔT		Maximum Longitudinal ΔT		Diurnal ΔT at Outflow	
	Mean (^{o}C)	σ (^{o}C)	Mean (^{o}C)	σ (^{o}C)	Mean (^{o}C)	σ (^{o}C)
December (1975)	5.2	2.0	8.0	2.5	1.9	0.9
January (1976)	6.0	1.5	9.5	1.8	2.3	1.0
February	4.6	1.3	7.7	1.7	2.5	1.3
March	3.2	2.7	6.9	3.1	3.4	1.6
April	1.9	1.8	5.6	1.6	5.3	1.9
May	1.8	1.3	5.7	1.4	4.4	2.2
June	2.7	1.5	4.8	1.6	4.0	0.0
July	1.7	0.9	4.0	0.9	3.5	0.8
August	0.9	1.1	4.5	2.0	3.7	1.5
September	1.7	0.7	3.5	0.9	2.9	1.2
October	0.9	1.0	3.4	2.6	2.9	1.2
November (1976)	1.0	1.0	5.7	3.9	2.5	2.4

TABLE 4.5. FREQUENCY ANALYSIS OF TEMPERATURE STRATIFICATION IN CHANNEL 1 (January 1 - December 31, 1976)

	Pool No.	Vertical ΔT $\geq 0.5^{o}C$	$\geq 1.0^{o}C$	$\geq 2.0^{o}C$
% days with stratification	6	48	29	9
	12	34	26	16
% hours with stratification	6	13	6	2
	12	11	8	3

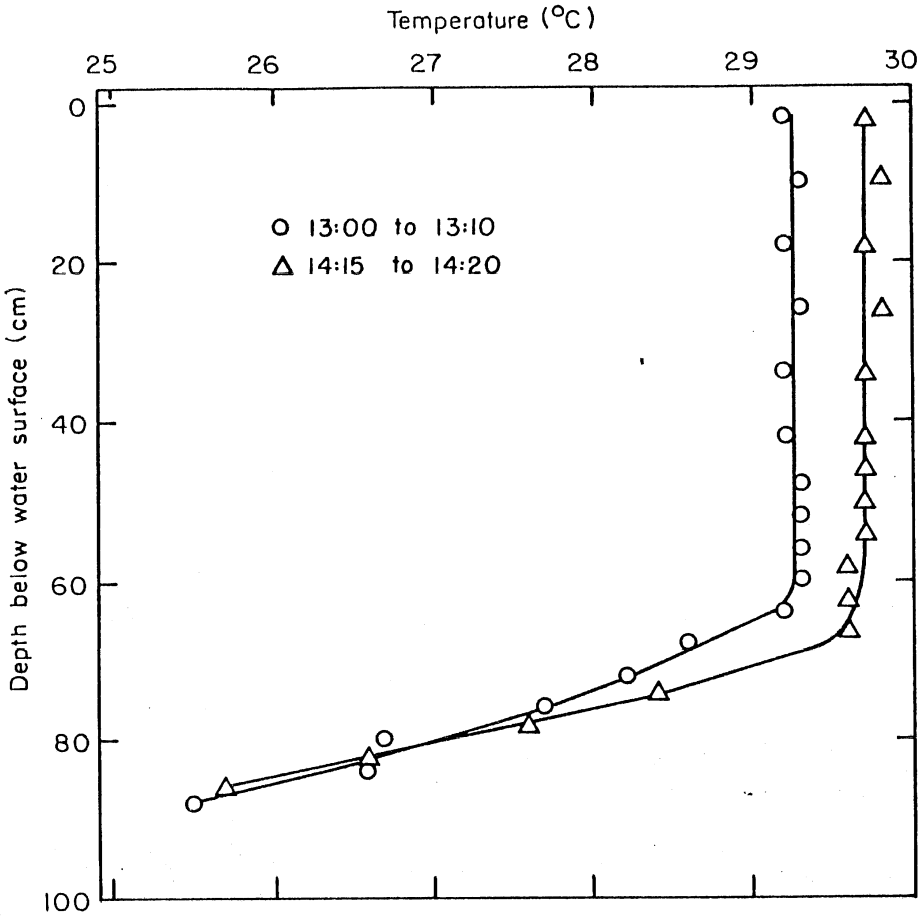

Fig. 4.18. Vertical temperature stratification in Channel 1, pool 6. Measured August 11, 1976.

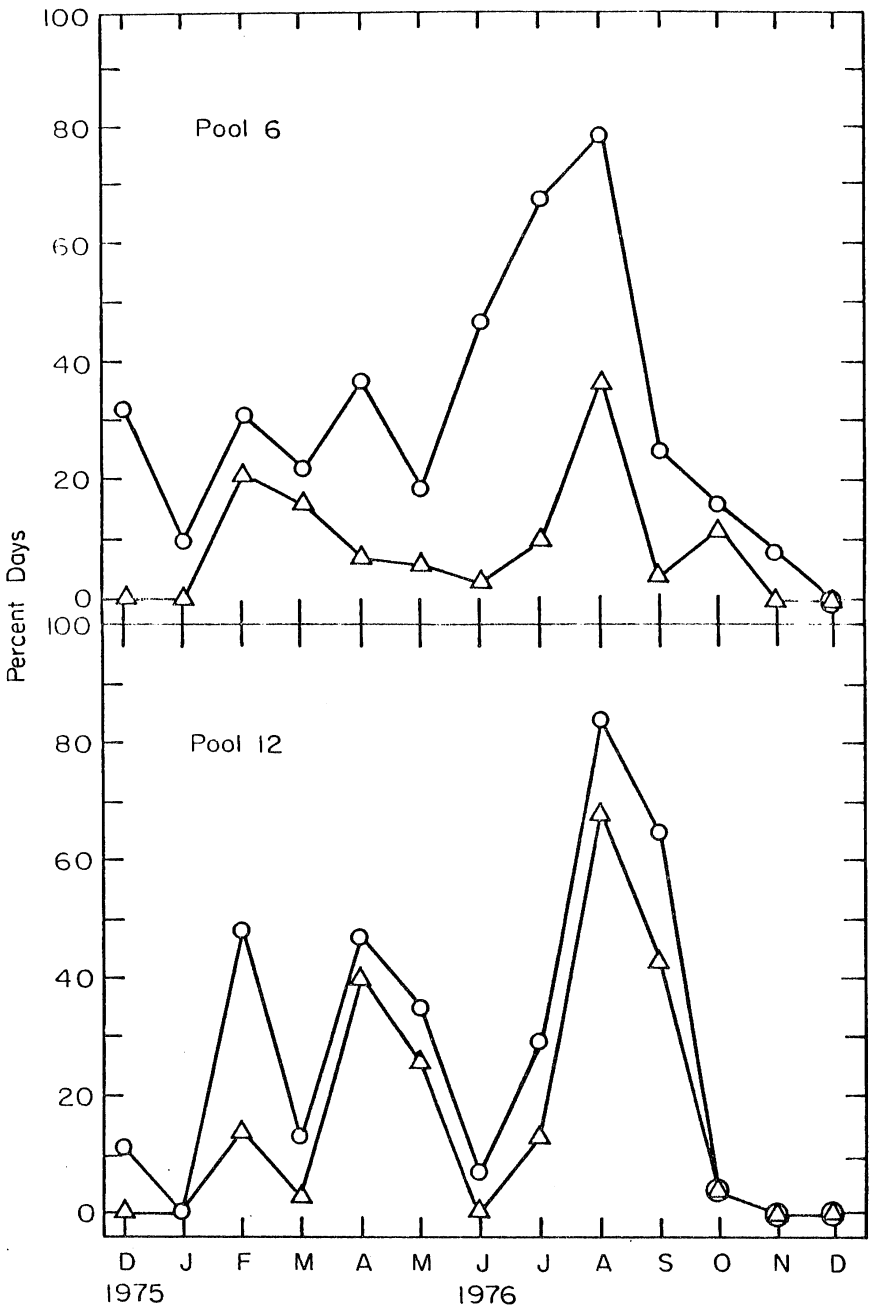

Fig. 4.19. Per cent days with stratification $\Delta T \geq 1.0^{\circ}C$ ⊙ and $\Delta T \geq 2.0^{\circ}C$ △ in Channel 1, pool 6 (top) and pool 12 (bottom). Average channel flow rate was 0.0175 m^3/s until August 1976 and 0.0317 m^3/s afterwards.

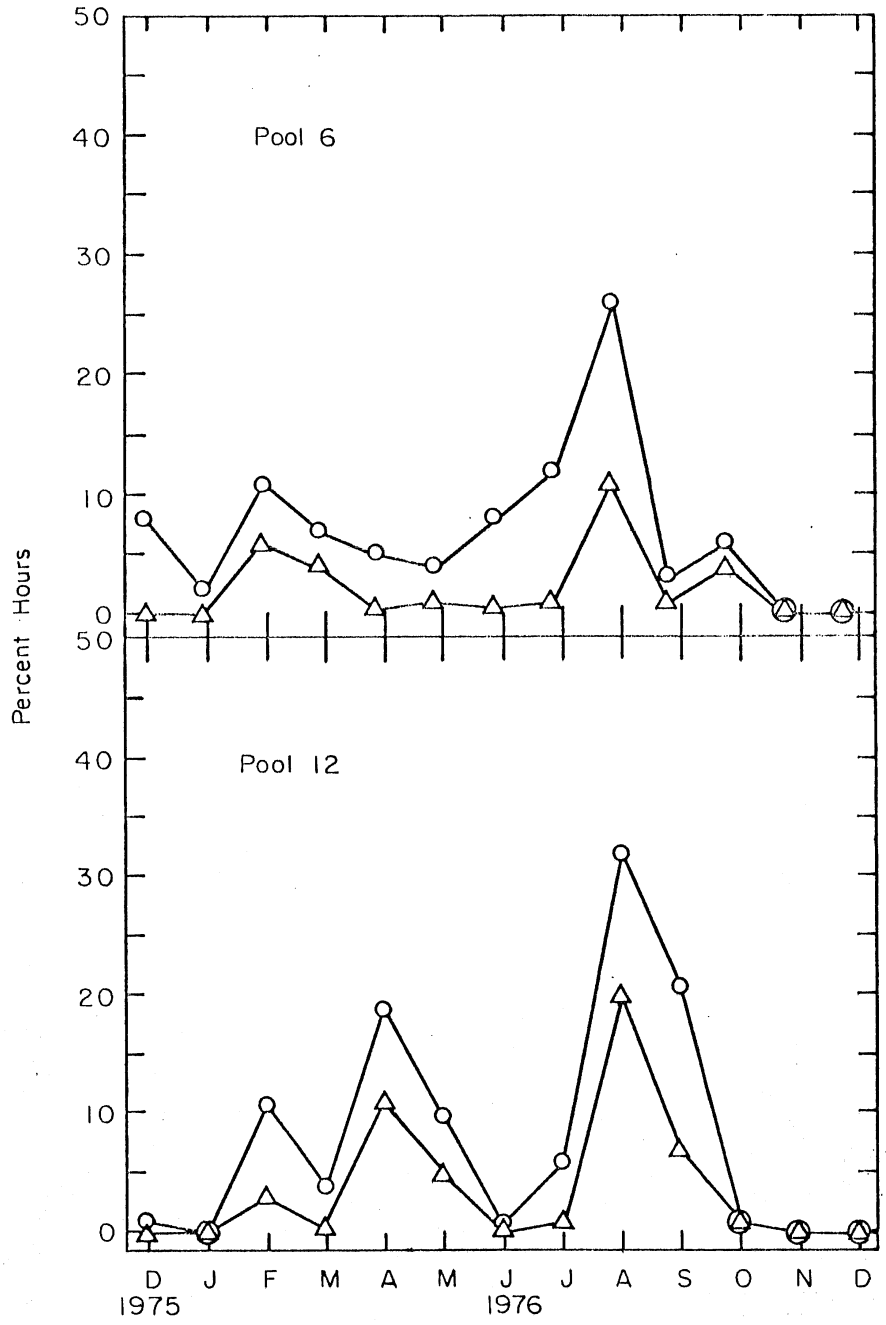

Fig. 4.20. Per cent hours with stratification $T \geq 1.0^{\circ}C$ ⊙ and $T \geq 2.0^{\circ}C$ △ in Channel 1, pool 6 (top) and pool 12 (bottom). Average channel flow rate was 0.175 m^3/sec until August 1976 and 0.0317 m^3/sec afterwards.

SECTION 5

A STUDY OF LONGITUDINAL DISPERSION IN THE MERS FIELD CHANNELS

5.1. BACKGROUND

The flow field in the MERS channels is very non-uniform and mean flow velocities are very small. Water moves through the MERS channels in a way far different from the movement of a piston in a cylinder (plug flow). Water may move faster in the center of a riffle or a pool than at its edges. Transverse and/or vertical mixing takes place between the faster and the slower water masses. Vegetation is present in pools and riffles in the summer. There is a weak jet effect at the transition from the riffles to the pools. In the pools water masses may be entrapped near the banks. There can be wind and there is intermittent stratification in the pool. As a result of all these interacting processes, heat or material contained in the water will spread out longitudinally along the channel. It was believed that the effect of longitudinal spreading had to be incorporated in the water temperature model.

Since a detailed study of the very complex low velocity channel hydrodynamics was not part of the research objective, the water temperature simulation could be based on two conceptually different models.

(a) a tanks in series model with an adjustable residence time parameter

(b) a uniform channel flow model with a longitudinal dispersion term

The latter approach was chosen arbitrarily because it was believed and later verified by the model results that the observed channel water temperature dynamics could be well predicted by a diffusion equation. The term *longitudinal dispersion coefficient* is used herein to describe a bulk coefficient which lumps the effects of all the processes mentioned above. It might also have been termed a *bulk or hydrodynamic longitudinal diffusion*

coefficient. To use separate coefficients for riffles and pools was considered but the frequent transitions and short lengths of these elements made it advisable not to use this approach.

The use of a diffusion equation to describe longitudinal mass transport in a channel is only justified after the initial convective period as shown by Fischer (1967). The MERS channels begin with a pool into which water is discharged from a weir producing a very well mixed upstream condition.

The mean residence time of the water is anywhere from 10 to 30 minutes depending on flow rate. The convective length estimated from the relationship

$$Z = 0.3 \frac{\ell^2}{h} \frac{h^{1/6}}{n\, g^{1/2}},$$

with ℓ 1.8 m for a pool
h 0.8 m for a pool
n 0.1 (0.06 to 0.3)
g 9.8 m/sec^2

gives a value of approximately 5 m or far less than the length of the first pool (30 m). It can therefore be considered that the convective length does not reach beyond the length of the first pool.

A study of longitudinal dispersion in the MERS field channels was made for two reasons. (1) A longitudinal dispersion coefficient was needed in the unsteady channel water temperature model to be discussed in Section 7, and (2) the size of the MERS channels is intermediate between laboratory flumes and full-size canals; size is an important factor for longitudinal dispersion and no studies had ever been made on a system of that intermediate size.

Longitudinal dispersion was first studied analytically in pipe flow by Taylor (1954) and was later applied to open channel flow by Elder (1959). For a straight, two-dimensional channel Elder obtained

$$D_L = 5.93\, h\, u_* \qquad (5\text{-}1)$$

where h is channel depth and u_* the shear velocity. Experimental verification of Eq. 5-1 by Elder (1959), Fischer (1968), Thackston and Krenkel (1967), and Sayre and Chang (1968) has indicated values of the constant from 5.3 to 15.7 for various flow and straight channel conditions.

Elder's equation, however, is not generally applicable to natural streams and larger channels in which dispersion coefficients are much larger than those predicted by Eq. 5-1. Fischer proposed that in natural streams velocity profiles and transverse mixing are dominant in determining longitudinal dispersion. Thus, the longitudinal dispersion coefficient depends upon shoreline configuration, bends, and bed formation, as well as the stream velocity (see e.g. Day, 1975).

A considerable amount of research on longitudinal dispersion in laboratory flumes and in natural streams has been reported since the above cited early studies. A recent summary of Fischer et al (1979) lists some of the investigators who have contributed analytical or experimental information. Prior reviews were given by Ditmars (1974) and Fischer (1973), El-Hadi and Davar (1976).

The prediction of longitudinal dispersion for a stream of given geometry without some form of field measurements of velocity profile or dye dispersion is still a difficult problem. Relationships based on geometrical and hydrologic stream characteristics were proposed, among others, by Bansal (1971), McQuivey and Keefer (1974), Jain (1976), Fischer et al (1979), and Liu and Chen (1980). These relationships are of a semiempirical nature, e.g.,

Liu and Chen: $D_L = (0.27 \text{ to } 1.25)\, u_* B^2/h$

Fischer: $D_L = 0.011\, \bar{U}^2 B^2/hu_*$

where D_L = longitudinal dispersion coefficient,

$\bar{U}$ = mean velocity,

B = stream width,

h = mean stream depth, and

u_* = shear velocity.

The channels investigated in this study do not have the accentuated longitudinal mixing characteristics of natural streams caused by meanders and large widths. They are also very different from laboratory channels. Abrupt changes in cross sectional areas from "riffle" to "pool" sections occur every 30 meters (100 ft). The parabolically shaped pool sections are 4 m wide and approximately 1 m deep. The repeated expansions and contractions in flow would be expected to affect longitudinal dispersion.

At elevated velocities longitudinal mixing is enhanced by jet effects of the flow from the riffle sections into the pool sections. Flow streamlines which could be expected from such jet mixing are sketched in Fig. 5.1. Lomax and Orsborn (1971) studied the effects of jet mixing in a small, experimental pool of circular shape and constant depth. A schematic of a measured outflow concentration curve is shown in Fig. 5.2. Inflow started at $t = 0$ with a concentration C_o in the pool. Concentration of the inflow was $C = 0$.

The pools at the Monticello Field Station have a length of nine times the width and very low flow velocity. This confines jet mixing effects to the upstream portion of each pool and reduced its significance. Jet mixing was therefore evaluated as part of the longitudinal dispersion coefficient.

Dispersion in the MERS channels can also be affected by wind mixing, plant growth, stratification and/or natural convection in the pools because the mean flow velocities in the pools are only on the order of 1 cm/sec. The measurements and the analysis integrated all those effects.

5.2. METHOD OF LONGITUDINAL DISPERSION COEFFICIENT DETERMINATION FROM TRANSIENT WATER TEMPERATURES

The contribution of longitudinal dispersion to longitudinal water temperature profiles increases with the transient character of water temperature. The effect of longitudinal dispersion is most evident when a temperature pulse or a front of elevated or depressed temperature moves downstream. In this section, temperature fronts will be related to longitudinal dispersion theory and used to estimate longitudinal dispersion coefficients in the MERS experimental channels.

The longitudinal dispersion coefficient for natural streams is often determined from an instantaneous injection of a conservative tracer. The one-dimensional mass transport equation for the tracer is

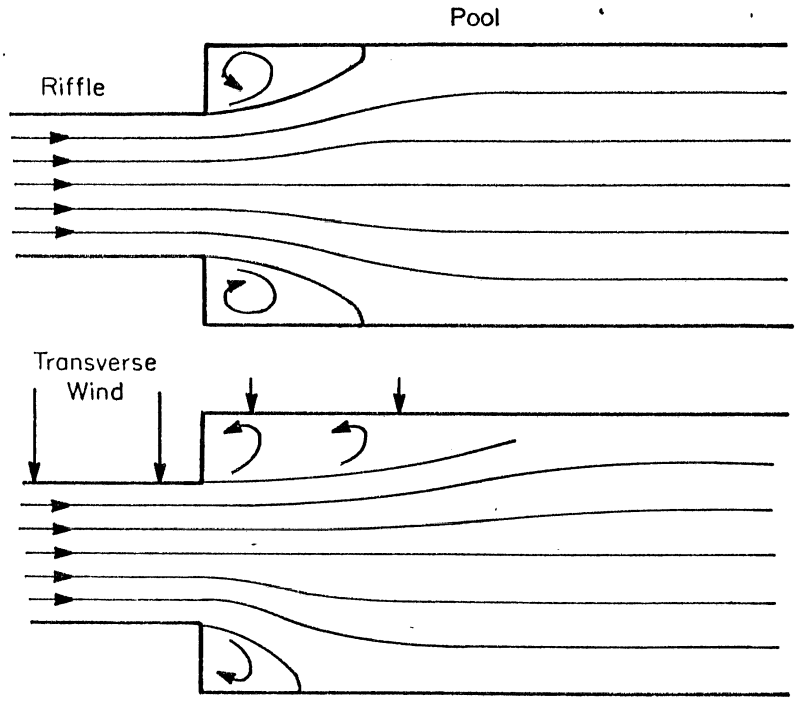

Fig. 5.1. Schematic streamlines at transition from riffle to pool in Monticello experimental channels without (above) and with (below) transverse winds.

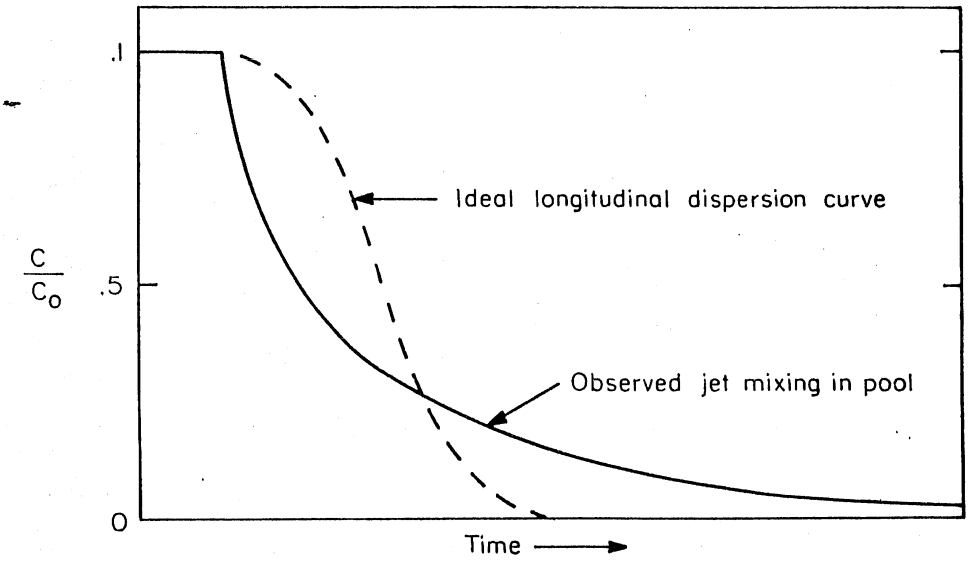

Fig. 5.2. Schematic outflow concentration curve for jet mixing in experimental pool (after Lomax and Orsborne, 1971).

$$\frac{\partial C}{\partial t} + U \frac{\partial C}{\partial x} - D_L \frac{\partial^2 C}{\partial x^2} = 0 \qquad (5\text{-}2)$$

with solution for an instantaneous injection

$$C(x) = \frac{M}{2A(\pi D_L t)^{1/2}} \exp\left[- \frac{(x-Ut)^2}{4 D_L t} \right] \qquad (5\text{-}3)$$

where C = tracer concentration (M/L^3),

M = mass of tracer injection (M),

A = channel cross-sectional area (L^2),

U = cross sectional mean flow velocity (L/T),

x = distance from point of injection (L),

t = time from moment of injection (T), and

D_L = longitudinal dispersion coefficient (L^2/T).

The use of Eq. 5-2 assumes that the shape of the tracer cloud will be Gaussian. By the method of moments, or by a routing method, the longitudinal dispersion coefficient between two points may be found. More comprehensive details of D_L determination from tracer pulses in natural streams are given by Godfrey and Frederick (1970), among others.

In the MERS experimental channels water temperature was used as a tracer to estimate longitudinal dispersion coefficients. The most readily obtainable trace, however, was not a heat impulse but a temperature front. Such fronts could be obtained by turning on or shutting off the heat exchanger in the feed line to Channel 1. (See Fig. 5.3 for examples.)

A longitudinal dispersion coefficient can be accurately determined by routing the temperature front downstream and adjusting D_L to minimize the error in measured and predicted water temperatures. The analytical solution for a temperature front assuming no sources or sinks is

$$\Theta = \frac{1}{2} \text{Erfc} \left[(x-Ut)/(4D_L t)^{1/2} \right] \qquad (5\text{-}4)$$

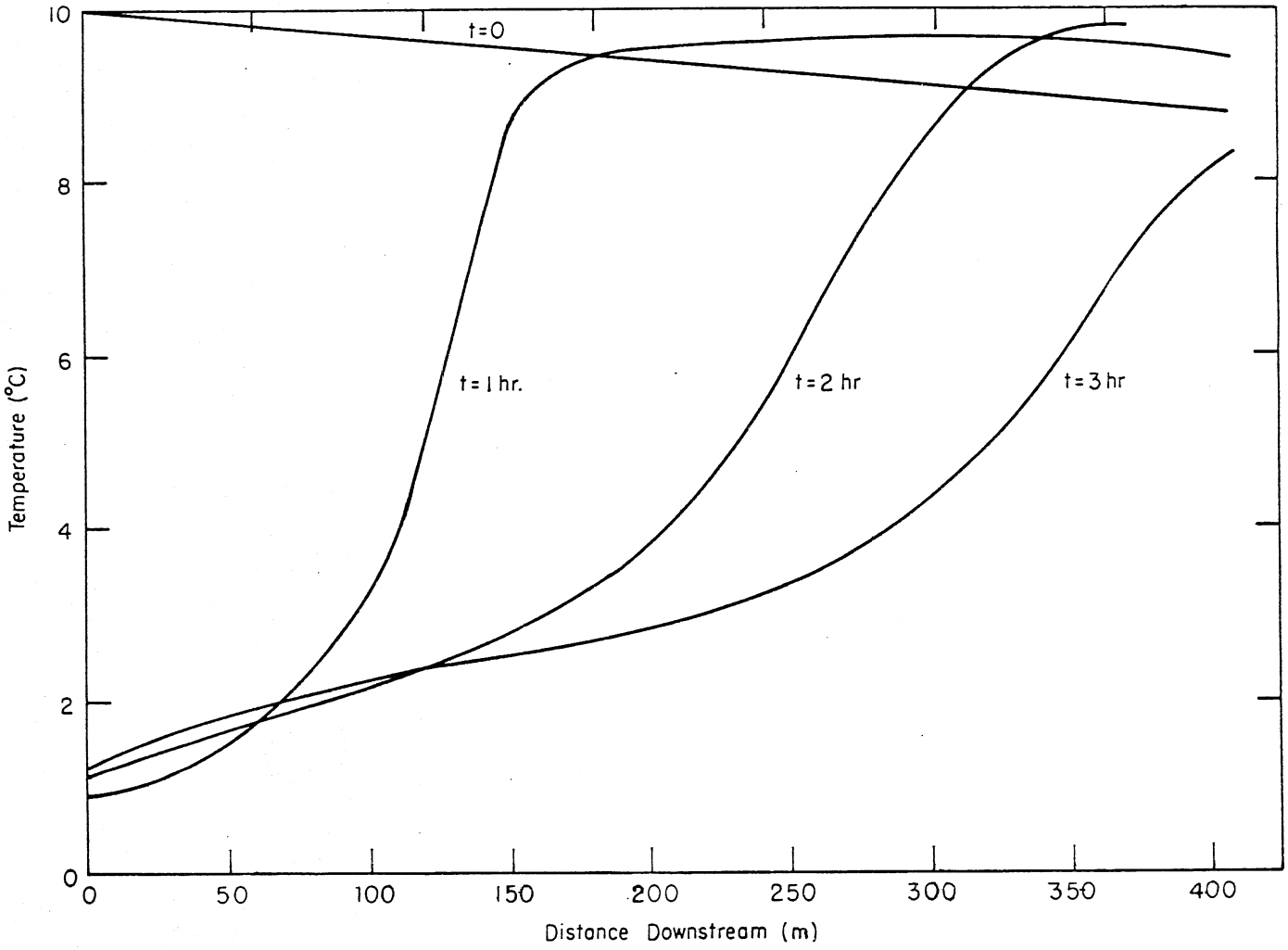

Fig. 5.3. Temperature fronts in MERS channel 1 on November 17, 1976. Front inception is at t=0.

where $\Theta = \frac{T(t) - T(0)}{T(\infty) - T(0)}$ and (5-5)

$$\text{Erfc}(g) = 1 - \frac{\sqrt{\pi}}{2} \int_0^g d^{-Q^2} \, dQ$$

Erfc is the complementary error function. Measured values of $\Theta(x,t)$ were compared to values computed by Eq. 5-4. The D_L value which minimizes the error between computed and observed Θ is the "measured" D_L for the test.

Heat transfer may also affect the longitudinal dispersion coefficient calculated from a temperature front. The order of magnitude of this error was estimated by computing a temperature front with and without heat transfer using typical values of channel depth and width, flow rate, and longitudinal dispersion coefficient, with upper limiting values for the bulk surface heat transfer coefficient, and the upstream temperature front (Gulliver, 1977). The computed results indicate that surface heat transfer has no appreciable effect upon the longitudinal dispersion coefficient determined by the routing method. Fig. 5.4 illustrates why this should be expected. Longitudinal dispersion can be directly visualized as the spread between the 0.16 and 0.84 values of dimensionless concentration Θ. Surface heat transfer reduces the values of Θ but not appeciably the longitudinal spread.

5.3. FORMULATION OF DIMENSIONLESS LONGITUDINAL DISPERSION NUMBERS

Many investigators have expressed longitudinal dispersion by a dimensionless number, $D_L/u_* h$, where u_* is bottom shear velocity. For the MERS channels flow rate, rather than water surface slope, is more accurately measured. With

$$U = \sqrt{8/f_b} \; u_*$$

and

$$f_b = \frac{8g \, n^2}{h^{1/3}}$$

where f_b = bottom friction factor for entire channel,

h = mean depth of channel, and

n = Manning's coefficient for the channel,

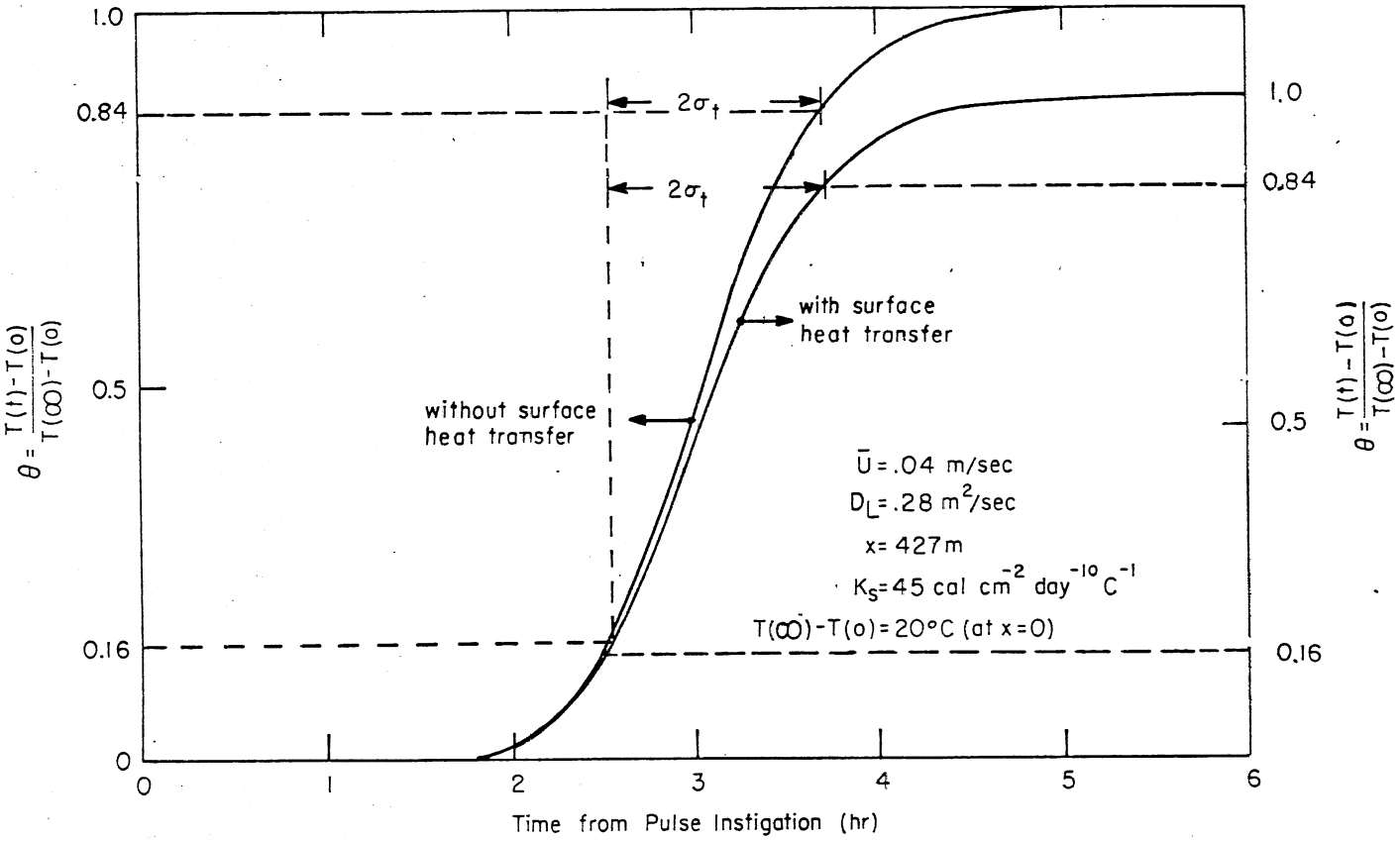

Fig. 5.4. Computed temperature fronts (normalized) which occur at location 17 in Channel 1 with and without heat transfer.

one derives for the dimensionless expression

$$\frac{D_L}{u_* h} = \frac{D_L}{Uh}\left(\frac{h^{1/3}}{g\, n^2}\right)^{\frac{1}{2}} = \left(\frac{h^{1/6}}{g^{\frac{1}{2}}\, n}\right)\frac{D_L\, B}{Q} \qquad (5\text{-}6)$$

where Q = flow rate and B = mean surface width. For constant mean channel depth h and constant Mannings 'n'

$$D^* = \frac{D_L\, B}{Q} \propto \frac{D_L}{u_* h} \qquad (5\text{-}7)$$

For a stream or channel of variable cross section, Bansal (1971) proposed a dimensionless local dispersion coefficient

$$D_B^* = \frac{U}{\bar{U}}\,\frac{D_L}{\bar{h}\,\bar{U}} = \frac{\bar{A}\,\bar{B}\,D_L}{AQ} \qquad (5\text{-}8)$$

where U = local cross sectionally averaged flow velocity,

$\bar{U}$ = average flow velocity, U, over stream reach,

$\bar{h}$ = average depth over stream reach,

$\bar{B}$ = average width over stream reach,

$\bar{A}$ = average cross sectional area over stream reach,

A = local cross sectional area, and

Q = flow rate.

D^* and D_B^* represent different expressions of the dimensionless longitudinal dispersion coefficient for a channel of variable morphology.

5.4. RESULTS OF TEMPERATURE ROUTING TESTS

Five recorded temperature fronts were routed through the MERS channels to determine the longitudinal dispersion coefficient D_L. These five events were selected by three criteria: 1) the temperature drop or increase had to be strong enough to be accurately traced as it moved downstream, 2) external conditions such as stratification, ice cover, or algal mats on the water surface which would alter the computed dispersion coefficient had to be absent, and 3) large diurnal variations or other transient water temperatures except for the temperature front had to be absent. The data for θ, channel morphology,

and travel times are given in Appendix A. Temperature records from 5, 6, or 7 stations were available. Values of Θ computed from Eq. 5.4 were compared to measured Θ values (for $\Theta \geq 0.05$ only). Values of D_L were chosen successively until the error between computed and measured Θ's was minimized. Below this range estimates of $\Theta(x,t)$ were considered to be more characteristic of entrapment rather than longitudinal dispersion.

A dispersion coefficient, representative of the entire channel, was calculated for each experiment using the temperature front data from all stations and the corresponding equation 5-4.

Each set of data was reduced for four D_L formulations: (1) D_L = constant, (2) $D_L = D^* Q/B$, (3) $D_L = D^*_B QA/(\overline{A}\ \overline{B})$, and (4) $D_L = D^*Q/\overline{B}$. Results are given in Table 5-1.

The D_L formulation which is most applicable may be selected by computing and comparing ratios of the standard deviation of the fitted coefficients to the mean of the five tests. These ratios represent the relative spread in fitted coefficients. Numerical values are shown in Table 5-1, last line. The dimensionless coefficients D^* and D^*_B represent about equally well the longitudinal dispersion for variable geometry and both are better than the constant D_L. The choice between D^* and D^*_B remains purely arbitrary. The reason for both coefficients giving equally good results will be examined in the next section.

Finally, the small standard errors and the consistency of the results indicate that the temperature front approach to determining longitudinal dispersion coefficient is valid and practical.

5.5. EFFECTS OF VARIABLE CROSS SECTIONAL AREA ON LONGITUDINAL DISPERSION

The subdivision of a channel into a series of pools of long residence time connected by riffles of short residence time makes the longitudinal dispersion almost entirely dependent upon the mixing processes in each pool and the number of pools. The processes are complicated and include:

- jet-like mixing at the transition from riffle to pool
- flow through the pool guided by vegetation and wind
- stratification effects.

It was not part of this project to analyze the motions in a pool in detail.

TABLE 5-1. LONGITUDINAL DISPERSION IN MERS-CHANNELS FROM TEMPERATURE FRONT DATA

Date of Experiment	Flow (m^3/sec)	D_L (m^2/sec)		$D^* = \frac{D_L B}{Q}$		$D_B^* = \frac{D_L \bar{A}\bar{B}}{QA}$		$\frac{D_L \bar{B}}{Q}$
11-17-76	.0349	0.100	(.0142)*	9.3	(.0143)*	4.8	(.0136)*	7.55
11-18-76	.0382	0.095	(.0084)	8.0	(.0082)	4.4	(.0095)	6.56
11-22-76	.0373	0.100	(.0152)	8.7	(.0153)	4.9	(.0153)	7.07
12-06-76	.0394	0.124	(.0172)	10.3	(.0168)	5.6	(.0182)	8.30
12-14-76	.0428	0.128	(.0106)	9.6	(.0108)	5.3	(.0103)	7.88
Mean		0.109	(.0131)	9.2	(.0131)	5.0	(.0134)	7.47
S.D.		0.015		0.88		0.46		0.68
$\frac{S.D.}{Mean}$		0.140		0.095		0.093		0.091

*Standard error.

TABLE 5-2. AVERAGE POOL AND RIFFLE D_L FROM TEMPERATURE FRONT ROUTING TESTS

Date of Experiment	$D_L(1)$=Const	$D_L(2) = D^* Q/B$		$D_L(3) = D_B^* QA/(\bar{A}\bar{B})$	
		$\bar{D}_L$(pools)	$\bar{D}_L$(riffles)	$\bar{D}_L$(pools)	$\bar{D}_L$(riffles)
	m^2/sec	m^2/sec	m^2/sec	m^2/sec	m^2/sec
11-17-76	0.100	0.099	0.174	0.102	0.026
11-18-76	0.095	0.093	0.164	0.102	0.026
11-22-76	0.100	0.100	0.176	0.114	0.029
12-06-76	0.124	0.124	0.219	0.135	0.034
12-14-76	0.128	0.124	0.217	0.139	0.035
Mean	.109	.100	.190	.118	.030

The measured longitudinal dispersion coefficients D^* (Table 5.1) are of the same order as those reported by Fischer (1973) for laboratory channels. This suggests that the combined effects of pool mixing and pool number were comparable to the effects of advective motion and transverse mixing in a straight channel.

That the pools dominate the effective longitudinal dispersion can be seen from an expression for the flux T of material in an open channel.

$$T = QC - AD_L \frac{\partial C}{\partial x} \qquad (5\text{-}9)$$

The advective flux QC in riffles and pools are comparable since Q and C are the same. The dispersive flux is, however, a function of cross sectional area A and D_L. The cross sectional areas of the pools are three to four times those of the riffles (Table 4.2). The dispersive transport in the pools is therefore dominant over the dispersive transport in the riffles. It is for this reason that in Table 5.2 for all five experiments, the dispersion coefficients in the pools are comparable, whereas the riffle values are not. (The values in Table 5.2 are computed from D^* and D^*_B values in Table 5.1 using riffle or pool values of B and A.)

5.6. COMPARISON WITH OTHER LONGITUDINAL DISPERSION MEASUREMENTS

If the mean flow velocity $U = Q/A$ in D^* is replaced by the shear velocity u_*, a comparison of these results with the dimensionless longitudinal dispersion coefficients, $D_L/(u_*\bar{h})$, cited by Fischer (1973) is possible. Field measurements on the MERS experimental channels have indicated that $u^*/U=0.55$ for these channels. The high value of u_*/U is misleading, however, when compared to the longitudinal dispersion coefficient. In the MERS channels most of the water surface drop occurs in the riffle sections. In fact, water surface slope in the pools is so small that it cannot be measured.

As shown in the previous section, longitudinal dispersion occurs predominently in the pool sections. Thus the dimensionless coefficient, $D_L/u_*\bar{h}$, compares u_* representing surface slope in the riffle sections and D_L representing longitudinal dispersion in pool sections. One would expect this value to be smaller than for most natural channels. For the mean value of $D^* = 9.2$,

$$\frac{D_L}{u_* \bar{h}} = \frac{D^*}{u_*/U} = 16.7 \qquad (5\text{-}10)$$

This value can be compared with others cited by Fischer (1973). It is found that the value given here is in the range of rectangular laboratory channels with smooth sides, in which longitudinal dispersion is much less than that found in natural channels. This is noteworthy since the geometry of the MERS channels is very different from a laboratory flume.

5.7. EFFECT OF ROUGHNESS (MANNING'S 'n') ON LONGITUDINAL DISPERSION IN THE MERS CHANNELS

The mixing processes in the pools of the MERS channels are not very dependent on Mannings 'n' values. Vegetation may be a factor, but it is doubtful that the relationship for shear flow in channels have much significance. Changes in Mannings 'n' caused by seasonal variations in vegetation are therefore not expected to have much significance on the longitudinal dispersion coefficients.

The longitudinal dispersion coefficients reported in Table 5.1 are for late fall/early winter conditions when vegetation was still present, although not as extensive as in mid-summer. Mannings 'n' values in November/December, when the measurements were made, are probably close to a seasonal average.

SECTION 6

HEAT TRANSFER ACROSS THE WATER SURFACE IN THE MERS FIELD CHANNELS

6.1. BACKGROUND

Net heat transfer across an air-water interface is the sum of several components. The source term in Eq. 1-1 may be written as

$$S = H_s - H_\ell - H_e - H_c \qquad (6\text{-}1)$$

where S = net heat flux per unit surface area,

H_s = net shortwave solar radiation entering the water surface ($E\ L^{-2}T^{-1}$),

H_ℓ = net long wave radiation leaving the water surface,

H_e = energy leaving the water surface due to evaporation, and

H_c = energy convection from the water to the air.

Many different empirical, semi-empirical, and deterministic relationships to determine the terms of Eq. 6-1 have been developed. Paily, Macagno, and Kennedy (1974a)provided a detailed summary. Only the equations to be used in this application will be given here. The parameters required to compute the net heat transfer are temperatures (water, air, and dew point), barometric pressure, solar radiation, cloud cover, and wind velocity. In this study the effect of wind direction on heat transfer in the MERS channels was also investigated.

A separate analysis of each term in Eq. 6-1 results in a net heat flux with nonlinear dependence on water temperature. In order to reduce complexity in analytical derivations and numerical computations, methods of computing heat flux as a linear function of water temperature have been proposed by Edinger, Duttweiller, and Geyer (1968), Brady, Graves and Geyer (1969), Dingman and Assur (1967), TVA (1968), Yotsukura, Jackman, and Faust (1973), Paily, Macagno, and Kennedy (1974b), Jobson and Yotsukura (1972) and others. The main drawback

to the linear models is that they are only valid over a limited water temperature range. Each of these methods may be expressed in a formulation first proposed by Edinger, Duttweiler, and Geyer (1968). Edinger, et al introduced a hypotehtical equilibrium temperature, T_E , and proposed that the net heat flux across an air-water interface may then be expressed as

$$S = -K_s (T_s - T_E) \qquad (6\text{-}2)$$

where T_s is water surface temperature and K_s is a bulk heat transfer coefficient at the water surface. Equation 6-2 indicates that net heat transfer will be small if (a) water surface temperature is close to equilibrium temperature and/or (b) K_s is small (calm wind, high relative humidity, etc.). T_E and K_s are indicative of water temperature response to weather conditions.

The MERS experimental channels are typical of many small streams and canals in that large diurnal variations in temperature occur. These diurnal variations are of interest for three reasons.

(a) The diurnal temperature maxima and minima affect the channel ecosystem studied by other investigators.

(b) Currently available water temperature prediction models use coefficients and time scales appropriate for deeper waters (typically one day). Water temperature analysis at much shorter time scales (3 hour) has not been much explored.

(c) Wind sheltering of the water surface in the MERS channels by the banks is a strong possibility and needs to be explored.

Thus, predicted temperature on less than daily time scales are required, and the heat transfer equations and time scale of data input are chosen accordingly.

6.2. NET SHORTWAVE (SOLAR) RADIATION

Essentially all shortwave radiation is from the sun to the water body (either direct or diffuse). In this study solar radiation is continually measured as a weather parameter and net shortwave radiation is expressed as the difference between (measured) incoming and (estimated) reflected radiation,

$$H_s = H_{si} - H_{sr} \tag{6-3a}$$

or

$$H_s = H_{si}(1-r) \tag{6-3b}$$

where H_{si} = incoming solar radiation ($EL^{-2}\ T^{-1}$),

H_{sr} = reflected solar radiation, and

r = total reflectivity of the water surface.

Anderson (1954) proposed an often used equation for total reflectivity of a water surface,

$$r = A\ \alpha^{B} \tag{6-4}$$

where α = solar angle in degrees, and

A and B = constants depending upon cloud cover.

If time increments of one day or greater are of interest, the relations of Koberg (1964) for H_{sr} are more appropriate. Brady, Graves, and Geyer (1969) calculated A and B as

$$A = 2.20 + \frac{C_r^{0.7}}{4.0} - (C_r^{0.7} - 0.4)^2/0.16 \tag{6-5}$$

and

$$B = -1.02 + \frac{C_r^{0.7}}{16.0} + (C_r^{0.7} - 0.4)^2/0.64 \tag{6-6}$$

where $C_r = 1 - H_{si}/H_{sm}$ = "Cloudiness ratio," and

H_{sm} = solar radiation which would occur with clear skies.

These are obviously empirical equations. The solar angle may be determined from the following equations as listed in Paily et al (1974a).

$$\sin\alpha = \sin\Phi\ \sin\delta\ + \cos\Phi\ \cos\delta\ \cos(h) \tag{6-7}$$

where ϕ = geographic latitude (radians)

δ = declination of the sun (radians)

$$= \frac{23.45\ \pi}{180}\ \cos\left[\frac{2\ \pi}{365}\ (172-D)\right] \tag{6-8}$$

D = day of the year (Jan. 1 = 1), and

h = hour angle of the sun (radians)

$\simeq \pi$ (day hour - 12)/12 (6-9)

For this particular application, however, the average value of sin α over a time increment is desired, rather than an instantaneous value. Thus, the solar angle which will be used is

$$\alpha(\text{rad}) = \sin^{-1} (\overline{\sin \alpha}) \tag{6-10a}$$

where

$$\sin \alpha = \frac{1}{h_2 - h_1} \int_{h_1}^{h_2} \sin \alpha \, dh$$

$$= \sin \Phi \sin \delta + \cos \Phi \cos \delta \frac{(\sin h_2 - \sin h_1)}{h_2 - h_1} \tag{6-10b}$$

The value of H_{sm} may be estimated from the equations which are listed in Paily et al (1974a).

$$H_{sm} = H_{so}(1-C_s) \left[a'' + 0.5(1-a')\right] \tag{6-11}$$

where C_s = a constant equal to the approximate value of some less significant parameters (such as dust depletion) which are difficult to determine,

$\simeq 0.01$,

H_{so} = solar radiation incident on the atmosphere,

$= I_o \sin \alpha / R^2$,

I_o = solar constant = 2 cal/cm^2/min=2880 cal/cm^2/day, and

R = ratio of the actual to the mean distance from the sun to the earth.

$$R = 1 + 0.017 \cos\left[\frac{2\pi}{365} (18.6-D)\right] \tag{6-13}$$

a' and a" are coefficients.

$$a' = \exp\left\{ m \left[- (0.465+0.130w)\right] \left[0.179+0.421 \, e^{-0.721m}\right]\right\} \tag{6-14}$$

$$a'' = \exp\left\{ m \left[- (0.465+0.134w)\right] \left[0.129+0.171 \, e^{-0.88m}\right]\right\} \tag{6-15}$$

where m = optical air mass

$$= \frac{P_a/P_o}{\sin \alpha + 0.15(\alpha + 3.885)^{-1.253}} \quad (6\text{-}16)$$

α = solar angle in degrees ,

P_a/P_o = ratio of air pressure at location altitude to sea level air pressure,

$$= \left(\frac{288 - 0.0065\ Alt}{288} \right)^{5.256} \quad (6\text{-}17)$$

Alt = altitude in meters.

w = atmospheric moisture content (cm)

$$= 0.85 \exp 0.110 + 0.0614\ T_d \text{ , and} \quad (6\text{-}18)$$

T_d = dewpoint temperature (^{o}C).

Although Eq. 6-4 through 6-18 are a rather long list to compute a simple parameter, r, to input a typical value of reflectivity can create large errors when time increments of less than one day are used. For the MERS experimental channels, r values from .04 to .2 have been computed over a day, and when the importance of the H_s term is considered, these variations are too large to be approximated accurately by "typical" or "average" values.

6.3. NET LONGWAVE RADIATION

Net longwave radiation is expressed as

$$H_\ell = \sigma \varepsilon_w (T_s^4 - \varepsilon_a T_a^4) \quad (6\text{-}19)$$

where T_s = water surface temperature (^{o}K),

T_a = air temperature (^{o}K),

ε_w = long-wave emissivity of the water surface (assumed equal to water surface long-wave reflectivity),

$\simeq 0.970$

ε_a = emissivity of the atmosphere, and

σ = Stefan-Boltzman constant.

For atmospheric emissivity without cloud cover, ε_{ac} , the Idso and Jackson (1969) formula will give accurate results for air temperatures above and below freezing point.

$$\varepsilon_{ac} = 1 - 0.261 \exp\left[-0.74\times10^{-4}\ T_a(^{o}C)^2\right] \qquad (6\text{-}20)$$

The Bolz formula is then used to find ε_a.

$$\varepsilon_a = \varepsilon_{ac}\ (1+K\ C_c^{\,2}) \qquad (6\text{-}21)$$

where C_c = fraction cloud cover, and
K = a coefficient which depends upon cloud height.

The coefficient K varies between 0.04 and 0.25. A TVA (1968) study recommends an average value of $K = 0.17$.

6.4. NET EVAPORATIVE AND CONVECTIVE HEAT TRANSFER

Evaporative heat transfer from a water surface may be expressed by the relation,

$$H_e = \rho L(Wftn)_z\ (e_{sw} - e_{az}) \qquad (6\text{-}22)$$

where e_{az} = vapor pressure of the air at height z,

e_{sw} = saturated vapor pressure at water surface temperature,

$Wftn_z$ = a wind function using wind velocity at height z,

L = latent heat of vaporization for water (E/M), and

ρ = density of water (M/L^3).

Saturation vapor pressure at any air temperature $T(^{o}K)$ may be computed over water by the Magnus-Tetons formula, (see Murray, 1967).

$$e_s\ (mb) = 6.1078 \exp\left[\frac{17.26939\ (T - 273.16)}{T - 35.86}\right] \qquad (6\text{-}23)$$

Atmospheric vapor pressure is computed from relative humidity, RH

$$e_a = \frac{RH}{100}\ e_{sa} \qquad (6\text{-}24)$$

The latent heat of vaporization is

$$L = 597.31 - 0.5631\ T_s \tag{6-25}$$

with L in cal/g and T_s in ^{o}C.

The convective heat transfer from an air-water interface, when evaluated according to Bowen (1926) may be expressed as

$$H_c = 0.61\ \frac{P_a(mb)}{1000}\ \rho L\ Wftn_z\ (T_s - T_{az}) \tag{6-26}$$

where T_{az} is air temperature at a height z above the water surface, P_a is in mb and $Wftn_z$ is the same as that for evaporative heat transfer.

A number of empirical wind function formulas $(Wftn)_z$ have been developed for various conditions. A formula used by many investigators, e.g. Marciano and Harbeck (1954), for natural water bodies is

$$(Wftn)_z = a + b\ W_z \tag{6-27}$$

where W_z = wind velocity at elevation z above the water surface, and

a and b = empirical constants.

Brady, Graves, and Geyer (1969) used the formula,

$$(Wftn)_z = a + b\ W_z^2 \tag{6-28}$$

for heat loss from power plant cooling ponds. Shulyakovskyi (1969) incorporated a natural convection term in Eq. 6-27 to describe accentuated heat loss from thermally loaded water bodies.

$$(Wftn)_z = a + b\ W_z + C(\Delta\theta_v)^{1/3}\ , \tag{6-29}$$

where θ_v = virtual temperature or the temperature of dry air at the same density as under the given conditions, and

$\Delta\theta_v$ = the difference in a virtual temperature between air at the water surface and at 2 m height.

The difference in virtual temperature is, in effect, a theoretical temperature difference which represents differences in density. The relation for $\Delta\theta_v$ is

$$\Delta\theta_v = T_s(1 + 0.378\ e_s/p_a) - T_a(1 + 0.378\ e_a/p_a) \qquad (6\text{-}30)$$

Ryan and Harleman (1973) excluded the constant term in Eq. 6-29 because of the large number of studies at natural water temperatures which found a = 0. They fitted laboratory natural convection and cooling pond data to the formula

$$(Wftn)_z = b\ W_z + c(\Delta\theta_v)^{1/3} \qquad (6\text{-}31)$$

Constants for the above equations have been determined for large water bodies. For smaller water bodies like the MERS channels, the forced convection constants (a and b) need to be evaluated separately. In the next section the constants in Eq. 6-27, 6-28, 6-29, and 6-31 will be determined from water temperature and weather data at the MERS and compared to results for water bodies with large surface areas.

6.5. DETERMINATION OF WIND RELATED HEAT TRANSFER COEFFICIENT FROM MEASURED STEADY-STATE LONGITUDINAL TEMPERATURE PROFILES

General Procedure

With constant inflow rate and inflow temperature and quasi-steady weather conditions, the longitudinal temperature profile in the channels will approach steady state. Conversely, when water temperature records indicate steady-state and weather conditions are nearly constant, the longitudinal water temperature profile in the channels may be used to determine coefficients in the steady-state equation of the longitudinal water temperature profile. If longitudinal temperature gradients are not large, and if Eq. 6-2 is used for the source term, water temperature is predicted by the solution to Eq. 1-1 for zero dispersion.

$$\ln \frac{\theta}{\theta_o} = -\frac{mx}{U} \qquad (6\text{-}32)$$

where $\dfrac{\theta}{\theta_o} = \dfrac{T(x) - T_E}{T_o - T_E}$,

T_E = equilibrium temperature,

$T_o = T(x=0)$,

U = bulk channel flow velocity,

$m = K_s/\rho c_p h$,

K_s = bulk surface heat transfer coefficient,

h = channel depth, and

c_p = specific heat of water.

From a measured longitudinal temperature profile and a computed equilibrium temperature, the value of K_s may be determined by Eq. 6-32 as

$$K_s = -\rho \frac{c_p h U}{x} \ln \frac{\theta}{\theta_o} \tag{6-33}$$

or

$$K_s = -\rho \frac{c_p Q}{\bar{B} x} \ln \frac{\theta}{\theta_o} \tag{6-34}$$

where Q = channel flow rate, and

$\bar{B}$ = mean channel surface width.

Errors in Computed Heat Transfer Coefficients

For a large measured longitudinal temperature gradient the contribution of longitudinal dispersion, D_L , to water temperature gradients may be significant. For this case the following solution to Eq. 1-1 with $D_L > 0$ must be applied.

$$\ell n \frac{\theta}{\theta_o} = \left(\frac{U}{2D_L} - \sqrt{\left(\frac{U}{2D_L}\right)^2 - \frac{m}{D_L}} \right) x \tag{6-35}$$

The error $Y(\%)$ in determining K_s from Eq. 6-34 by assuming $D_L=0$ is

$$Y = -100 \frac{\ln \theta/\theta_o \ (D_L=0) - \ln \theta/\theta_o \ (D_L > 0)}{\ln \theta/\theta_o \ (D_L > 0)} \tag{6-36}$$

For the calculations it is convenient to rewrite Eq. 6-35 as,

$$\ln \frac{\theta}{\theta_o} \ (D_L > 0) = -\frac{x}{\bar{D}} \left[(1 + \bar{K} \bar{D})^{1/2} - 1 \right] \tag{6-37}$$

where $\bar{D} = 2 D_L/U$

$\bar{K} = 2 m/U$.

For a given per cent error Y, equations 6-34, 6-36, and 6-37 may be combined to give

$$\left(\frac{Y}{100}\right)^2 - \frac{Y}{100} - \frac{\bar{K}\,\bar{D}}{4} = 0 \qquad (6\text{-}38)$$

Eq. 6-38 may be solved for Y. Typical input parameters for $\bar{K}$ and $\bar{D}$ at the MERS channels are

$$0 < D_L < 1.0 \text{ m/sec}$$

$$9 \times 10^{-5} < m < 2 \times 10^{-4} \text{ sec}^{-1}$$

$$.05 < U < .2 \text{ m/sec}$$

It is found that Y does not exceed 2 per cent. Longitudinal dispersion therefore will not significantly affect the surface heat transfer coefficients computed from steady-state longitudinal water temperature profiles, while ignoring longitudinal dispersion.

Equation 6-34 also implies that the longitudinal temperature profile has achieved steady-state. True steady-state can be approached but is rarely, if ever, achieved precisely. Therefore an estimate of the unsteady character of the longitudinal temperature profile and its effect on computations of K_s is also needed. With $D_L = 0$, Eq. 1-1 may be written as,

$$\frac{\partial T}{\partial t} + \frac{Q}{Bh}\frac{\partial T}{\partial x} = -m(T-T_E) = -m\theta \qquad (6\text{-}39)$$

or

$$\frac{NS + SS}{\theta_o} = -m\frac{\theta}{\theta_o} \qquad (6\text{-}40)$$

where $NS = \partial T/\partial t$ is the unsteady contribution and

$SS = (Q/Bh)\,\partial T/\partial x$ is the steady-state contribution.

The per cent error Z in θ/θ_o created by assuming $NS = 0$ is

$$\frac{Z}{100} = \left(1 - \frac{SS}{SS+NS}\right) = \left(1 - \frac{1}{1+NS/SS}\right) \qquad (6\text{-}41)$$

If, for each assumed steady-state θ/θ_o, the location with the maximum $\partial T/\partial t$ is used to compute NS, and SS is taken as the average over channel length, Eq. 6-41 will give an estimate of the largest possible error in K_s computations.

Determination of Wind Function Coefficients

The bulk surface heat transfer coefficient K_s (cal cm^{-2} day^{-1} $^oC^{-1}$) is given by Edinger and Geyer (1965) as

$$K_s = 9.256 + \rho L(Wftn)(\beta + 0.61) \qquad (6\text{-}42)$$

where Wftn = wind function (cm mb^{-1} day^{-1}), L = latent heat of vaporization (cal/g), and β (mb/ ^oC) = mean slope of the saturated vapor pressure versus temperature curve between water surface and dew point temperatures. Brady, Graves, and Geyer (1969) suggested the formula

$$\beta = .4604 + .0197\,\bar{T} + .001585\,\bar{T}^2 \qquad (6\text{-}43)$$

where $\bar{T} = (T_s + T_d)/2$ (^oC)

T = water surface temperature (^oC), and

T_d = dew point temperature (^oC).

Equations 6-37 and 6-29 may be combined to give the wind function for a steady-state longitudinal temperature profile.

$$F_w = \rho L(Wftn) = \frac{\frac{\rho C_p Q}{Bx}\ln\left(\frac{\theta}{\theta_o}\right) - 9.256}{\beta + .61} \quad \left(\text{cal } cm^{-2}\ day^{-1}\ mb^{-1}\right) \qquad (6\text{-}44)$$

Equation 6-44 is not dependent upon channel depth, indicating pool stratification does not affect computations of F_w. This is so because stratification decreases not only the effective channel depth, but also residence time as long as the flow rate is constant.

Using Eqs. 6-34 and 6-44, K_s and F_w were computed for 47 cases of near steady-state longitudinal temperature profiles. The parameter NS/SS and the maximum per cent error in K_s due to unsteady water temperatures were also computed for each case. The data and computational results of all cases is given in Appendix B, Table B-1. A sample calculation is also given in Appendix B.

A least-squares fit to determine the coefficients in Eqs. 6-27, 6-28, 6-29, and 6-31 was undertaken with all 47 cases. In addition, the data were also fitted to the equation

$$F_{w_z} = \rho L(Wftn)_z = b\, W_z + 5.52(\Delta\theta_v)^{1/3} \qquad (6\text{-}45)$$

where $c = 5.52$ was found by Ryan and Harleman (1973). Equation 6-45 was included because natural convection should not depend strongly on water surface area, and Ryan and Harleman's (1973) results may be applicable to the MERS channels.

The following five equations result from a least squares fit on computed F_w values from the MERS field channels:

1. $F_w(\text{cal cm}^{-2}\ \text{day}^{-1}\ \text{mb}^{-1}) = a + b\, W_9(\text{m/sec})$ (6-46)

   with $a = 17.5$
   $b = 2.40$
   and a standard error = 3.79

2. $F_w = a + b\, W_9^2$ (6-47)

   with $a = 21.18$
   $b = .316$
   and a standard error = 3.74

3. $F_w = a + b\, W_9 + c(\Delta\theta_v)^{1/3}$ (6-48)

   with $a = 9.17$
   $b = 2.68$
   $c = 2.78$
   and a standard error = 3.72

4. $F_w = b\, W_9 + c(\Delta\theta_v)^{1/3}$ (6-49)

   with $b = 3.10$
   $c = 5.68$
   and a standard error = 3.81

5. $F_w = b\, W_9 + 5.52\ (\Delta\theta_v)^{1/3}$ (6-50)

with b = 3.21

and a standard error = 3.77

Equations 6-46 and 6-47 are compared to experimental (field) values of F_w in Figure 6-1. Three ranges of the parameter NS/SS are indicated by different symbols. The scatter in Fig. 6-1 is not uncommon, as indicated e.g. by similar plots by Brady, Graves, and Geyer (1969). Equations 6-48, 6-49, and 6-50 are compared to computed values of $F_w - 2.78(\Delta\theta_v)^{1/3}$, $F_w - 5.68(\Delta\theta_v)^{1/3}$, and $F_w - 5.52(\Delta\theta_v)^{1/3}$ in Figs. 6-2, 6-3, and 6-4, respectively. Comparison of the standard errors of Eqs. 6-46 through 6-50 and comparison of the individual curves with F_w data indicates that all five equations give a remarkably similar fit to the data. This indicates that for a given type of water body, in this case narrow open channels with constant thermal loading, any of the five equations may be applied as a wind function.

Paily, Macagno, and Kennedy (1974a)compiled a list of wind function formulas given by various authors for different water bodies. Some of the wind function formulas which compare with those used here are given in Table 6-1. Table 6-1 gives $(Wftn)_2 = F_{w_2}/(\rho L)$ as a function of wind velocity at 2 m above the water surface. Equations 6-46 through 6-50 were converted to the form of Table 4 and added on the bottom.

Wind velocities at 9 m above the water surface were related to wind velocities at 2 m, W_2, by the formula

$$W_2 = W_9(2/9)^{.3} \qquad (6\text{-}51)$$

as suggested by Paily, Macagno, and Kennedy (1974a)for wind over land. Because of the small size of the Monticello channels, the vertical wind velocity profile is essentially that over land. A comparison of the relationships found in the MERS-channels and from previous investigations as shown in Table 6-1 can now be made.

A number of the investigators (Kohler, Marciano and Harbeck, Harbeck, Hughes, Turner, and Ficke) listed in Table 6-1 used a wind function formula

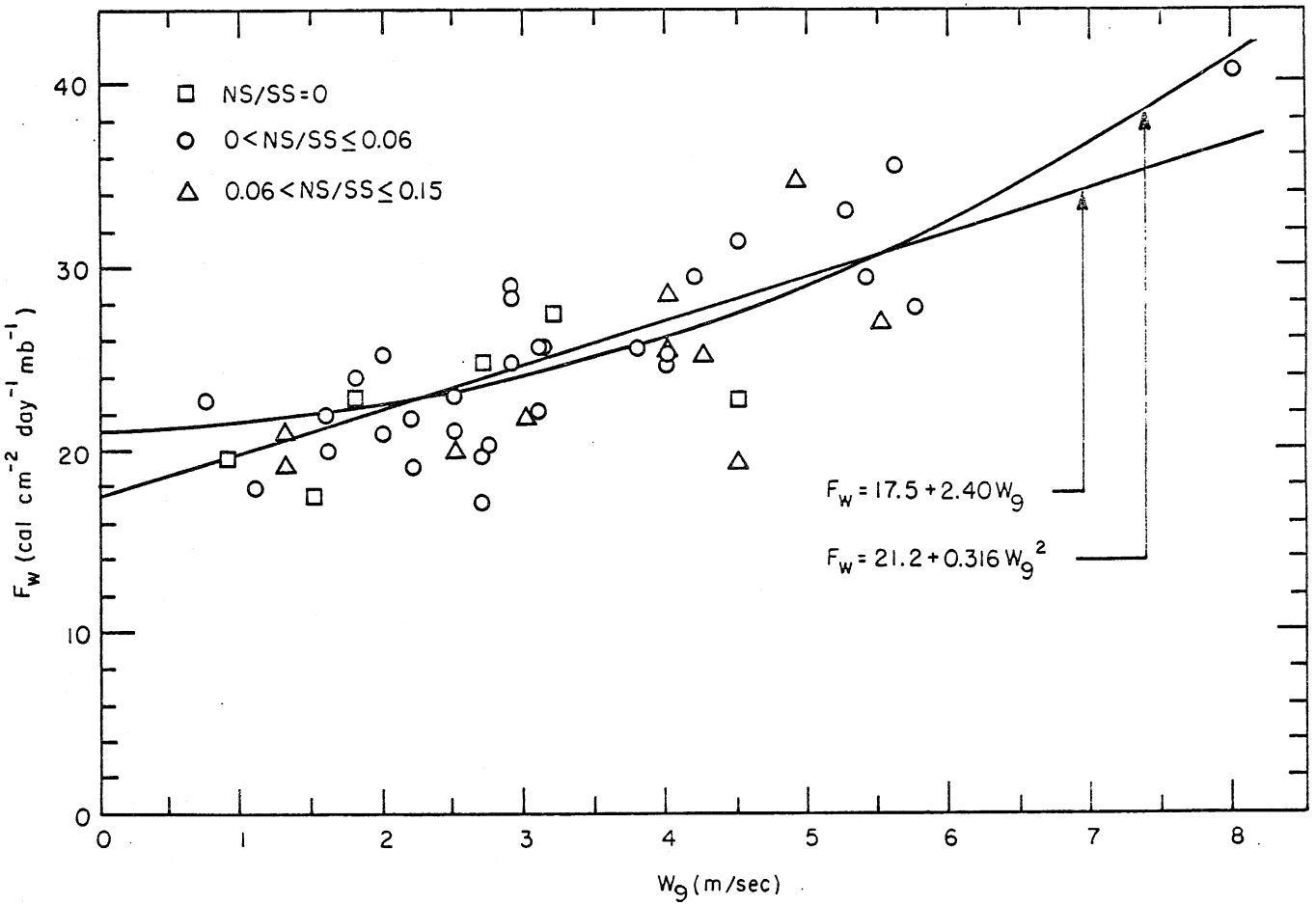

Fig. 6.1. Comparison of Eq. 6-46 and 6-47 with computed values of the wind function, F_w.

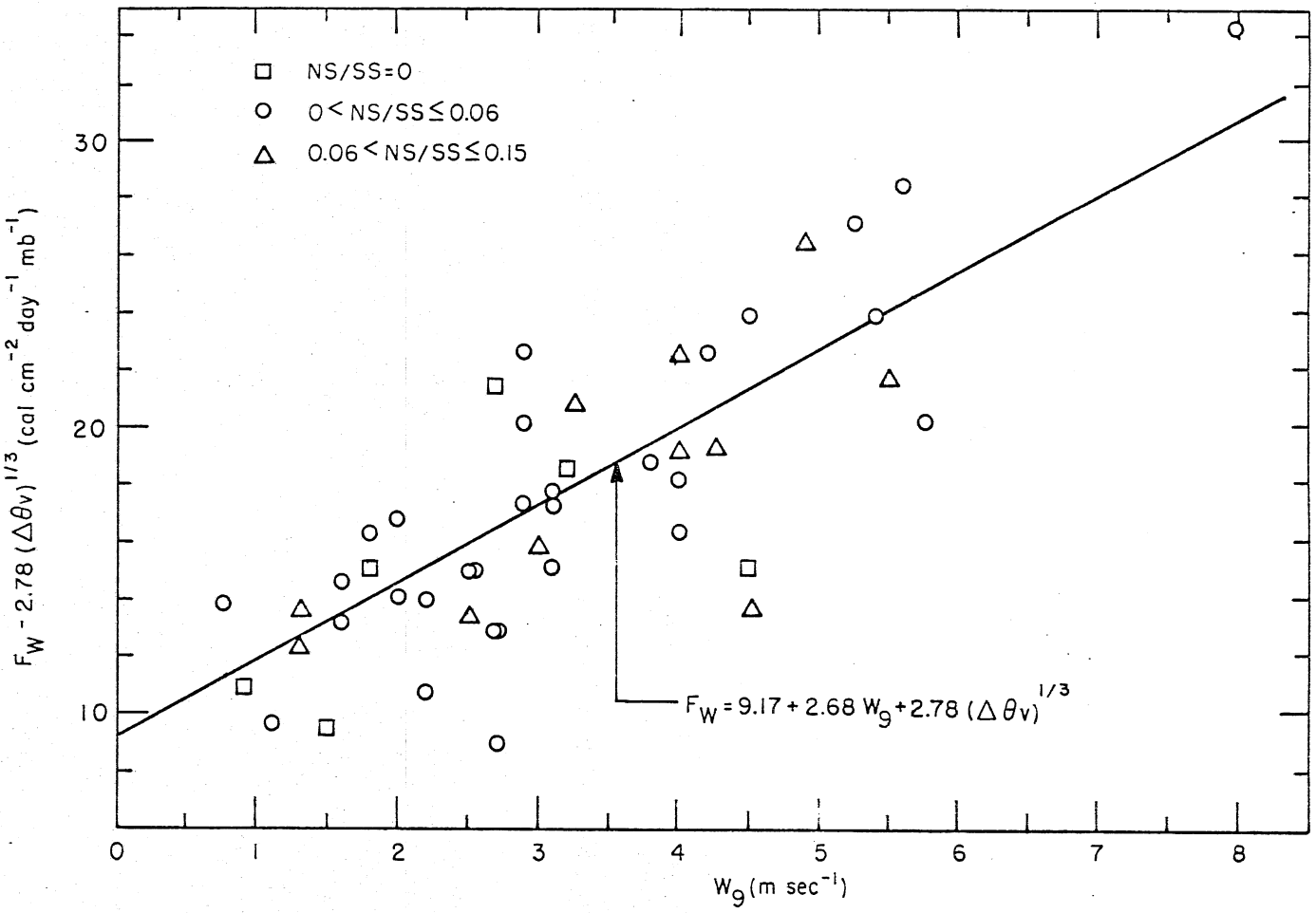

Fig. 6.2. Comparison of Eq. 6-48 with computed values of the wind function minus natural convection term.

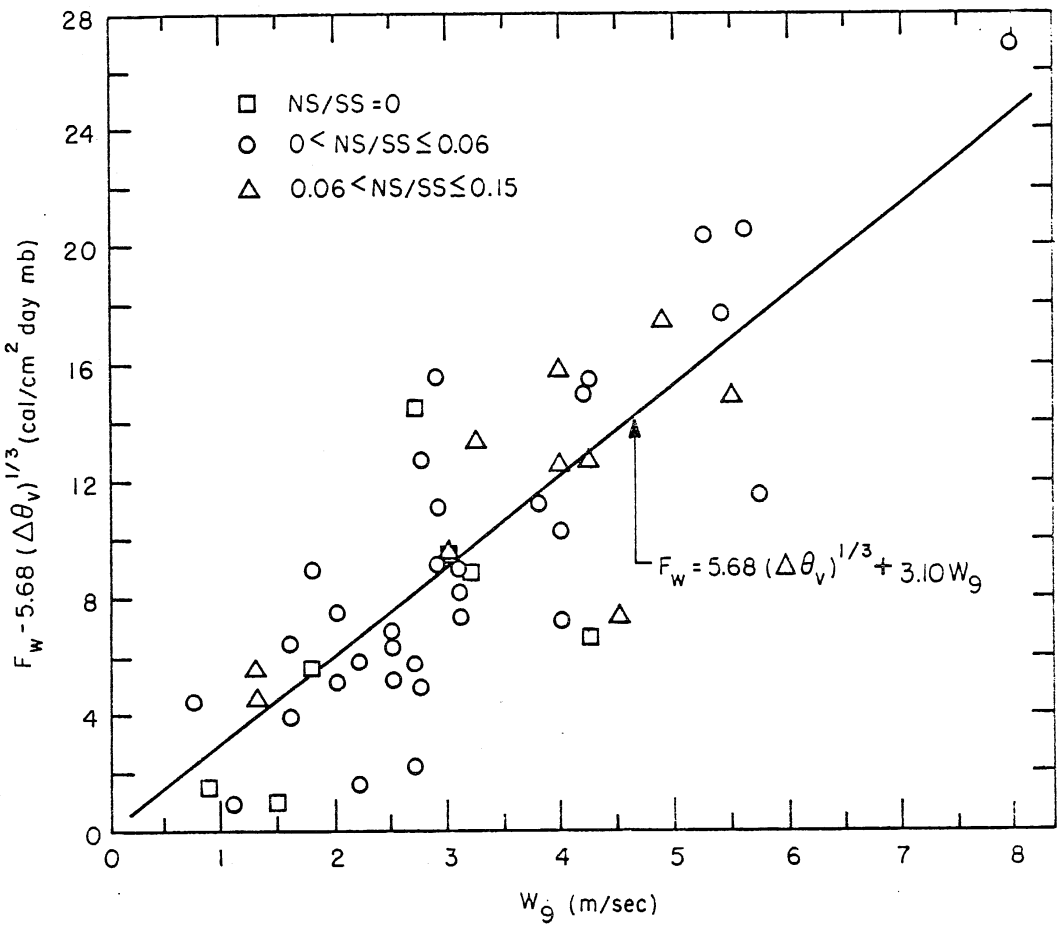

Fig. 6.3. Comparison of Eq. 6-49 with computed values of the wind function, F_w, minus natural convection term.

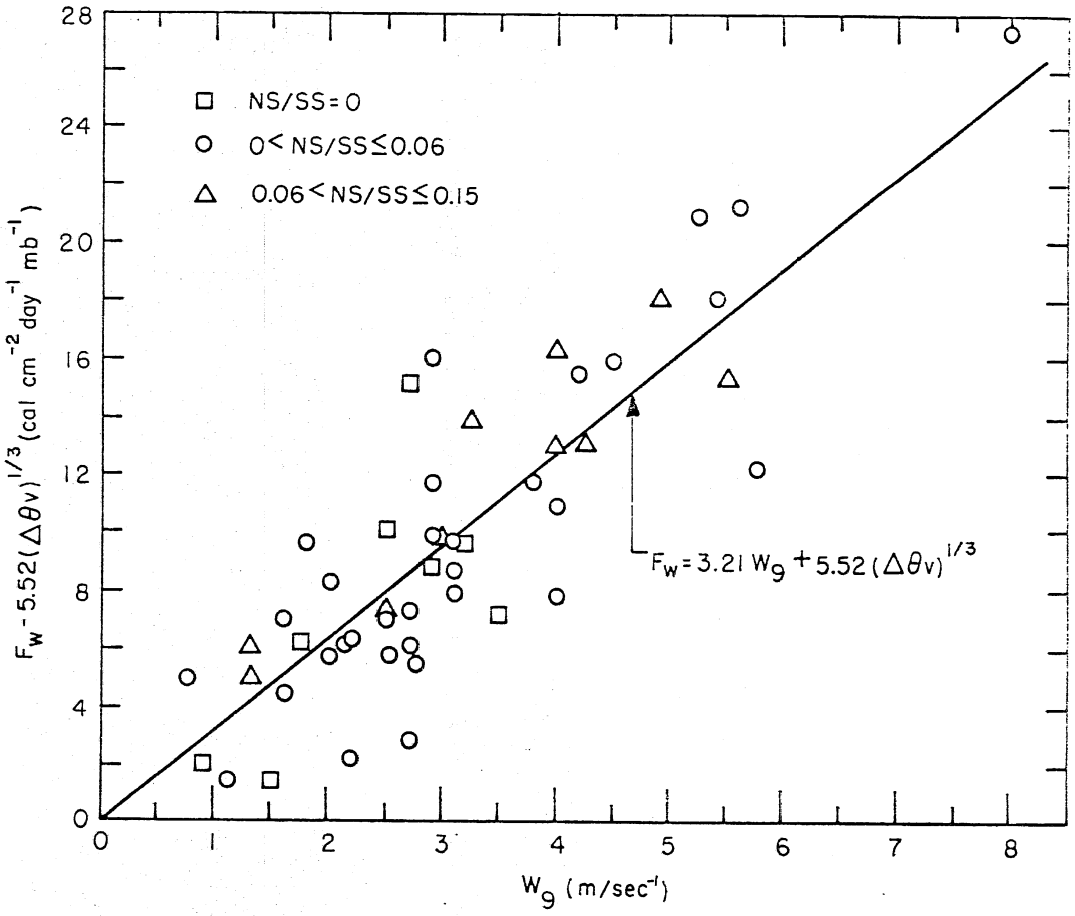

Fig. 6.4. Comparison of Eq. 6-50 with computed values of the wind function, F_w, minus natural convection term.

TABLE 6-1. WIND FUNCTION FORMULAS DETERMINED BY VARIOUS INVESTIGATORS*

Investigator	Wind Function Formula (Wftn) (cm/day-mb)	Water Body
Kohler (1954)	$0.005175+4.995\times10^{-4}\ W_2$	Lake Hefner, barge and midlake stations
Marciano and Harbeck (1954)	$0.01134\ W_2$	Lake Hefner
Harbeck (1958)	$0.01309\ W_2$	Lake Mead
Rymsha and Doschenko (1958)	$0.0209+9.107\times10^{-4}(T-Ta_2)+0.01018\ W_2$	Winter Time Rivers
Hughes (1964)	$0.008864\ W_2$	Salton Sea, California
Turner (1966)	$0.02045\ W_2$	Lake Michie, No. Carolina
Brady, Graves, and Geyer (1969)	$0.0239+0.00147\ W_2^2$	Power Plant Cooling Ponds
Shulyyakovskyi (1969)	$0.015+0.0094\ (\Delta\theta_v)^{1/3}+0.0112\ W_2$	
Ficke (1972)	$0.0125\ W_2$	Pretty Lakes, Indiana
Ryan and Harleman (1973)	$0.00934\ (\Delta\theta_v)^{1/3}+0.01107\ W_2$	Cooling Ponds and Laboratory Data
		MERS channels
Stefan, Gulliver Hahn & Fu	$0.0296+0.00637\ W_2$	6-46
	$0.0358+0.00132\ W_2^2$	6-47
	$0.0155+0.0047(\Delta\theta_v)^{1/3}+0.00711\ W_2$	6-48
	$0.0096\ (\Delta\theta_v)^{1/3}+0.00832\ W_2$	6-49
	$0.00934\ (\Delta\theta_v)^{1/3}+0.00852\ W_2$	6-50

*Listed by Paily, Macagno, and Kennedy (1974a).

like Eq. 6-46 for lakes with natural water surface temperatures. These investigators found a very small or zero constant term. The large constant term in Eq. 6-46 is believed to reflect natural convection due to the artificially elevated water surface temperatures in the Monticello Field channels studied herein.

Brady, Graves, and Geyer (1969) used a wind function similar to Eq. 6-47 for heat loss from power plant cooling ponds, given in Table 6-1. Their constant term is smaller than that of Eq. 6-47. The explanation for this is similar to that for the higher constant term in Eq. 6-46. The virtual temperature difference ($\Delta\theta_v$) in the cooling ponds studied by Brady et al varied from 5 to 12°C. The range of $\Delta\theta_v$ in the open channel studied here was 7 to 35°C, resulting in stronger natural convection effects.

Equation 6-48b has the same form as that used by Shulyakovskyi (1969). The constant terms in the two equations are strikingly similar. However, the natural convection term in Eq. 6-48 is approximately half that of Shulyakovskyi's. With three fitted constants, this equation should give the best fit, but the standard error is only slightly smaller than with two fitted constants.

The natural convection constant in Eq. 6-49 is very similar to that proposed by Ryan and Harleman (1973), which was found to be satisfactory in a number of evaporation experiments at the laboratory scale and the field scale. The Monticello data essentially confirm Ryan and Harleman's natural convection term. In fact, the results are so close that a least-squares fit using Ryan and Harleman's (1973) natural convection constant, Eq. 3-50, gave a smaller standard error than Eq. 6-49.

As expected, Eqs. 6-46 through 6-50 have smaller forced convection terms than the corresponding equations in Table 6-1. One possible cause is that the Monticello channels experience a land surface rather than a water surface wind boundary layer. More important yet is the observation that, except for a narrow range of wind directions, the relatively high channel sides at Monticello create a separated wind boundary layer over the channel water surface. The reduced wind velocities near the water surface in a separated boundary layer would cause less forced convection than in an unseparated boundary layer.

Since any of the equations 6-46 through 6-50 will give similar accuracy in determining a wind function for the channel studied, criteria for selection of a wind function equation will be based upon how well the equation describes physically real processes and whether the equation may be used for channels which do not have heat additions. Equation 6-49 fits both of these criteria. Equations 6-46, 6-47, and 6-48 are not as good as Eqs. 6-49 or 6-50 because they contain an unexplained constant rather than a natural convection term. In addition, for natural water surface temperatures where $\Delta\theta_v$ is small, Eq. 6-49 will reduce to a form similar to wind functions determined from lake evaporation in Table 6-1. Finally, the natural convection term determined by least-squares fit from the MERS field channel data is very close to the one derived from laboratory data by Ryan and Harleman (1973). This gives further credibility to the wind function in Eq. 6-49, which is selected as the most appropriate relationship.

SECTION 7

DYNAMIC WATER TEMPERATURE PREDICTION IN OPEN CHANNELS

7.1. GENERAL OBJECTIVE

To describe water temperature dynamics in an open channel under all types of weather conditions, a numerical solution of Eq. 1-1 is necessary. The most important terms to be described numerically are the source terms which incorporate heat transfer across the air-water interface and longitudinal dispersion. The source terms are highly non-linear and require an iterative scheme to accurately predict air-water heat transfer. Linearized source terms may be used to solve Eq.1-1 analytically for temperature distribution but the solutions with linearized equilibrium temperature relationships are limited to specific upstream water temperature and steady-state weather conditions. A one-dimensional unsteady finite difference model for stream temperature prediction titled MNSTREM for Minnesota Stream Water Temperature Prediction Model has been developed. MNSTREM will be described herein and applied to water temperature prediction in the MERS field channels. MNSTREM has unusually high time resolution, meaning that it can predict rapid water temperature changes in very shallow water.

7.2. FORMULATION OF ONE-DIMENSIONAL FINITE DIFFERENCE EQUATIONS FOR WATER TEMPERATURE PREDICTION

The finite difference equation for water temperature with convection, longitudinal dispersion, and air-water heat exchange will be formulated in a Crank-Nicholson implicit scheme. The basic transport equation is

$$A \frac{\partial T}{\partial t} + \frac{\partial (QT)}{\partial x} = \frac{\partial}{\partial x} \left(A D_L \frac{\partial T}{\partial x} \right) + \frac{BS}{\rho c_p} \qquad (7\text{-}1)$$

where T = temperature (^{o}C),

t = time (T),

x = distance (L),

A = cross-sectional area (L^2),

Q = flow rate (L^3/T),

D_L = longitudinal dispersion coefficient (L^2/T),

B = channel surface width (L),

ρ = density of water (M/L^3),

c_p = specific heat ($E\ M^{-1}\ {}^oC^{-1}$), and

S = net rate of heat transfer through air-water interface (E/L^2).

The equations will be formulated in the control volume, shown in Fig. 7.1, about the $i,j+\frac{1}{2}$ location. Then

$$A \frac{\partial T}{\partial t} = A_i \frac{(T_{i,j+1} - T_{i,j})}{\Delta t}$$

and

$$\frac{BS}{\rho c_p} = \frac{B_i\ S_{i,j+\frac{1}{2}}}{\rho c_p} = \frac{B_i (S_{i,j+1} + S_{i,j})}{2\ \rho c_p} ,$$

since Crank-Nicholson implicit differences are being used. Formulation of the x-differences depends upon the grid Peclet number.

$$Pe = \frac{Q\ \Delta x}{A\ D_L} \tag{7-2}$$

If Pe is large, an upstream difference scheme is appropriate (as in QUAL I), and if Pe is small a central difference scheme is appropriate. For many open channel conditions where D_L is significant, Pe is in an intermediate region. For the MERS experimental channels,

$Q \simeq .05\ m^3/sec$

$A \simeq 1.5\ m^3$

$D_L \simeq .1\ m^2/sec$

$\Delta X = 3 \rightarrow 8$ m, and

$Pe \simeq 1 \rightarrow 3$

which is in the range where neither the upstream nor central difference formulations are accurate (the greatest error occurs at Pe=2). The exact solution to the steady-state transport equation without a source term gives (Chien, 1977)

$$Q \frac{\partial T}{\partial x}\bigg|_i - \frac{\partial}{\partial x}\left(AD_L \frac{\partial T}{\partial x}\right)\bigg|_i = \frac{Q}{\Delta x}\left[T_i - T_{i-1} + \frac{T_i - T_{i+1}}{\exp(Pe_{i+1}) - 1} + \frac{T_i - T_{i-1}}{\exp(Pe_{i-1}) - 1}\right] \tag{7-3}$$

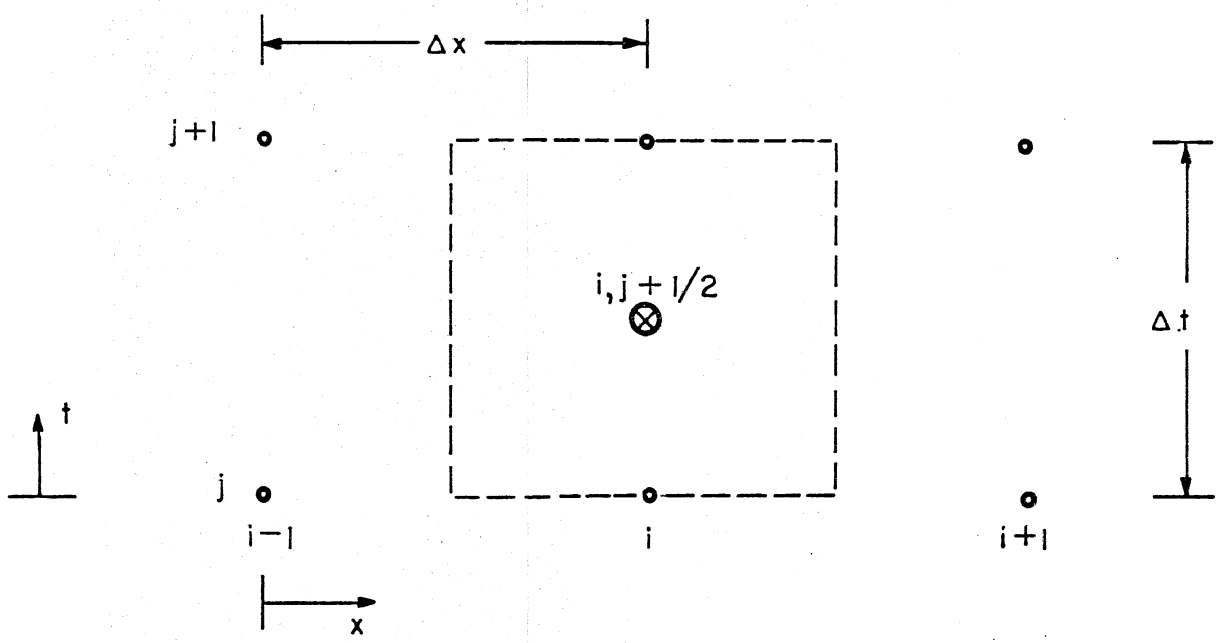

i= distance node

j= time node

x= distance

t= time

Δx= distance increment

Δt= time increment

Fig. 7.1. Control volume in time-distance coordinates for formulation of finite differences.

At large values of Pe, however, the exponential terms are expensive to compute. A power law approximation to Eq. 7-3 which has been developed by Patankar and Baliga (1978) is

$$Q \left.\frac{\partial T}{\partial x}\right|_i - \left.\frac{\partial}{\partial x}\left(AD_L \frac{\partial T}{\partial x}\right)\right|_i = \frac{Q}{\Delta x}\left\{T_i - T_{i-1} + (T_i - T_{i+1})\left[0, \frac{\left(1-0.1\left|Pe_{i+\frac{1}{2}}\right|\right)^5}{Pe_{i+\frac{1}{2}}}\right] + (T_i - T_{i-1})\left[0, \frac{\left(1-0.1\left|Pe_{i-\frac{1}{2}}\right|\right)^5}{Pe_{i-\frac{1}{2}}}\right]\right\} \quad (7\text{-}4)$$

In Eq. 7-4 the terms in brackets signify the largest of the individual terms. Because one temperature is assumed to be valid over a whole control volume, the Peclet numbers between matrix locations use the hormonic mean of D_L.

$$Pe_{i+\frac{1}{2}} = \frac{U\Delta x}{D_{Li+\frac{1}{2}}} \quad (7\text{-}5a)$$

$$D_{Li+\frac{1}{2}} = \frac{2\, D_{Li}\, D_{Li+1}}{D_{Li} + D_{Li+1}} \quad (7\text{-}5b)$$

Because the finite difference equation is to be Crank-Nickolson implicit (rather than fully implicit) the convective-dispersive term in Eq. 7-4 should be:

$$Q \left.\frac{\partial T}{\partial x}\right|_{i,j+\frac{1}{2}} - \left.\frac{\partial}{\partial x}\left(AD_L \frac{\partial T}{\partial x}\right)\right|_{i,j+\frac{1}{2}} = \frac{Q}{2}\left[\left.\frac{\partial T}{\partial x}\right|_{i,j+1} + \left.\frac{\partial T}{\partial x}\right|_{i,j}\right] - \frac{1}{2}\left[\left.\frac{\partial}{\partial x}\left(AD_L \frac{\partial T}{\partial x}\right)\right|_{i,j+1} + \left.\frac{\partial}{\partial x}\left(AD_L \frac{\partial T}{\partial x}\right)\right|_{i,j}\right] \quad (7\text{-}6)$$

Combining Eq. 7-1, 7-4, and 7-6 gives the finite difference equation:

$$a\, T_{i-1,j+1} - b\, T_{i,j+1} + c\, T_{i+1,j+1} + Z_{i,j} = 0 \quad (7\text{-}7)$$

where $$a = \frac{Q\,\Delta t}{2\, A_i\, \Delta x}\left\{1 + \left[0, \frac{\left(1-0.1\left|Pe_{i-\frac{1}{2}}\right|\right)^5}{Pe_{i-1}}\right]\right\}$$

$$c = \frac{Q\,\Delta t}{2\,A_i\,\Delta x}\left[0,\ \frac{\left(1-0.1\left|Pe_{i+\frac{1}{2}}\right|\right)^5}{Pe_{i+\frac{1}{2}}}\right]$$

$$b = 1 + a + c \text{ , and}$$

$$Z_{i,j} = (1-a-c)T_{i,j} + a\,T_{i-1,j} + c\,T_{i+1,j} + \frac{\Delta t\,B_i\,S_{i,j+\frac{1}{2}}}{\rho\,c_p\,A_i}$$

To solve for the longitudinal temperature profile at t=j+1, Eq. 7-7 is first rewritten as

$$T_{i,j+1} + W_i\,T_{i+1,\,j+1} = G_i \tag{7-8}$$

were at all locations except the boundaries.

$$W_i = -\frac{c}{b + a\,W_{i-1}} \tag{7-9}$$

and

$$G_i = \frac{a\,G_{i-1} + Z_{i,j}}{b + a\,W_{i-1}} \tag{7-10}$$

At i=1, $T_{1,\,j+1}$ is known and

$$W_2 = -c/b \quad \text{and} \quad G_2 = \frac{Z_a + a\,T_{1,j+1}}{b} \tag{7-11}$$

At the lower end of the channel reach to be studied (i=I), a constant gradient of temperature will be assumed, or

$$T_{I+1,\,j+1} = 2\,T_{I,j+1} - T_{I-1,\,j+1}$$

Then,

$$W_I = 0$$

$$G_I = \frac{(a-c)\,G_{I-1} + Z_I}{b-2c+(a-c)W_{I-1}}$$

and finally

$$T_{I,\,j+1} = G_I\ . \tag{7-12}$$

The longitudinal temperature profile is then found through back substitution from i=I-1 to i=2 through a rearranged form of Eq. 7-8.

$$T_{i,\ j+1} = G_i - W_i\ T_{i+1,\ j+1}$$

Eq. 7-8 through 7-12 comprise a tri-diagonal matrix algorithm (TDMA).

The implicit method of solution is always stable and convergent (Mickley et al, 1957). However, because a Crank-Nicholson implicit scheme, rather than fully implicit, is used oscillation matrices in the solution for temperatures can develop. A Crank-Nicholson scheme is used because it is more accurate when the transition to the final steady values of the dependent variable are of interest. For finite difference procedures which are both convergent and stable, a reduction of increment step size gives a good indication of result reliability (Mickley et al, 1957). To assure that no oscillation occurs in the matrix, and to test the significance of numerical damping, the numerical solution is computed with half the original time step. If no significant difference exists between the three runs, then no oscillation or numerical damping problems are assumed to exist.

The source term in Eq. 7-1 is nonlinearly dependent upon water temperature. Therefore, the term $S_{i,j+1}$ cannot be included in the TDMA scheme and is included through iteration. First, it is assumed that $S_{i,j+1} = S_{i,j}$. Then $S_{i,j+1}$ is computed from $T_{i,j+1}$ determined from the TDMA. Finally, $S_{i,j+1}$ is used to solve new $T_{i,j+1}$ values. These two steps are repeated until there is no significant change in the $T_{i,j+1}$ values. For open channels, such as the MERS field channels, where heat exchange is important this type of iteration can significantly reduce errors in the prediction of water temperature.

7.3. DESCRIPTION OF NUMERICAL FINITE DIFFERENCE COMPUTER PROGRAM FOR WATER TEMPERATURE PREDICTION

The water temperature prediction program MNSTREM begins with a channel reach of specified length, distance increment, time increment, and initial water temperature in each segment. The channel reach is divided into a number of segments. Each segment is assumed to have a constant surface width and cross sectional area and may consist of one or more distance increments.

MNSTREM reads cross sectional area and surface width for each segment as well as dimensionless longitudinal dispersion coefficient for the channel and latitude and longitude of the study site. Upstream water temperatures, flow rates, and the required weather parameters are read by MNSTREM to continuously compute water temperatures. Measured water temperatures may be input to MNSTREM for comparison with computed water temperatures. Individual residuals, the residual sum of squares, and the RMS residual are then computed. A more detailed description of all required input parameters is given in Appendix C (User's guide). A general flow chart for MNSTREM is given in Fig. 7.2. The program listing, given in Appendix D, provides a more detailed description of the required computations. A sample input is given in Appendix E. Appendix F gives a partial sample output which includes a comparison with measured water temperatures and computed residuals.

The most important input parameters for accurate water temperature prediction with MNSTREM are:

a. Flow rate and cross sectional areas since water temperature prediction is very sensitive to residence time,

b. Solar radiation, relative humidity, air temperature, and wind velocity measurements for accurate air-water heat transfer prediction, and

c. If temperature fronts or pulses are being routed D_L, Δt, and Δx must be chosen carefully to match real longitudinal dispersion with the combination of D_L and numerical dispersion in the model.

7.4. EXAMPLES OF WATER TEMPERATURE PREDICTIONS IN THE MERS FIELD CHANNELS

The wind function (Eq. 6-49 in Table 6-1) and the dimensionless longitudinal dispersion coefficient $D^* = D_L \bar{B}/Q = 7.47$ (Section 5.4) are used in MNSTREM to predict water temperatures in the MERS field channels. MNSTREM is applied to water temperature prediction over four different time periods and compared to recorded water temperatures.

a. January 31 through February 4, 1976, with weather data averaged over 1 hour time increments (Run A).

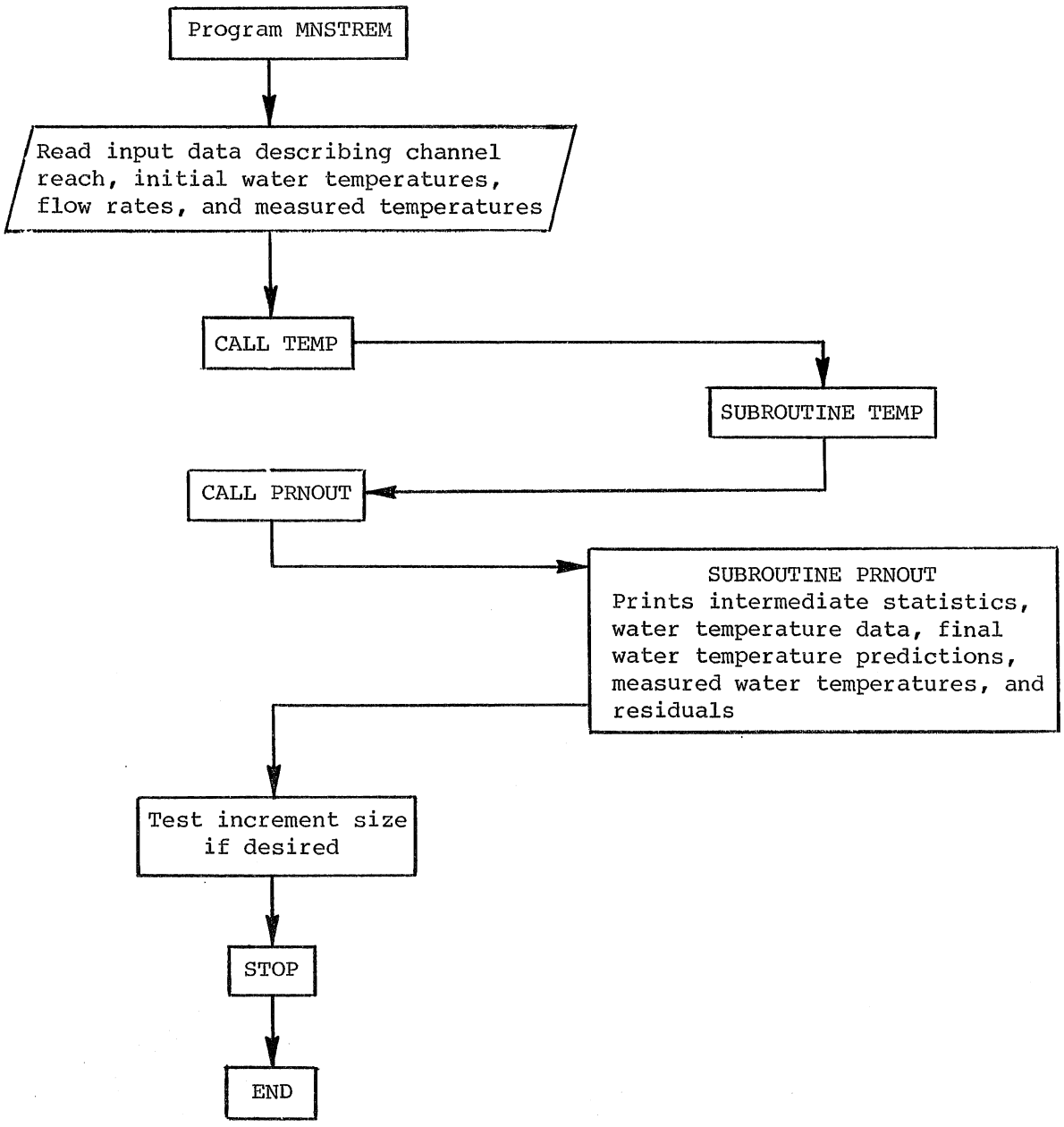

Fig. 7.2. General flow chart for MNSTREM, the Minnesota Stream Water Temperature Prediction Model. (Cont'd)

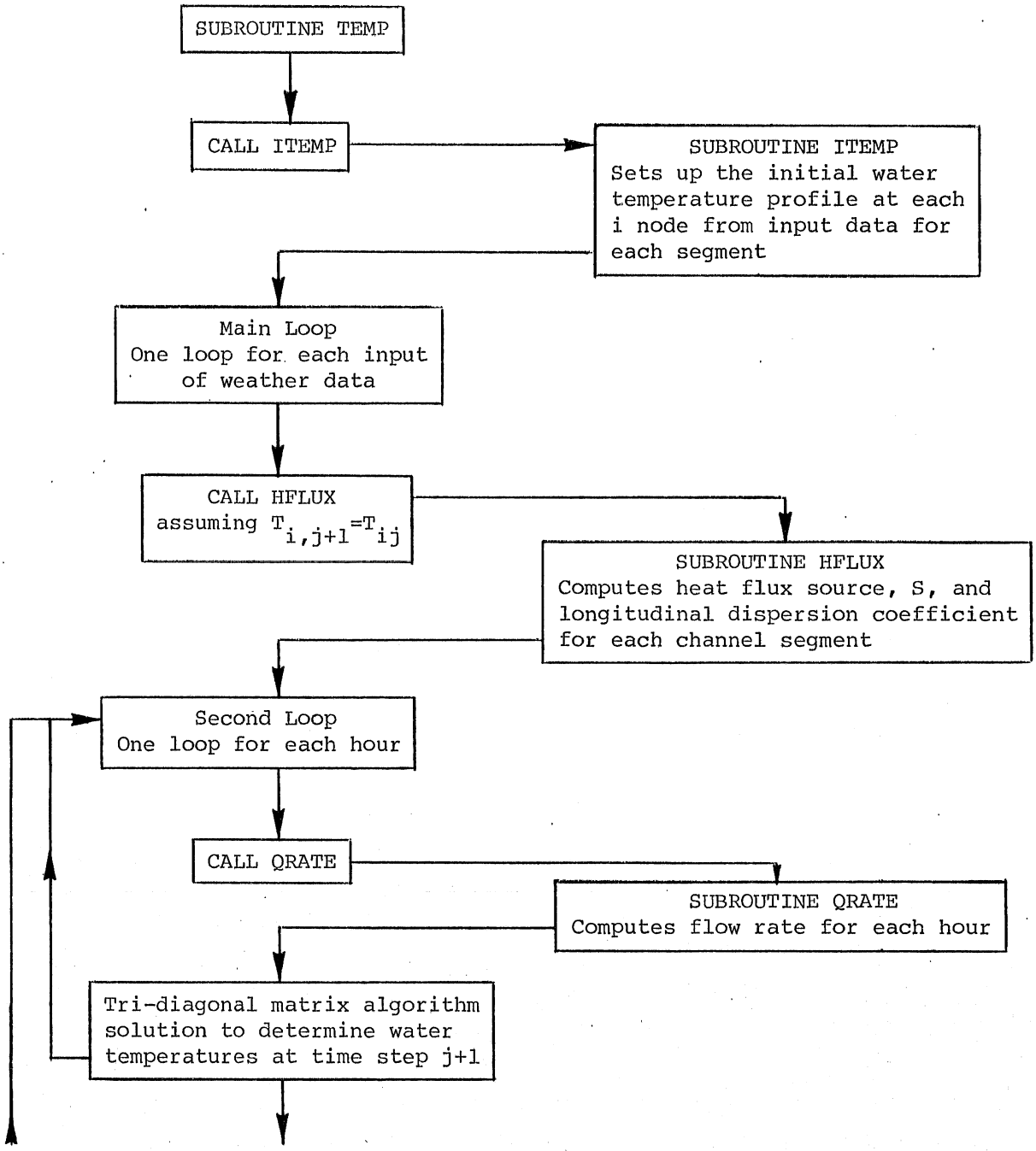

Fig. 7.2. General flow chart for MNSTREM, the Minnesota Stream Water Temperature Prediction Model. (Cont'd)

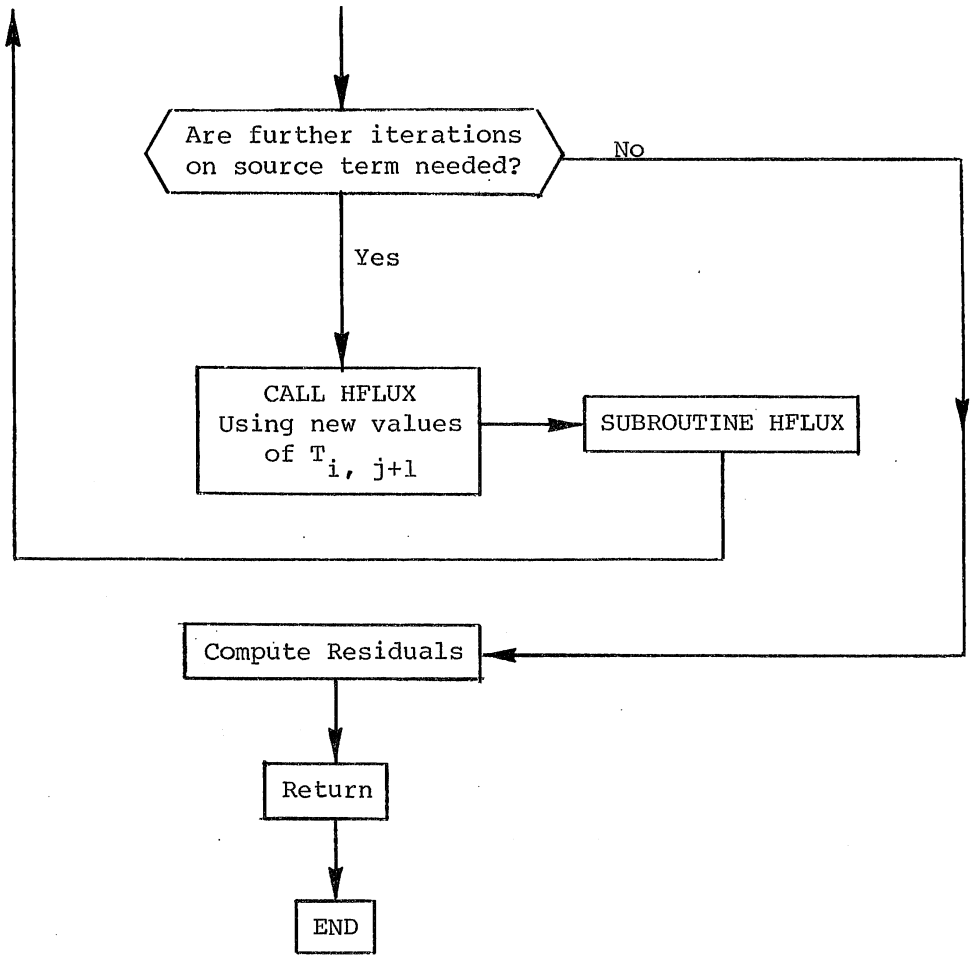

Fig. 7.2 (Cont'd). General flow chart for MNSTREM, the Minnesota Stream Water Temperature Prediction Model.

b. April 3 through April 12, 1976, with weather data averaged over 3 hour time increments (Run B).

c. June 20 through July 19, 1977, with weather data averaged over 3 hour time increments (Run C).

d. November 16 through December 6, 1976, with weather data averaged over 3 hour time increments (Run D).

Finally, the accuracy of using instantaneous rather than time-averaged readings of weather data is evaluated by comparison of water temperature predictions with the two types of data input to the model. In addition, the predictive capabilities of time-averaged weather data over various averaging time periods is analyzed.

In order to predict water temperatures the input data listed in Section 7.3 and Appendix C must be obtained. The water data acquisition system has been described in Section 4.4. The MERS weather station is described in Appendix G. Hourly inflow water temperatures and channel water temperatures were read on water temperature strip charts and adjusted according to calibration measurements as described in Section 4.4. A weather station to measure and record weather parameters was installed near the center of the MERS. Solar radiation was measured with a 50 junction Epply pyranometer at 2 m height. Wind velocity was measured at 9 m height with a Science Associate's anemometer. YSI 80 recorders were calibrated and used for recording both wind velocity and solar radiation. Air temperature and relative humidity were recorded on a Belfort spring wound hygrothermograph, with a bimetal temperature sensor and hair hygrothermograph. The hygrothermograph was calibrated weekly. When instrumentation breakdown occurred, the required weather data were obtained from Northern States Power Company records at the nearby Monticello Power Plant. Fraction cloud cover was estimated from NOAA Minneapolis-St. Paul and St. Cloud local weather data and from the Epply solar radiation records. Finally, cross sectional area and surface width at each channel segment were determined from field measurements as in Section 4.1.

When a convective-diffusive equation such as Eq. 6-1 is modelled through finite differences, care must be taken to insure that the numerical dispersion caused by the finite size of the well-mixed control volumes is small when compared to the physical dispersion. Longitudinal dispersion is included

in Eq. 6-1 as a diffusive term. Banks (1974) studied a one-dimensional unsteady mixed cell model with a concentration front similar to the temperature fronts in Section 5. He found that at an infinite number of cells the model is equivalent to Eq. 6-1 without the source term where the term $Q\,\Delta x/(2A)$ replaced the longitudinal dispersion coefficient (D_L). If we define an approximate numerical longitudinal dispersion coefficient,

$$D_{num} = \frac{Q\,\Delta x}{2A} \tag{7-13}$$

then the grid Peclet number may be expressed as

$$Pe = 2\,D_{num}/D_L \tag{7-14}$$

Although D_{num} is only truly equivalent to a diffusion coefficient at an infinite number of cells, it gives a valid estimate of existing numerical diffusion with a finite number of cells. It is interesting to note that the greatest difference between central difference or upstream difference formulations as described in Section 7.2 occurred at $D_{num} = D_L$. For the hybrid formulation used here (Eq. 7-4) a small grid Peclet number must be used if longitudinal dispersion is important. The use of various distance increments indicated that in the four water temperature prediction, Runs A through D, longitudinal dispersion was crucial only to Run D, where two temperature fronts were routed through the channel.

Run A: 1800 h January 31 through 2200 h February 4, 1976, with weather data averaged over 1 hour time increments.

This four day period includes a temporary decrease in upstream water temperature and a severe cold front. Upstream water temperature was mostly maintained at 15°C through the heat exchangers. Because of the artificially high water temperature, air-water heat transfer was large. The mean channel flow velocity was constant at 0.016 m/sec. Air and dew point temperatures were obtained from records at the NSP Monticello weather station. Computed water temperatures were compared to observed hourly water temperatures at channel locations 3, 7, 9, 13, 15, and 17. The standard error was computed to be 0.22°C. When one considers that a decrease in water temperature of

7°C along the channel was common, this standard error can be considered very low. Predicted and observed water temperatures from channel locations 3, 9, and 17 are shown in Fig. 7.3.

Run B: 0000 h April 3 through 2400 h April 12, 1976, with weather data averaged over 3-hour time increments

For these ten days in early spring the relatively high solar radiation and low relative humidity are in contrast to Run A for the winter period. Air temperature was mild, between 20 and -3°C. The mean channel flow velocity during this period was approximately 0.013 m/sec. With the large solar radiation values, a small error in measured solar radiation or predicted water surface reflectivity can cause significant errors in computed water temperatures at 1200, 1500, and 1800 hr. This is shown to occur periodically in Fig. 7.4, where computed and observed water temperatures for channel locations 3, 12, and 17 are compared. While longwave, evaporative, and conductive heat transfer were all of similar values for the winter Run A, the larger air temperatures and lower relative humidity of Run B decreased the importance of conductive heat transfer and increased the importance of evaporative heat transfer. Residuals of predicted and observed water temperatures were taken every 3 hours at channel locations 3, 6, 12, and 17, and the standard error was determined to be 0.22°C. This standard error compares very well to the daily variation of 7-8°C at location 17.

Run C: 1500 h June 20 through 2100 h July 19, 1977. with weather data averaged over 3 hour increments

This run encompasses a full month in midsummer when solar radiation is of the greatest importance. Large variations in cloud cover, wind velocity, and solar radiation occurred over the month period. In declining importance, most of the air-water heat transfer was due to solar radiation, evaporation, and longwave radiation. Convective heat transfer provided a very small contribution. The mean channel flow velocity throughout the period for Run C (Period C) was approximately 0.020 m/sec. Computed and observed water temperatures for channel locations 3 and 17 are compared in Figs. 7.5a, 7.5b, and 7.5c. As with Run A and Run B, upstream water temperature was maintained 10-15°C above ambient so that the heat transfer is about what is expected from cooling ponds. The temperature regime which would occur under ambient

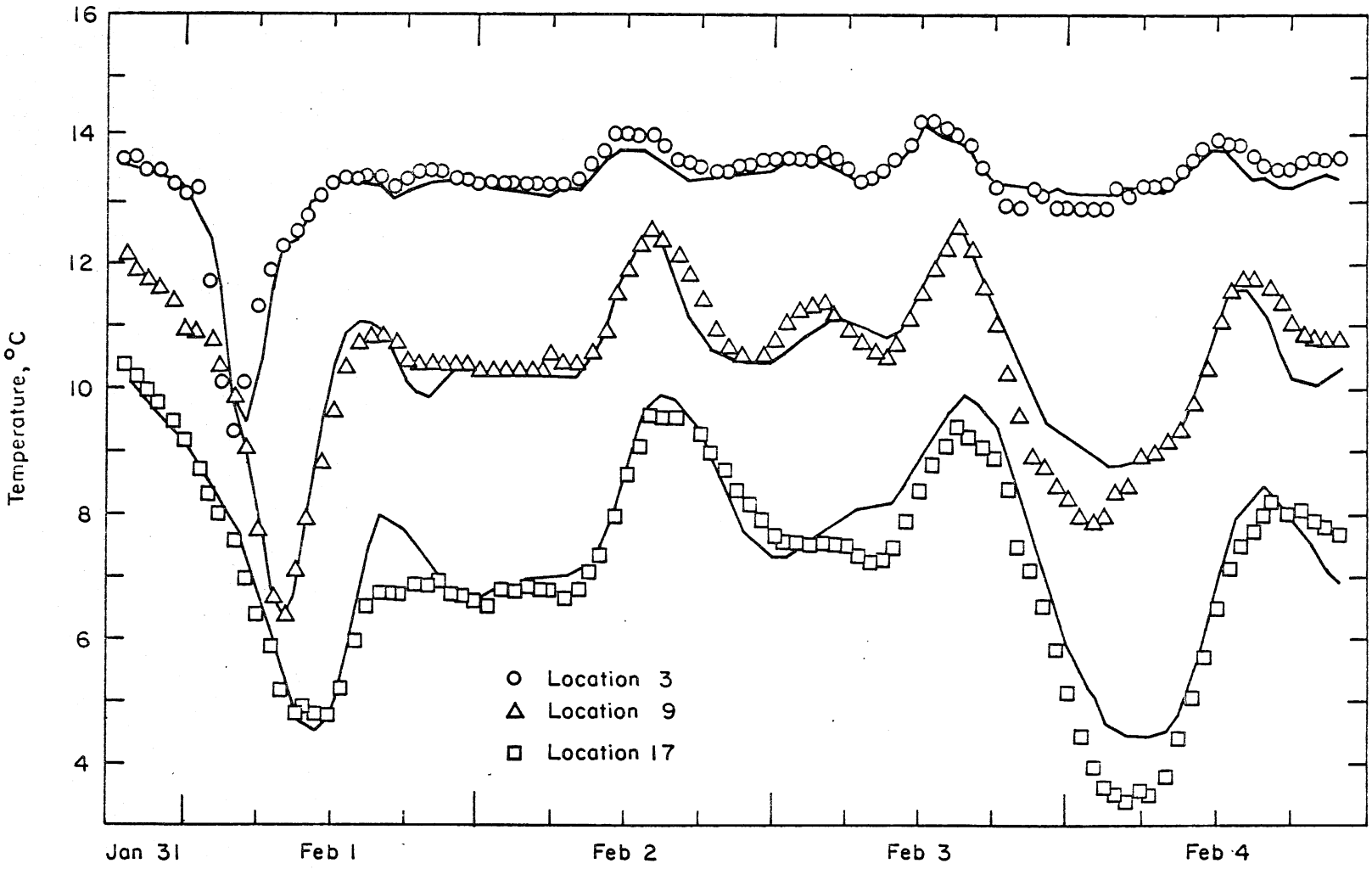

Fig. 7.3. Run A. Hourly water temperatures at three stations in channel 1 from January 31 through February 4, 1976. Station locations are identified in Fig. 4.13. Symbols are recorded values; solid lines are values simulated with MNSTREM.

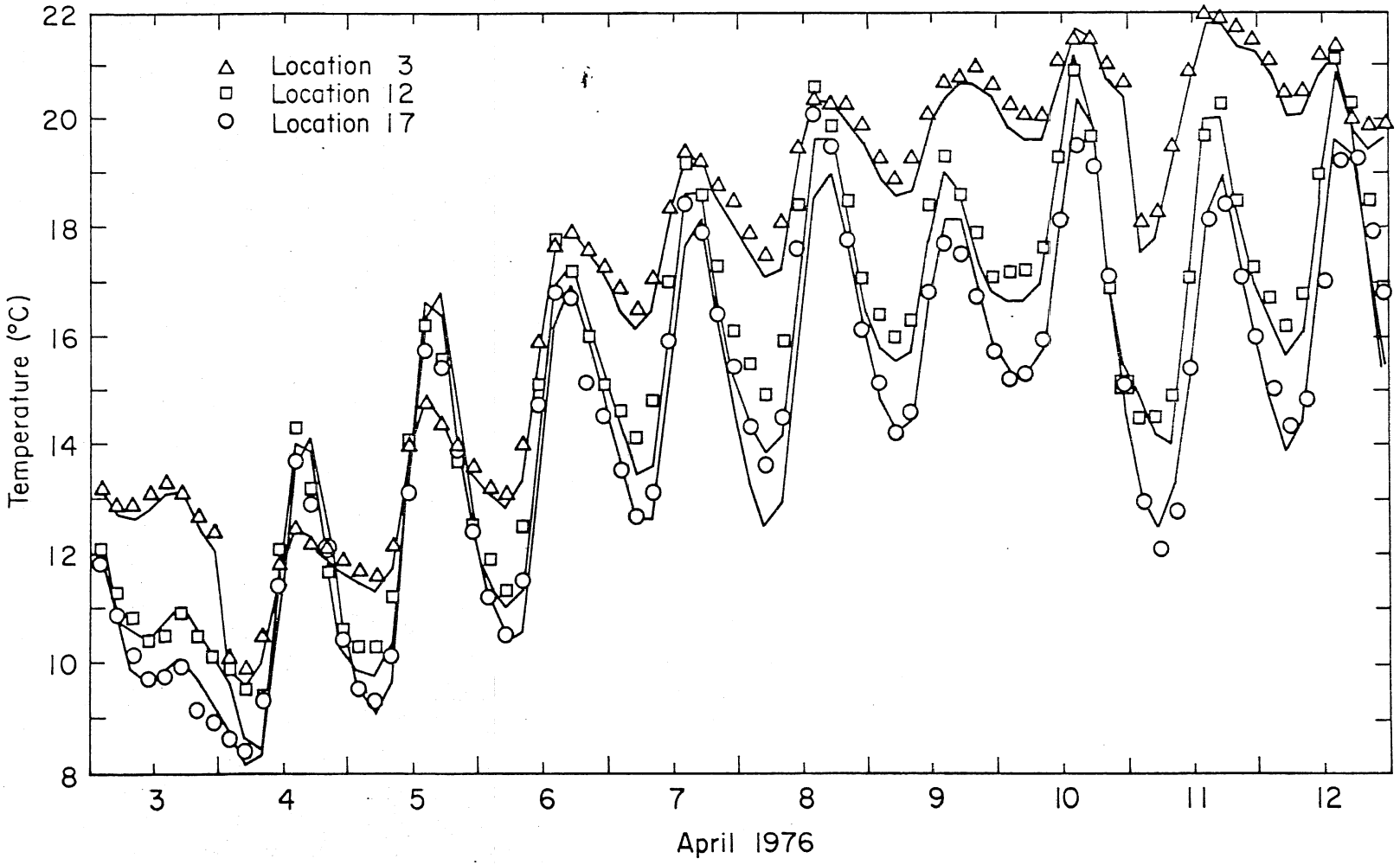

Fig. 7.4. Run B. Three-hour water temperatures at three stations in Channel 1. Station locations are identified in Fig. 4.13 (3 is upstream and 17 is downstream). Symbols are recorded values; solid lines are values simulated with MNSTREM.

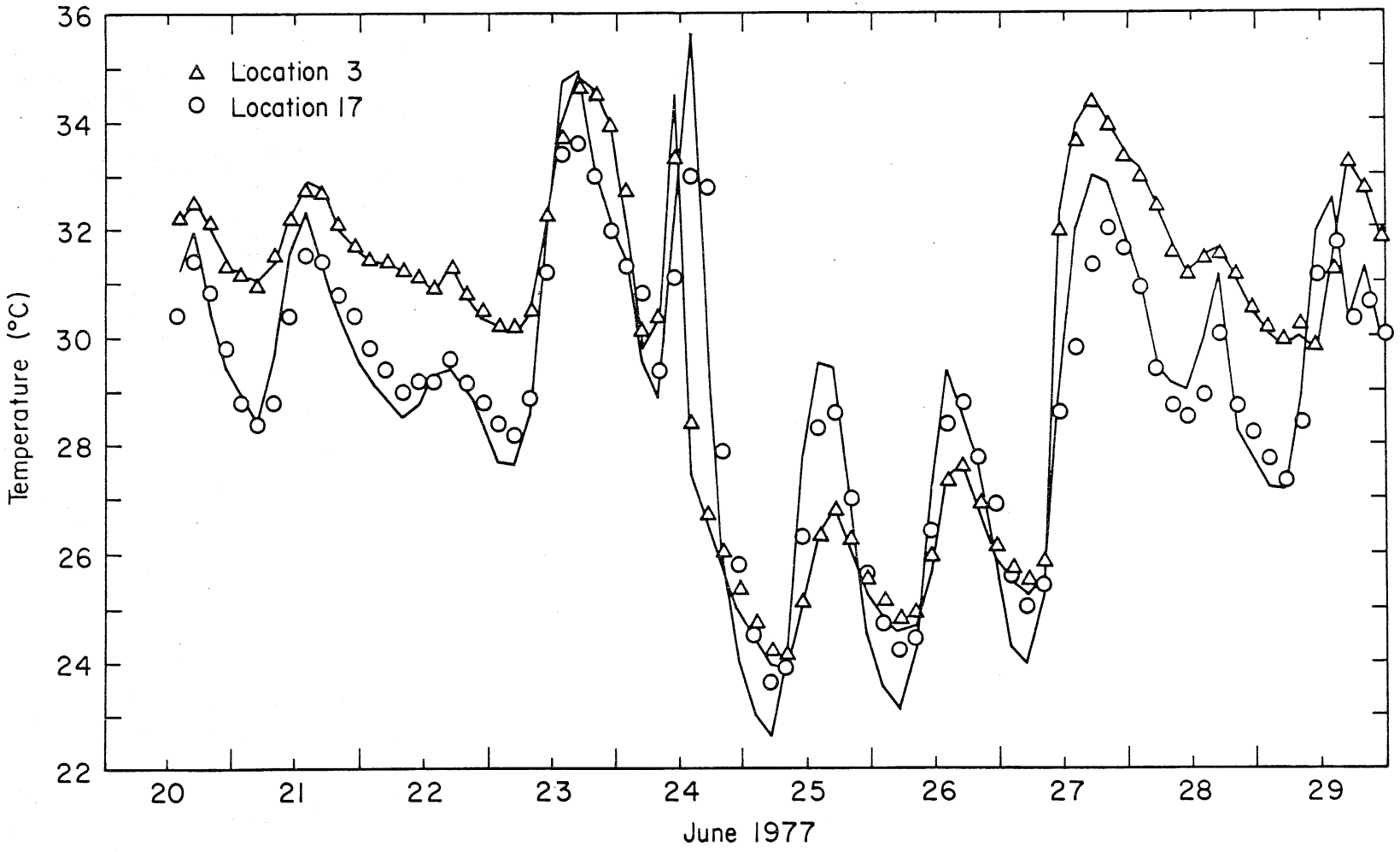

Fig. 7.5a. Run C. Three-hour water temperatures at Station 3 (upstream) and Station 17 (downstream) in Channel 8. Symbols are recorded values; solid lines are values simulated with MNSTREM.

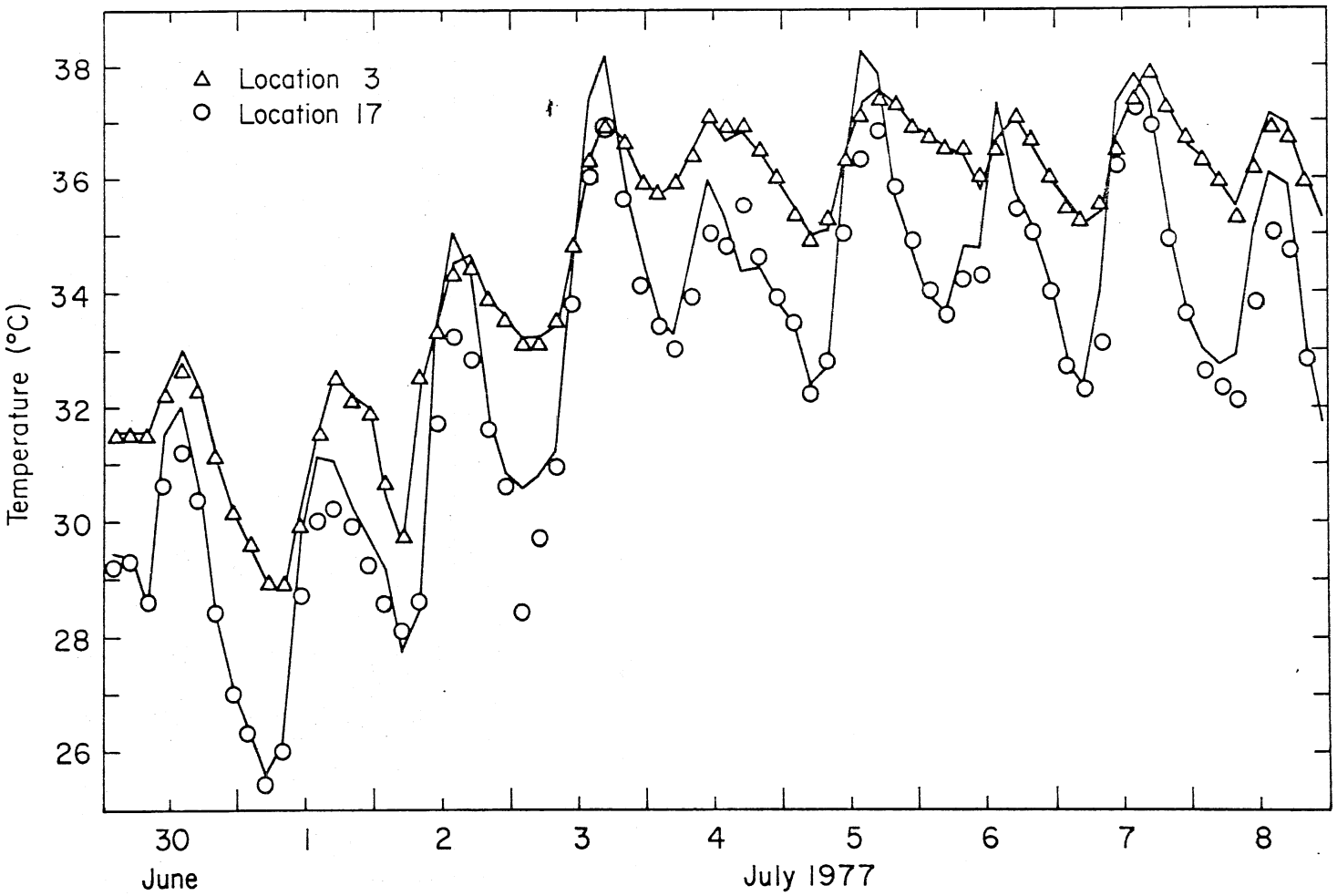

Fig. 7.5b. Run C. Three-hour water temperatures at Station 3 (upstream) and Station 17 (downstream) in Channel 8. Symbols are recorded values; solid lines are values simulated with MNSTREM.

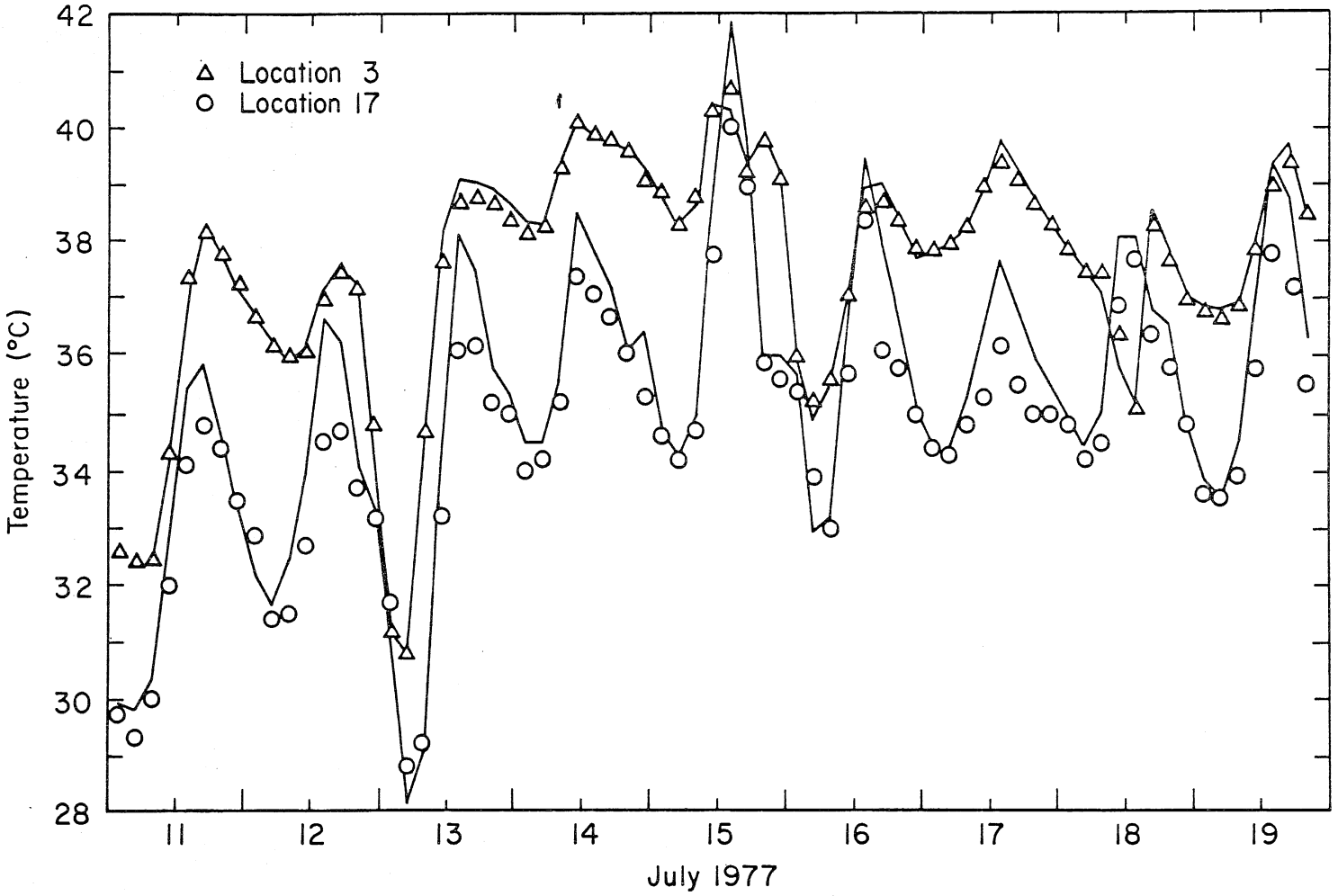

Fig. 7.5c. Run C. Three-hour water temperatures at Station 3 (upstream) and Station 17 (downstream) in Channel 8. Symbols are recorded values; solid lines are values simulated with MNSTREM.

conditions is shown during the period June 24 through June 26 when no additional heat was supplied to inflowing water upstream. Residuals of predicted and observed water temperatures were taken every 3 hours at channel locations 3, 9, and 17, and the standard error was determined to be 0.29°C.

Run D: 0000 h November 16 through 2400 h December 5, 1976, with weather data averaged over 3 hour increments

This late fall period includes four temperature fronts (2 increases and 2 decreases), a steady decrease in air temperature from approximately 5°C to -20°C, and consistently large wind velocities. Upstream water temperatures were maintained around 10°C above ambient. During the temperature front periods, the computational time increment was reduced from 3600 sec to 400 sec to prevent oscillations in the solution matrix. This is usually required when $\partial T/\partial x$ is very large, as in a temperature front or pulse. Grid Peclet number was approximately 1 in the pools, so $D_{num}/D_L \simeq 1/2$ during this run and D^* was adjusted accordingly. The mean channel flow velocity during this period was approximately 0.015 m/sec. As with Run A, air temperature and dew point temperature were obtained from weather station records for the NSP Monticello Power Plant. The predicted and observed water temperature, from channel locations 3 and 17 are compared in Fig. 7.6a and 7.6b. During much of the period predicted downstream temperatures are larger than observed. This could be because the wind direction was predominantly parallel to the downstream channel sections, and wind direction is not included in the wind function determined in section 6.5. In the later half of Period D, low air temperatures and a variable wind velocity created a highly dynamic temperature regime with large longitudinal gradients. As with Run A, evaporative, convective, longwave radiation and solar radiation heat transfer were all of equal importance. Residuals of predicted and observed water temperatures were taken every 3 hours at channel locations 3, 6, 12, and 17 and the standard error was determined to be 0.32°C.

The water temperature predictions were chosen to cover all four seasons of the year. Runs A, B, C, and D indicate that MNSTREM accurately predicted water temperatures which were both ambient and artificially heated for each season of the year. Upstream water temperature varied from 0° to 40°C and air temperature varied from -25°C to +35°C. With this wide range of conditions,

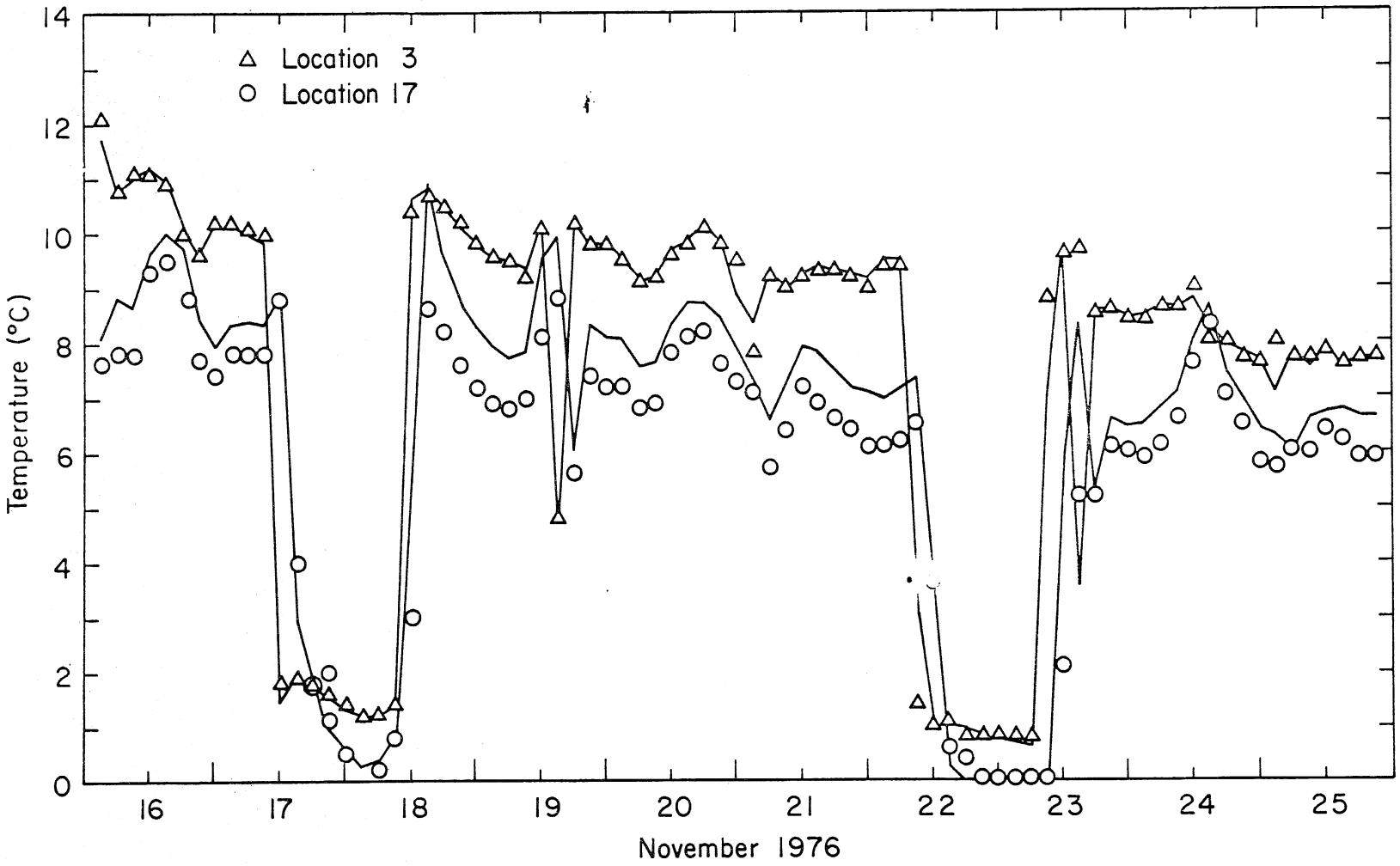

Fig. 7.6a. Run D. Three-hour water temperatures at Station 3 (upstream) and Station 17 (downstream) in Channel 1. Symbols are recorded values; solid lines are values simulated with MNSTREM.

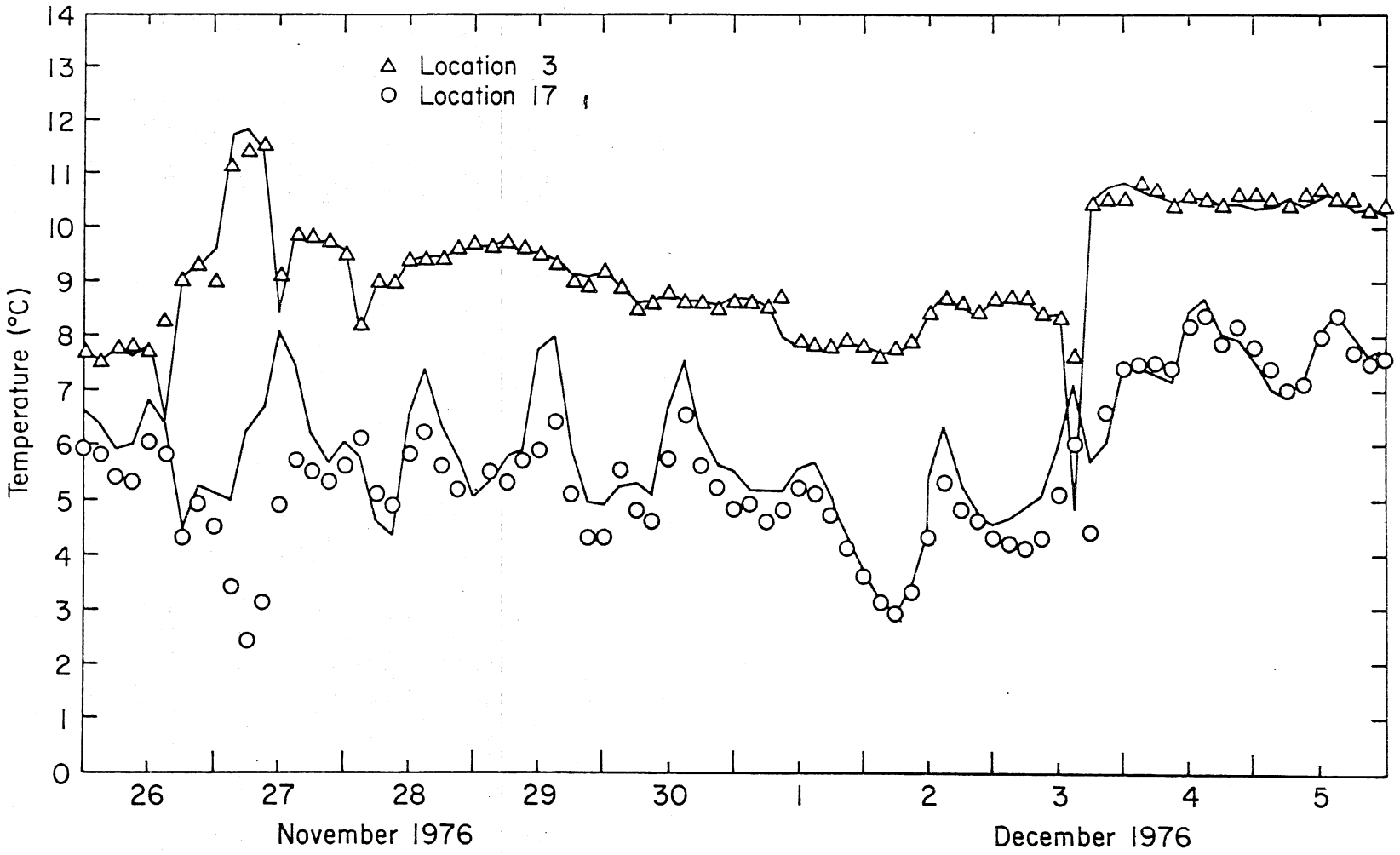

Fig. 7.6b. Run D. Three-hour water temperatures at Station 3 (upstream) and Station 17 (downstream) in Channel 1. Symbols are recorded values; solid lines are values simulated with MNSTREM.

the maximum standard error for any run was 0.316°C, which compares to a calibration error of 0.10 to 0.2°C for the thermistors which measured water temperature. The low standard errors are a good indication of MNSTREM's capability for predicting water temperature, especially when one considers that MNSTREM has no coefficients determined from the data of any of the predictive Runs A, B, C, or D.

When predicting water temperatures over a stream reach, an investigator must decide what time period is adequate for averaging measured weather parameters. Since hourly averages of weather data were used for Run A, this period was used to compare the accuracy of water temperature predictions with weather data averaged over 1, 3, 6, and 12 hour periods. The results, given in Table 7.1, indicate that for the period in Run A, averaging weather parameters over 1, 3, and 6 hour periods gave equally good predictions.

TABLE 7.1. STANDARD ERROR OF WATER TEMPERATURE PREDICTIONS WHEN WEATHER PARAMETERS ARE AVERAGED OVER 1, 3, 6, AND 12 HR PERIODS

Time Period for Averaging Weather Parameters	Standard Error of Prediction
(hr)	(°C)
1	0.222
3	0.243
6	0.239
12	0.407

It should be noted that Run A was for a winter period when daily variations of solar radiation are small. Other weather parameters such as wind velocity and air temperature, however, were highly variable in Run A.

Instantaneous values of weather data are more easily obtained than time averaged values. Much of the NOAA Local Climatological Data, for example, is given as instantaneous values every three hours. To test the accuracy of water temperature prediction with instantaneous rather than time-averaged readings of weather data, water temperatures were predicted with 3, 6, and 12 hour instantaneous weather data for Period A. In addition, the effect of

lead time in the input of the instantaneous data to the computer model was studied. The results are given in Table 7.2. For six-hour instantaneous weather data, a lead time of 1.5 hours means the weather data is applied 4.5 hours before the reading and 1.5 hours after the reading time. The results of Table 7.2 indicate that, for example

1) a three-hour instantaneous reading of weather data taken at 1200 would give the best prediction if applied from 1030 to 1330, based on the lowest standard error of prediction

2) a six-hour instantaneous reading at 1200 should be applied from 0830 to 1430, and

3) a 12-hour instantaneous reading at 0100 should be applied from 0230 to 1430.

The results given in Table 7.2 are only strictly applicable to the MERS channels for Period A. They give an indication of what can be expected in a shallow channel.

TABLE 7.2. STANDARD ERROR OF WATER TEMPERATURE PREDICTIONS WITH INSTANTANEOUS READINGS OF WEATHER DATA TAKEN AT 3, 6, AND 12 HOUR INCREMENTS*

Lead Time in Input of Weather Data	Data Readings every:	Standard Error		
		3 (hrs)	6 (hrs)	12 (hrs)
(hr)		(^{o}C)	(^{o}C)	(^{o}C)
0.5		0.265	0.379	0.678
1.5		0.248	0.271	0.474
2.5		0.278	0.261	0.297
3.5			0.308	0.344
4.5			0.420	0.534
5.5			0.364	0.402
6.5				0.539
7.5				0.649
8.5				0.661
9.5				0.705
10.5				0.793
11.5				0.845

*A lead time of 2.5 hours means the instantaneous data is applied for 2.5 hours after the reading time, and N-2.5 hours before the reading time, where N = 3, 6, or 12.

REFERENCES

Anderson, E. R. (1954) "Energy Budget Studies," Water-Loss Investigations, Lake Hefner Studies, U. S. Geological Survey Professional Paper No. 269.

Banks, R. B. (1974) "A Mixing Cell Model for Longitudinal Dispersion in Open Channels," Water Resources Research, Vol. 10,No. 2.

Bansal, M. K. (1971) "Dispersion in Natural Streams," Proc. ASCE, Vol. 97, No. HY11.

Barnes, Jr., H. H. (1967) "Roughness Characteristics of Natural Channels," U. S. Geological Survey Water Supply Paper No. 1849.

Bowen, I. S. (1926) "The Ratio of Heat Losses by Conduction and by Evaporation from any Water Surface," Physical Review, Vol. 27.

Brady, D. K., W. L. Graves, and J. C. Geyer (1969) "Surface Heat Exchange at Power Plant Cooling Lakes," The Johns Hopkins University, Dept. of Geography and Environmental Engineering, Report No. 49-5.

Chien, J. C. (1977) "A General Finite-Difference Formulation with Application to Navier-Stokes Equations," Computers and Fluids, Vol. 5(1):15.

Day, T. J. (1975) "Longitudinal Dispersion in Natural Channels," Water Resources Research, Vol. 11, No. 6, p. 909.

Dingman, S. L. and A. Assur (1967) "The Effect of Thermal Pollution on River-Ice Conditions--Part II, U. S. Army Cold Regions Research and Engineering Laboratory, Hanover, New Hampshire.

Ditmars, J. D. (1974) "Mixing and Transport"(literature review), Journal of the Water Pollution Control Federation, Vol. 46, No. 6, pp. 1591-1604.

Edinger, J. E. and J. C. Geyer (1965) Heat Exchange in the Environment, The Johns Hopkins University, R.P. 49-2.

Edinger, J. E., D. W. Duttweiler, and J. C. Geyer (1968) "The Response of Water Temperatures to Meteorological Conditions," Water Resources Research, Vol. 4, No. 5.

Elder, J. W. (1959) "The Dispersion of Marked Fluid in Turbulent Shear Flow," Journal of Fluid Mechanics, Vol. 5, pp. 554-560.

El-Hadi, N.D.A. and K. S. Davar (1976) "Longitudinal Dispersion for Flow Over Rough Beds," Journal of Hydraulic Div., ASCE, Vol. 102, HY4, pp. 483-498.

Ficke, J. F. (1972) "Comparison of Evaporation Computation Methods, Pretty Lakes, Lagrange City,Northwestern Indiana," U. S. Geological Survey Professional Paper No. 65.

Fischer, H. B. (1967) "The Mechanics of Dispersion in Natural Streams," Proc.. ASCE. Vol. 93, HY6.

Fischer, H. B. (1968) "Dispersion Prediction in Natural Streams," Proc. ASCE, Vol. 94, SA5.

Fischer, H. B. (1973) "Longitudinal Dispersion and Turbulent Mixing in Open-Channel Flow," Annual Reviews of Fluid Mechanics, Vol. 5, pp. 59-78.

Fischer, H. B. et al (1979) Chapter 5 in Mixing in Inland and Coastal Waters, Academic Press.

Fu, A. Y. and H. Stefan (1979a) "User's Manual for Operational Water Temperature Statistics Computer Programs WTEMP1 AND WTEMP2," St. Anthony Falls Hydrulic Laboratory, University of Minnesota, External Memorandum No. 162.

Fu, A. Y. and H. Stefan (1979b) "Water Temperature Data Processing for the Experimental Field Channels at the USEPA Ecological Research Station in Monticello, Minnesota," St. Anthony Falls Hydraulic Laboratory, University of Minnesota, External Memorandum No. 167, 32 pp.

Godfrey, R. G. and B. J. Frederick (1970) "Stream Dispersion at Selected Sites," U. S. Geological Survey Professional Paper 433-K.

Gulliver, J. S. (1977) "Analysis of Surface Heat Exchange and Longitudinal Diapersion in a Narrow Open Field Channel with Application to Water Temperature Prediction," M.S. Thesis, University of Minnesota, Department of Civil and Mineral Engineering, 187 pp.

Gulliver, J. S. and H. Stefan (1980) "Soil Thermal Conductivity and Temperature Prediction in the Bed of the Experimental Field Channels at the USEPA Ecological Research Station in Monticello, Minnesota," St. Anthony Falls Hydraulic Laboratory, University of Minnesota, External Memorandum No. 165.

Hahn, M. G., J. S. Gulliver, and H. Stefan (1978a) "Operational Water Temperature Characteristics in Channel No. 1 of the USEPA Monticello Ecological Research Station," St. Anthony Falls Hydraulic Laboratory, University of Minnesota, External Memorandum No. 151, 46 pp.

Hahn, M. G., J. S. Gulliver, and H. Stefan (1978b) "Physical Characteristics of the Experimental Field Channels at the USEPA Ecological Research Station in Monticello, Minnesota," St. Anthony Falls Hydraulic Laboratory, University of Minnesota, External Memorandum No. 156, 36 pp.

Hahn, M. G. (1978) "Experimental Studies of Vertical Mixing in Temperature Stratified Waters," M.S. Thesis, University of Minnesota, Minneapolis, Minnesota, 179 pp.

Harbeck, G. E. (1958) "Water Loss Investigations, Lake Mead Studies," U.S. Geological Survey Professional Paper No. 298.

Hughes, G. H. (1964) "Analysis of Techniques Used to Measure Evaporation from Salton Sea, California," U. S. Geological Survey, Professional Paper No. 272-H.

Idso, S. B. and R. D. Jackson (1969) "Thermal Radiation from the Atmosphere," Journal of Geophysical Research, Vol. 74, No. 23.

Jain, S. C. (1976) "Longitudinal Dispersion Coefficients for Streams," Journal of the Environmental Engineering Division, ASCE, Vol. 102, No. EE2, April 1976, pp. 465-474.

Jobson, H. E. and N. Yotsukura (1972) "Mechanics of Heat Transfer in Non-Stratified Open Channel Flows," Institute of River Mechanics Paper, Colorado State University.

Koberg, G. E. (1964) "Methods to Compute Long-wave Radiation from the Atmosphere and Reflected Solar Radiation from a Water Surface," U. S. Geological Survey, Professional Paper 272-F.

Kohler, M. A. (1954) "Lake and Pan Evaporation," Lake Hefner Studies, U. S. Geological Survey Professional Paper No. 269.

Limerinos, J. T. (1970) "Determination of the Manning Coefficient from Measured Bed Roughness in Natural Channels," U. S. Geological Survey Water Supply Paper 1898-B.

Liu, H. and A.H.D. Cheng (1980) "Modified Fickian Model for Predicting Dispersion," Journal of the Hydraulics Div.,ASCE, Vol. 106, No. HY6, June 1980, pp. 1021-1040.

Lomax, C. C. and J. F. Orsborn (1971) "Flushing of Small Streams," USEPA Water Pollution Control Research Series, 16010, DMG.

Marciano, J. J. and G. E. Harbeck (1954) "Mass Transfer Studies," Lake Hefner Studies, U. S. Geological Survey Professional Paper No. 267.

McQuivey, P. S. and T. N. Keefer (1974) "Simple Method for Predicting Dispersion in Streams," Journal Env. Engrg. Div., ASCE, Vol. 100, EE4, pp. 997-1011.

Mickley, H. S., T. K. Sherwood, and C. E. Reed (1957) Applied Mathematics in Chemical Engineering, McGraw-Hill, New York.

Murray, F. W. (1967) "On the Computation of Saturation Vapor Pressure," Journal of Applied Meteorology, Vol. 6, No. 1.

Olsen, R. M. (1973) Essentials of Engineering Fluid Mechanics, Intext Educational Publishers, New York.

Paily, P. P., E. O. Macagno, and J. F. Kennedy (1974a) "Winter-Regime Surface Heat Loss from Heated Streams," Institute of Hydraulic Research, Report No. 155, University of Iowa.

Paily, P. P., E. O. Macagno, and J. F.Kennedy (1974b) "Winter Regime Thermal Response of Heated Streams," Proc. ASCE, Vol. 100, HY4.

Patankar, S. V. and B. R. Baliga (1978) "A New Finite Difference Scheme for Parabolic Differential Equations," Numerical Heat Transfer, Vol. 1: 27-37.

Ryan, P. J. and D.R.F. Harleman (1973) "An Analytical and Experimental Study of Transient Cooling Pond Behavior," Parsons Laboratory for Water Resources and Hydrodynamics Report No. 161, Massachusetts Institute of Technology

Rymsha, V. A. and R. V. Doschenko (1958) "The Investigations of Heat Loss from Water Surfaces in Winter Time," (in Russian), Turdy GGl, No. 65.

Sayre, W. W. and F. M. Chang (1968) "A Laboratory Investigation of the Open Channel Dispersion Process for Dissolved, Suspended and Floating Dispersants," U. S. Geological Survey Professional Paper 433-E.

Shulyakovskyi, L. G. (1969) "Formula for Computing Evaporation with Allowance for the Temperature of Free Water Surface," Soviet Hydrology - Selected Papers, No. 6.

Stefan, H. and J. S. Gulliver (1980) "Pore Water Temperatures and Heat Transfer in a Riffle (Rock) Section of the Experimental Field Channels at the USEPA Ecological Research Station at Monticello, Minnesota," St. Anthony Falls Hydraulic Laboratory, University of Minnesota, External Memorandum No. 166.

Taylor G. I. (1954) "The Dispersion of Matter in Turbulent Flow Through a Pipe," Proc. Royal Society of London, No. 223-A, pp. 446-468.

Tennessee Valley Authority (1968) "The Water Temperature Regime of Fully Mixed Streams," Water Resources Research Laboratory, Report No. 15.

Thackston, E. L. and P. A.Krenkel (1967) "Longitudinal Mixing in Natural Streams," Proc. ASCE, Vol. 93, SA5.

Turner, J. F. (1966) "Evaporation Study in a Humid Region--Lake Michie, North Carolina," U. S. Geological Survey Professional Paper No. 272-G.

Yotsukura, N., A. P. Jackman, and C. R. Faust (1973) "Approximations of Heat Exchange at the Air-Water Interface," Water Resources Research, Vol. 9, No. 1.

APPENDIX A

TEMPERATURE FRONT DATA FOR DETERMINATION OF LONGITUDINAL DISPERSION COEFFICIENT

TABLE A-1. CHANNEL 1 CROSS-SECTIONAL AREAS AND SURFACE WIDTHS FOR TEMPERATURE FRONT EXPERIMENTS

Section Nr	Cross-sectional Area (m^2)	Surface Width (m)
2	1.17	3.05
3	0.46	2.01
4	1.44	3.35
5	0.48	1.89
6	1.62	3.35
7	0.37	2.04
8	1.64	3.35
9	0.37	1.95
10	1.77	3.35
11	0.37	1.80
12	1.76	3.35
13	0.39	1.80
14	1.83	3.26
15	0.38	1.80
16	1.37	3.20
17	0.38	1.65

TABLE A-2. RESIDENCE TIMES TO EACH STATION IN TEMPERATURE FRONT EXPERIMENTS (HRS)

Date of Experiment	Stations 3	5	7	9	1	13	15	17
11/17/76	0.31	0.76	1.25	1.72	2.22	2.83	3.64	4.15
11/18/76	0.37	0.82	1.28	1.68	2.14	2.58	3.04	3.41
11/22/76	0.31	0.74	1.20	1.65	2.06	2.64	3.13	3.58
12/06/76	0.15	0.56	1.06	1.50	1.98	2.50	2.99	3.46
12/14/76	0.29	0.67	1.08	1.47	1.88	2.30	2.86	--

TABLE A-3. MEASURED Θ VALUES FOR 11/17/76 TEMPERATURE FRONT (Cont'd)

Time Since Front Inception	Stations 3	5	7	9	11	13	15
(hr)							
.25	.83	1.00	1.00	1.00	1.00	1.00	1.00
.31	.49	1.00	"	"	"	"	"
.38	.33	1.00	"	"	"	"	"
.44	.23	1.00	"	"	"	"	"
.50	.15	.96	1.00	"	"	"	"
.56	.10	.94	1.00	"	"	"	"
.63	.06	.80	1.00	"	"	"	"
.69	.03	.65	1.00	"	"	"	"
.75	--	.52	1.00	"	"	"	"
.81	--	.39	--	1.00	"	"	"
.88	--	.31	--	1.00	"	"	"
.94	--	.23	.99	1.00	"	"	"
1.00	--	.15	.94	1.00	"	"	"
1.13	--	.10	.76	--	1.00	"	"
1.25	--	.05	.49	--	1.00	"	"
1.38	--	--	.32	.97	1.00	"	"
1.50	--	--	.21	.83	1.00	"	"
1.63	--	--	.14	.63	1.00	"	"
1.75	--	--	.09	.46	--	1.00	"
1.88	--	--	.05	.32	.90	1.00	"
2.00	--	--	--	.21	.78	1.00	"
2.13	--	--	--	.15	.60	1.00	"
2.25	--	--	--	.11	.47	.97	1.00
2.38	--	--	--	.06	.37	.89	1.00
2.50	--	--	--	--	.29	.76	1.00
2.63	--	--	--	--	.22	.67	--
2.75	--	--	--	--	.18	.55	.96
2.88	--	--	--	--	.14	.47	.89
3.00	--	--	--	--	.11	.40	.80
3.13	--	--	--	--	.08	.35	.73
3.25	--	--	--	--	--	.31	.66
3.38	--	--	--	--	--	.27	.60
3.50	--	--	--	--	--	.24	.55
3.63	--	--	--	--	--	--	.51
3.75	--	--	--	--	--	--	.47
4.00	--	--	--	--	--	--	.40
4.25	--	--	--	--	--	--	.36
4.50	--	--	--	--	--	--	.33
4.75	--	--	--	--	--	--	.30
5.00	--	--	--	--	--	--	.23

Note: Θ is defined by Eq. 5.5.

$$\Theta = [T(t) - T(0)]/[T(\infty) - T(0)]$$

TABLE A-3. MEASURED θ VALUES FOR 11/18/76 TEMPERATURE FRONT (Cont'd)

Time Since Front Inception (hr)	Stations 3	5	7	9	11	13	15
.25	.89	1.00	1.00	1.00	1.00	1.00	1.00
.31	.66	"	"	"	"	"	"
.38	.51	1.00	"	"	"	"	"
.44	.38	--	"	"	"	"	"
.50	.28	--	"	"	"	"	"
.56	.20	.95	"	"	"	"	"
.63	.15	.86	"	"	"	"	"
.69	.10	.73	"	"	"	"	"
.75	.08	.61	1.00	"	"	"	"
.81	.07	.50	1.00	"	"	"	"
.88	.05	.40	--	1.00	"	"	"
.94	--	.31	--	1.00	"	"	"
1.00	--	.23	.91	--	1.00	"	"
1.13	--	.13	.72	--	1.00	"	"
1.25	--	.09	.53	--	1.00	"	"
1.38	--	.07	.45	.90	--	1.00	"
1.50	--	--	.22	.75	--	1.00	"
1.63	--	--	.13	.57	.95	--	1.00
1.75	--	--	.08	.42	.88	--	1.00
1.88	--	--	.07	.31	.76	--	1.00
2.00	--	--	--	.21	.64	.93	--
2.13	--	--	--	.13	.52	.87	--
2.25	--	--	--	.08	.37	.77	--
2.38	--	--	--	--	.27	.68	.92
2.50	--	--	--	--	.17	.57	.87
2.63	--	--	--	--	.10	.45	.79
2.75	--	--	--	--	.05	.32	.68
2.88	--	--	--	--	--	.21	.62
3.00	--	--	--	--	--	.15	.52
3.13	--	--	--	--	--	.10	.42
3.25	--	--	--	--	--	.06	.34
3.38	--	--	--	--	--	--	.22
3.50	--	--	--	--	--	--	.16
3.63	--	--	--	--	--	--	.10
3.75	--	--	--	--	--	--	.07

TABLE A-3. MEASURED Θ VALUES FOR 11/22/76 TEMPERATURE FRONT (Cont'd)

Time Since Front Inception	Stations 3	5	7	9	11	13	15
(hr)							
.19	.99	1.00	1.00	1.00	1.00	1.00	1.00
.25	.76	"	"	"	"	"	"
.31	.46	"	"	"	"	"	"
.38	.30	"	"	"	"	"	"
.44	.18	1.00	"	"	"	"	"
.50	.12	.96	"	"	"	"	"
.56	.07	.86	"	"	"	"	"
.63	.05	.75	"	"	"	"	"
.69	--	.57	1.00	"	"	"	"
.75	--	.47	1.00	"	"	"	"
.81	--	.37	.99	"	"	"	"
.88	--	.28	.96	"	"	"	"
.94	--	.20	.92	"	"	"	"
1.00	--	.14	.84	1.00	"	"	"
1.13	--	.09	.59	1.00	"	"	"
1.25	--	.05	.43	.96	"	"	"
1.38	--	--	.28	.85	1.00	"	"
1.50	--	--	.20	.69	.98	"	"
1.63	--	--	.13	.51	.96	"	"
1.75	--	--	.08	.39	--	"	"
1.88	--	--	.05	.29	.75	1.00	"
2.00	--	--	--	.22	.62	.98	"
2.13	--	--	--	.18	.46	.91	1.00
2.25	--	--	--	.14	.40	.84	1.00
2.38	--	--	--	.10	.33	.72	.97
2.50	--	--	--	.08	.26	.60	.92
2.63	--	--	--	.07	.20	.48	.85
2.75	--	--	--	.05	.17	.42	.77
2.88	--	--	--	--	.14	.36	.68
3.00	--	--	--	--	.12	.30	.59
3.13	--	--	--	--	--	.25	.50
3.25	--	--	--	--	.09	.21	.42
3.38	--	--	--	--	--	.17	.36
3.50	--	--	--	--	--	.15	.31
3.63	--	--	--	--	.06	--	.28
3.75	--	--	--	--	--	.12	.23
3.88	--	--	--	--	--	--	.20
4.00	--	--	--	--	--	.09	.17

TABLE A-3. MEASURED Θ VALUES FOR 12/06/76 TEMPERATURE FRONT (Cont'd)

Time Since Front Inception (hr)	Stations 3	5	7	9	11	13	15
.13	.64	1.00	1.00	1.00	1.00	1.00	1.00
.19	.37	1.00	"	"	"	"	"
.25	.24	1.00	"	"	"	"	"
.31	.15	--	"	"	"	"	"
.38	.10	.95	"	"	"	"	"
.44	.07	.84	"	"	"	"	"
.50	--	.69	"	"	"	"	"
.56	--	.50	"	"	"	"	"
.63	--	.36	1.00	"	"	"	"
.69	--	.27	--	"	"	"	"
.75	--	.21	.97	1.00	"	"	"
.81	--	.15	.93	"	"	"	"
.88	--	.12	.87	"	"	"	"
.94	--	.08	.77	1.00	"	"	"
1.00	--	.07	.63	--	"	"	"
1.13	--	--	.38	.95	"	"	"
1.25	--	--	.26	.86	"	"	"
1.38	--	--	.18	.70	1.00	"	"
1.50	--	--	.12	.50	--	"	"
1.63	--	--	.08	.38	.91	"	"
1.75	--	--	.05	.27	.77	1.00	"
1.88	--	--	--	.20	.62	--	"
2.00	--	--	--	.16	.47	.95	"
2.13	--	--	--	.12	.35	.85	1.00
2.25	--	--	--	.09	.27	.73	1.00
2.38	--	--	--	.07	.21	.61	.97
2.50	--	--	--	--	.14	.50	.90
2.63	--	--	--	--	.11	.41	.79
2.75	--	--	--	--	--	.35	.69
2.88	--	--	--	--	.08	.29	.60
3.00	--	--	--	--	--	.24	.48
3.13	--	--	--	--	--	.21	.42
3.25	--	--	--	--	--	.18	.35
3.38	--	--	--	--	--	.15	.29
3.50	--	--	--	--	--	--	.21
3.75	--	--	--	--	--	.11	.18
3.88	--	--	--	--	--	--	.15
4.00	--	--	--	--	--	.09	.13

TABLE A-3(Cont'd). MEASURED Θ VALUES FOR 12/14/76 TEMPERATURE FRONT

Time Since Front Inception (hr)	Stations 3	5	7	9	11	13	15
.25	.72	1.00	1.00	1.00	1.00	1.00	1.00
.31	.42	"	"	"	"	"	"
.38	.26	"	"	"	"	"	"
.44	.15	--	"	"	"	"	"
.50	.09	.88	"	"	"	"	"
.56	.05	.78	"	"	"	"	"
.63	--	.61	"	"	"	"	"
.69	--	.45	--	"	"	"	"
.75	--	.34	--	"	"	"	"
.81	--	.25	.95	"	"	"	"
.88	--	.21	.88	"	"	"	"
.94	--	.16	.79	"	"	"	"
1.00	--	.13	.65	1.00	"	"	"
1.13	--	.08	.43	.95	1.00	"	"
1.25	--	.05	.29	.82	--	"	"
1.38	--	--	.19	.64	.95	"	"
1.50	--	--	.10	.47	.90	1.00	"
1.63	--	--	.07	.35	.79	--	"
1.75	--	--	--	.24	.66	.95	"
1.88	--	--	--	.16	.51	.88	1.00
2.00	--	--	--	.11	.39	.81	--
2.13	--	--	--	.06	.29	.69	.97
2.25	--	--	--	--	.21	.55	.90
2.38	--	--	--	--	.15	.45	.84
2.50	--	--	--	--	.11	.36	.76
2.63	--	--	--	--	.10	.29	.66
2.75	--	--	--	--	--	.24	.56
2.88	--	--	--	--	--	.19	.48
3.00	--	--	--	--	--	.16	.44
3.13	--	--	--	--	--	.12	.37
3.25	--	--	--	--	--	.10	.32
3.38	--	--	--	--	--	.09	.29
3.50	--	--	--	--	--	--	.26
3.63	--	--	--	--	--	.07	--
3.75	--	--	--	--	--	--	.19
4.00	--	--	--	--	--	--	.13

APPENDIX B

DATA AND COMPUTATIONS OF BULK SURFACE HEAT TRANSFER COEFFICIENT AND WIND FUNCTION PARAMETERS FROM STEADY-STATE LONGITUDINAL WATER TEMPERATURE PROFILES

TABLE B-1. DATA AND COMPUTATIONAL RESULTS FOR DETERMINATION OF BULK SURFACE HEAT TRANSFER COEFFICIENT AND WIND FUNCTION PARAMETERS FROM STEADY STATE LONGITUDINAL WATER TEMPERATURE PROFILES (Cont'd)

Date	T_a (°C)	T_d (°C)	T_w (°C)	$\Delta\theta_v$ (°C)	Q (ℓ/s)	NS/SS	W_9 (m/sec)	θ/θ_o (x=487.7m)	K_s (cal cm^{-2} day^{-1} °C^{-1})	F_w	$F_w-5.52(\Delta\theta_v)^{1/3}$ (cal cm^{-2} day^{-1} mb^{-1})
12-4-75	-1.4	-2.9	7.6	9.2	11.7	.10	4.5	.647	31.1	19.4	7.9
12-4-75	4.2	1.3	9.8	8.4	11.7	.04	5.4	.530	45.3	29.4	18.1
12-19-75	-6.7	-8.3	12.5	20.0	21.1	.04	2.75	.780	32.1	20.4	5.5
12-21-75	-17.2	-17.2	8.2	26.1	17.8	.03	1.1	.778	27.3	17.8	1.5
12-21-75	-7.2	-8.3	8.9	16.6	17.8	.10	1.3	.760	29.9	19.2	5.1
12-24-75	-7.2	-8.3	10.1	17.9	22.0	.06	5.6	.700	48.1	35.6	21.2
12-26-75	-6.9	-7.8	12.3	20.1	22.0	.04	2.9	.759	37.2	24.8	9.8
12-28-75	-5.6	-6.9	11.7	18.0	22.9	.06	2.7	.815	28.7	17.2	2.8
12-29-75	-3.3	-3.9	12.2	16.2	22.9	.05	4.2	.721	44.1	29.5	15.6
12-30-75	-3.9	-5.0	12.6	17.3	22.0	.06	3.1	.770	35.2	22.2	8.0
1-5-76	-2.7	-6.1	12.2	15.7	21.1	.03	3.8	.742	38.6	25.6	11.8
1-8-76	-22.8	-23.9	8.8	33.8	21.1	0	3.2	.751	37.0	27.4	9.6
1-9-76	-20.6	-21.7	10.1	32.2	21.1	.03	1.6	.784	31.5	22.0	4.4
1-9-76	-16.7	-17.8	11.4	29.0	21.1	.04	2.0	.778	32.5	22.7	5.7
1-11-76	-11.7	-11.7	12.0	24.6	21.1	.03	2.5	.769	34.0	23.0	7.0
1-13-76	-8.9	-10.0	11.7	21.4	20.2	.02	2.2	.767	32.9	21.7	6.4
1-14-76	-15	-15	11.2	27.1	20.2	.05	2.9	.732	38.7	28.3	11.7
1-15-76	-12.2	-12.2	11.1	24.1	20.2	.04	3.1	.710	36.5	25.7	9.7
1-17-76	-20.6	-20.6	11.2	32.7	20.2	.04	.75	.771	32.2	22.7	5.0
1-19-76	-17.2	-18.3	9.7	27.7	19.4	.09	4.9	.687	44.5	34.7	18.0
1-22-76	-12.2	-12.2	11.2	24.6	19.4	0	1.5	.779	27.8	17.5	1.5
1-25-76	-8.9	-10.0	12.0	21.8	19.4	.03	2.5	.761	32.4	21.2	5.8
1-27-76	-19.4	-19.4	9.4	33.6	21.1	0	1.8	.772	33.5	24.0	6.2
1-31-76	-5.6	-7.8	11.3	17.6	20.2	.05	4.0	.740	37.3	25.3	10.9
2-2-76	-21.1	-21.1	10.3	32.6	20.2	0	.9	.787	29.1	19.6	2.0
2-5-76	-17.2	-18.3	10.6	28.7	20.2	.02	2.2	.772	32.1	19.1	2.2
2-6-76	-17.2	-17.8	9.3	28.2	19.4	.06	3.1	.743	35.2	25.6	8.8

TABLE B-1(Cont'd). DATA AND COMPUTATIONAL RESULTS FOR DETERMINATION OF BULK SURFACE HEAT TRANSFER COEFFICIENT AND WIND FUNCTION PARAMETERS FROM STEADY STATE LONGITUDINAL WATER TEMPERATURE PROFILES

Date	T_a	T_d	T_w	$\Delta\theta_v$	Q	NS/SS	W_9	θ/θ_o	K_s	F_w	$F_w-5.52(\Delta\theta_v)^{1/3}$
	(^oC)	(^oC)	(^oC)	(^oC)	(ℓ/s)		(m/sec)	(x=487.7m)	(cal cm^{-2} day^{-1} $^oC^{-1}$)		(cal cm^{-2} day^{-1} mb^{-1})
2-7-76	-18.3	-21.1	9.3	28.2	20.2	.06	4.0	.758	34.3	25.6	8.8
2-12-76	-1.1	-3.3	12.3	14.1	19.4	.96	2.7	.760	32.5	19.6	6.2
2-13-76	-6.5	-7.5	12.2	20.0	16.3	.04	1.6	.711	34.0	22.0	7.0
2-15-76	3	2.5	11.7	11.1	14.8	.11	4.0	.578	46.1	28.6	16.3
2-17-76	3	2.5	12.7	10.5	14.8	.13	4.0	.586	42.2	25.1	13.0
2-18-76	2.5	2.3	12.7	11.0	15.5	0	2.7	.622	45.1	27.4	15.1
2-19-76	1.2	-.7	12.4	12.1	13.4	.09	2.5	.632	34.2	20.1	7.4
3-6-76	-20.5	-20.5	8.0	29.5	15.5	.04	2.0	.693	34.8	25.3	8.3
3-7-76	-9.5	-9.8	9.2	19.7	15.5	.14	1.3	.717	31.6	21.0	6.1
3-9-76	-2	-2	11.2	14.1	15.5	.06	1.8	.680	36.6	22.9	9.6
3-14-76	-1	-1.3	10.8	12.6	14.8	.04	2.9	.616	44.0	28.9	16.1
3-27-76	2.2	0.7	10.8	9.3	22.9	.10	5.5	.750	42.6	27.0	15.3
4-10-76	10	8.3	19.0	10.2	15.5	.08	3.0	.623	44.9	21.8	9.8
11-16-76	.5	-1.3	9.1	10.2	29.8	.10	4.25	.809	38.7	25.1	13.2
11-19-76	-2.0	-4.0	8.3	10.9	37.9	.03	5.25	.819	46.3	33.1	20.9
11-22-76	-4.0	-4.6	9.2	14.0	36.7	.04	8.0	.783	55.0	40.7	27.4
11-24-76	-7.0	-7.3	7.2	14.9	39.1	.08	3.25	.851	38.6	27.5	13.9
11-29-76	-14	-14	8.0	23.0	29.8	.05	4.5	.796	41.7	31.6	15.9
12-1-76	-15	-15.2	6.8	22.7	29.8	0	4.5	.832	32.4	22.8	7.1
12-3-76	-13	-13.5	8.7	22.7	28.8	.03	5.75	.806	38.0	27.8	12.2

Sample Calculation of Bulk Surface Heat Transfer Coefficient and Wind Function Parameters from Steady State Longitudinal Temperature Profile

A near steady-state longitudinal temperature profile was observed on strip chart records of water temperature on November 29, 1976. Weather records indicated that $T_a = -14^{\circ}C$, $W_9 = 4.5 \pm 1$ m/sec, and relative humidity (RH) was 91 per cent. Using psychometric tables, dew point was determined to be $-14^{\circ}C$ for the given T_a and RH. This and all other steady-state periods occurred during non-daylight hours, so $T_E = T_d$ was a good approximation.

Water temperatures were adjusted by the corresponding temperature calibration and values of $\theta/\theta_o = [T(x)-T_d]/(T_o-T_d)$ were computed and plotted on semi-log paper as shown in Fig. B-1. A best fit line through all points gave θ/θ_o(x=487.7 m)*= .796. All points, however, are enclosed by maximum and minimum θ/θ_o(x=487.7 m) values of .865 and .760, respectively.

Sample Computation:

For $\theta/\theta_o = .796$, x = 1600 ft = 487.7 m, Q = 473 gpm = 29.8 ℓ/s

and b = 9.5 ft = 2.9 m, K_s from Eq. 6-34 = 41.66 cal cm^{-2} day^{-1} $^{o}C^{-1}$

T_w = 8.0 (mean channel water temperature) ^{o}C

$T_d = -14^{\circ}C$.

Then

β = from Eq. 6-43 = .4156 mb/ ^{o}C .

and

F_w from Eq. 6-42 = 31.59 cal cm^{-2} day^{-1} mb^{-1}

p_a = air pressure = 1013 mb (assumed)

e_s = saturation vapor pressure at T_w = 8.05 mb

e_{a2} = saturation vapor pressure at T_d = 1.56 mb .

Then

$\Delta\theta_v$ = from Eq. 6-30 = $22.95^{\circ}C$

and

$F_w = 5.88(\Delta\theta_v)^{1/3}$ from Eq. 3-45 = 15.91 cal cm^{-1} day^{-1} mb^{-1} .

---

* 1600 ft.

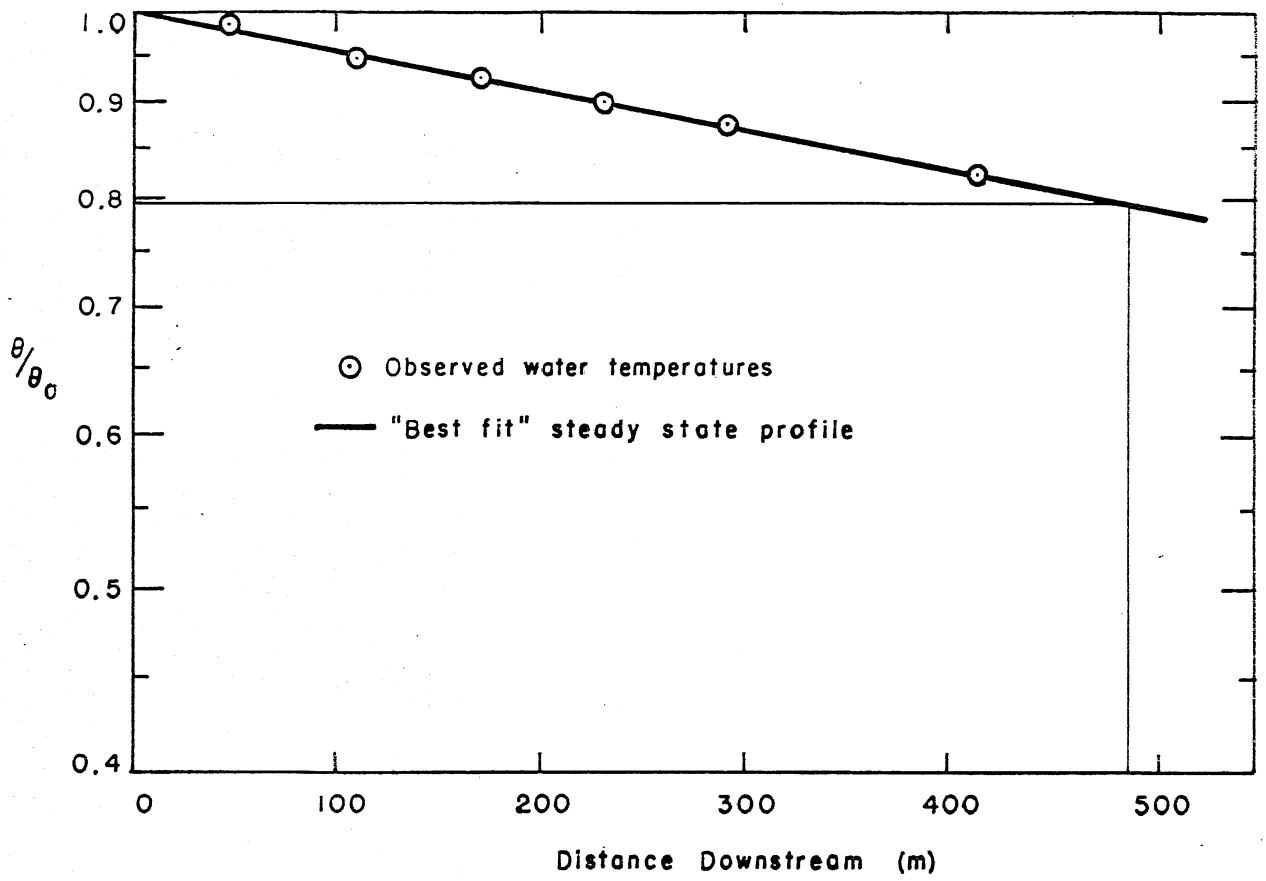

Fig. B-1. Steady state water temperature profile and "best fit" curve for November 29, 1976.

The maximum $\Delta T/\Delta t$ of all channel locations was $2.0^{o}C$/day, and the temperature difference between inflow and outflow temperatures was $\Delta T = 5.0^{o}C$. Thus the steady state parameter was

$$\frac{NS}{SS} = \frac{\Delta T/day}{30.39\ Q(gpm)(\Delta T)} = .05$$

where $Q = 473$ gpm. The maximum per cent error in $T(x)$ from non-steady-state temperatures is $100(1 - 1/1.05) = 5\%$. Since $\theta_o = T_o - T_E = 15^{o} + 14^{o} = 29^{o}C$, from Fig. B-1

$$T(x = 1600\ ft) = .796\ \theta_o + T_E = 9.08^{o}C$$

and the maximum per cent error Z in $\theta/\theta_o(x = 1600\ ft)$

$$Z = 100\ \frac{\theta/\theta_o - [.95T)x = 1600) - T_E]/\theta_o}{\theta/\theta_o} = 2\%$$

Then the maximum error in K_s calculations is

$$\%(NS/SS)\ error\ in\ K_s = \pm\ 100\ \frac{\ln\ \theta/\theta_o - \ln(1.02\ \theta/\theta_o)}{\ln\ \theta/\theta_o} = \pm\ 8.7\%$$

At a flow of 473 gpm, the accuracy of flow rate measurement in the MFS experimental channels is $\pm$ 4 per cent. Equation 6-34 indicates that this will transfer directly to a $\pm$ 4 per cent error in K_s computations. Thus, there are three significant contributions to errors in K_s.

Equations 6-42 and 6-47 indicate that the magnitude of the maximum error in K_s, rather than the per cent error, is carried to both F_w and $F_w - 5.52(\Delta\theta_v)^{1/3}$. The maximum and minimum values of K_s, F_w, and $F_w - 5.52(\Delta\theta_v)^{1/3}$ which would occur due to each component of error and with a combination of all three errors are given in Table B-2. With such a large potential error, the scatter in Figs. 6-1 through 6-4 is understandable.

TABLE B-2. MAXIMUM AND MINIMUM VALUES OF K_s, F_w, and $F_w - 5.52(\Delta\theta_v)^{1/3}$ IN SAMPLE COMPUTATION DUE TO MAXIMUM POSSIBLE ERRORS IN DATA

	K_s (cal cm^{-2} day^{-1} $^oC^{-1}$)	F_w (cal cm^{-2} mb^{-1})	$F_w - 5.52(\Delta\theta_v)^{1/3}$ (cal cm^{-2} day^{-1} mb^{-1})
Best estimate	41.66	31.59	15.91
Ranges of estimates:			
Including estimate of θ/θ_o			
Maximum	50.11	39.83	24.15
Minimum	26.48	16.79	1.11
Including errors due to unsteady character of water temperature			
Maximum	45.28	35.12	19.44
Minimum	38.04	28.07	12.38
Including errors in flow measurement			
Maximum	43.33	32.22	17.54
Minimum	40.0	29.98	14.29
Including combination of all sources of error			
Maximum	56.65	46.21	30.52
Minimum	23.21	13.61	- 2.08

APPENDIX C

USER'S GUIDE TO THE MINNESOTA

STREAM WATER TEMPERATURE PREDICTION MODEL (MNSTREM)

As noted in Section 7.3, the most important parameters for accurate water temperature prediction with MNSTREM are flow rate, cross-sectional area, solar radiation, air temperature, relative humidity, and sometimes longitudinal dispersion coefficient. There are also a number of other parameters necessary in running the model. This appendix gives a line by line description of the input file with format specifications given in parenthesis. Sample data from Appendix E are given in brackets.

Line 1 (8F 10.2)
DSTAR, TSTART, DELX, DTIME, DAY1, TLNGTH , LAT, ALT

DSTAR = Dimensionless longitudinal dispersion coefficient = $D_L \bar{B}/Q$ [7.47]

TSTART = Starting hour of day (hours.minutes) [00.00]
DELX = Distance increment (ft) for computations [12.50]
DTIME = Time increment (sec) for computations [3600]
DAY1 = Day of month for starting day [16]
TLNGTH = Total length of channel reach (ft) [1700]
LAT = Latitude of study site (degrees) [45]
ALT = Altitude of study site (ft) [1000]

Line 2 (8F 10.2)
DATE, CHDATE

DATE = Month.Day of starting day [11.16]
CHDATE = Number of days in month/100 [.30]

Line 3 (9I5)
NHOUR, MHOUR, NRES, NF, NSECT, IFLAG, JFLAG, KFLAG, LFLAG

NHOUR = Total hours of time period for computer run [480]
MHOUR = Number of hours between weather data input [3]
NRES = Number of channel locations with observed water temperatures [3]
NF = Number of flow rates read in [11]
NSECT = Number of constant cross-sectional segments in channel reach [17]
IFLAG = 1 if observed water temperatures are read in
JFLAG = 0 if the longitudinal dispersion model is used
JFLAG = 1 if computations are by upstream differences (numerical dispersion only)
KFLAG = 1 if D_L, rather than DSTAR, is specified at each segment
LFLAG = 1 if test of increment size is called

Set 4 (9F5.1) Two lines
TO(1) (TI(I), I=1, 17)

TO(1) = inflow temperature for first time step (^{o}C) [11.3]
TI(I) = initial temperature at channel segment I [TI(1)=10.7,TI(16)=8.1]

Line 5 (10A8)
HEAD (I), I=1, 10

HEAD = Heading for output of weather data which includes date and time of run

Set 6 (7F 10.4). NHOUR/MHOUR lines
TA(J), RH(J), RAD(J), W(J), WDIR(J), P(J), CC(J), TIME

Set 6 is repeated for J=1 to J=NHOUR/MHOUR

TA(J) = Air temperature (^{o}C) [TA(1)=-10]
RH(J) = Relative humidity (%) [RH(1)=100]
RAD(J) = Total solar radiation (cal cm^{-2} min^{-1}) [RAD(3)=.09]
W(J) = Wind velocity (m/sec) [W(4)=3]
WDIR(J) = Wind direction (degrees) [Blank column in Appendix E]
P(J) = Air Pressure (Bars) [PA(1)=979]
CC(J) = Fraction cloud cover [CC(13)=0.5]
TIME = Time of day (hours) [03 in first row of Set 6]
The last column gives data, which is not read into MNSTREM.

If IFLAG = 0, the next set of lines is skipped.

Set 7(18F 6.2). NHOUR/MHOUR lines
TO(J), (TT(IT+1, IT+NSECT)

Set 7 is repeated for
J=1 to J=NHOUR/MHOUR, where IT=(J-1)*NSECT

TT(I) = Observed water temperatures. Use 0.0 if no observed water temperature is input at segment. [Not in Appendix E]
Temperature measurements taken at a given time would occupy one row.

Set 8(12F 5.1). NHOUR/12+1 lines
TO(J), J=1, NHOUR+1 [TO(1)=11.1, TO(13)=10.8]

TO(J) = Upstream water temperature which is read for each hour

Date and hour given in the last two columns is not read into MNSTREM

Set 9 (10F 7.0). NF/10+1 lines
Q(I), I=1, NF

Q(I) = Flow rate (gpm) [Q(1)=473, Q(11)=456]
NF = Number of input flow rates

Set 10 (10I5). NF/10+1 lines
IF(I), I=1, NF

IF(I) = Number of hours Q(I) is applied [IF(1)=8, IF(11)=192]

Set 11(10F 7.2). NSECT/10+1 lines
A(I), I=1, NSECT

A(I) = Cross-sectional area of segment I(ft^{2}) [A(1)=14.2, A(17)=20]

Set 12 (10F 7.2). NSECT/10+1 lines
B(I), I=1, NSECT

B(I) = surface width of channel segment I(ft^{2}) [B(1)=10.8, B(17)=10.5]

Set 13 (10F 7.2). NSECT/10+1 lines
DL(I), I=1, NSECT

DL(I) = Longitudinal dispersion coefficient for channel segment I (m^2/sec) [Not in Appendix E]

APPENDIX D

PROGRAM LISTING FOR THE MINNESOTA STREAM WATER TEMPERATURE MODEL

MNSTREM

```
00001       PROGRAM MNSTREM(INPUT,OUTPUT,TAPE6,TAPE7=INPUT)                    NSFTN
00002C        MINNESOTA STREAM TEMPERATURE MODEL
00003C        PREDICTION OF OPEN CHANNEL WATER TEMPERATURES
00004C        DEVELOPED FOR
00005C           MONTICELLO ECOLOGICAL RESEARCH STATION
00006C           U. S. ENVIRONMENTAL PROTECTION AGENCY
00007C        BY
00008C           SAINT ANTHONY FALLS HYDRAULICS LABORATORY
00009C           UNIVERSITY OF MINNESOTA
00010C
00011C
00012C        THIS PROGRAM COMPUTES WATER TEMPERATURES IN AN OPEN CHANNEL
00013C        WITH LONGITUDINAL DISPERSION BY A HYBRID IMPLICIT
00014C        FINITE DIFFERENCE SCHEME
00015C
00016C        COMPARISON WITH ACTUAL WATER TEMPERATURES AND A TEST OF
00017C        INCREMENT SIZE ARE POSSIBLE.
00018C
00019C        REQUIRED INPUTS ARE FLOW RATE,CHANNEL CROSS-SECTIONS AND
00020C        SURFACE WIDTHS, LONGITUDINAL DISPERSION COEFFICIENT, UPSTREAM
00021C        TEMPERATURE, AND WEATHER PARAMETERS.
00022C
00023C        THE PROGRAM IS SPECIFICALLY DESIGNED FOR SITUATIONS WHERE
00024C        DIURNAL VARIATIONS ARE OF INTEREST. IF (MHOUR .GE. 1 DAY), THE
00025C        SHORTWAVE REFLECTIVITY EQUATIONS SHOULD BE CHANGED.
00026C
00027C        THE PROGRAM IS WRITTEN IN MINNESOTA FORTRAN
00028C        NON-STANDARD FORTRAN STATEMENTS ARE INDICATED BY *NSFTN* IN
00029C        COLUMNS 73-80
00030C        NON-STANDARD CONVENTIONS USED ARE:
00031C             1. 7-CHARACTER NAMES
00032C             2. NON-STANDARD SUBSCRIPTS AND DO LOOP INDICES
00033C             3. PRINT, RATHER THAN WRITE, STATEMENTS
00034C             4. NON-STANDARD FORMAT
00035C
00036C        VARIABLE LIST;
00037C        A(K) = SECTION CROSS-SECTIONAL AREA (M**2)
00038C        ALT = ALTITUDE(M)
00039C        B(K) = SURFACE WIDTH (M)
00040C        CC(I) = FRACTION CLOUD COVER FOR TIME INCREMENT I
00041C        CHDATE = THE NUMBER OF DAYS IN THE STARTING MONTH /100
00042C        DATE = MONTH.DAY
00043C        DAY1 = STARTING DAY OF YEAR
00044C        DELX = DISTANCE INCREMENT FOR COMPUTATIONS
00045C        DL = LONGITUDINAL DISPERSION COEFFICIENT (M**2/SEC)
00046C        DSTAR = DIMENSIONLESS LONGITUDINAL DISPERSION COEFFICIENT
00047C        DTIME = TIME INCREMENT FOR COMPUTATIONS (SEC)
00048C        ERRMAX = MAXIMUM ERROR DUE TO CHANGE IN INCREMENT SIZE
00049C        ERRMEAN = MEAN ERROR DDUE TO CHANGE IN INCREMENT SIZE
00050C        FI = COEFFICIENT WHICH SPECIFIES TIME STEP METHOD
00051C        FI = 0.5 FOR CRANK-NICOLSON IMPLICIT METHOD
00052C        FI = 1.0 FOR FULLY IMPLICIT METHOD
00053C        HEAD = HEADING FOR WEATHER DATA OUTPUT
00054C        ITEST = 0 IF NO INCREMENT SIZE TEST HAS OCCURED
00055C        LAT = LATITUDE(RADIANS)
00056C        M= TOTAL NUMBER OF RESIDUALS
00057C        MHOUR= NUMBER OF HOURS BETWEEN WATER TEMPERATURE AND
00058C               WEATHER DATA INPUT
00059C        NITER = NUMBER OF ITERATIONS ON SOURCE TERM FOR EACH TIME STEP
00060C        NF= NUMBER OF FLOW RATES READ IN
00061C        NHOUR= TOTAL HOURS OF TIME PERIOD
00062C        NSECT = NUMBER OF SECTIONS IN TOTAL CHANNEL LENGTH
00063C        NT = TOTAL NUMBER OF TIME INCREMENT STEPS
00064C        P= AIR PRESSURE (MB)
00065C        PRNOUT = A SUBROUTINE FOR OUTPUT OF WATER TEMPERATURES
```

```
00066C         Q = CHANNEL FLOW RATE
00067C         RAD= INCOMING SHORTWAVE RADIATION (CAL/DAY/CM**2)
00068C         RH= RELATIVE HUMIDITY(PERCENT)
00069C         SIGMA= STEFAN -BOLTZMAN CONSTANT
00070C         SUMERR = SUM OF SQUARES OF THE ERRORS IN INCREMENT SIZE TEST
00071C         T(I,J)= COMPUTED WATER TEMPERATURE AT LOCATION I AND TIME J
00072C         TA= AIR TEMPERATURE (C) AT 2M.
00073C         TLNGHT = TOTAL LENGTH OF CHANNEL
00074C         TT(I)= ACTUAL WATER TEMPERATURES
00075C         TIME= DAY HOUR
00076C         TSTART= STARTING DAY HOUR
00077C         W= WIND VELOCITY AT 9M. (M/SEC)
00078C         WDIR= WIND DIRECTION (DEGREES)
00079        COMMON/A/ T(150,2),TIME,IX,IPOOL,KPOOL,MHOUR
00080        COMMON/B/ TF(4000),TT(4000),RESID(4000)
00081        COMMON/C/ TSTART,TLNGTH,IFLAG,JFLAG,KFLAG,JTIME,NSECT,NDELEAT        NSFTN
00082        COMMON/D/ TO(710),TI(18)
00083        COMMON/E/ Q(30),IF(30),NF
00084        COMMON/F/ TA(250),RH(250),RAD(250),W(250),WDIR(250),P(250),CC(250)
00085        COMMON/G/ S(17),SIGMA,DAY1,LAT,ALT,TOLD(150)
00086        COMMON/H/ A(17),B(17),AK(17),BK(17),CK(17),DL(17),DELX,
00087       $DTIME ,PE(17),FC(17),FI
00088        DIMENSION HEAD(10)
00089        REAL LAT
00090        EXTERNAL TEMP,PRNOUT
00091C          READ PARAMETERS AND FLAGS
00092        READ(7,800) DSTAR,TSTART,DELX,DTIME,DAY1,TLNGTH,LAT,ALT
00093C          DELX SHOULD BE CHOSEN SUCH THAT TLENGTH/NSECT/DELX = EVEN NO.
00094        READ(7,800) DATE,CHDATE,FI
00095        LAT=LAT*3.14/180.
00096C          CONVERT TO METRIC
00097        DELX=DELX*.3048
00098        TLNGTH=TLNGTH*.3048
00099        READ(7,810) NHOUR,MHOUR,NF,NSECT,IFLAG,JFLAG,KFLAG,LFLAG,NITER
00100C          IF IFLAG=0, NO OBSERVED WATER TEMPERATURES ARE READ
00101C          IF JFLAG=0, THE LONGITUDINAL DISPERSION MODEL IS USED
00102C          IF JFLAG = 1, COMPUTATIONS ARE BY UPSTREAM DIFFERENCES
00103C                        (NUMERICAL DISPERSION ONLY)
00104C          IF KFLAG=0, DSTAR, RATHER THAN DL, IS SPECIFIED
00105C          IF LFLAG=1, TEST OF INCREMENT SIZE IS CALLED
00106        SIGMA=1.17E-7
00107        NT=NHOUR/MHOUR
00108        ITEST=0
00109        ITER=0
00110        NDELEAT=0                                                          NSFTN
00111C          READ INITIAL WATER TEMPERATURES
00112        READ(7,820) TO(1),(TI(I),I=1,17)
00113C          READ AND CONVERT UNITS OF WEATHER DATA
00114        READ(7,830) (HEAD(I),I=1,10)
00115        PRINT 835, (HEAD(I),I=1,10)                                        NSFTN
00116        PRINT 840                                                          NSFTN
00117        TIME=TSTART+FLOAT(MHOUR)
00118        DO 4 J=1,NT
00119        NH=J*MHOUR
00120        ITER=ITER+1
00121        IF(ITER.EQ.87) PRINT 840                                           NSFTN
00122        IF(TIME.GE.24.) TIME=TIME-24.
00123        READ(7,850) TA(J),RH(J),RAD(J),W(J),WDIR(J),P(J),CC(J)
00124        RAD(J)=RAD(J)*1440.
00125        PRINT 860,NH,TA(J),RH(J),RAD(J),W(J),WDIR(J),P(J),CC(J),TIME       NSFTN
00126        TIME=TIME+FLOAT(MHOUR)
00127 4      CONTINUE
00128        IF(IFLAG.EQ.0) GO TO 7
00129C          READ WATER TEMPERATURE TEMPERATURE DATA
00130        IT=0
00131        DO 5 J=1,NT
```

```
00132       NH=J*MHOUR
00133       READ(6,870) TO(NH+1),(TT(I),I=IT+1,IT+NSECT)                    NSFTN
00134 5     IT=IT+NSECT
00135 7     READ(7,880)(TO(J),J=1,NHOUR+1)                                  NSFTN
00136C         READ FLOW RATES AND NUMBER OF HOURS FOR APPLICATION OF EACH
00137C         FLOW RATE
00138       READ(7,890)(Q(I),I=1,NF)
00139       READ(7,895)(IF(I),I=1,NF)
00140       DO 10 I=1,NF
00141 10    Q(I)=Q(I)*.00228*.3048**3
00142C         READ CROSS-SECTIONAL AREAS AND SURFACE WIDTHS
00143       PRINT 910                                                       NSFTN
00144       READ(7,900) (A(I),I=1,NSECT)
00145       READ(7,900) (B(I),I=1,NSECT)
00146C         CONVERT TO METRIC
00147       DO 15 I=1,NSECT
00148       A(I)=A(I)*.3048*.3048
00149 15    B(I)=B(I)*.3048
00150       PRINT 920,(A(I),I=1,NSECT)                                      NSFTN
00151       PRINT 930,(B(I),I=1,NSECT)                                      NSFTN
00152       IF(JFLAG.EQ.1) GO TO 40
00153       IF(KFLAG.NE.1) GO TO 40
00154C         READ SECTION-SPECIFIC LONGITUDINAL DISPERSION COEFF.
00155       READ(7,900) (DL(I),I=1,NSECT)
00156       PRINT 940,(DL(I),I=1,NSECT)                                     NSFTN
00157 40    CONTINUE
00158       PRINT 950,(IF(I),I=1,NF)                                        NSFTN
00159       PRINT 955,(Q(I),I=1,NF)                                         NSFTN
00160       PRINT 980                                                       NSFTN
00161C         CALL NUMERICAL WATER TEMPERATURE PROGRAM
00162       CALL TEMP(NT,DSTAR,ITEST,ERRMAX,SUMERR,IT,NITER)
00163       M=NT*NSECT-NDELEAT                                              NSFTN
00164       CALL PRNOUT(NT,M,DATE,CHDATE)
00165       IF(LFLAG.NE.1) STOP
00166C         TEST INCREMENT SIZE
00167       ITEST=1
00168       SUMERR=0.0
00169       ERRMAX=0.0
00170       DTIME=DTIME/2.
00171       CALL TEMP(NT,DSTAR,ITEST,ERRMAX,SUMERR,IT,NITER)
00172       ERRMEAN=SQRT(SUMERR/FLOAT(IT))                                  NSFTN
00173       PRINT 960, ERRMAX,ERRMEAN                                       NSFTN
00174       STOP
00175C
00176 800   FORMAT(8F10.2)
00177 810   FORMAT(9I5)
00178 820   FORMAT(9F5.1)
00179 830   FORMAT(10A8)
00180 835   FORMAT(20X,7A8//36X,3A8)
00181 840   FORMAT(//5X,* HOUR AIR TEMP  REL HUM   RADIATION    WIND    WIND D NSFTN
00182      1IR  PRESSURE CLD COVER   TIME*/14X,*(C)      PERCENT  LANG/DAY   (
00183      2M/SEC)   DEGREES     MB     FRACTION*)
00184 850   FORMAT(7F10.4)
00185 860   FORMAT(I10,7F10.4,F7.2)
00186 870   FORMAT(18F6.2)
00187 880   FORMAT(12F5.1)
00188 890   FORMAT(10F7.0)
00189 895   FORMAT(10I5)
00190 900   FORMAT(10F7.2)
00191 910   FORMAT(///10X,*MORPHOLOGIC AND LONGITUDINAL MIXING PARAMETERS*//   NSFTN
00192      160X,*CHANNEL LOCATION*/17X,*   2      3      4      5      6
00193      27      8      9      10     11     12     13     14     15     16
00194      3    17     18*/)
00195 920   FORMAT(1X,*CROSS-SECTIONAL*,17F7.2/5X,*AREA (M)*)                NSFTN
00196 930   FORMAT(1X,*WIDTH (M)      *,17F7.2)                             NSFTN
00197 940   FORMAT(1X,"DL (M**2/SEC)  ",17F7.2)                             NSFTN
```

```
00198 950  FORMAT(//10X,*HOURS OF APPLICATION FOR EACH FLOW RATE*/3X,18I7)     NSFTN
00199 955  FORMAT(10X,"FLOW RATES (M**3/SEC)"/5X,18F7.5)                       NSFTN
00200 960  FORMAT(//10X,*TEST OF COMPUTATIONAL ERROR BY HALVING TIME INCREMEN NSFTN
00201     1T*//20X,*MAXIMUM ERROR =*,F7.4/20X,*MEAN ERROR=*,F7.4)
00202 980  FORMAT(///10X,*COEFFICIENTS IN HFLUX SUBROUTINE AT X = NSECT/2*/    NSFTN
00203     1*   NH      CR          CC          R          SINA       TDEW       AMASS
00204     2    AMC        HSM         HS        HLR         HE         HC       S*)
00205      END
00206      SUBROUTINE PRNOUT(NT,M,DATE,CHDATE)
00207C        THIS SUBROUTINE PRINTS INTERMEDIATE STATISTICS, WATER
00208C        TEMPERATURE DATA, AND FINAL ESTIMATED WATER TEMPERATURES
00209C        AND RESIDUALS.
00210C
00211C        VARIABLE LIST
00212C        IPOOL=NUMBER OF LENGTH INCREMENTS IN ONE POOL OR RIFFLE
00213C        IX= TOTAL NUMBER OF LENGTH INCERMENTS IN THE CHANNEL
00214C        KPOOL= 1/2 IPOOL
00215C        MONTH = MONTH OF THE YEAR = 1 TO 12
00216C        TF = PREDICTED WATER TEMPERATURES (C)
00217C        TT = OBSERVED WATER TEMPERATURES (C)
00218C        STD= STANDARD ERROR IN PREDICTED WATER TEMPERATURE
00219C        SUMF= RESIDUAL SUM OF SQUARES
00220C        VAR= RESIDUAL VARIANCE
00221      COMMON/A/ T(150,2),TIME,IX,IPOOL,KPOOL,MHOUR
00222      COMMON/B/ TF(4000),TT(4000),RESID(4000)
00223      COMMON/C/ TSTART,TLNGTH,IFLAG,JFLAG,KFLAG,JTIME,NSECT,NDELEAT       NSFTN
00224      COMMON/D/ TO(710),TI(18)
00225      COMMON/H/ A(17),B(17),AK(17),BK(17),CK(17),DL(17),DELX,
00226     $DTIME ,PE(17),FC(17),FI
00227      PRINT 300,DELX,DTIME                                                 NSFTN
00228      PRINT 305,IX,JTIME,IPOOL,KPOOL                                       NSFTN
00229      PRINT 310                                                            NSFTN
00230      PRINT 330, (TI(I),I=1,NSECT)                                         NSFTN
00231      MONTH =DATE
00232      IT=1
00233      TIME=TSTART
00234      DO 120 L=1,NT
00235      TIME=TIME+FLOAT(MHOUR)
00236      IF(TIME.LT.24.) GO TO 112
00237      TIME = TIME-24.
00238      DATE=DATE+0.01
00239      IF(DATE-FLOAT(MONTH).GT.CHDATE) DATE=FLOAT(MONTH)+1.01
00240      MONTH =DATE
00241      PRINT 315,DATE                                                       NSFTN
00242 112  NH=L*MHOUR
00243      PRINT 320,NH,(TF(I),I=IT,IT+NSECT-1),TIME                            NSFTN
00244      IF(IFLAG EQ.0) GO TO 115
00245      PRINT 330,(TT(I),I=IT,IT+NSECT-1)                                    NSFTN
00246      PRINT 340,(RESID(I),I=IT,IT+NSECT-1)                                 NSFTN
00247 115  IT=IT+NSECT
00248 120  CONTINUE
00249      IF(IFLAG.EQ.0) RETURN
00250      SUMF=0.0
00251      DO 140 I=1,M
00252 140  SUMF=SUMF+RESID(I)**2
00253      PRINT 350,SUMF                                                       NSFTN
00254      VAR=SUMF/(M-1)                                                       NSFTN
00255      STD=SQRT(VAR)
00256      PRINT 360,STD                                                        NSFTN
00257      PRINT 370,NDELEAT                                                    NSFTN
00258      RETURN
00259C
00260 300  FORMAT(///10X,*WATER TEMPERATURES FROM FINITE DIFFERENCE MODEL WIT NSFTN
00261     1H*//20X,*X-INCREMENT (FT) =*,F7.2/20X,*TIME INCREMENT (SEC) =*,
00262     2F7.2)
00263 305  FORMAT(12X,*IX=*,I4,5X,*JTIME=*,I4,5X,*IPOOL=*,I3,5X,*KPOOL=*,I3)   NSFTN
```

```
00264 310  FORMAT(60X,*POOL NUMBER*/15X,* HOUR   2     3     4     5     6    NSFTN
00265     $  7     8     9     10    11    12    13    14    15    16    17
00266     $  18      TIME*/)
00267 315  FORMAT(4X,F5.2)
00268 320  FORMAT(4X,*EST. TEMP   *,I3,2X,17F6.2,F9.2)                          NSFTN
00269 330  FORMAT(4X,*ACT TEMP*,9X,17F6.2)                                      NSFTN
00270 340  FORMAT(4X,*RESIDUAL*,9X,17F6.2)                                      NSFTN
00271 350  FORMAT(//10X,*RESIDUAL SUM OF SQUARES =*,F10.4)                      NSFTN
00272 360  FORMAT(10X,*STANDARD ERROR=*,F6.4)                                   NSFTN
00273 370  FORMAT(10X,*DELEATED CASES =*,I5)                                    NSFTN
00274      END
00275      SUBROUTINE TEMP(NT,DSTAR,ITEST,ERRMAX,SUMERR,IT,NITER)
00276C       THIS SUBROUTINE NUMERICALLY PREDICTS WATER TEMPERATURES IN
00277C       A ONE-DIMENSIONAL OPEN CHANNEL WITH LONGITUDINAL DISPERSION
00278C       BY A HYBRID IMPLICIT FINITE DIFFERENCE ROUTINE.
00279C
00280C       VARIABLE LIST:
00281C       A(K) = SECTION CROSS-SECTIONAL AREA (M**2)
00282C       B(K) = SURFACE WIDTH (M)
00283C       BBAR= MEAN CHANNEL WIDTH (COMPLETE CHANNEL) (M)
00284C       DELX=LENGTH INCREMENT (M)
00285C       DISPERS = A SUBROUTINE TO COMPUTE COEFFICIENTS FOR HYBRID
00286C                 DIFFERENCES
00287C       DL = LONGITUDINAL DISPERSION COEFFICIENT (M**2/SEC)
00288C       DSTAR = DIMENSIONLESS LONGITUDINAL DISPERSION COEFFICIENT
00289C       DTIME= TIME INCREMENT (SEC)
00290C       ERRMAX = MAXIMUM ERROR DUE TO CHANGE IN INCREMENT SIZE
00291C       FC(K) = FLUX COEFFICIENT FOR THE FINITE DIFFERENCE SOLUTION
00292C       FI = COEFFICIENT WHICH SPECIFIES TIME STEP METHOD
00293C       FI = 0.5 FOR CRANK-NICOLSEN IMPLICIT METHOD
00294C       FI = 1.0 FOR FULLY IMPLICIT METHOD
00295C       FLOW= FLOW RATE(M**3/SEC)
00296C       IPOOL=NUMBER OF LENGTH INCREMENTS IN ONE POOL OR RIFFLE
00297C       ITEMP = SUBROUTINE TO COMPUTE INITIAL TEMPERATURE PROFILE
00298C       IX= TOTAL NUMBER OF LENGTH INCERMENTS IN THE CHANNEL
00299C       JTIME=NUMBER OF TIME INCREMENTS IN ONE HOUR
00300C       KPOOL= 1/2 IPOOL
00301C       MHOUR= NUMBER OF HOURS BETWEEN WATER TEMPERATURE AND
00302C              WEATHER DATA INPUT
00303C       NDELEAT= NUMBER OF COMPUTED WATER TEMPERATURES FOR WHICH
00304C       NITER = NUMBER OF ITERATIONS ON SOURCE TERM FOR EACH TIME STEP
00305C                THERE IS NO INPUT WATER TEMPERATURE DATA
00306C       NSECT = NUMBER OF SECTIONS IN TOTAL CHANNEL LENGTH
00307C       NT = TOTAL NUMBER OF TIME INCREMENT STEPS
00308C       PE(K) = GRID PECLET NUMBER
00309C       RESID = RESIDUAL, = TF-TT
00310C       ROECP= DENSITY OF WATER (KG/M**3)
00311C       S(I) = TOTAL HEAT SOURCE FOR LOCATION I (KCAL/SEC/M**2)
00312C       SUMERR = SUM OF SQUARES OF THE ERRORS IN INCREMENT SIZE TEST
00313C       T(I,J)= COMPUTED WATER TEMPERATURE AT LOCATION I AND TIME J
00314C       TIME = DAY HOUR
00315C       TF(I)=COMPUTED WATER TEMPERATURE AT PROBE LOCATION I
00316C       TLNGHT = TOTAL LENGTH OF CHANNEL
00317C       TSTART= STARTING DAY HOUR
00318C       TT(I)= ACTUAL WATER TEMPERATURES
00319C       UPSTREM = A SUBROUTINE TO COMPUTE COEFFICIENTS FOR UPSTREAM
00320C                 DIFFERENCES
00321      EXTERNAL ITEMP,QRATE,HFLUX,DISPERS,UPSTREM                          NSFTN
00322      COMMON/A/ T(150,2),TIME,IX,IPOOL,KPOOL,MHOUR
00323      COMMON/B/ TF(4000),TT(4000),RESID(4000)
00324      COMMON/C/ TSTART,TLNGTH,IFLAG,JFLAG,KFLAG,JTIME,NSECT,NDELEAT       NSFTN
00325      COMMON/D/ TO(710),TI(18)
00326      COMMON/G/ S(17),SIGMA,DAY1,LAT,ALT,TOLD(150)
00327      COMMON/H/ A(17),B(17),AK(17),BK(17),CK(17),DL(17),DELX,
00328     $DTIME ,PE(17),FC(17),FI
00329      DIMENSION Z(500),G(500),F(500),TITER(150)
```

```
00330       REAL KS
00331       ROECP=1000.
00332       IX=TLNGTH/DELX+.1
00333       IPOOL=IX/NSECT
00334       KPOOL=FLOAT(IPOOL)/2.+.6
00335       JJ=1
00336       TIME=TSTART
00337       IT=1
00338       SUMB=0.0
00339C        COMPUTE MEAN CHANNEL WIDTH
00340       DO 3 K=1,NSECT
00341  3    SUMB=SUMB+B(K)
00342       BBAR=SUMB/FLOAT(NSECT)
00343       CALL ITEMP
00344       NH=0
00345C        BEGIN MAIN LOOP
00346       DO 300 LOOP=1,NT
00347       MFLAG=0
00348       DO 5 I=1,IX
00349       TITER(I)=T(I,1)
00350  5    TOLD(I)=T(I,1)
00351       CALL HFLUX(LOOP,MFLAG)
00352 10    DO 200 ILOOP=1,MHOUR
00353       NH=NH+1
00354       DTIME=3600.
00355       JTIME=3600./DTIME+.1
00356C        DETERMINE FLOW RATE
00357       CALL QRATE(FLOW,NH)
00358       IF(KFLAG.EQ.1) GO TO 25
00359C         COMPUTE LONGITUDINAL DISPERSION,DL(FT**2/SEC), FOR POOL I
00360       DO 20 K=1,NSECT
00361 20    DL(K)=DSTAR*FLOW/BBAR
00362C        COMPUTE PECLET NO. FOR EACH SECTION
00363 25    DO 30 K=1,NSECT
00364       FC(K)=FLOW*DTIME/A(K)/DELX*FI
00365       PE(K)=FLOW*DELX/A(K)/DL(K)
00366 30    CONTINUE
00367 35    DO 200 J=1,JTIME
00368       TIME=TIME+1./FLOAT(JTIME)
00369       IF(TIME.GE.24.) TIME=TIME-24.
00370C        DETERMINE INFLOW TEMPERATURE
00371       R=1.-FLOAT(J)/FLOAT(JTIME)
00372       T(1,JJ+1)=R*TN+(1.-R)*TO(NH+1)
00373       T(1,JJ+1)=T(1,JJ+1)+0.2
00374C        SUBSTITUTION AND ELIMINATION SOLUTION FOR TEMP. PROFILE
00375       I=2
00376       K=1
00377       L=0
00378       IF(JFLAG.EQ.0) CALL DISPERS(K,L)                                    NSFTN
00379       IF(JFLAG.NE.0) CALL UPSTREM(K)                                      NSFTN
00380       Z(I)=T(I,1)+(1.-FI)/FI*(AK(K)*T(I-1,1)-(AK(K)+CK(K))*T(I,1)+CK(K)
00381      1*T(I+1,1))+S(K)*B(K)*DTIME/A(K)/ROECP
00382       G(2)=(Z(2)+AK(K)*T(1,2))/BK(K)
00383       F(2)=-CK(K)/BK(K)
00384       DO 110 I=3,IX-1                                                     NSFTN
00385       K=(I-1)/IPOOL+1
00386       L=0
00387       IF(I.EQ.IPOOL*(K-1)+1) L=1
00388       IF(JFLAG.EQ.0) CALL DISPERS(K,L)                                    NSFTN
00389       IF(JFLAG.NE.0) CALL UPSTREM(K)                                      NSFTN
00390       Z(I)=T(I,1)+(1.-FI)/FI*(AK(K)*T(I-1,1)-(AK(K)+CK(K))*T(I,1)+CK(K)
00391      1*T(I+1,1))+S(K)*B(K)*DTIME/A(K)/ROECP
00392       G(I)=(Z(I)+AK(K)*G(I-1))/(BK(K)+AK(K)*F(I-1))
00393 110   F(I)=-CK(K)/(BK(K)+AK(K)*F(I-1))
00394       I=IX
00395       K=NSECT
```

```
00396       L=0
00397       IF(JFLAG.EQ.0) CALL DISPERS(K,L)                                  NSFTN
00398       IF(JFLAG.NE.0) CALL UPSTREM(K)                                    NSFTN
00399       T(I+1,1)=T(I,1)*2.-T(I-1,1)
00400       Z(I)=T(I,1)+(1.-FI)/FI*(AK(K)*T(I-1,1)-(AK(K)+CK(K))*T(I,1)+CK(K)
00401      1*T(I+1,1))+S(K)*B(K)*DTIME/A(K)/ROECP
00402       G(I)=((AK(K)-CK(K))*G(I-1)+Z(I))/(BK(K)-2.*CK(K)+(AK(K)-CK(K))
00403      1*F(I-1))
00404C          BACK-SUBSTITUTE FOR WATER TEMPERATURE
00405       T(IX,JJ+1)=G(IX)
00406       DO 130 I=1,IX-2                                                   NSFTN
00407 130   T(IX-I,JJ+1)=G(IX-I)-F(IX-I)*T(IX-I+1,JJ+1)                       NSFTN
00408       DO 140 I=1,IX
00409 140   T(I,JJ)=T(I,JJ+1)
00410 200   CONTINUE
00411C          NITER ITERATIONS ON WATER TEMPERATURE IN SOURCE TERM
00412       IF(MFLAG.EQ.NITER) GO TO 202
00413       NFLAG=0
00414       DO 2005 I=1,IX
00415 2005  IF(ABS(T(I,2)-TITER(I)).GT.0.1) NFLAG=1
00416       IF(NFLAG.EQ.0) GO TO 202
00417       MFLAG=MFLAG+1
00418       TIME=TIME-FLOAT(MHOUR)
00419       NH=NH-MHOUR
00420       CALL HFLUX(LOOP,MFLAG)
00421       DO 201 I=1,IX
00422       TITER(I)=T(I,2)
00423 201   T(I,1)=TOLD(I)
00424       GO TO 10
00425 202   DO 220 I=IT,IT+NSECT-1                                            NSFTN
00426       II=(I-IT+1)*IPOOL-KPOOL+1
00427       IF(ITEST.NE.1) GO TO 205
00428C          COMPUTE PARAMETERS FOR INCREMENT SIZE TEST
00429       ERR=ABS(T(II,JJ)-TF(I))
00430       IF(ERR.GT.ERRMAX) ERRMAX=ERR
00431       SUMERR=SUMERR+ERR**2
00432       GO TO 220
00433C          STORE WATER TEMPERATURE AND DETERMINE RESIDUAL
00434 205   TF(I)=T(II,JJ)
00435       IF(IFLAG.EQ.0) GO TO 220
00436       RESID(I)=TF(I)-TT(I)
00437       IF(TT(I).GT.4.5) GO TO 220
00438       RESID(I)=0.0
00439       NDELEAT=NDELEAT+1
00440 220   CONTINUE
00441       IT=IT+NSECT
00442 300   CONTINUE
00443       RETURN
00444       END
00445       SUBROUTINE ITEMP
00446C          THIS SUBROUTINE SETS UP THE INITIAL WATER TEMPERATURE PROFILE
00447       COMMON/A/ T(150,2),TIME,IX,IPOOL,KPOOL,MHOUR
00448       COMMON/D/ TO(710),TI(18)
00449       I=1
00450       II=1
00451       IF(TI(17).LT.0.1) TI(17)=TI(16)-.5*(TI(14)-TI(16))
00452       DO 40 J=2,IX
00453       IF(I.EQ.17) TI(I+1)=TI(I)
00454       IF(TI(I).GT.0.1.AND.TI(I+1).GT.0.1) GO TO 15
00455       K=0
00456 10    K=K+1
00457       IF(I.NE.1) GO TO 12
00458       IF(TI(I+K).GE.0.1) TI(I)=TO(1)+(TI(I+K)-T(1,1))/(FLOAT(K)+.5)     NSFTN
00459       IF(TI(I+K).GE.0.1) TI(I+1)=TI(I)+(TI(I+K)-TI(I))/FLOAT(K)         NSFTN
00460       GO TO 13
00461 12    IF(TI(I+K).GE.0.1) TI(I+1)=TI(I)+(TI(I+K)-TI(I))/FLOAT(K)         NSFTN
```

```
00462 13   IF(TI(I+K).LT.0.1) GO TO 10                                    NSFTN
00463 15   IF(J.GT.KPOOL) GO TO 20
00464      R=FLOAT(J-1)/FLOAT(KPOOL-1)
00465      T(J,1)=TO(1)*(1.-R)+R*TI(I)
00466      GO TO 40
00467 20   R=FLOAT(II)/FLOAT(IPOOL)
00468      T(J,1)=TI(I)*(1.-R)+R*TI(I+1)
00469      II=II+1
00470      IF(II.NE.IPOOL+1) GO TO 40
00471      I=I+1
00472      II=1
00473 40   CONTINUE
00474      RETURN
00475      END
00476      SUBROUTINE QRATE(FLOW,NH)
00477C        THIS SUBROUTINE COMPUTES FLOW RATE FOR EACH HOUR
00478      COMMON/E/ Q(30),IF(30),NF
00479      IFF=1                                                           NSFTN
00480      DO 10 I=1,NF+1
00481      IF(IFF+IF(I).LT.NH) GO TO 5
00482      IF(IFF.GT.NH) GO TO 10
00483      FLOW=Q(I)
00484 5    IFF=IFF+IF(I)
00485 10   CONTINUE
00486      RETURN
00487      END
00488      SUBROUTINE HFLUX(NH,MFLAG)
00489C         THIS SUBROUTINE COMPUTES HEAT FLUX SOURCE,S, FOR EACH POOL
00490C
00491C        LIST OF VARIABLES:
00492C        A AND B= CONSTANTS FOR ANDERSONS EQN.
00493C        ALPHA=SOLAR ANGLE (DEGREES) FOR TIME INCREMENT I
00494C        ALT = ALTITUDE(M)
00495C        AMASS = OPTICAL AIR MASS
00496C        AMC = ATMOSPHERIC MOISTURE CONTENT(CM)
00497C        CC(I) = FRACTION CLOUD COVER FOR TIME INCREMENT I
00498C        CL = LATENT HEAT OF VAPORIZATION (CAL/G)
00499C        CR = CLOUDINESS RATIO = 1.-RAD(I)/HSM
00500C        DAY = DAY OF YEAR(JAN. 1 = 1)
00501C        DAY1 = STARTING DAY OF YEAR
00502C        DELTV= DIFFERENCE IN VIRTUAL TEMPERATURE (C) BETWEEN WATER
00503C               SURFACE AND 2M.HEIGHT
00504C        E= RATE OF EVAPORATION (G/DAY)
00505C        EA=AIR VAPOR PRESSURE(MB) AT 2M. HEIGHT
00506C        EPS=ATMOSPHERIC EMISSIVITY
00507C        ES=SATRUATION VAPOR PRESSURE AT WATER SURFACE TEMPERATURE(MB)
00508C        ESA = SATURATED VAPOR PRESSURE AT AIR TEMPERATURE
00509C        HC= CONVECTIVE HEAT FLUX(CAL/DAY/CM**2)
00510C        HE=EVAPORATIVE HEAT FLUX (CAL/DAY/CM**2)
00511C        HLR= NET LONGWAVE RADIATIVE HEAT FLUX (CAL/DAY/CM**2)
00512C        HS= NET SHORTWAVE RADIATIVE HEAT FLUX (CAL/DAY/CM**2)
00513C        HSM = CLEAR SKY SOLAR RADIATION(CAL/DAY/CM**2)
00514C        HSO = SOLAR RADIATION INCIDENT ON THE ATMOSPHERE(CAL/DAY/CM**2)
00515C        HOURO = DAY HOUR AT SUNRISE( ALPHA=0)
00516C        LAT = LATITUDE(RADIANS)
00517C        IPOOL=NUMBER OF LENGTH INCREMENTS IN ONE POOL OR RIFFLE
00518C        KPOOL= 1/2 IPOOL
00519C        MHOUR= NUMBER OF HOURS BETWEEN WATER TEMPERATURE AND
00520C               WEATHER 4ATA INPUT
00521C        NSECT = NUMBER OF SECTIONS IN TOTAL CHANNEL LENGTH
00522C        P= AIR PRESSURE (MB)
00523C        R= REFLECTIVITY OF WATER SURFACE
00524C        RAD= INCOMING SHORTWAVE RADIATION (CAL/DAY/CM**2)
00525C        RH= RELATIVE HUMIDITY(PERCENT)
00526C        S(I) = TOTAL HEAT SOURCE FOR LOCATION I (KCAL/SEC/M**2)
00527C        SIGMA= STEFAN -BOLTZMAN CONSTANT
```

```
00528C         SINA = MEAN SINE OF THE SOLAR ANGLE
00529C         SUNDEC = DECLINATION OF THE SUN(RADIANS)
00530C         T(I,J)= COMPUTED WATER TEMPERATURE AT LOCATION I AND TIME J
00531C         TIME= DAY HOUR
00532C         TA= AIR TEMPERATURE (C) AT 2M.
00533C         TDEW = DEW POINT TEMPERATURE (C)
00534C         W= WIND VELOCITY AT 9M. (M/SEC)
00535C         WDIR= WIND DIRECTION (DEGREES)
00536C         WFTN = WIND FUNCTION FOR EVAPORATIVE AND CONVECTIVE HEAT
00537C                LOSSES (CAL/CM**2/DAY/MB)
00538       COMMON/A/ T(150,2),TIME,IX,IPOOL,KPOOL,MHOUR
00539       COMMON/C/ TSTART,TLNGTH,IFLAG,JFLAG,KFLAG,JTIME,NSECT,NDELEAT      NSFTN
00540       COMMON/F/ TA(250),RH(250),RAD(250),W(250),WDIR(250),P(250),CC(250)
00541       COMMON/G/ S(17),SIGMA,DAY1,LAT,ALT,TOLD(150)
00542       REAL LAT
00543       IF(MFLAG.GE.1) GO TO 8
00544C            CLEAR SKY SOLAR RADIATION
00545       C1=1.0
00546       C2=1.0
00547       IF(RAD(NH).GT.0.0) GO TO 5
00548       HS=RAD(NH)
00549       GO TO 7
00550C            COMPUTE AVERAGE SINE OF SOLAR ALTITUDE,SINA.
00551 5     HOUR1=0.262*(TIME-12.)
00552       IF(HOUR1.LT.0.0) C1=-C1
00553       HOUR2=0.262*(TIME+FLOAT(MHOUR)-12.)
00554       IF(HOUR2.LT.0.0) C2=-C2
00555       DAY=DAY1+FLOAT(NH*MHOUR/24)
00556       SUNDEC=0.409*COS(0.0172*(172.-DAY))
00557       HOURO=ACOS(-SIN(LAT)*SIN(SUNDEC)/COS(LAT)/COS(SUNDEC))
00558       IF(COS(HOUR1).LT.COS(HOURO)) HOUR1=C1*HOURO
00559       IF(COS(HOUR2).LT.COS(HOURO)) HOUR2=C2*HOURO
00560       SINA=((HOUR2-HOUR1)*SIN(LAT)*SIN(SUNDEC)+(SIN(HOUR2)-SIN(HOUR1))
00561      $*COS(LAT)*COS(SUNDEC))/FLOAT(MHOUR)/0.262
00562       IF(SINA.LE.0.0) SINA=1.E-40
00563C            COMPUTE AVERAGE EXTRA-TERRESTRIAL RADIATION OVER TIME PERIOD
00564       HSO=2880.*SINA/(1.+0.017*COS(0.0172*(186.-DAY)))**2
00565C            COMPUTE OPTICAL AIR MASS, AMASS.
00566       FALT=(1.-2.26E-5*ALT)**5.256
00567       AMASS=FALT/(SINA+0.15/(ASIN(SINA)+3.885)**1.253)
00568C            COMPUTE ATMOSPHERIC MOISTURE CONTENT,AMC (CM).
00569       CRH=1.-RH(NH)/100.
00570       TDEW=TA(NH)-CRH*(14.55+0.114*TA(NH))-(CRH*(2.5+.007*TA(NH)))**3
00571      $-(15.9+0.117*TA(NH))*CRH**14
00572       AMC=0.85*EXP(0.11+0.0614*TDEW)
00573C            COMPUTE CLEAR SKY SOLAR RADIATION, HSM (LANGLYS/DAY).
00574       A1=EXP(AMASS*(-0.465-0.130*AMC)*(0.179+0.421*EXP(-.721*AMASS)))
00575       A2=EXP(AMASS*(-0.465-0.134*AMC)*(0.129+0.171*EXP(-.880*AMASS)))
00576       HSM=HSO*(A1+0.5*(1.-A2))
00577C            COMPUTE CLOUDINESS RATIO.
00578       IF(RAD(NH).GT.HSM) GO TO 6
00579       CR=1.-RAD(NH)/HSM
00580  6    IF(RAD(NH).GT.HSM) CR=0.0
00581C            SHORTWAVE REFLECTIVITY WITH ANDERSONS EQN.
00582       A=2.20+CR**0.7/4.-(CR**0.7-0.4)**2/0.16
00583       B=-1.02+CR**0.7/16.+(CR**0.7-0.4)**2/0.64
00584       R=A*(ASIN(SINA)*57.3)**B
00585       IF(R.GT.1.0) R=1.0
00586C             NET SHORTWAVE RADIATION
00587       HS=(1.-R)*RAD(NH)
00588C            COMPUTE AIR VAPOR PRESSURE
00589 7     ESA=6.1078*EXP(17.26939*TA(NH)/(TA(NH)+309.))
00590       EA=ESA*RH(NH)/100.
00591C            COMPUTE SKY EMISSIVITY FOR LONG-WAVE RADIATION
00592       EPS=(1.+0.17*CC(NH)**2)*(1.-.261*EXP(-.74E-4*TA(NH)**2))
00593  8    DO 10 I=1,NSECT
```

```
00594       II=I*IPOOL-KPOOL+1
00595C          COMPUTE NET LONGWAVE RADIATION,HLR.
00596       TWS=(T(II,1)+TOLD(II))/2.
00597       HLR=SIGMA*.97*((TWS+273.)**4-EPS*(TA(NH)+273.)**4)
00598C          COMPUTE EVAPORATIVE HEAT TRANSFER,HE.
00599       ES=6.1078*EXP(17.26939*TWS/(TWS+309.))
00600       DELTV=(TWS+273.)*(1.+.378*ES/P(NH))-(TA(NH)+273.)
00601      $*(1.+.378*EA/P(NH))
00602       IF(DELTV.LE.0.0) DELTV=1.E-40
00603       WFTN=.00960*DELTV**(1./3.)+.0053*W(NH)
00604       E=WFTN*(ES-EA)
00605       CL=597.5-.592*TWS
00606       HE=E*(CL+TWS)
00607C          COMPUTE CONDUCTIVE HEAT TRANSFER,HC.
00608       HC=.61*P(NH)/1000.*WFTN*(TWS-TA(NH))*CL
00609C         COMPUTE TOTAL NET HEAT SOURCE,S(KCAL/SEC/M**2) FOR POOL I.
00610       S(I)=(HS-HE-HLR-HC)*10./3600./24.
00611C          OUTPUT COEFFICIENTS AT X=TLENGTH/2
00612       IF(I.EQ.IX/2/IPOOL)PRINT 100,NH,CR,CC(NH),R,SINA,                  NSFTN
00613      1TDEW,AMASS,AMC,HSM,HS,HLR,HE,HC,S(I)
00614 10    CONTINUE
00615       RETURN
00616 100   FORMAT(I5,13F10.4)
00617       END                                                                NSFTN
00618       SUBROUTINE DISPERS(K,L)
00619C         THIS SUBROUTINE DETERMINES COEFFICIENTS FOR THE SUBSTITUTION-
00620C         ELIMINATION SOLUTION WHEN LONGITUDINAL DISPERSION IS INCLUDED
00621       COMMON/H/ A(17),B(17),AK(17),BK(17),CK(17),DL(17),DELX,
00622      $DTIME ,PE(17),FC(17),FI
00623       AK(K)=FC(K)*(1.+AMAX1(0.,(1.-0.1*PE(K-L))**5/PE(K-L)))             NSFTN
00624       CK(K)=FC(K)*AMAX1(0.,(1.-0.1*PE(K))**5/PE(K))
00625       BK(K)=1.+AK(K)+CK(K)
00626       RETURN
00627       END                                                                NSFTN
00628       SUBROUTINE UPSTREM(K)
00629C         THIS SUBROUTINE DETERMINES COEFFICIENTS FOR THE SUBSTITUTION-
00630C         ELIMINATION SOLUTION WITHOUT LONGITUDINAL DISPERSION
00631       COMMON/H/ A(17),B(17),AK(17),BK(17),CK(17),DL(17),DELX,
00632      $DTIME ,PE(17),FC(17),FI
00633       AK(K)=FC(K)
00634       CK(K)=0.0
00635       BK(K)=1.+AK(K)
00636       RETURN
00637       END
```

APPENDIX E

SAMPLE INPUT DATA FOR MNSTREM

Variable names and formats
are specified in Appendix C

7.47 00.00 12.50 3600. 16. 1700. 45. 1000.
11.16 .30 .7
480 3 11 17 1 0 0 0 5
11.3 10.7 9.9
9.0 8.1

WEATHER DATA FROM 11-16-76 THROUGH12-06-76

-10.	100.	.	.
-11.1	100.	.00	00.0
-10.	100.	.09	.
2.	64.	.46	3.
7.	42.	.38	6.5
3.5	52.	.06	3.5
-3.	75.	.	2.
.5	61.	.	4.
.5	65.	.	4.
0.0	69.	.	3.5
-1.	68.	.11	4.
6.5	37.	.46	7.
10.	36.	.43	10.
6.	44.	.05	8.5
1.	58.	.	3.
-2.5	76.	.	2.5
-4.5	87.	.	2.
-3.	71.	.	3.
3.	46.	.00	5.
12.	47.	.29	8.5
13.	37.	.32	12.
8.5	34.	.03	8.
4.5	36.	.	6.
4.	38.	.	7.
2.	43.	.	6.
1.	50.	.	5.5
0.	56.	.09	4.5
5.5	46.	.46	6.
7.	40.	.43	6.5
2.5	49.	.06	4.5
-1.	63.	.	2.
-4.	80.	.	1.5
-6.5	94.	.	0.
-11.	100.	.	00.
-8.	98.	.03	.
0.	61.	.11	1.5
2.5	69.	.08	4.
1.5	96.	.03	4.
.5	97.	.	7.
-.5	97.	.	8.
-1.	97.	.	5.
-2.	90.	.	7.
-1.5	80.	.08	8.
1.5	58.	.25	9.
.5	72.	.09	8.
-.5	81.	.	8.5
-2.	85.	.	9.
-2.5	82.	.	8.
-3.5	82.	.	8.
-4.	84.	.	7.5
-4.	85.	.00	6.5
-3.5	80.	.09	6.
-3.5	71.	.09	7.
-5.	72.	.01	6.5
-7.	76.	.	6.
-9.	83.	.	5.5
-9.	82.	.	3.
-8.	79.	.	6.
-8.	77.	.01	4.5

THREE-HOURLY AVERAGE

979.	.	03 11-16-7
979.	0.0	06 11-16
979.	.	09 11-16
979.	0.0	12 11-16
979.	0.0	15 11-16
979.	0.0	18 11-16
979.	0.0	21 11-16
979.	0.0	24 11-16
971.	.	03 11-17
971.	0.0	06 11-17
971.	0.0	09 11-17
971.	0.0	12 11-17
971.	0.5	15 11-17
971.	0.0	18 11-17
971.	0.0	21 11-17
971.	0.0	24 11-17
969.	0.0	03 11-18
969.	.9	06 11-18
969.	1.0	09 11-18
969.	.6	12 11-18
969.	.5	15 11-18
969.	.3	18 11-18
969.	0.0	21 11-18
969.	0.0	24 11-18
975.	.0	03 11-19
975.	0.0	06 11-19
975.	0.0	09 11-19
975.	0.0	12 11-19
975.	0.0	15 11-19
975.	0.0	18 11-19
975.	0.0	21 11-19
975.	0.0	24 11-19
975.	0.0	03 11-20
975.	.0	06 11-20
975.	1.0	09 11-20
975.	1.0	12 11-20
975.	1.0	15 11-20
975.	1.0	18 11-20
975.	1.0	21 11-20
975.	.7	24 11-20
980.	1.0	03 11-21
980.	1.0	06 11-21
980.	.5	09 11-21
980.	.7	12 11-21
980.	1.0	15 11-21
980.	1.0	18 11-21
980.	1.0	21 11-21
980.	1.0	24 11-21
985.	1.0	03 11-22
985.	1.0	06 11-22
985.	1.0	09 11-22
985.	1.0	12 11-22
985.	1.0	15 11-22
985.	1.0	18 11-22
985.	1.0	21 11-22
985.	.6	24 11-22
985.	1.0	03 11-22
985.	1.0	06 11-22
985.	1.0	09 11-22

-6.5	70.	.15	4.5	985.	1.0	12 11-22
-5.5	64.	.20	5.5	985.	1.0	15 11-22
-7.	72.	.02	4.	985.	1.0	18 11-22
-7.	75.	.	3.	985.	1.0	21 11-22
-8.	79.	.	3.	985.	.3	24 11-22
-7.5	92.	.	3.5	985.	1.0	03 11-24
-5.5	96.	.	3.	974.	1.0	06 11-24
-4.	92.	.02	3.5	974.	1.0	09 11-24
-1.	72.	.22	3.	974.	.9	12 11-24
4.5	53.	.28	4.5	974.	.9	15 11-24
3.	68.	.00	3.	974.	1.0	18 11-24
0.	92.	.	1.5	974.	1.0	21 11-24
-5.	100.	.	1.	974.	.6	24 11-24
-4.5	100.	.	1.	965.	.8	03 11-25
-2.5	100.	.	2.5	965.	.4	06 11-25
-.5	96.	.00	3.	965.	1.0	09 11-25
2.	77.	.02	4.5	965.	1.0	12 11-25
1.5	98.	.00	5.5	965.	1.0	15 11-25
1.	100.	.00	4.5	965.	1.0	18 11-25
1.	100.	.	4.	965.	1.0	21 11-25
1.	99.	.	5.5	965.	1.0	24 11-25
-.5	95.	.	4.5	974.	.5	03 11-26
-3.5	100.	.	4.	974.	.2	06 11-26
-4.5	97.	.08	4.5	974.	1.0	09 11-26
2.	93.	.15	7.	974.	1.0	12 11-26
-2.5	92.	.09	6.5	974.	1.0	15 11-26
-4.5	83.	.00	8.	974.	1.0	18 11-26
-8.	68.	.	8.	974.	1.0	21 11-26
-10.	65.	.	9.	974.	1.0	24 11-26
-12.	64.	.	9.	985.	1.0	03 11-27
-14.5	75.	.	8.	985.	1.0	06 11-27
-16.	82.	.03	6.5	985.	1.0	09 11-27
-13.	74.	.40	7.	985.	.6	12 11-27
-11.5	59.	.49	7.5	985.	.6	15 11-27
-14.	61.	.06	6.	985.	.6	18 11-27
-16.	74.	.	3.	985.	0.0	21 11-27
-17.5	87.	.	1.	985.	0.0	24 11-27
-19.	92.	.	2.5	985.	.4	03 11-28
-18.5	86.	.	4.5	985.	.5	06 11-28
-19.5	86.	.08	4.	985.	0.0	09 11-28
-15.	73.	.49	6.	985.	.3	12 11-28
-13.	62.	.46	6.5	985.	.8	15 11-28
-12.5	68.	.06	4.5	985.	.8	18 11-28
-16.5	81.	.	2.5	985.	0.0	21 11-28
-17.	85.	.	6.5	985.	0.0	24 11-28
-16.5	90.	.	4.5	985.	.8	03 11-29
-15.5	91.	.	3.5	985.	.1	06 11-29
-15.	88.	.06	4.	985.	.5	09 11-29
-10.5	73.	.52	6.5	985.	.7	12 11-29
-9.5	62.	.49	8.	985.	.6	15 11-29
-13.	69.	.03	6.5	985.	.6	18 11-29
-15.	78.	.	6.	985.	.5	21 11-29
-16.5	84.	.	4.5	985.	.2	24 11-29
-18.	89.	.	2.5	985.	0.0	03 11-30
-20.	91.	.	1.5	985.	0.0	06 11-30
-21.	90.	.11	2.5	985.	0.0	09 11-30
-14.	77.	.46	4.	985.	0.0	12 11-30
-10.	58.	.43	4.	985.	.1	15 11-30
-11.5	73.	.05	2.5	985.	.5	18 11-30
-15.5	93.	.	.5	985.	.6	21 11-30
-13.5	85.	.	3.	985.	1.0	24 11-30
-13.5	83.	.	4.5	985.	1.0	03 12-01
-15.	84.	.	3.5	985.	1.0	06 12-01
-13.5	85.	.02	4.5	985.	1.0	09 12-01
-10.5	79.	.17	6.	985.	1.0	12 12-01
-9.	75.	.20	5.5	985.	1.0	15 12-01

-10.			75.			.05			5.5				985.	1.0	18 12-01
-13.5			79.			.			5.				985.	.8	21 12-01
-18.			72.			.			5.				985.	.6	24 12-01
-21.5			73.			.			4.5				991.	.0	03 12-02
-24.5			76.			.			4.				991.	0.0	06 12-02
-25.5			74.			.05			2.				991.	.5	09 12-02
-21.5			61.			.38			1.5				991.	.5	12 12-02
-19.			60.			.37			2.5				991.	.7	15 12-02
-18.			65.			.02			3.				991.	.8	18 12-02
-16.5			67.			.			4.				991.	1.0	21 12-02
-15.			70.			.			5.5				991.	1.0	24 12-02
-13.5			83.			.			6.				980.	1.0	03 12-03
-13.			85.			.			6.				980.	1.0	06 12-03
-12.5			90.			.00			5.				980.	1.0	09 12-03
-11.5			92.			.15			3.5				980.	1.0	12 12-03
-8.5			80.			.23			2.5				980.	1.0	15 12-03
-9.5			88.			.02			3.5				980.	1.0	18 12-03
-13.			100.			.			2.				980.	1.0	21 12-03
-12.5			99.			.			2.				980.	1.0	24 12-03
-13.5			96.			.			2.5				986.	1.0	03 12-04
-13.5			97.			.			2.5				986.	1.0	06 12-04
-15.			98.			.06			2.				986.	.2	09 12-04
-7.5			92.			.28			3.5				986.	.8	12 12-04
-5.5			92.			.18			5.				986.	1.0	15 12-04
-6.			99.			.02			4.				986.	1.0	18 12-04
-5.			99.			.			3.				986.	1.0	21 12-04
-7.5			97.			.			4.5				986.	1.0	24 12-04
-12.5			100.			.			3.				989.	.7	03 12-05
-16.5			99.			.			1.				989.	.4	06 12-05
-17.5			97.			.03			.5				989.	1.0	09 12-05
-12.			99.			.22			2.5				989.	1.0	12 12-05
-8.5			96.			.17			3.5				989.	1.0	15 12-05
-7.			100.			.01			3.5				989.	1.0	18 12-05
-6.			100.			.			4.				989.	.8	21 12-05
-3.5			100.			.			5.				989.	1.0	24 12-05
11.1	12.	12.3	11.6	11.2	10.9	10.8	10.6	11.0	11.0	3.6	10.6	11-16-76	00		
10.8	11.2	10.9	10.8	10.8	10.6	9.9	9.6	9.6	9.6	9.8	10.	11-16-76	12		
10.3	10.2	10.2	10.1	10.1	10.0	10.0	9.8	9.8	9.8	.9	1.0	11-17-76	00		
1.2	1.4	1.6	1.7	1.6	1.6	1.5	1.4	1.4	1.4	1.3	1.2	11-17-76	12		
1.2	1.1	1.1	1.1	1.1	1.1	1.1	1.2	1.2	1.2	11.	10.2	11-18-76	00		
10.4	10.6	10.6	10.6	10.6	10.5	10.5	10.4	10.2	10.1	10.0	9.9	11-18-76	12		
9.8	9.7	9.6	9.6	9.6	9.5	9.5	9.3	9.2	9.4	9.6	9.8	11-19-76	00		
10.1	9.	4.6	4.6	10.2	10.2	10.2	10.0	10.0	9.6	9.7	9.9	11-19-76	12		
9.8	9.7	9.6	9.5	9.3	9.2	9.2	9.1	9.1	9.2	9.4	9.6	11-20-76	00		
9.6	9.7	9.8	9.8	9.9	10.1	10.1	10.0	9.9	9.8	9.7	9.6	11-20-76	12		
8.6	7.5	7.6	8.6	9.2	9.4	9.3	9.1	9.1	9.0	9.1	9.1	11-21-76	00		
9.2	9.3	9.4	9.4	9.4	9.4	9.3	9.3	9.3	9.3	9.3	9.3	11-21-76	12		
9.2	9.4	9.6	9.6	9.6	9.6	9.6	9.6	9.6	.8	.8	.8	11-22-76	00		
.8	.8	.8	.9	.9	.9	.9	.8	.8	.8	.8	.7	11-22-76	12		
.7	.7	.7	.6	.6	.6	.6	.6	.6	9.4	9.2	9.4	11-23-76	00		
9.8	10.0	10.2	3.4	8.6	8.6	8.5	8.6	8.6	8.6	8.5	8.6	11-23-76	12		
8.4	8.3	8.4	8.5	8.5	8.6	8.6	8.6	8.6	8.6	8.7	8.8	11-24-76	00		
8.6	8.2	8.	8.	7.9	7.9	7.8	7.8	7.7	7.7	7.6	7.6	11-24-76	12		
7.6	7.6	7.	7.	7.8	7.7	7.7	7.6	7.6	7.6	7.7	7.8	11-25-76	00		
7.8	7.6	7.6	7.6	7.6	7.5	7.6	7.6	7.6	7.6	7.6	7.6	11-25-76	12		
7.7	7.6	7.6	7.5	7.5	7.4	7.9	7.8	7.8	7.6	7.6	7.9	11-26-76	00		
7.6	7.5	3.	8.6	9.0	9.3	9.2	9.3	9.6	9.5	9.4	9.4	11-26-76	12		
10.2	12.6	12.2	12.0	12.1	12.2	12.3	12.2	12.1	11.7	11.	6.	11-27-76	00		
10.2	10.3	10.2	10.0	10.0	9.9	10.1	10.0	10.0	10.0	10.0	9.8	11-27-76	12		
9.8	9.9	8.7	8.2	8.4	9.	9.4	9.1	9.2	9.2	9.3	9.4	11-28-76	00		
9.4	9.4	9.5	9.5	9.6	9.6	9.7	9.8	9.8	9.8	9.9	10.0	11-28-76	12		
10.0	10.1	10.0	9.9	9.8	10.0	10.0	10.0	9.9	9.7	9.6	9.5	11-29-76	00		
9.5	9.4	9.4	9.5	9.5	9.5	9.4	9.4	9.4	9.4	9.4	9.4	11-29-76	12		
9.5	9.3	9.2	9.2	9.2	9.0	8.8	8.9	9.0	8.8	8.8	9.0	11-30-76	00		
8.6	8.6	8.6	8.6	8.7	8.8	8.8	8.8	8.8	8.7	8.8	8.8	11-30-76	12		
8.9	8.9	8.9	8.9	8.8	8.8	8.8	8.8	8.9	8.9	9.1	9.0	12-01-76	00		

```
 9.0  9.1  8.9  9.0  9.0  9.0  9.0  9.2  9.2  9.2  9.1  9.1 12-01-76 12
 9.3  9.2  9.2  9.1  9.3  9.2  9.2  9.2  9.2  9.2  9.3  9.4 12-02-76 00
 9.6  9.7  9.8 10.0 10.0  9.9  9.9 10.0  9.9  9.7  9.9 10.0 12-02-76 12
10.0 10.1 10.1 10.1 10.0 10.0 10.0  9.9  9.8  9.7  9.6  9.5 12-03-76 00
 9.4  9.2  9.3  2.0 10.0 10.2 10.6 10.5 10.8 11.0 10.9 11.0 12-03-76 12
11.0 10.8 10.8 10.9 10.7 10.8 10.8 10.7 10.8 10.6 10.7 10.6 12-04-76 00
10.5 10.4 10.7 10.5 10.5 10.5 10.5 10.5 10.5 10.5 10.6 10.4 12-04-76 12
10.6 10.4 10.4 10.7 10.4 10.8 10.6 10.6 10.5 10.6 10.6 10.6 12-05-76 00
10.6 10.6 10.7 10.6 10.6 10.4 10.4 10.4 10.4 10.5 10.5 10.2 12-05-76 12
10.4 10.4
  473.   601.   582.   601.   582.   620.   601.   582.   456.   473.
  456.
    8   24   24   48   72   24   24   24   48   48
  192
  14.2    3.4   16.7    4.0   18.2    4.0   17.8    3.3   17.0    3.2
  17.7    3.0   18.5    3.2   17.2    2.3   20.0
  10.8    6.6   11.0    6.2   10.9    6.7   11.9    6.4   11.3    5.9
  11.0    5.9   10.9    5.4   10.8    5.6   10.5
END OF FILE
```

APPENDIX F

PARTIAL SAMPLE OUTPUT FROM MNSTREM

WATER TEMPERATURES FROM FINITE DIFFERENCE MODEL WITH

X-INCREMENT (FT) = 3.81
TIME INCREMENT (SEC) =3600.00
IX= 136 JTIME= 1 IPOOL= 8 KPOOL= 4

		POOL NUMBER																	
	HOUR	2	3	4	5	6	7	8	9	10	11	12	13	14	15	16	17	18	TIME
ACT.TEMP		10.83	10.70	10.43	10.17	9.90	9.75	9.60	9.45	9.30	9.15	9.00	8.82	8.64	8.46	8.28	8.10	12.15	
EST. TEMP	3	11.83	11.78	11.68	11.54	11.25	11.02	10.61	10.36	9.95	9.71	9.34	9.13	8.80	8.63	8.37	8.18	8.00	3.00
ACT.TEMP		0	12.10	0	0	10.80	0	0	0	0	0	8.50	0	0	0	0	7.60	0	
RESIDUAL		0	-.32	0	0	.45	0	0	0	0	0	.84	0	0	0	0	.58	0	
EST. TEMP	6	10.88	10.72	10.52	10.38	10.24	10.13	10.01	9.91	9.81	9.72	9.61	9.51	9.35	9.22	9.01	8.86	8.58	6.00
ACT.TEMP		0	10.80	0	0	10.00	0	0	0	0	0	9.00	0	0	0	0	7.80	0	
RESIDUAL		0	-.08	0	0	.24	0	0	0	0	0	.61	0	0	0	0	1.06	0	
EST. TEMP	9	11.14	11.02	10.79	10.64	10.39	10.23	9.98	9.84	9.62	9.49	9.29	9.17	8.99	8.89	8.75	8.66	8.53	9.00
ACT.TEMP		0	11.10	0	0	10.00	0	0	0	0	0	8.70	0	0	0	0	7.80	0	
RESIDUAL		0	-.08	0	0	.39	0	0	0	0	0	.59	0	0	0	0	.86	0	
EST. TEMP	12	11.33	11.26	10.47	9.96	9.13	8.82	8.52	8.47	8.53	8.62	8.83	8.97	9.21	9.34	9.52	9.60	9.71	12.00
ACT.TEMP		0	11.10	0	0	10.40	0	0	0	0	0	6.40	0	0	0	0	9.30	0	
RESIDUAL		0	.16	0	0	-1.27	0	0	0	0	0	2.43	0	0	0	0	.30	0	
EST. TEMP	15	10.99	11.02	11.05	11.06	11.11	11.15	11.23	11.26	11.25	11.21	11.06	10.96	10.59	10.54	10.26	10.14	9.87	15.00
ACT.TEMP		0	10.90	0	0	10.50	0	0	0	0	0	10.20	0	0	0	0	9.50	0	
RESIDUAL		0	.12	0	0	.61	0	0	0	0	0	.86	0	0	0	0	.64	0	
EST. TEMP	18	10.14	10.14	10.18	10.16	10.14	10.09	10.02	9.96	9.89	9.83	9.78	9.74	9.73	9.71	9.72	9.70	9.73	18.00
ACT.TEMP		0	10.00	0	0	9.90	0	0	0	0	0	9.20	0	0	0	0	8.80	0	
RESIDUAL		0	.14	0	0	.24	0	0	0	0	0	.58	0	0	0	0	.90	0	
EST. TEMP	21	9.72	9.60	9.43	9.32	9.16	9.05	8.91	8.82	8.73	8.66	8.60	8.55	8.51	8.47	8.44	8.39	8.37	21.00
ACT.TEMP		0	9.60	0	0	9.00	0	0	0	0	0	8.10	0	0	0	0	7.70	0	
RESIDUAL		0	.00	0	0	.16	0	0	0	0	0	.50	0	0	0	0	.69	0	
11.17																			
EST. TEMP	24	10.37	10.21	9.98	9.83	9.60	9.46	9.23	9.10	8.89	8.77	8.58	8.47	8.29	8.19	8.03	7.94	7.80	0
ACT.TEMP		0	10.20	0	0	9.40	0	0	0	0	0	8.20	0	0	0	0	7.40	0	
RESIDUAL		0	.01	0	0	.20	0	0	0	0	0	.38	0	0	0	0	.54	0	
EST. TEMP	27	10.23	10.13	9.98	9.89	9.75	9.65	9.50	9.40	9.25	9.15	9.00	8.90	8.73	8.63	8.47	8.36	8.18	3.00
ACT.TEMP		0	10.20	0	0	9.60	0	0	0	0	0	8.70	0	0	0	0	7.80	0	
RESIDUAL		0	-.07	0	0	.15	0	0	0	0	0	.30	0	0	0	0	.56	0	
EST. TEMP	30	10.11	10.00	9.85	9.75	9.61	9.51	9.36	9.26	9.13	9.03	8.90	8.82	8.69	8.61	8.49	8.41	8.29	6.00
ACT.TEMP		0	10.10	0	0	9.40	0	0	0	0	0	8.50	0	0	0	0	7.80	0	
RESIDUAL		0	-.10	0	0	.21	0	0	0	0	0	.40	0	0	0	0	.61	0	
EST. TEMP	33	9.92	9.81	9.65	9.55	9.41	9.32	9.18	9.09	8.97	8.89	8.78	8.70	8.59	8.51	8.40	8.33	8.22	9.00
ACT.TEMP		0	10.00	0	0	9.30	0	0	0	0	0	8.20	0	0	0	0	7.80	0	
RESIDUAL		0	-.19	0	0	.11	0	0	0	0	0	.58	0	0	0	0	.53	0	
EST. TEMP	36	1.42	1.46	1.50	1.53	1.59	1.65	1.91	2.15	2.95	3.53	4.98	5.74	7.13	7.71	8.50	8.78	9.18	12.00
ACT.TEMP		0	1.70	0	0	2.20	0	0	0	0	0	6.50	0	0	0	0	8.80	0	
RESIDUAL		0	0	0	0	0	0	0	0	0	0	-1.52	0	0	0	0	-.02	0	
EST. TEMP	39	1.97	2.06	2.19	2.28	2.39	2.47	2.57	2.65	2.74	2.80	2.87	2.91	2.95	2.98	2.99	3.02	3.05	15.00
ACT.TEMP		0	1.90	0	0	2.30	0	0	0	0	0	3.00	0	0	0	0	4.00	0	
RESIDUAL		0	0	0	0	0	0	0	0	0	0	0	0	0	0	0	0	0	
EST. TEMP	42	1.70	1.68	1.66	1.64	1.62	1.59	1.56	1.54	1.52	1.51	1.54	1.55	1.60	1.63	1.71	1.74	1.85	18.00
ACT.TEMP		0	1.80	0	0	1.70	0	0	0	0	0	1.40	0	0	0	0	1.80	0	
RESIDUAL		0	0	0	0	0	0	0	0	0	0	0	0	0	0	0	0	0	

RESIDUAL		0	.05	0	0	.09	0	0	0	0	0	.20	0	0	0	0	.16	0		
EST. TEMP	405	8.65	8.42	8.12	7.90	7.59	7.35	7.00	6.76	6.43	6.21	5.90	5.69	5.40	5.21	4.94	4.76	4.51	21.00	
ACT.TEMP		0	8.40	0	0	7.50	0	0	0	0	0	5.70	0	0	0	0	4.60	0		
RESIDUAL		0	.02	0	0	.09	0	0	0	0	0	.20	0	0	0	0	.16	0		
12.03																				
EST. TEMP	408	8.90	8.62	8.23	7.95	7.55	7.27	6.86	6.60	6.25	6.02	5.70	5.49	5.20	5.01	4.73	4.54	4.28	0	
ACT.TEMP		0	8.70	0	0	7.40	0	0	0	0	0	5.50	0	0	0	0	4.30	0		
RESIDUAL		0	-.08	0	0	.15	0	0	0	0	0	.20	0	0	0	0	0	0		
EST. TEMP	411	9.00	8.73	8.36	8.11	7.75	7.50	7.11	6.86	6.51	6.28	5.93	5.71	5.37	5.16	4.84	4.64	4.33	3.00	
ACT.TEMP		0	8.70	0	0	7.70	0	0	0	0	0	5.60	0	0	0	0	4.20	0		
RESIDUAL		0	.03	0	0	.05	0	0	0	0	0	.33	0	0	0	0	0	0		
EST. TEMP	414	8.91	8.64	8.27	8.03	7.69	7.46	7.11	6.88	6.56	6.34	6.04	5.83	5.53	5.34	5.05	4.86	4.55	6.00	
ACT.TEMP		0	8.70	0	0	7.60	0	0	0	0	0	5.50	0	0	0	0	4.10	0		
RESIDUAL		0	-.06	0	0	.09	0	0	0	0	0	.54	0	0	0	0	0	0		
EST. TEMP	417	8.64	8.42	8.13	7.93	7.65	7.45	7.15	6.94	6.65	6.46	6.17	5.98	5.70	5.52	5.25	5.07	4.79	9.00	
ACT.TEMP		0	8.40	0	0	7.60	0	0	0	0	0	5.60	0	0	0	0	4.30	0		
RESIDUAL		0	.02	0	0	.05	0	0	0	0	0	.57	0	0	0	0	0	0		
EST. TEMP	420	9.26	8.93	8.51	8.29	8.00	7.83	7.58	7.42	7.20	7.05	6.83	6.69	6.45	6.31	6.08	5.93	5.68	12.00	
ACT.TEMP		0	8.30	0	0	7.90	0	0	0	0	0	6.20	0	0	0	0	5.10	0		
RESIDUAL		0	.63	0	0	.10	0	0	0	0	0	.63	0	0	0	0	.83	0		
EST. TEMP	423	3.79	4.92	6.45	7.04	7.79	8.01	8.21	8.22	8.16	8.09	7.91	7.80	7.57	7.44	7.21	7.09	6.84	15.00	
ACT.TEMP		0	7.60	0	0	4.30	0	0	0	0	0	6.70	0	0	0	0	6.00	0		
RESIDUAL		0	-2.68	0	0	0	0	0	0	0	0	1.21	0	0	0	0	1.09	0		
EST. TEMP	426	10.54	10.46	10.17	9.76	8.70	8.05	7.04	6.57	6.02	5.78	5.61	5.53	5.59	5.60	5.71	5.71	5.83	18.00	
ACT.TEMP		0	10.40	0	0	9.50	0	0	0	0	0	6.50	0	0	0	0	4.40	0		
RESIDUAL		0	.06	0	0	-.80	0	0	0	0	0	-.89	0	0	0	0	0	0		
EST. TEMP	429	11.01	10.75	10.38	10.13	9.77	9.55	9.26	9.07	8.77	8.56	8.13	7.84	7.26	6.93	6.36	6.06	5.52	21.00	
ACT.TEMP		0	10.50	0	0	9.50	0	0	0	0	0	7.80	0	0	0	0	6.60	0		
RESIDUAL		0	.25	0	0	.27	0	0	0	0	0	.33	0	0	0	0	-.54	0		
12.04																				
EST. TEMP	432	11.05	10.83	10.52	10.32	10.03	9.83	9.53	9.33	9.03	8.84	8.55	8.36	8.09	7.92	7.66	7.49	7.19	0	
ACT.TEMP		0	10.50	0	0	9.80	0	0	0	0	0	8.10	0	0	0	0	7.40	0		
RESIDUAL		0	.33	0	0	.23	0	0	0	0	0	.45	0	0	0	0	.09	0		
EST. TEMP	435	10.91	10.66	10.32	10.09	9.80	9.59	9.30	9.10	8.84	8.66	8.41	8.24	8.00	7.84	7.60	7.44	7.20	3.00	
ACT.TEMP		0	10.80	0	0	9.60	0	0	0	0	0	8.00	0	0	0	0	7.50	0		
RESIDUAL		0	-.14	0	0	.20	0	0	0	0	0	.41	0	0	0	0	-.06	0		
EST. TEMP	438	10.84	10.60	10.27	10.05	9.75	9.54	9.23	9.02	8.74	8.55	8.28	8.10	7.84	7.67	7.43	7.27	7.04	6.00	
ACT.TEMP		0	10.70	0	0	9.50	0	0	0	0	0	8.00	0	0	0	0	7.50	0		
RESIDUAL		0	-.10	0	0	.25	0	0	0	0	0	.28	0	0	0	0	-.23	0		
EST. TEMP	441	10.68	10.47	10.18	9.97	9.68	9.46	9.15	8.94	8.64	8.45	8.17	7.99	7.72	7.55	7.30	7.13	6.89	9.00	
ACT.TEMP		0	10.40	0	0	9.50	0	0	0	0	0	7.90	0	0	0	0	7.40	0		
RESIDUAL		0	.07	0	0	.18	0	0	0	0	0	.27	0	0	0	0	-.27	0		
EST. TEMP	444	10.64	10.55	10.45	10.37	10.26	10.17	10.02	9.91	9.73	9.61	9.40	9.28	9.03	8.90	8.65	8.52	8.24	12.00	
ACT.TEMP		0	10.60	0	0	10.00	0	0	0	0	0	8.90	0	0	0	0	8.20	0		
RESIDUAL		0	-.05	0	0	.26	0	0	0	0	0	.50	0	0	0	0	.32	0		
EST. TEMP	447	10.66	10.55	10.36	10.22	10.01	9.87	9.67	9.55	9.40	9.30	9.18	9.09	8.98	8.90	8.79	8.71	8.59	15.00	
ACT.TEMP		0	10.50	0	0	9.80	0	0	0	0	0	8.70	0	0	0	0	8.40	0		
RESIDUAL		0	.05	0	0	.21	0	0	0	0	0	.48	0	0	0	0	.31	0		
EST. TEMP	450	10.57	10.39	10.14	9.97	9.73	9.57	9.34	9.19	8.99	8.85	8.67	8.55	8.38	8.27	8.12	8.01	7.89	18.00	
ACT.TEMP		0	10.40	0	0	9.60	0	0	0	0	0	8.30	0	0	0	0	7.90	0		
RESIDUAL		0	-.01	0	0	.13	0	0	0	0	0	.37	0	0	0	0	.11	0		
EST. TEMP	453	10.58	10.42	10.20	10.05	9.84	9.69	9.46	9.31	9.09	8.95	8.74	8.61	8.40	8.27	8.08	7.96	7.78	21.00	
ACT.TEMP		0	10.60	0	0	9.80	0	0	0	0	0	8.40	0	0	0	0	8.20	0		
RESIDUAL		0	-.18	0	0	.04	0	0	0	0	0	.34	0	0	0	0	-.24	0		

12.05																			
EST. TEMP	456	10.60	10.36	10.06	9.87	9.60	9.41	9.14	8.96	8.72	8.56	8.35	8.20	8.01	7.88	7.70	7.57	7.40	0
ACT.TEMP		0	10.60	0	0	9.40	0	0	0	0	0	7.90	0	0	0	0	7.80	0	
RESIDUAL		0	-.24	0	0	.20	0	0	0	0	0	.45	0	0	0	0	-.23	0	
EST. TEMP	459	10.66	10.37	9.98	9.74	9.41	9.19	8.87	8.66	8.38	8.19	7.94	7.76	7.52	7.37	7.15	7.00	6.80	3.00
ACT.TEMP		0	10.50	0	0	9.20	0	0	0	0	0	7.70	0	0	0	0	7.40	0	
RESIDUAL		0	-.13	0	0	.21	0	0	0	0	0	.24	0	0	0	0	-.40	0	
EST. TEMP	462	10.69	10.48	10.14	9.91	9.58	9.35	9.00	8.77	8.45	8.24	7.94	7.74	7.45	7.27	7.00	6.82	6.57	6.00
ACT.TEMP		0	10.40	0	0	9.30	0	0	0	0	0	7.50	0	0	0	0	7.00	0	
RESIDUAL		0	.08	0	0	.28	0	0	0	0	0	.44	0	0	0	0	-.18	0	
EST. TEMP	465	10.62	10.40	10.10	9.90	9.64	9.45	9.17	8.98	8.71	8.53	8.27	8.09	7.81	7.64	7.37	7.19	6.91	9.00
ACT.TEMP		0	10.60	0	0	9.40	0	0	0	0	0	7.80	0	0	0	0	7.10	0	
RESIDUAL		0	-.20	0	0	.24	0	0	0	0	0	.47	0	0	0	0	.09	0	
EST. TEMP	468	10.70	10.55	10.36	10.24	10.06	9.92	9.71	9.57	9.35	9.21	8.99	8.85	8.61	8.47	8.24	8.11	7.86	12.00
ACT.TEMP		0	10.70	0	0	10.00	0	0	0	0	0	8.70	0	0	0	0	8.00	0	
RESIDUAL		0	-.15	0	0	.06	0	0	0	0	0	.29	0	0	0	0	.11	0	
EST. TEMP	471	10.72	10.59	10.39	10.26	10.06	9.92	9.71	9.57	9.38	9.26	9.09	8.97	8.80	8.70	8.53	8.42	8.25	15.00
ACT.TEMP		0	10.50	0	0	9.80	0	0	0	0	0	8.60	0	0	0	0	8.40	0	
RESIDUAL		0	.09	0	0	.26	0	0	0	0	0	.49	0	0	0	0	.02	0	
EST. TEMP	474	10.46	10.28	10.05	9.90	9.69	9.54	9.33	9.18	8.98	8.85	8.67	8.54	8.38	8.26	8.10	7.99	7.84	18.00
ACT.TEMP		0	10.50	0	0	9.40	0	0	0	0	0	8.00	0	0	0	0	7.70	0	
RESIDUAL		0	-.22	0	0	.29	0	0	0	0	0	.67	0	0	0	0	.29	0	
EST. TEMP	477	10.54	10.33	10.05	9.86	9.60	9.42	9.15	8.98	8.74	8.59	8.38	8.23	8.04	7.91	7.73	7.61	7.45	21.00
ACT.TEMP		0	10.30	0	0	9.40	0	0	0	0	0	7.90	0	0	0	0	7.50	0	
RESIDUAL		0	.03	0	0	.20	0	0	0	0	0	.48	0	0	0	0	.11	0	
12.06																			
EST. TEMP	480	10.42	10.22	9.98	9.84	9.65	9.51	9.30	9.16	8.94	8.80	8.59	8.44	8.22	8.09	7.88	7.75	7.54	0
ACT.TEMP		0	10.40	0	0	9.20	0	0	0	0	0	7.90	0	0	0	0	7.60	0	
RESIDUAL		0	-.18	0	0	.45	0	0	0	0	0	.69	0	0	0	0	.15	0	

RESIDUAL SUM OF SQUARES = 55.2382
STANDARD ERROR= .3161
DELEATED CASES = 2166

APPENDIX G

MERS WEATHER STATION

The MERS channel water temperatures are controlled by inflow and weather conditions. A station to measure and record weather parameters was therefore installed near the center of the field station. Solar radiation and wind velocity were recorded since December 3, 1975. A 50 - junction Epply pyranometer and a Science Associate's anemometer were mounted at 2 m and 9 m, respectively, above the ground. A Belfort hydrothermograph, with a bimetal temperature sensor and hair hydrometer, were mounted in a weather shelter and recorded air temperature and relative humidity since January 29, 1976. A Texas Electronics wind direction vane and transmitter, mounted at 4 m, with power supply unit and Rustrak recorder was put in operation on April 2, 1976. Sample strip chart records are shown in Figs. G-1 and G-2. The weather station is shown in Fig. G-3. A one-year cycle of measured air temperatures is shown in Fig. G-4.

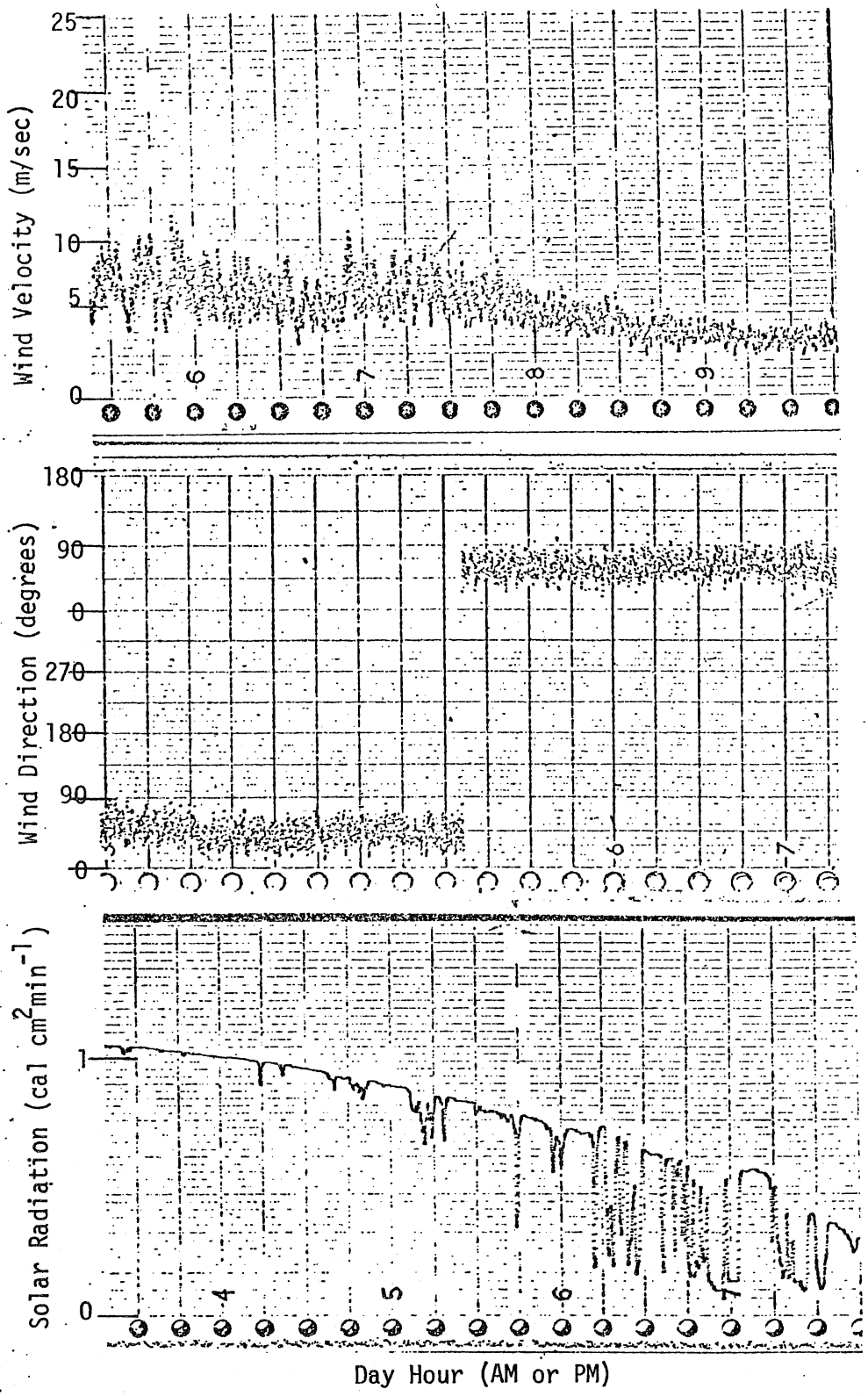

Fig. G-1 - Sample strip charts for wind velocity, wind direction, and solar radiation.

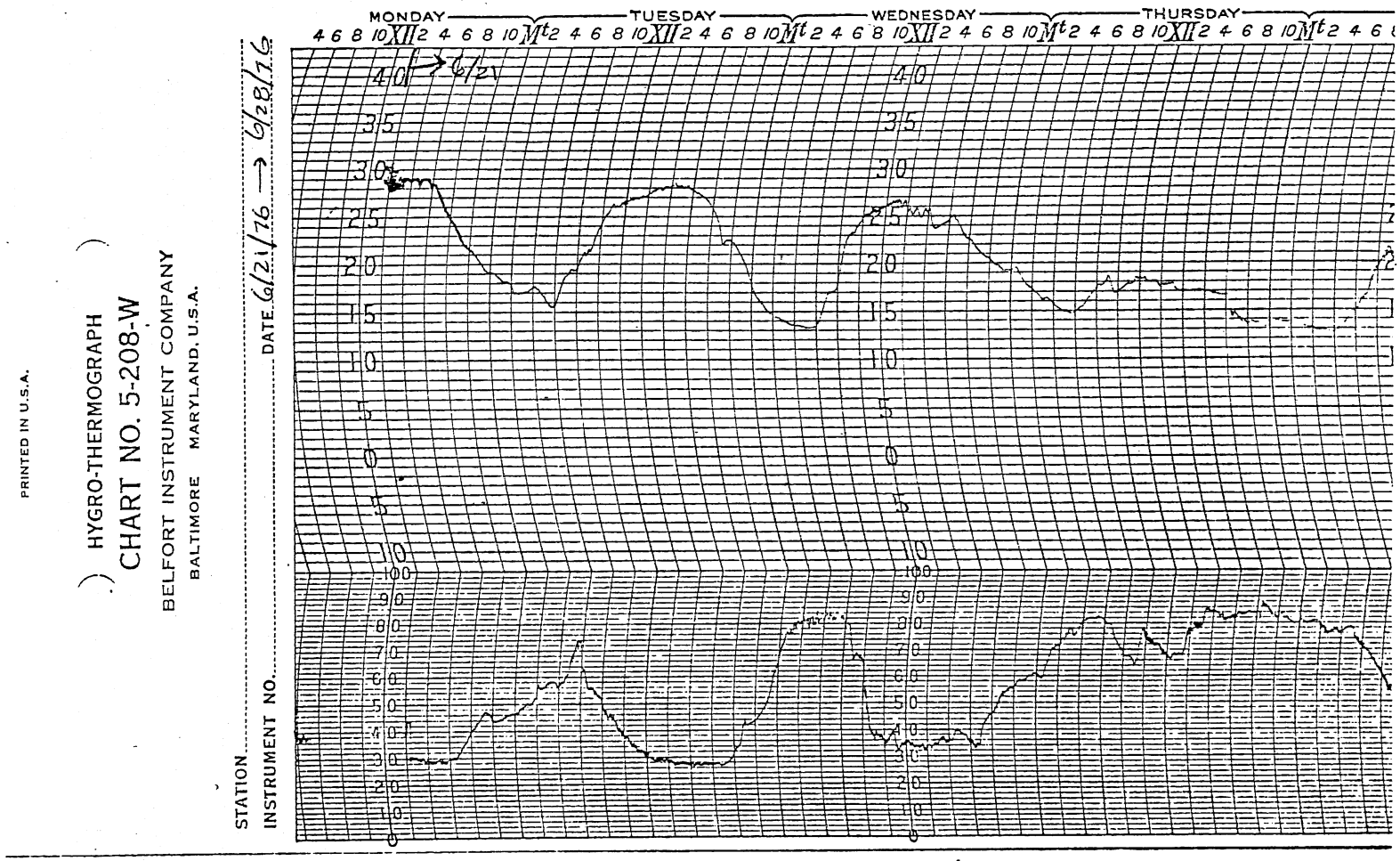

Fig. G-2 - Sample hygrothermograph strip chart for degrees Celcius air temperature (top) and percent relative humidity (bottom).

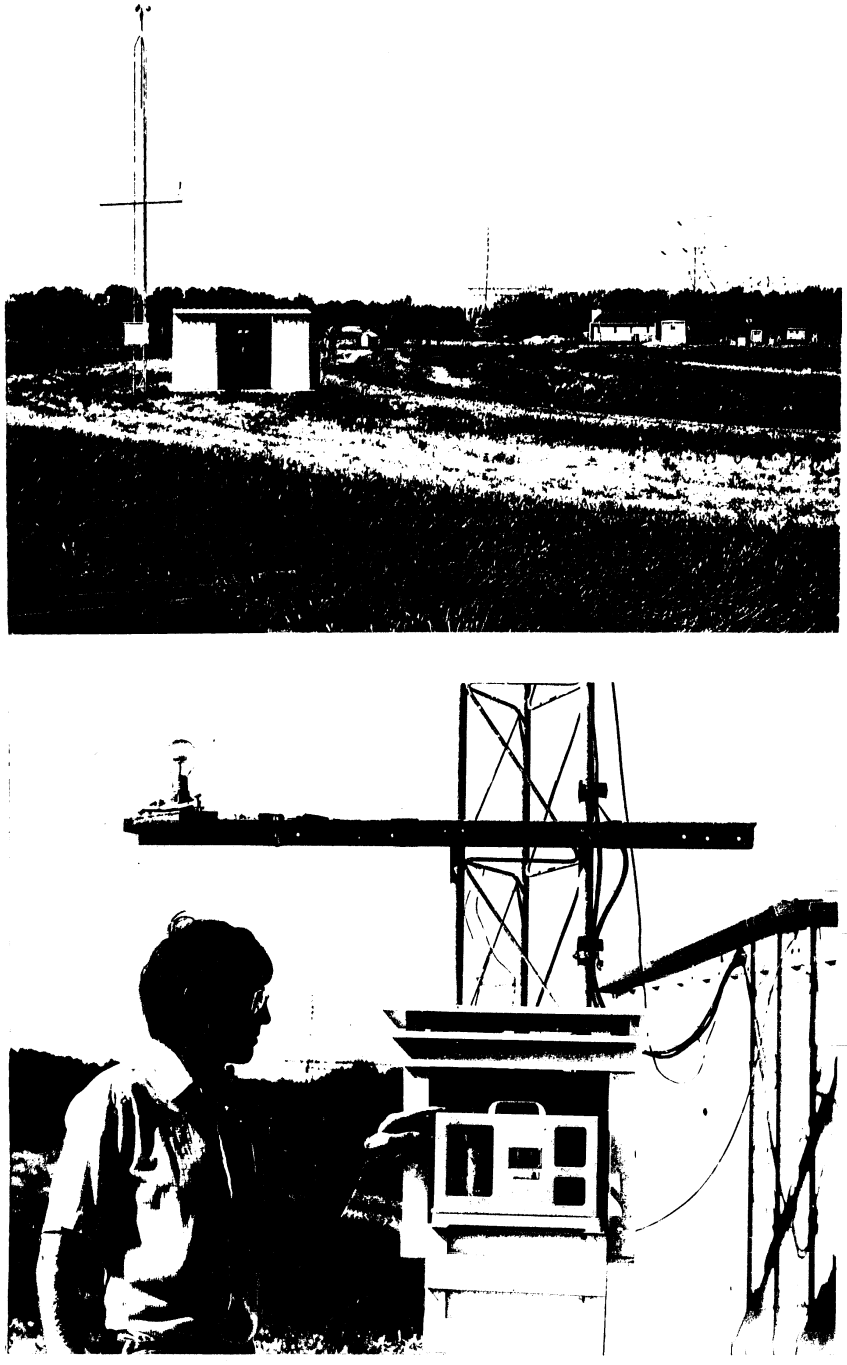

Fig. G-3. Weather station with hygrothermograph and shelter, pyranometer, wind vane, and anemometer. Top - complete weather station. Bottom - hygrothermograph, small weather shelter, and pyranometer.

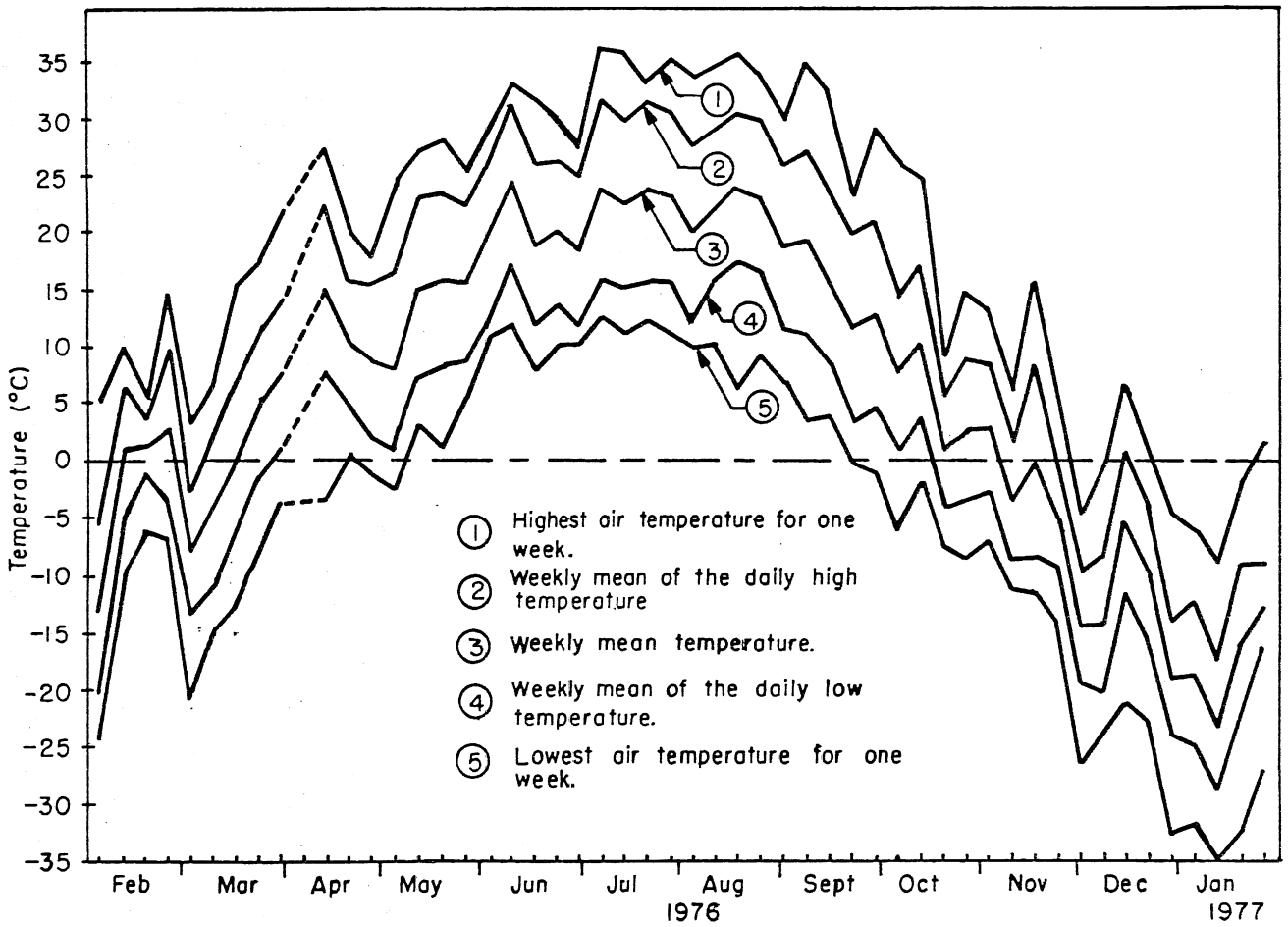

Fig. G-4. One-year cycle of air temperatures. February 1976 through January 1977.

APPENDIX H

SAMPLE OUTPUT FROM PROGRAM WTEMP1

WATER TEMPERATURE STATISTICS

****

WATER TEMPERATURE STUDY

US EPA MONTICELLO ECOLOGICAL RESEARCH STATION

CONDUCTED BY

UNIVERSITY OF MINNESOTA
ST. ANTHONY FALLS HYDRAULIC LABORATORY

STATISTICAL ANALYSIS OF OPERATIONAL WATER TEMPERATURES FOR

CHANNEL 4, STATION 2

NOTES:

PERIOD OF ANALYSIS IS FROM 10/20/76 TO 9/19/77. ALL STATISTICS RECORDED ARE SLIDING 7-DAILY PARAMETERS, COMPUTED FROM THREE-HOURLY DATA. ALL STATISTICS, EXCEPT SKEWNESS, ARE RECORDED IN DEGREES CELCIUS, SKEWNESS IS DIMENSIONLESS. ALL CALENDAR WEEKS START ON SUNDAY.

DATE	CALENDAR DAY/WEEK	DAY OF THE WEEK	MINIMUM TEMPERATURE	PROBABILITIES IN PERCENT 95.0	50.0	5.0	MAXIMUM TEMPERATURE	MEAN	STANDARD DEVIATION	SKEWNESS COEFFICIENT	NO. OF EST. DATA POINTS
10-23-76	297/43	SAT.	4.4	7.0	5.7	4.6	7.2	5.7	.68	.30	0
10-24-76	298/44	SUN.	3.4	6.1	5.4	3.8	6.8	5.3	.71	-.62	0
10-25-76	299/44	MON.	3.4	6.0	5.3	3.7	6.1	5.1	.71	-.54	0
10-26-76	300/44	TUE.	3.4	6.1	5.1	3.7	6.3	5.0	.72	-.39	0
10-27-76	301/44	WED.	3.4	6.5	5.1	3.7	6.7	5.1	.84	-.14	0
10-28-76	302/44	THU.	3.4	6.6	5.1	3.7	6.7	5.2	.91	-.09	0
10-29-76	303/44	FRI.	3.4	6.7	5.1	3.7	6.9	5.3	1.00	-.14	0
10-30-76	304/44	SAT.	3.4	6.9	6.0	3.7	7.0	5.6	1.06	-.59	0
10-31-76	305/45	SUN.	3.6	6.9	6.0	3.9	7.0	5.8	.92	-.71	0
11- 1-76	306/45	MON.	3.4	6.9	6.0	3.6	7.0	5.7	1.06	-.81	0
11- 2-76	307/45	TUE.	3.1	6.9	6.0	3.2	7.0	5.4	1.32	-.56	0
11- 3-76	308/45	WED.	2.7	6.9	5.0	2.9	7.0	4.9	1.52	-.07	0
11- 4-76	309/45	THU.	1.4	6.9	3.8	1.6	7.0	4.3	1.73	.19	0
11- 5-76	310/45	FRI.	.8	6.8	3.3	.9	7.0	3.5	1.84	.40	0
11- 6-76	311/45	SAT.	.7	5.5	2.9	.8	6.2	2.7	1.46	.35	0
11- 7-76	312/46	SUN.	.7	3.8	1.8	.7	4.4	2.1	1.16	.26	0
11- 8-76	313/46	MON.	.6	3.4	1.3	.6	4.4	1.7	1.02	.75	0
11- 9-76	314/46	TUE.	.6	3.1	1.1	.6	3.5	1.5	.86	.85	0
11-10-76	315/46	WED.	.6	3.1	1.0	.6	3.5	1.3	.67	1.71	0
11-11-76	316/46	THU.	.5	3.1	.9	.6	3.5	1.1	.65	2.37	0
11-12-76	317/46	FRI.	.5	3.1	.9	.5	3.5	1.1	.67	2.30	0
11-13-76	318/46	SAT.	.5	3.1	.9	.5	3.5	1.0	.67	2.41	0
11-14-76	319/47	SUN.	.5	3.1	.8	.5	3.5	1.1	.67	2.25	0
11-15-76	320/47	MON.	.5	3.1	.9	.5	3.5	1.1	.69	1.92	0
11-16-76	321/47	TUE.	.5	2.0	.9	.5	2.1	1.1	.47	.81	0
11-17-76	322/47	WED.	.5	2.0	1.0	.5	2.1	1.1	.47	.72	0
11-18-76	323/47	THU.	.5	2.0	1.0	.5	2.1	1.1	.43	.70	0
11-19-76	324/47	FRI.	.6	3.2	1.1	.7	3.6	1.3	.68	1.82	0
11-20-76	325/47	SAT.	.6	3.5	1.3	.7	3.6	1.5	.82	1.38	0
11-21-76	326/48	SUN.	.6	3.5	1.1	.7	3.6	1.5	.84	1.38	0
11-22-76	327/48	MON.	.5	3.5	1.0	.6	3.6	1.4	.88	1.49	0
11-23-76	328/48	TUE.	.5	3.5	.8	.5	3.6	1.2	.90	1.82	0
11-24-76	329/48	WED.	.5	3.5	.8	.5	3.6	1.1	.91	1.96	0
11-25-76	330/48	THU.	.5	3.5	.7	.5	3.6	1.1	.93	2.02	0
11-26-76	331/48	FRI.	.5	3.4	.7	.5	3.5	.9	.69	3.23	0
11-27-76	332/48	SAT.	.5	.8	.7	.5	.8	.7	.09	-.44	0
11-28-76	333/49	SUN.	.5	.8	.7	.5	.8	.7	.08	-.48	0
11-29-76	334/49	MON.	.5	.8	.7	.5	.8	.7	.08	-.83	0
11-30-76	335/49	TUE.	.5	.9	.7	.7	1.0	.7	.07	.75	0
12- 1-76	336/49	WED.	.6	.9	.7	.7	1.0	.7	.07	1.61	0
12- 2-76	337/49	THU.	.5	.9	.7	.6	1.0	.7	.09	.37	0
12- 3-76	338/49	FRI.	.5	.9	.7	.5	1.0	.7	.10	.51	0
12- 4-76	339/49	SAT.	.5	.9	.7	.5	1.0	.7	.12	.51	0
12- 5-76	340/50	SUN.	.5	.9	.6	.5	1.0	.6	.13	.78	0
12- 6-76	341/50	MON.	.4	.9	.6	.5	1.0	.6	.14	1.12	0
12- 7-76	342/50	TUE.	.4	.8	.5	.4	.9	.6	.10	1.28	0
12- 8-76	343/50	WED.	.4	.6	.5	.4	.7	.5	.06	.51	0
12- 9-76	344/50	THU.	.4	.6	.5	.4	.7	.5	.05	.82	0
12-10-76	345/50	FRI.	.4	.5	.5	.4	.7	.5	.05	.75	0
12-11-76	346/50	SAT.	.4	.5	.5	.4	.7	.5	.05	.61	0
12-12-76	347/51	SUN.	.4	.5	.5	.4	.7	.5	.06	.63	0
12-13-76	348/51	MON.	.3	.5	.5	.4	.7	.5	.07	.26	0
12-14-76	349/51	TUE.	.3	.5	.5	.4	.5	.4	.06	-.53	0
12-15-76	350/51	WED.	.3	1.3	.4	.3	1.5	.5	.25	3.19	0
12-16-76	351/51	THU.	.3	1.4	.4	.3	1.5	.5	.32	2.26	0
12-17-76	352/51	FRI.	.2	1.4	.4	.2	1.5	.5	.33	2.14	0
12-18-76	353/51	SAT.	.2	1.4	.4	.2	1.5	.5	.34	2.19	0
12-19-76	354/52	SUN.	.2	1.4	.4	.2	1.5	.5	.35	1.86	0
12-20-76	355/52	MON.	.2	1.5	.4	.2	1.5	.7	.45	.95	0
12-21-76	356/52	TUE.	.2	1.5	.5	.2	1.5	.8	.51	.29	0

DATE	CALENDAR DAY/WEEK	DAY OF THE WEEK	MINIMUM TEMPERATURE	PROBABILITIES IN PERCENT 95.0	50.0	5.0	MAXIMUM TEMPERATURE	MEAN	STANDARD DEVIATION	SKEWNESS COEFFICIENT	NO. OF EST. DATA POINTS
12-22-76	357/52	WED.	.2	1.5	.8	.2	1.6	.9	.53	.02	0
12-23-76	358/52	THU.	.2	1.6	1.4	.2	1.6	1.0	.55	-.33	0
12-24-76	359/52	FRI.	.3	1.6	1.4	.3	1.6	1.2	.48	-.98	0
12-25-76	360/52	SAT.	.3	1.6	1.4	.4	1.6	1.3	.34	-2.02	0
12-26-76	361/ 1	SUN.	.8	1.6	1.4	1.3	1.6	1.4	.12	-2.52	0
12-27-76	362/ 1	MON.	1.3	1.6	1.4	1.3	1.6	1.4	.09	.21	0
12-28-76	363/ 1	TUE.	1.3	1.6	1.5	1.3	1.6	1.5	.08	-.26	0
12-29-76	364/ 1	WED.	1.3	1.8	1.5	1.3	1.9	1.5	.13	.90	0
12-30-76	365/ 1	THU.	1.3	1.8	1.5	1.3	1.9	1.5	.15	.63	0
12-31-76	366/ 1	FRI.	1.0	1.8	1.5	1.1	1.9	1.5	.21	-.20	0
1- 1-77	1/ 1	SAT.	1.0	1.8	1.5	1.1	1.9	1.4	.24	.01	0
1- 2-77	2/ 2	SUN.	1.0	1.8	1.4	1.1	1.9	1.4	.26	.18	0
1- 3-77	3/ 2	MON.	1.0	1.8	1.2	1.1	1.9	1.3	.28	.48	0
1- 4-77	4/ 2	TUE.	1.0	1.8	1.2	1.1	1.9	1.3	.28	.90	0
1- 5-77	5/ 2	WED.	1.0	1.8	1.2	1.1	1.8	1.2	.21	1.68	0
1- 6-77	6/ 2	THU.	1.0	1.3	1.2	1.1	1.3	1.2	.08	.12	0
1- 7-77	7/ 2	FRI.	1.0	1.3	1.2	1.1	1.3	1.2	.07	-.09	0
1- 8-77	8/ 2	SAT.	1.0	1.3	1.2	1.1	1.3	1.2	.07	-.25	0
1- 9-77	9/ 3	SUN.	1.0	1.3	1.2	1.1	1.3	1.2	.07	-.39	3
1-10-77	10/ 3	MON.	1.1	1.3	1.2	1.1	1.4	1.2	.06	.18	3
1-11-77	11/ 3	TUE.	1.1	1.3	1.2	1.1	1.4	1.2	.06	.18	4
1-12-77	12/ 3	WED.	1.1	1.3	1.2	1.1	1.4	1.2	.06	.28	4
1-13-77	13/ 3	THU.	1.1	1.3	1.2	1.1	1.4	1.2	.06	.28	4
1-14-77	14/ 3	FRI.	1.0	1.3	1.2	1.1	1.4	1.2	.07	-.51	6
1-15-77	15/ 3	SAT.	1.0	1.3	1.2	1.0	1.4	1.2	.10	-.67	11
1-16-77	16/ 4	SUN.	1.0	1.3	1.2	1.0	1.4	1.2	.09	-.65	8
1-17-77	17/ 4	MON.	1.0	1.3	1.2	1.0	1.3	1.2	.08	-.82	8
1-18-77	18/ 4	TUE.	.9	1.2	1.2	1.0	1.3	1.1	.09	-.73	7
1-19-77	19/ 4	WED.	.9	1.2	1.1	.9	1.3	1.1	.11	-.46	7
1-20-77	20/ 4	THU.	.9	1.2	1.1	.9	1.3	1.1	.12	-.03	7
1-21-77	21/ 4	FRI.	.9	1.2	1.0	.9	1.3	1.0	.11	.20	5
1-22-77	22/ 4	SAT.	.9	1.2	1.0	.9	1.2	1.0	.10	.05	0
1-23-77	23/ 5	SUN.	.9	1.2	1.0	.9	1.2	1.0	.09	.33	0
1-24-77	24/ 5	MON.	.9	1.1	1.0	.9	1.2	1.0	.08	.38	0
1-25-77	25/ 5	TUE.	.9	1.1	1.0	.9	1.2	1.0	.07	.56	0
1-26-77	26/ 5	WED.	.9	1.1	1.0	.9	1.1	1.0	.07	.24	0
1-27-77	27/ 5	THU.	.9	1.1	1.0	.9	1.1	1.0	.07	.33	0
1-28-77	28/ 5	FRI.	.9	1.1	1.0	.9	1.1	1.0	.07	.41	0
1-29-77	29/ 5	SAT.	.9	1.1	1.0	.9	1.1	1.0	.07	.52	0
1-30-77	30/ 6	SUN.	.9	1.1	1.0	.9	1.1	1.0	.07	.51	0
1-31-77	31/ 6	MON.	.9	1.1	1.0	.9	1.4	1.0	.10	1.70	0
2- 1-77	32/ 6	TUE.	.9	1.1	1.0	.9	1.4	1.0	.10	1.43	0
2- 2-77	33/ 6	WED.	.9	1.1	1.0	.9	1.4	1.0	.10	1.19	0
2- 3-77	34/ 6	THU.	.8	1.1	1.0	.9	1.4	1.0	.11	.83	0
2- 4-77	35/ 6	FRI.	.7	1.1	1.0	.8	1.4	1.0	.11	.58	0
2- 5-77	36/ 6	SAT.	.5	1.1	.9	.6	1.4	.9	.16	-.59	0
2- 6-77	37/ 7	SUN.	.5	1.1	.9	.5	1.4	.9	.18	-.38	0
2- 7-77	38/ 7	MON.	.4	1.1	.9	.5	1.1	.8	.19	-.57	0
2- 8-77	39/ 7	TUE.	.4	1.1	.8	.5	1.1	.8	.19	-.19	0
2- 9-77	40/ 7	WED.	.4	1.0	.7	.5	1.1	.7	.18	.20	0
2-10-77	41/ 7	THU.	.4	1.0	.6	.5	1.1	.7	.17	.60	0
2-11-77	42/ 7	FRI.	.4	.9	.6	.5	1.1	.6	.15	1.02	0
2-12-77	43/ 7	SAT.	.4	.9	.6	.5	1.1	.6	.15	1.06	0
2-13-77	44/ 8	SUN.	.4	1.0	.6	.5	1.1	.6	.16	1.12	0
2-14-77	45/ 8	MON.	.4	1.0	.6	.5	1.1	.6	.17	1.13	0
2-15-77	46/ 8	TUE.	.3	1.0	.6	.4	1.0	.6	.16	.82	0
2-16-77	47/ 8	WED.	.3	1.0	.6	.4	1.0	.6	.17	.82	0
2-17-77	48/ 8	THU.	.3	1.0	.6	.4	1.0	.6	.17	.70	0
2-18-77	49/ 8	FRI.	.3	1.0	.6	.4	1.0	.6	.18	.77	0
2-19-77	50/ 8	SAT.	.3	1.0	.6	.4	1.0	.6	.17	.73	0

DATE	CALENDAR DAY/WEEK	DAY OF THE WEEK	MINIMUM TEMPERATURE	PROBABILITIES IN PERCENT 95.0	50.0	5.0	MAXIMUM TEMPERATURE	MEAN	STANDARD DEVIATION	SKEWNESS COEFFICIENT	NO. OF EST. DATA POINTS
2-20-77	51/ 8	SUN.	.2	.9	.5	.3	1.0	.6	.17	.68	0
2-21-77	52/ 9	MON.	.2	.8	.5	.2	1.2	.5	.20	.83	2
2-22-77	53/ 9	TUE.	.2	.8	.5	.2	1.2	.5	.20	1.01	2
2-23-77	54/ 9	WED.	.2	.8	.4	.2	1.2	.5	.20	1.17	2
2-24-77	55/ 9	THU.	.2	.8	.4	.2	1.2	.5	.20	1.34	2
2-25-77	56/ 9	FRI.	.2	.8	.4	.2	1.2	.5	.21	1.25	2
2-26-77	57/ 9	SAT.	.2	.8	.4	.2	1.2	.4	.19	1.37	2
2-27-77	58/10	SUN.	.2	.9	.4	.2	1.2	.5	.20	1.15	2
2-28-77	59/10	MON.	.2	.8	.5	.2	.9	.5	.16	.64	0
3- 1-77	60/10	TUE.	.3	.8	.5	.3	.9	.5	.15	.64	0
3- 2-77	61/10	WED.	.3	.8	.5	.4	.9	.6	.16	.39	0
3- 3-77	62/10	THU.	.3	.8	.5	.3	.9	.6	.16	.24	0
3- 4-77	63/10	FRI.	.3	.8	.6	.3	.9	.6	.15	.11	0
3- 5-77	64/10	SAT.	.3	.8	.6	.3	.9	.6	.15	.02	0
3- 6-77	65/11	SUN.	.3	.8	.6	.3	.9	.6	.14	-.13	0
3- 7-77	66/11	MON.	.3	.8	.6	.3	.9	.6	.15	-.31	0
3- 8-77	67/11	TUE.	.3	.8	.6	.3	.9	.6	.15	-.30	0
3- 9-77	68/11	WED.	.3	.8	.6	.3	.9	.6	.14	-.18	0
3-10-77	69/11	THU.	.3	.8	.6	.3	.9	.6	.14	.00	0
3-11-77	70/11	FRI.	.3	.9	.6	.3	.9	.6	.15	.31	0
3-12-77	71/11	SAT.	.3	.9	.6	.4	.9	.6	.16	.52	0
3-13-77	72/12	SUN.	.2	.9	.6	.3	.9	.6	.17	.36	0
3-14-77	73/12	MON.	.2	.9	.6	.4	.9	.6	.16	.38	7
3-15-77	74/12	TUE.	.2	.9	.6	.4	.9	.6	.16	.43	15
3-16-77	75/12	WED.	.2	.9	.5	.2	.9	.5	.19	.22	15
3-17-77	76/12	THU.	.2	.9	.5	.2	.9	.5	.21	.22	15
3-18-77	77/12	FRI.	.2	.8	.4	.2	.9	.5	.21	.31	15
3-19-77	78/12	SAT.	.2	.8	.4	.2	.9	.4	.21	.26	15
3-20-77	79/13	SUN.	.2	.8	.5	.2	1.0	.5	.21	.25	15
3-21-77	80/13	MON.	.2	1.5	.4	.2	2.1	.5	.37	2.42	8
3-22-77	81/13	TUE.	.2	3.9	.4	.2	4.0	.8	.97	2.19	0
3-23-77	82/13	WED.	.2	4.4	.6	.2	4.6	1.4	1.55	1.15	0
3-24-77	83/13	THU.	.2	4.5	1.0	.2	4.6	1.9	1.70	.47	0
3-25-77	84/13	FRI.	.2	4.5	2.7	.2	4.6	2.4	1.64	-.07	0
3-26-77	85/13	SAT.	.2	4.5	3.2	.3	4.6	2.7	1.43	-.54	0
3-27-77	86/14	SUN.	.2	4.5	3.2	.3	4.6	3.0	1.16	-.88	0
3-28-77	87/14	MON.	1.6	4.5	3.3	1.8	4.6	3.3	.79	-.30	0
3-29-77	88/14	TUE.	2.1	4.5	3.3	2.2	4.6	3.4	.67	.13	0
3-30-77	89/14	WED.	2.1	4.2	3.2	2.2	4.5	3.2	.57	.31	0
3-31-77	90/14	THU.	2.1	3.8	3.0	2.2	4.2	3.1	.48	.09	0
4- 1-77	91/14	FRI.	2.1	3.8	3.0	2.2	4.2	3.1	.47	.08	0
4- 2-77	92/14	SAT.	2.1	3.9	3.0	2.2	4.2	3.1	.50	.01	0
4- 3-77	93/15	SUN.	2.1	3.9	3.2	2.4	4.2	3.1	.48	-.05	0
4- 4-77	94/15	MON.	2.3	5.2	3.2	2.4	5.5	3.3	.65	1.66	0
4- 5-77	95/15	TUE.	2.3	6.1	3.4	2.4	6.5	3.6	1.03	1.23	0
4- 6-77	96/15	WED.	2.3	8.3	3.5	2.4	8.7	4.2	1.59	1.26	0
4- 7-77	97/15	THU.	2.3	11.2	4.1	2.4	11.4	5.2	2.53	1.06	0
4- 8-77	98/15	FRI.	2.3	12.7	5.5	2.4	13.5	6.4	3.38	.61	0
4- 9-77	99/15	SAT.	2.3	12.7	6.8	2.6	13.5	7.5	3.44	.05	0
4-10-77	100/16	SUN.	3.2	12.7	9.6	3.2	13.5	8.7	3.10	-.36	0
4-11-77	101/16	MON.	4.6	12.7	11.0	5.1	13.5	9.8	2.52	-.79	0
4-12-77	102/16	TUE.	5.9	13.2	11.2	6.0	13.5	10.7	1.87	-1.23	0
4-13-77	103/16	WED.	8.6	13.5	11.4	8.8	13.8	11.6	1.20	-.40	0
4-14-77	104/16	THU.	10.4	14.1	11.8	10.5	14.1	12.1	1.14	.32	1
4-15-77	105/16	FRI.	10.4	14.4	12.5	10.5	14.6	12.4	1.31	.07	6
4-16-77	106/16	SAT.	10.5	14.4	13.2	10.6	14.6	12.9	1.29	-.45	6
4-17-77	107/17	SUN.	10.8	14.4	13.6	11.1	14.6	13.2	1.13	-.79	6
4-18-77	108/17	MON.	10.8	14.4	13.7	11.2	14.6	13.3	1.01	-1.08	6
4-19-77	109/17	TUE.	11.2	14.6	13.8	11.7	14.8	13.6	.82	-1.08	6
4-20-77	110/17	WED.	11.2	14.9	13.9	11.7	15.2	13.7	.84	-1.22	6

DATE	CALENDAR DAY/WEEK	DAY OF THE WEEK	MINIMUM TEMPERATURE	PROBABILITIES IN PERCENT 95.0	50.0	5.0	MAXIMUM TEMPERATURE	MEAN	STANDARD DEVIATION	SKEWNESS COEFFICIENT	NO. OF EST. DATA POINTS
4-21-77	111/17	THU.	11.2	14.9	13.9	11.7	15.2	13.7	.86	-1.10	5
4-22-77	112/17	FRI.	11.2	14.9	13.8	11.7	15.2	13.7	.86	-.90	0
4-23-77	113/17	SAT.	11.2	15.2	13.8	11.7	15.7	13.7	.94	-.47	0
4-24-77	114/18	SUN.	11.2	15.8	13.9	11.7	16.2	14.0	1.11	-.28	0
4-25-77	115/18	MON.	12.6	15.8	14.2	12.8	16.2	14.3	.91	.18	0
4-26-77	116/18	TUE.	12.7	16.4	14.5	13.0	16.9	14.5	.96	.31	0
4-27-77	117/18	WED.	12.7	17.1	14.8	13.0	17.6	14.8	1.16	.32	0
4-28-77	118/18	THU.	12.7	17.2	15.2	13.2	17.6	15.2	1.21	-.06	0
4-29-77	119/18	FRI.	13.2	17.2	15.6	13.5	17.6	15.6	1.07	-.21	0
4-30-77	120/18	SAT.	13.4	17.2	15.6	14.2	17.6	15.8	.90	-.13	0
5- 1-77	121/19	SUN.	13.4	17.2	15.6	14.2	17.6	15.7	.90	-.08	0
5- 2-77	122/19	MON.	14.5	17.6	15.9	14.8	17.9	16.0	.84	.36	0
5- 3-77	123/19	TUE.	14.8	17.7	16.0	14.9	17.9	16.2	.84	.25	0
5- 4-77	124/19	WED.	14.8	17.8	16.3	14.9	18.0	16.3	.86	.15	0
5- 5-77	125/19	THU.	14.8	18.6	16.4	14.9	19.1	16.5	1.03	.53	0
5- 6-77	126/19	FRI.	14.8	18.9	16.6	14.9	19.1	16.7	1.14	.29	0
5- 7-77	127/19	SAT.	14.8	19.1	17.1	14.9	19.3	17.1	1.18	-.01	0
5- 8-77	128/20	SUN.	15.7	19.5	17.5	15.8	19.8	17.5	1.06	.20	0
5- 9-77	129/20	MON.	15.9	20.4	17.8	16.4	21.0	18.0	1.19	.49	0
5-10-77	130/20	TUE.	15.9	22.2	18.4	16.4	22.9	18.6	1.62	.71	0
5-11-77	131/20	WED.	16.4	22.8	18.9	16.7	23.0	19.3	1.81	.42	0
5-12-77	132/20	THU.	17.1	22.8	19.6	17.2	23.0	19.9	1.79	.10	0
5-13-77	133/20	FRI.	17.1	22.9	20.4	17.2	23.3	20.4	1.72	-.17	0
5-14-77	134/20	SAT.	17.8	22.9	21.1	18.2	23.3	20.9	1.46	-.49	0
5-15-77	135/21	SUN.	18.4	23.8	21.4	18.8	24.6	21.5	1.29	-.18	0
5-16-77	136/21	MON.	20.0	24.9	22.0	20.2	25.7	22.1	1.29	.75	0
5-17-77	137/21	TUE.	20.0	24.9	22.3	20.3	25.7	22.3	1.22	.56	0
5-18-77	138/21	WED.	20.0	24.9	22.1	20.3	25.7	22.2	1.29	.60	0
5-19-77	139/21	THU.	19.6	24.9	21.7	19.8	25.7	21.9	1.51	.40	0
5-20-77	140/21	FRI.	18.8	24.9	21.7	19.2	25.7	21.8	1.62	.25	0
5-21-77	141/21	SAT.	18.8	24.9	21.6	19.2	25.7	21.9	1.72	.20	0
5-22-77	142/22	SUN.	18.8	25.4	22.4	19.2	25.8	22.1	1.84	.14	0
5-23-77	143/22	MON.	18.8	25.8	22.4	19.2	26.6	22.2	1.93	.20	0
5-24-77	144/22	TUE.	18.8	25.8	22.4	19.2	26.6	22.3	2.06	.12	0
5-25-77	145/22	WED.	18.8	25.8	23.3	19.2	26.6	22.8	2.06	-.34	0
5-26-77	146/22	THU.	18.8	25.8	23.7	19.2	26.6	23.4	1.78	-.87	0
5-27-77	147/22	FRI.	21.2	25.8	24.0	21.5	26.6	23.9	1.20	-.23	0
5-28-77	148/22	SAT.	21.1	25.8	23.8	22.1	26.6	23.9	1.19	.08	1
5-29-77	149/23	SUN.	20.0	25.8	23.4	20.3	26.6	23.5	1.53	-.35	1
5-30-77	150/23	MON.	20.0	25.5	23.0	20.3	25.8	23.0	1.58	-.13	1
5-31-77	151/23	TUE.	20.0	25.5	22.4	20.3	25.8	22.7	1.54	.26	1
6- 1-77	152/23	WED.	20.0	25.1	22.2	20.3	25.8	22.4	1.41	.58	1
6- 2-77	153/23	THU.	20.0	24.4	22.1	20.3	25.0	22.1	1.16	.60	1
6- 3-77	154/23	FRI.	20.0	23.7	22.0	20.3	24.3	21.9	.88	.15	1
6- 4-77	155/23	SAT.	20.0	23.7	22.0	20.3	24.3	22.0	.91	.13	0
6- 5-77	156/24	SUN.	20.5	23.7	22.2	20.8	24.3	22.2	.80	.26	0
6- 6-77	157/24	MON.	20.0	23.7	22.1	20.7	24.3	22.1	.85	.11	0
6- 7-77	158/24	TUE.	18.7	23.7	22.0	19.1	24.3	21.8	1.20	-.77	0
6- 8-77	159/24	WED.	18.7	23.7	21.9	19.1	24.3	21.8	1.24	-.59	0
6- 9-77	160/24	THU.	18.7	23.3	22.0	19.1	23.5	21.7	1.16	-.84	0
6-10-77	161/24	FRI.	18.7	23.3	21.6	19.1	23.5	21.5	1.17	-.44	0
6-11-77	162/24	SAT.	18.7	23.2	21.3	19.1	23.5	21.4	1.17	-.24	0
6-12-77	163/25	SUN.	18.7	23.2	21.1	19.1	23.5	21.3	1.10	-.07	0
6-13-77	164/25	MON.	18.7	23.2	21.2	19.1	23.5	21.3	1.14	-.09	0
6-14-77	165/25	TUE.	20.0	23.5	21.4	20.3	23.8	21.7	1.03	.28	0
6-15-77	166/25	WED.	20.0	23.3	21.6	20.3	23.8	21.7	.99	.22	0
6-16-77	167/25	THU.	20.0	23.3	21.6	20.3	23.8	21.7	.98	.22	0
6-17-77	168/25	FRI.	20.4	23.3	21.7	20.4	23.8	21.8	.90	.27	0
6-18-77	169/25	SAT.	20.4	23.2	21.7	20.4	23.8	21.8	.82	.29	0
6-19-77	170/26	SUN.	20.4	23.2	21.7	20.4	23.8	21.8	.81	.32	0

DATE	CALENDAR DAY/WEEK	DAY OF THE WEEK	MINIMUM TEMPERATURE	PROBABILITIES IN PERCENT 95.0	50.0	5.0	MAXIMUM TEMPERATURE	MEAN	STANDARD DEVIATION	SKEWNESS COEFFICIENT	NO. OF EST. DATA POINTS
6-20-77	171/26	MON.	20.1	23.9	21.7	20.5	24.6	21.9	.97	.76	0
6-21-77	172/26	TUE.	20.1	25.3	21.8	20.5	25.9	22.2	1.38	1.11	0
6-22-77	173/26	WED.	20.1	25.8	22.1	20.5	26.2	22.6	1.67	.66	0
6-23-77	174/26	THU.	20.1	26.3	22.6	20.5	27.0	23.1	1.94	.32	0
6-24-77	175/26	FRI.	20.1	26.7	24.1	20.5	27.0	23.7	2.03	-.19	0
6-25-77	176/26	SAT.	20.1	26.7	24.3	20.5	27.0	24.0	1.90	-.55	0
6-26-77	177/27	SUN.	20.1	26.7	24.5	20.5	27.0	24.2	1.69	-.75	0
6-27-77	178/27	MON.	21.5	26.7	24.4	21.8	27.0	24.4	1.33	-.10	0
6-28-77	179/27	TUE.	20.4	26.7	24.1	20.9	27.0	23.9	1.68	-.20	0
6-29-77	180/27	WED.	20.4	26.7	23.7	20.9	27.0	23.7	1.69	.09	0
6-30-77	181/27	THU.	20.4	26.3	23.4	20.9	26.7	23.5	1.60	.14	0
7- 1-77	182/27	FRI.	20.4	26.4	23.4	20.9	26.6	23.6	1.66	.18	0
7- 2-77	183/27	SAT.	20.4	26.9	23.7	20.9	27.2	23.8	1.88	.10	0
7- 3-77	184/28	SUN.	20.4	26.9	24.2	20.9	27.2	24.4	2.01	-.25	0
7- 4-77	185/28	MON.	20.4	27.2	25.6	20.9	27.6	24.8	2.08	-.65	0
7- 5-77	186/28	TUE.	21.7	27.2	25.9	21.9	27.6	25.5	1.55	-1.09	0
7- 6-77	187/28	WED.	23.1	27.2	25.9	23.2	27.6	25.7	1.17	-.75	0
7- 7-77	188/28	THU.	23.1	27.2	25.8	23.3	27.6	25.6	1.23	-.55	0
7- 8-77	189/28	FRI.	22.3	27.2	25.3	22.4	27.6	25.2	1.48	-.37	0
7- 9-77	190/28	SAT.	22.3	27.2	25.0	22.4	27.6	25.0	1.47	-.02	0
7-10-77	191/29	SUN.	22.3	27.2	24.4	22.4	27.6	24.6	1.34	.36	0
7-11-77	192/29	MON.	22.3	26.5	24.4	22.4	26.8	24.4	1.14	.11	0
7-12-77	193/29	TUE.	22.3	26.1	24.3	22.4	26.8	24.3	1.01	.12	0
7-13-77	194/29	WED.	22.3	26.9	24.6	22.4	27.5	24.5	1.24	.34	0
7-14-77	195/29	THU.	22.3	26.9	25.0	22.4	27.5	24.9	1.28	-.18	0
7-15-77	196/29	FRI.	23.2	27.6	25.1	23.2	28.7	25.3	1.25	.42	0
7-16-77	197/29	SAT.	23.2	28.7	25.8	23.5	29.0	25.8	1.40	.31	0
7-17-77	198/30	SUN.	23.8	28.7	26.1	24.4	29.0	26.3	1.23	.28	0
7-18-77	199/30	MON.	23.8	28.7	26.3	24.0	29.0	26.3	1.28	.03	0
7-19-77	200/30	TUE.	24.0	28.7	26.4	24.6	29.0	26.4	1.19	.15	0
7-20-77	201/30	WED.	24.0	28.7	26.1	24.5	29.0	26.2	1.21	.35	0
7-21-77	202/30	THU.	24.0	28.7	26.0	24.3	29.0	26.1	1.31	.35	0
7-22-77	203/30	FRI.	24.0	28.5	25.9	24.3	29.0	26.0	1.22	.39	0
7-23-77	204/30	SAT.	22.4	27.3	25.4	23.7	28.0	25.5	1.14	-.11	0
7-24-77	205/31	SUN.	22.4	27.0	25.0	23.3	27.1	25.0	1.10	-.02	0
7-25-77	206/31	MON.	21.7	26.7	24.8	22.0	27.0	24.7	1.31	-.36	0
7-26-77	207/31	TUE.	21.7	26.6	24.6	22.0	27.0	24.4	1.33	-.16	0
7-27-77	208/31	WED.	21.7	26.6	24.0	22.0	27.0	24.3	1.30	.18	0
7-28-77	209/31	THU.	21.0	26.4	23.8	21.4	26.7	23.7	1.44	.08	0
7-29-77	210/31	FRI.	20.1	25.6	23.3	20.5	26.5	23.1	1.47	-.01	0
7-30-77	211/31	SAT.	20.1	25.6	22.8	20.5	26.5	22.8	1.43	.22	0
7-31-77	212/32	SUN.	20.1	25.6	22.5	20.5	26.5	22.8	1.49	.41	0
8- 1-77	213/32	MON.	20.1	25.6	22.8	20.5	26.5	22.8	1.45	.38	0
8- 2-77	214/32	TUE.	20.1	24.8	22.4	20.5	25.4	22.5	1.26	.22	0
8- 3-77	215/32	WED.	20.1	24.7	22.0	20.2	25.4	22.2	1.21	.42	0
8- 4-77	216/32	THU.	20.1	24.9	22.4	20.2	25.4	22.4	1.34	.35	0
8- 5-77	217/32	FRI.	20.2	25.3	22.8	20.7	25.4	22.8	1.32	.26	0
8- 6-77	218/32	SAT.	20.2	25.3	22.8	20.7	25.4	22.9	1.28	.16	0
8- 7-77	219/33	SUN.	20.2	25.0	22.6	20.7	25.4	22.7	1.25	.25	0
8- 8-77	220/33	MON.	19.5	25.0	22.3	20.1	25.4	22.4	1.41	.26	0
8- 9-77	221/33	TUE.	19.2	25.0	22.2	19.5	25.4	22.2	1.56	.13	0
8-10-77	222/33	WED.	19.2	25.0	22.3	19.5	25.4	22.2	1.51	.15	0
8-11-77	223/33	THU.	19.2	24.8	22.1	19.5	25.4	22.0	1.42	.16	0
8-12-77	224/33	FRI.	19.2	23.9	21.6	19.5	24.3	21.6	1.23	.15	0
8-13-77	225/33	SAT.	19.0	23.0	21.0	19.2	23.3	21.1	1.15	.10	0
8-14-77	226/34	SUN.	19.0	23.0	20.8	19.2	23.3	20.9	1.15	.36	0
8-15-77	227/34	MON.	17.9	23.0	20.5	18.9	23.3	20.7	1.26	.20	0
8-16-77	228/34	TUE.	17.9	22.8	20.5	18.5	23.3	20.6	1.24	.15	0
8-17-77	229/34	WED.	17.9	22.5	20.3	18.5	23.3	20.4	1.15	.23	0
8-18-77	230/34	THU.	17.9	22.3	20.4	18.5	22.4	20.4	1.08	-.07	0

DATE	CALENDAR DAY/WEEK	DAY OF THE WEEK	MINIMUM TEMPERATURE	PROBABILITIES IN PERCENT 95.0	50.0	5.0	MAXIMUM TEMPERATURE	MEAN	STANDARD DEVIATION	SKEWNESS COEFFICIENT	NO. OF EST. DATA POINTS
8-19-77	231/34	FRI.	17.9	22.3	20.4	18.5	22.4	20.4	1.10	-.10	0
8-20-77	232/34	SAT.	17.9	22.3	20.5	18.5	22.4	20.4	1.10	-.15	0
8-21-77	233/35	SUN.	17.9	22.3	20.4	18.5	22.4	20.4	1.14	-.10	0
8-22-77	234/35	MON.	18.6	22.3	20.4	18.8	22.4	20.4	1.13	.12	0
8-23-77	235/35	TUE.	18.7	22.3	20.3	18.8	22.4	20.3	1.11	.24	0
8-24-77	236/35	WED.	18.7	22.3	20.5	18.8	22.3	20.4	1.12	.04	0
8-25-77	237/35	THU.	18.7	22.0	20.6	18.8	22.3	20.3	1.05	-.07	0
8-26-77	238/35	FRI.	18.7	22.0	20.5	18.8	22.3	20.2	1.03	.04	0
8-27-77	239/35	SAT.	18.7	22.0	20.3	18.8	22.3	20.2	.98	.14	0
8-28-77	240/36	SUN.	18.8	22.0	20.3	18.8	22.3	20.3	.96	.12	0
8-29-77	241/36	MON.	18.8	22.0	20.3	19.0	22.3	20.4	.85	.16	0
8-30-77	242/36	TUE.	18.5	22.0	20.3	19.0	22.3	20.4	.85	.22	0
8-31-77	243/36	WED.	18.5	21.4	20.0	19.0	21.8	20.1	.74	.28	0
9- 1-77	244/36	THU.	18.5	21.3	19.8	19.0	21.8	19.9	.64	.79	0
9- 2-77	245/36	FRI.	18.4	21.2	19.8	18.7	21.8	19.8	.63	.52	0
9- 3-77	246/36	SAT.	18.4	21.2	19.8	18.7	21.8	19.8	.66	.51	0
9- 4-77	247/37	SUN.	18.4	20.7	19.8	18.6	20.9	19.7	.57	-.28	0
9- 5-77	248/37	MON.	18.1	20.8	19.7	18.2	21.0	19.6	.70	-.24	0
9- 6-77	249/37	TUE.	18.0	20.8	19.6	18.1	21.0	19.5	.78	-.24	0
9- 7-77	250/37	WED.	17.0	20.8	19.5	17.5	21.0	19.3	.98	-.38	0
9- 8-77	251/37	THU.	17.0	20.8	19.1	17.5	21.0	19.1	.99	.01	0
9- 9-77	252/37	FRI.	17.0	20.8	18.7	17.5	21.0	18.9	1.02	.37	0
9-10-77	253/37	SAT.	17.0	20.6	18.5	17.4	21.0	18.7	.93	.70	0
9-11-77	254/38	SUN.	17.0	21.5	18.4	17.2	22.2	18.7	1.18	1.36	0
9-12-77	255/38	MON.	17.0	22.1	18.5	17.2	22.2	19.0	1.54	.99	0
9-13-77	256/38	TUE.	17.0	22.1	18.8	17.2	22.2	19.3	1.69	.47	0
9-14-77	257/38	WED.	17.1	22.1	19.3	17.5	22.2	19.8	1.68	-.02	0
9-15-77	258/38	THU.	17.1	22.1	20.9	17.5	22.2	20.1	1.66	-.53	0
9-16-77	259/38	FRI.	17.1	22.1	20.9	17.7	22.2	20.4	1.41	-1.04	4

WATER TEMPERATURE DATA

NUMBER OF DAYS = 335
NUMBER OF STATIONS TO BE AVERAGED = 1
CHANNEL NUMBER = 4
STATION NUMBER = 2

****

DATE	HOUR= 00	03	06	09	12	15	18	21	DATE	HOUR= 00	03	06	09	12	15	18	21
10-20-76	7.0	6.7	6.5	6.4	6.6	7.2	7.2	7.0	10-21-76	6.8	6.4	6.1	5.9	6.0	6.1	5.9	5.8
10-22-76	5.6	5.3	5.0	4.7	5.0	6.0	5.9	5.9	10-23-76	5.6	5.4	5.3	5.2	5.3	5.7	5.8	5.9
10-24-76	5.8	5.7	5.5	5.3	5.4	5.9	6.1	6.1	10-25-76	6.0	5.8	5.6	5.4	5.3	5.5	5.5	5.3
10-26-76	5.0	4.7	4.5	4.4	4.6	4.8	4.8	4.8	10-27-76	4.5	4.1	3.8	3.4	3.7	4.4	4.6	4.5
10-28-76	4.3	4.0	3.8	3.6	3.9	4.8	5.1	5.2	10-29-76	5.1	4.9	4.8	4.7	5.0	5.8	6.2	6.3
10-30-76	6.2	6.1	6.0	5.8	6.0	6.5	6.7	6.7	10-31-76	6.6	6.2	6.0	5.7	6.1	6.6	6.6	6.5
11- 1-76	6.3	6.0	5.8	5.8	6.2	6.7	6.9	6.9	11- 2-76	6.8	6.7	6.6	6.4	6.7	7.0	6.9	6.6
11- 3-76	6.2	5.8	5.4	5.1	4.9	4.8	4.5	4.3	11- 4-76	4.0	3.8	3.6	3.4	3.4	3.8	3.8	3.7
11- 5-76	3.6	3.4	3.2	3.1	3.3	4.4	3.2	3.1	11- 6-76	3.0	2.9	2.7	2.7	2.9	3.1	3.0	2.9
11- 7-76	2.6	2.3	1.9	1.6	1.7	1.9	1.6	1.4	11- 8-76	1.1	.9	.8	.8	1.0	1.1	1.0	1.0
11- 9-76	1.0	.9	.8	.7	1.0	1.3	1.4	1.3	11-10-76	1.1	.9	.8	.7	.9	1.0	.9	.7
11-11-76	.6	.6	.6	.6	1.5	1.7	.9	1.2	11-12-76	1.0	.7	3.5	3.1	1.9	2.0	3.4	2.0
11-13-76	1.6	1.2	1.3	1.0	.9	1.2	.9	.6	11-14-76	.6	.6	.6	.6	.6	.8	.6	.5
11-15-76	.5	.5	.5	.5	.7	1.0	.9	.8	11-16-76	.7	.7	.7	.7	.9	1.2	1.0	.9
11-17-76	.6	.7	.7	.7	1.0	1.5	1.4	1.3	11-18-76	.8	1.0	1.0	1.1	1.6	2.0	2.1	2.0
11-19-76	1.8	1.6	1.4	1.3	1.6	2.1	2.0	1.8	11-20-76	1.6	1.3	1.0	1.0	1.1	1.2	1.3	1.3
11-21-76	1.2	1.1	1.0	.9	1.0	1.0	1.0	.9	11-22-76	.8	.8	.8	1.3	2.9	3.2	3.6	3.5
11-23-76	3.4	3.4	3.5	2.8	1.5	1.1	.9	.8	11-24-76	.8	.7	.7	.7	.8	.8	.8	.6
11-25-76	.6	.6	.6	.5	.6	.7	.6	.6	11-26-76	.6	.6	.6	.6	.6	.6	.5	.5
11-27-76	.5	.7	.8	.7	.8	.8	.8	.8	11-28-76	.7	.7	.7	.7	.7	.8	.7	.7
11-29-76	.7	.7	.7	.8	.8	.8	.7	.7	11-30-76	.7	.7	.7	.7	.7	.8	.8	.8
12- 1-76	.7	.7	.7	.7	.7	.7	.7	.7	12- 2-76	.7	.7	.7	.7	.7	.7	.7	.8
12- 3-76	.9	.9	1.0	.8	.8	.7	.7	.8	12- 4-76	.9	.8	.8	.7	.7	.7	.7	.6
12- 5-76	.6	.5	.6	.6	.6	.6	.6	.5	12- 6-76	.6	.6	.6	.6	.6	.6	.6	.5
12- 7-76	.5	.5	.5	.5	.5	.5	.5	.5	12- 8-76	.5	.5	.5	.5	.5	.5	.5	.5
12- 9-76	.5	.5	.5	.4	.5	.4	.5	.5	12-10-76	.5	.4	.4	.5	.5	.7	.5	.5
12-11-76	.5	.5	.5	.5	.5	.5	.5	.5	12-12-76	.5	.5	.5	.4	.5	.5	.5	.5
12-13-76	.5	.4	.4	.4	.5	.5	.5	.5	12-14-76	.5	.5	.5	.5	.5	.5	.4	.4
12-15-76	.4	.4	.4	.4	.5	.4	.4	.4	12-16-76	.4	.4	.3	.3	.4	.4	.4	.4
12-17-76	.4	.4	.4	.4	.5	.4	.5	.4	12-18-76	.4	.4	.3	.6	1.2	1.5	1.5	1.3
12-19-76	.5	.3	.4	1.1	1.4	1.4	.5	.3	12-20-76	.3	.3	.2	.2	.2	.3	.3	.3
12-21-76	.3	.3	.3	.3	.4	.4	.4	.4	12-22-76	.3	.3	.4	.4	.5	.9	.9	.8
12-23-76	.8	1.3	1.3	1.4	1.4	1.5	1.5	1.5	12-24-76	1.4	1.4	1.4	1.4	1.4	1.4	1.4	1.4
12-25-76	1.4	1.4	1.5	1.5	1.5	1.6	1.5	1.6	12-26-76	1.6	1.5	1.5	1.5	1.6	1.6	1.6	1.4
12-27-76	1.4	1.4	1.5	1.5	1.5	1.5	1.4	1.4	12-28-76	1.5	1.5	1.5	1.4	1.3	1.4	1.4	1.4
12-29-76	1.4	1.5	1.5	1.4	1.3	1.3	1.3	1.3	12-30-76	1.4	1.3	1.4	1.4	1.4	1.5	1.5	1.6
12-31-76	1.5	1.5	1.5	1.5	1.5	1.5	1.5	1.5	1- 1-77	1.6	1.7	1.7	1.7	1.8	1.7	1.8	1.9
1- 2-77	1.8	1.7	1.8	1.8	1.7	1.7	1.6	1.6	1- 3-77	1.1	1.0	1.2	1.1	1.1	1.1	1.1	1.1
1- 4-77	1.1	1.1	1.2	1.1	1.2	1.2	1.2	1.3	1- 5-77	1.2	1.1	1.1	1.1	1.1	1.1	1.1	1.1
1- 6-77	1.0	1.1	1.2	1.2	1.1	1.1	1.1	1.1	1- 7-77	1.2	1.2	1.2	1.1	1.2	1.3	1.3	1.3
1- 8-77	1.3	1.3	1.3	1.2	1.2	1.2	1.2	1.2	1- 9-77	1.2	1.2	1.2	1.3	1.2	1.2	1.2	1.2
1-10-77	1.2	1.2	1.2	1.2	1.2	1.2	1.2	1.2	1-11-77	1.2	1.2	1.2	1.2	1.2	1.2	1.2	1.3
1-12-77	1.3	101.1	101.1	101.1	1.3	1.3	1.3	1.3	1-13-77	1.2	1.2	1.3	1.3	1.3	1.4	1.3	1.3
1-14-77	1.3	1.3	101.1	1.3	1.2	1.2	1.2	1.2	1-15-77	1.2	1.1	1.2	1.2	1.2	1.2	1.2	1.2
1-16-77	1.2	1.2	1.2	1.2	1.2	1.2	1.2	1.3	1-17-77	1.2	1.2	1.2	1.2	1.2	1.2	101.0	101.0
1-18-77	101.0	101.0	101.0	101.0	101.0	1.3	1.2	1.2	1-19-77	1.2	1.1	1.2	1.2	1.2	1.2	1.1	1.0
1-20-77	1.1	1.1	1.1	1.2	1.2	1.2	1.2	1.1	1-21-77	1.1	1.0	1.1	1.1	1.0	1.1	1.0	.9
1-22-77	.9	.9	.9	1.2	1.0	1.0	.9	.9	1-23-77	1.0	.9	.9	.9	.9	1.0	1.0	.9
1-24-77	1.0	.9	.9	1.1	1.1	1.1	1.0	1.0	1-25-77	1.0	1.1	1.0	1.1	1.1	1.1	1.0	1.0
1-26-77	1.0	1.0	1.0	.9	.9	1.0	.9	1.0	1-27-77	1.0	1.0	.9	1.0	1.0	1.0	1.0	1.0

1-28-77	1.0	1.0	1.0	1.0	1.0	1.0	.9	.9	1-29-77	.9	1.0	1.0	.9	.9	.9	.9	.9
1-30-77	.9	.9	.9	.9	1.0	.9	.9	.9	1-31-77	.9	.9	.9	1.0	1.1	1.1	1.0	.9
2- 1-77	.9	.9	1.0	1.1	1.1	1.1	1.1	1.0	2- 2-77	.9	.9	.9	1.0	1.1	1.1	1.1	1.0
2- 3-77	.9	.9	.9	1.0	1.4	1.1	1.1	1.0	2- 4-77	1.0	1.0	1.0	1.1	1.1	1.1	1.0	.9
2- 5-77	.9	.9	.9	.9	1.1	1.1	1.1	1.0	2- 6-77	.8	.8	.9	.9	1.1	1.0	1.0	.9
2- 7-77	.9	.9	.9	1.0	1.0	.9	1.0	.7	2- 8-77	.6	.5	.5	.7	.9	.8	.8	.6
2- 9-77	.5	.6	.6	.8	.9	.9	.8	.6	2-10-77	.6	.5	.4	.8	.9	.8	.7	.6
2-11-77	.6	.7	.6	.9	1.1	.6	.6	.6	2-12-77	.6	.6	.5	.6	.6	.6	.5	.5
2-13-77	.5	.5	.5	.5	.7	.6	.5	.5	2-14-77	.5	.5	.5	.6	.7	.8	.6	.5
2-15-77	.5	.5	.5	.7	1.0	.9	.8	.5	2-16-77	.5	.6	.6	.9	1.0	.9	.7	.5
2-17-77	.5	.5	.4	.7	1.0	.9	.8	.6	2-18-77	.6	.3	.4	.8	.8	.7	.6	.6
2-19-77	.6	.6	.6	.5	.5	.5	.5	.4	2-20-77	.5	.4	.4	.5	.7	.7	.4	.4
2-21-77	.4	.5	.5	.5	.7	.6	.5	.4	2-22-77	.4	.5	.5	.8	1.0	.8	.7	.6
2-23-77	.5	.5	.5	.3	.4	.4	.3	.2	2-24-77	.2	.2	.2	1.2	100.6	100.3	.2	.2
2-25-77	.2	.2	.2	.3	.5	.5	.6	.4	2-26-77	.3	.3	.4	.5	.5	.4	.4	.6
2-27-77	.5	.5	.4	.5	.4	.4	.4	.4	2-28-77	.4	.4	.4	.6	.8	.8	.6	.4
3- 1-77	.3	.4	.5	.7	.8	.7	.5	.4	3- 2-77	.4	.3	.5	.6	.9	.9	.5	.5
3- 3-77	.5	.4	.5	.7	.6	.6	.6	.5	3- 4-77	.5	.6	.5	.7	.8	.7	.7	.7
3- 5-77	.7	.7	.7	.8	.8	.6	.5	.4	3- 6-77	.3	.3	.4	.5	.5	.6	.5	.5
3- 7-77	.5	.6	.6	.8	.7	.7	.6	.5	3- 8-77	.4	.3	.4	.6	.8	.7	.7	.7
3- 9-77	.6	.5	.6	.8	.9	.6	.6	.5	3-10-77	.5	.3	.3	.7	.8	.7	.6	.6
3-11-77	.6	.6	.6	.8	.8	.8	.6	.6	3-12-77	.6	.6	.6	.5	.6	.6	.5	.5
3-13-77	.5	.5	.4	.5	.4	.4	.4	.4	3-14-77	.4	.5	.5	.5	.9	.9	.6	.5
3-15-77	.5	.4	.4	.8	.9	.8	.5	.4	3-16-77	.4	.4	.2	.6	.9	.8	.6	.6
3-17-77	.5	100.6	100.5	100.7	100.8	100.8	100.7	100.6	3-18-77	100.6	100.6	100.6	100.7	100.7	100.7	100.6	100.4
3-19-77	.4	.3	.2	.2	.3	.3	.2	.2	3-20-77	.3	.3	.3	.3	.3	.2	.2	.2
3-21-77	.2	.2	.2	.3	.6	.6	.4	.3	3-22-77	.2	.2	.2	.4	.6	.6	.6	.6
3-23-77	.6	.6	.6	.6	1.0	.7	.6	.4	3-24-77	.2	.2	.3	.5	1.0	1.5	2.1	1.7
3-25-77	1.8	1.6	1.7	2.4	3.1	3.9	4.0	3.9	3-26-77	4.1	4.3	4.4	4.3	4.3	4.4	4.6	4.5
3-27-77	4.2	3.8	3.5	3.3	3.7	4.5	4.5	4.0	3-28-77	3.7	3.7	3.6	3.6	3.3	3.3	3.3	3.3
3-29-77	3.2	3.2	3.0	2.9	3.0	3.1	3.1	2.8	3-30-77	2.5	2.3	2.2	2.2	2.8	3.2	3.0	2.8
3-31-77	2.6	2.6	2.4	2.1	3.3	4.2	4.1	3.7	4- 1-77	3.5	3.4	3.2	3.1	2.9	3.0	2.9	2.8
4- 2-77	2.7	2.6	2.5	2.4	2.6	3.5	3.7	3.2	4- 3-77	3.0	3.0	3.0	2.9	3.0	3.6	3.8	3.6
4- 4-77	3.5	3.4	3.4	3.3	3.2	3.6	3.7	3.4	4- 5-77	3.4	2.9	2.4	2.6	3.4	3.9	3.6	3.2
4- 6-77	2.9	2.6	2.4	2.3	3.0	3.5	3.4	3.3	4- 7-77	3.2	3.2	3.2	3.2	4.3	5.5	5.5	5.1
4- 8-77	5.1	5.1	4.8	4.6	5.3	6.2	6.5	6.1	4- 9-77	6.0	5.9	5.9	6.0	7.0	8.3	8.7	8.6
4-10-77	8.6	8.7	8.8	9.0	10.2	11.4	11.4	11.2	4-11-77	11.2	11.3	11.4	12.0	12.8	13.5	12.7	11.6
4-12-77	11.5	11.5	10.8	10.4	11.0	11.4	11.2	11.0	4-13-77	10.7	10.6	10.5	10.5	11.9	12.7	12.7	12.0
4-14-77	11.7	11.8	11.7	11.6	11.4	11.1	11.1	11.2	4-15-77	11.2	11.0	10.8	11.2	12.1	13.2	13.2	13.0
4-16-77	13.0	12.8	12.5	12.5	12.6	13.5	13.8	13.8	4-17-77	13.9	14.0	14.1	114.1	14.1	14.0	13.6	13.4
4-18-77	113.6	113.8	114.0	114.2	114.4	14.6	14.4	14.2	4-19-77	14.0	13.9	13.7	13.6	14.0	14.6	14.4	14.2
4-20-77	14.2	14.2	13.9	13.7	13.5	13.4	13.8	12.3	4-21-77	12.0	11.7	11.2	11.4	12.6	13.8	13.9	13.4
4-22-77	13.4	13.2	12.8	12.6	13.2	14.6	14.8	14.4	4-23-77	14.2	14.0	13.5	13.4	14.4	15.2	15.2	14.4
4-24-77	14.1	14.0	13.4	12.8	13.6	14.5	14.7	13.9	4-25-77	13.6	13.5	13.0	12.7	13.6	14.5	14.5	14.0
4-26-77	13.9	13.9	13.5	13.2	14.0	15.2	15.7	15.4	4-27-77	15.1	15.1	14.8	14.6	15.3	16.2	16.2	15.6
4-28-77	15.0	14.5	14.0	13.4	14.2	15.5	15.7	15.1	4-29-77	15.0	15.0	14.7	14.5	15.2	16.4	16.9	16.4
4-30-77	16.0	15.9	15.6	15.3	16.0	17.2	17.6	17.1	5- 1-77	16.7	16.5	16.3	16.1	15.9	17.0	17.3	16.7
5- 2-77	16.0	15.6	15.3	15.2	15.8	16.8	17.2	16.8	5- 3-77	16.6	16.4	16.1	15.6	15.4	15.4	15.4	15.3
5- 4-77	15.2	15.0	14.9	14.8	14.9	15.6	15.9	15.8	5- 5-77	15.8	15.8	15.7	15.7	16.6	17.6	17.9	17.5
5- 6-77	17.0	16.7	16.5	16.4	17.2	17.7	17.8	17.4	5- 7-77	17.1	16.7	16.2	15.9	16.4	17.4	18.0	17.6
5- 8-77	16.8	16.4	16.4	16.7	17.0	18.9	19.1	18.5	5- 9-77	18.0	17.5	17.2	17.1	17.8	18.9	19.1	18.4
5-10-77	17.7	17.2	17.1	17.2	18.0	19.0	19.3	18.8	5-11-77	18.5	18.2	17.9	17.8	18.5	19.5	19.8	19.5
5-12-77	19.2	18.9	18.5	18.4	19.3	20.4	21.0	20.7	5-13-77	20.4	20.3	20.2	20.3	21.3	22.6	22.9	22.1
5-14-77	21.4	21.1	20.9	21.0	22.0	23.0	22.8	22.0	5-15-77	21.4	21.4	21.0	21.2	22.2	22.7	22.3	21.6
5-16-77	20.7	20.2	20.0	20.3	21.4	22.7	23.3	22.9	5-17-77	22.1	21.6	21.7	21.6	21.7	22.0	22.5	22.2
5-18-77	21.6	21.2	21.0	21.4	22.6	23.9	24.6	23.8	5-19-77	23.1	22.7	22.6	22.8	23.8	25.2	25.7	24.9
5-20-77	23.8	23.2	23.1	22.9	22.8	23.0	22.9	22.6	5-21-77	21.6	21.0	20.7	20.8	21.1	21.1	20.6	20.3
5-22-77	20.0	19.8	19.6	19.7	19.9	20.1	20.4	20.0	5-23-77	19.6	19.2	18.8	19.0	20.2	21.9	22.5	22.2
5-24-77	21.5	21.2	21.2	21.6	22.8	24.2	24.6	24.0	5-25-77	23.3	22.7	22.4	22.6	23.8	25.3	25.8	24.8
5-26-77	23.8	23.4	23.3	23.4	24.4	26.6	25.8	24.9	5-27-77	23.9	23.4	23.2	23.3	24.4	25.6	25.2	24.2
5-28-77	23.4	23.0	22.8	23.1	24.0	24.9	25.5	24.9	5-29-77	24.3	24.0	23.7	23.7	24.6	25.5	25.8	25.0
5-30-77	24.1	23.4	23.0	22.9	24.0	25.0	25.0	24.2	5-31-77	22.9	22.4	22.2	22.2	22.4	122.1	21.8	21.1
6- 1-77	20.7	20.2	20.0	20.3	21.3	21.9	21.8	21.4	6- 2-77	21.0	20.8	20.5	20.6	21.3	22.3	22.6	22.2
6- 3-77	21.8	21.5	21.2	21.0	21.3	22.2	22.6	22.4	6- 4-77	22.1	22.1	21.7	21.9	22.6	22.4	22.6	22.0
6- 5-77	21.6	21.6	21.4	21.2	22.4	23.8	24.3	23.7	6- 6-77	23.0	22.4	22.0	21.5	22.1	23.0	23.0	22.5
6- 7-77	22.3	22.0	21.8	21.7	22.3	23.4	23.2	22.8	6- 8-77	22.4	22.2	21.8	21.5	22.2	23.0	23.3	22.7

6- 9-77	22.1	21.5	21.0	20.7	21.0	20.9	20.4	20.0	6-10-77	19.7	19.2	18.8	18.7	19.3	20.9	21.8	21.7
6-11-77	21.4	21.2	21.0	21.2	22.1	23.2	23.5	22.8	6-12-77	22.0	21.3	21.0	21.1	22.0	23.0	22.9	22.0
6-13-77	21.0	20.3	20.0	20.0	20.4	21.2	21.8	21.5	6-14-77	20.9	20.6	20.5	20.8	22.0	23.2	23.1	23.0
6-15-77	22.4	21.1	21.8	21.3	21.0	20.9	21.2	20.9	6-16-77	20.5	20.4	20.4	20.4	21.2	22.4	23.1	22.8
6-17-77	22.3	22.8	21.7	21.9	22.8	23.8	23.6	22.8	6-18-77	22.1	21.6	21.1	21.1	21.7	22.7	22.8	22.2
6-19-77	21.7	21.2	21.2	21.2	22.1	22.8	22.8	22.2	6-20-77	21.0	21.4	21.0	20.9	21.6	22.1	22.4	21.9
6-21-77	21.4	21.1	21.0	21.5	22.1	22.7	22.5	22.1	6-22-77	21.8	21.6	21.6	21.4	21.2	21.0	21.0	20.8
6-23-77	20.5	20.3	20.1	20.5	21.8	23.6	24.6	24.4	6-24-77	23.9	23.6	23.7	24.1	24.9	25.8	25.9	25.2
6-25-77	24.7	24.2	23.6	23.5	24.5	25.8	26.2	25.6	6-26-77	24.6	24.5	24.2	24.3	25.3	26.9	27.0	26.2
6-27-77	25.6	25.2	25.0	25.2	26.3	26.7	26.2	25.8	6-28-77	25.6	25.2	24.6	24.0	23.5	23.3	23.5	22.9
6-29-77	22.2	21.8	21.5	21.7	23.1	24.6	24.6	24.1	6-30-77	23.3	23.1	23.1	23.0	23.6	24.1	23.8	22.5
7- 1-77	21.6	21.0	20.5	20.4	21.2	22.0	22.3	22.2	7- 2-77	22.0	21.9	21.7	21.8	22.7	23.9	24.3	24.0
7- 3-77	23.6	23.1	23.1	23.2	24.1	25.4	26.4	26.2	7- 4-77	25.8	25.6	25.6	25.9	26.6	26.4	26.5	26.2
7- 5-77	26.8	25.3	24.9	24.8	25.7	26.4	27.2	27.2	7- 6-77	26.9	26.9	26.6	26.3	26.0	26.8	26.9	26.7
7- 7-77	26.2	25.8	25.3	25.2	26.2	27.2	27.6	27.3	7- 8-77	26.8	26.8	26.0	25.5	25.8	26.4	26.5	25.8
7- 9-77	25.0	24.5	23.9	23.6	24.1	25.1	25.2	23.7	7-10-77	24.2	23.9	23.5	23.3	24.3	23.3	23.3	23.1
7-11-77	22.8	22.4	22.3	22.3	23.2	24.6	25.3	25.0	7-12-77	24.6	24.1	23.6	23.2	23.4	24.2	24.7	24.4
7-13-77	23.9	23.5	23.2	23.2	23.8	24.9	25.4	25.4	7-14-77	25.2	25.0	24.9	25.1	25.8	25.5	25.3	25.2
7-15-77	24.9	24.4	24.2	23.8	24.8	26.0	26.5	26.8	7-16-77	26.1	25.0	24.8	25.0	26.2	27.5	27.4	26.8
7-17-77	26.3	26.1	25.9	26.0	26.2	26.6	26.4	26.0	7-18-77	25.6	25.1	24.7	24.8	25.8	27.4	28.2	28.7
7-19-77	27.1	27.0	27.0	27.0	27.7	29.0	28.5	28.7	7-20-77	28.0	27.6	27.2	27.0	26.8	26.8	26.8	26.0
7-21-77	25.0	25.4	24.0	24.0	25.0	26.5	27.1	26.4	7-22-77	25.5	25.0	24.8	25.0	25.8	26.6	27.0	26.4
7-23-77	26.0	25.6	25.4	25.2	25.1	24.8	24.6	24.8	7-24-77	24.6	24.5	24.4	24.3	25.0	26.6	27.0	26.5
7-25-77	25.8	25.2	24.8	24.8	25.5	26.4	26.7	25.8	7-26-77	24.6	23.8	23.3	22.4	24.0	25.5	25.6	24.6
7-27-77	24.0	23.6	23.3	23.3	24.0	23.8	24.0	23.2	7-28-77	22.4	21.8	21.7	22.0	22.6	24.0	24.7	24.2
7-29-77	23.3	22.8	22.5	22.8	24.0	25.6	26.5	25.8	7-30-77	25.0	24.2	23.8	23.7	23.6	23.7	24.0	23.4
7-31-77	22.7	22.0	21.4	21.0	21.1	21.8	22.1	21.7	8- 1-77	21.1	20.5	20.1	20.2	20.7	21.8	22.4	22.4
8- 2-77	21.9	21.3	21.2	21.2	21.1	23.3	23.4	23.7	8- 3-77	22.9	22.2	21.8	22.0	23.1	24.7	25.4	24.8
8- 4-77	23.8	22.8	22.4	22.3	22.4	23.1	23.7	23.6	8- 5-77	22.8	21.8	21.2	21.2	21.2	22.6	23.2	22.8
8- 6-77	21.8	20.8	20.2	20.4	21.5	23.0	23.8	23.4	8- 7-77	22.6	21.9	21.5	21.6	23.0	24.8	25.3	24.7
8- 8-77	23.8	22.9	22.4	22.3	23.4	24.8	25.4	24.9	8- 9-77	23.9	22.8	22.2	22.0	22.0	23.2	24.3	24.0
8-10-77	22.3	21.4	21.0	20.7	21.2	22.4	22.7	22.4	8-11-77	21.4	20.5	19.8	19.5	20.2	21.6	22.2	21.8
8-12-77	21.1	20.0	19.4	19.2	20.4	22.0	23.0	23.0	8-13-77	22.3	21.6	20.9	20.6	21.7	22.8	23.1	22.5
8-14-77	21.8	20.8	20.3	20.1	21.1	22.3	23.3	22.8	8-15-77	22.0	21.2	20.8	20.4	20.2	20.4	20.2	20.1
8-16-77	20.0	19.7	19.2	19.0	19.4	20.4	21.2	21.0	8-17-77	20.5	20.1	19.6	19.3	19.9	21.1	21.8	20.9
8-18-77	20.1	19.2	18.2	17.9	19.1	20.7	20.7	20.5	8-19-77	20.0	19.3	18.8	18.6	19.6	21.1	21.9	21.8
8-20-77	21.0	20.3	19.7	19.4	19.8	21.5	22.4	22.2	8-21-77	21.8	21.1	20.6	20.2	21.0	22.3	22.3	21.8
8-22-77	21.2	20.4	19.9	19.6	20.4	21.6	21.7	21.2	8-23-77	20.7	19.8	19.4	18.8	19.0	20.5	21.4	20.8
8-24-77	20.4	19.6	19.1	18.7	19.5	21.0	22.0	20.6	8-25-77	20.8	20.1	19.4	18.9	18.8	18.8	18.9	18.8
8-26-77	18.8	19.0	18.9	19.0	19.2	19.8	20.6	21.0	8-27-77	21.2	20.9	20.7	20.8	21.4	22.2	22.3	22.0
8-28-77	21.4	21.0	20.8	20.7	20.9	21.2	21.2	20.6	8-29-77	20.1	19.7	19.5	19.4	20.1	21.2	21.3	20.7
8-30-77	20.0	19.8	19.5	19.6	20.0	20.3	20.4	20.3	8-31-77	19.9	19.5	19.4	19.3	20.4	21.5	21.8	21.1
9- 1-77	20.8	20.6	20.2	19.8	20.0	20.3	20.2	19.8	9- 2-77	19.4	19.2	19.0	18.5	19.0	20.0	20.2	19.8
9- 3-77	19.6	19.3	19.2	19.0	19.4	19.9	20.1	19.8	9- 4-77	19.7	19.7	19.7	19.6	19.6	19.7	20.0	19.9
9- 5-77	19.5	20.0	18.7	18.4	20.1	19.8	20.4	20.0	9- 6-77	19.8	19.8	19.5	19.5	20.0	20.7	20.9	20.6
9- 7-77	20.2	20.0	19.6	18.9	18.6	18.8	19.1	19.9	9- 8-77	18.4	18.2	18.2	18.1	19.4	20.6	21.0	20.8
9- 9-77	20.6	19.9	19.1	18.4	18.1	18.6	18.5	18.0	9-10-77	17.7	17.5	17.2	17.0	17.9	19.0	19.1	18.6
9-11-77	18.5	18.7	18.5	18.0	18.2	19.2	19.4	18.9	9-12-77	18.7	18.6	18.2	17.6	17.5	17.7	18.1	17.8
9-13-77	17.8	17.8	17.7	17.4	18.2	19.1	19.2	18.8	9-14-77	18.8	18.3	17.7	17.1	17.8	21.4	22.2	22.0
9-15-77	21.9	21.8	21.6	21.2	21.2	21.7	22.2	22.1	9-16-77	21.8	21.4	21.2	20.8	20.6	20.9	21.4	21.4
9-17-77	21.5	21.2	21.1	20.9	20.7	20.9	21.4	21.5	9-18-77	21.4	21.2	21.0	20.9	20.9	21.0	21.3	21.2
9-19-77	20.9	20.7	20.4	20.1	120.1	120.1	120.1	120.1									

Project Report No. 193
September, 1980

WATER TEMPERATURE DYNAMICS IN EXPERIMENTAL FIELD CHANNELS: ANALYSIS AND MODELING

(SUMMARY)

by

Heinz G. Stefan
John Gulliver
Alec Y. Fu
and
Michael G. Hahn

University of Minnesota
St. Anthony Falls Hydraulic Laboratory
Mississippi River at 3rd Ave. S. E.
Minneapolis, Minnesota 55414

Grant Nos. R 80368601 and R 80473601

Project Officer

Kenneth E. F. Hokanson
Monticello Ecological Research Station
Box 500, Monticello, Minnesota 55362

ENVIRONMENTAL RESEARCH LABORATORY - DULUTH
OFFICE OF RESEARCH AND DEVELOPMENT
U. S. ENVIRONMENTAL PROTECTION AGENCY
DULUTH, MINNESOTA 55804

PROJECT SUMMARY

A research program on the effects of elevated water temperatures resulting from waste heat discharges on fish and other aquatic organisms was initiated in August 1973 by the Monticello Ecological Research Station (MERS), a field laboratory of the USEPA Environmental Research Laboratory - Duluth. The purpose of these studies was (a) to validate water quality criteria data produced in the laboratory under semi-natural field (mesoscale) conditions and (b) to identify significant response by aquatic organisms under field monitoring conditions. The field channels in which the experimental studies were conducted were supplied with water heated artificially by waste heat from a nuclear electric generating plant.

The MERS is located approximately 40 miles northwest of Minneapolis, near Monticello, Minnesota, on 34 acres adjacent to a nuclear electric generating plant owned and operated by Northern States Power Company. The MERS has eight soil bottom experimental open channels of approximately 520 m (1700 ft) length each. The Mississippi River serves as the main source of water for the channels which operate in a once-through mode with the discharge returned to the river. Heat exchangers using waste heat (i.e. maximum Δt 19°C in winter, 13°C in summer) from the power plant can be used to artificially heat the water in any of the channels. Flow rates in each of the channels as well as water stages can be controlled.

To provide assistance in the ecological studies, it was necessary to document, analyze, and predict water temperature characteristics in the field channels and to identify sources of variation and error. Water temperatures in small open channels are highly dynamic due to the time dependent character of the controlling processes: advective transport, wind and flow induced mixing, and heat exchange with the air and the channel bed. In the MERS field channels the unsteady character of water temperature is especially acute since neither the mixing characteristics nor the effect of advective transport are negligible in the channels. The channels are exposed to a wide range of air temperatures, humidities, wind velocities, and solar radiation. The corresponding heat transfer with the environment is significant: a difference in temperature between the upper and lower

end as high as 15°C has been recorded and diurnal variations above 5°C have been observed at the downstream end. The experimental channels provide an excellent medium for the study of unsteady water temperatures in open channel flow and their relationship to meteorological parameters.

The work performed for the USEPA Monticello Ecological Research Station (MERS) under this grant had two basically different purposes. One was to provide background material and general information in support of the biological work conducted by the MERS field station staff. The second purpose was to investigate surface heat transfer, longitudinal dispersion, and water temperature predictions in streams under field conditions. This second purpose is basic and includes verification of the applicability of relationships developed for larger water bodies to smaller streams.

The report is divided into sections which address the two above purposes separately. Section 4, Hydraulic and Thermal Characteristics of the MERS Field Channels, provides general background information. Section 5, Longitudinal Dispersion; Section 6, Heat Budget; and Section 7, Water Temperature Predictions, give results of basic experimental and analytical studies. Additional details on the substudies can be found in several St. Anthony Falls Hydraulic Laboratory memoranda.

1. Operational Water Temperature Characteristics in Channel No. 1 of the USEPA Monticello Ecological Research Station, SAFHL Memo No. 151, Jan. 1978, 48 pp.

2. Physical Characteristics of the Experimental Field Channels at the USEPA Ecological Research Station in Monticello, Minnesota, SAFHL Memo No. 156, April 1978, 39 pp.

3. User's Manual for Operational Water Temperature Statistics, Computer Programs WTEMP1 and WTEMP2, SAFHL Memo No. 162, July 1979, 51 pp.

4. Soil Thermal Conductivity and Temperature Prediction in the Bed of the Experimental Field Channels at the USEPA Ecological Research Station in Monticello, Minnesota, SAFHL Memo No. 165, Jan., 1980, 58 pp.

5. Pore Water Temperatures and Heat Transfer in a Riffle(Rock) Section of the Experimental Field Channels at the USEPA Ecological Research Station, Monticello, Minn., SAFHL Memo No. 166, April, 1980, 11 pp.

6. Water Temperature Data Processing for the Experimental Field Channels at the USEPA Ecological Research Station, Monticello, Minnesota, SAFHL Memo No. 167, April, 1979,39 pp.

The final report and memoranda can be purchased from the St. Anthony Falls Hydraulic Laboratory, University of Minnesota, Mississippi River at 3rd Ave. S.E., Minneapolis, Minnesota 55414. The final report reference is "Water Temperature Dynamics in Experimental Field Channels: Analysis and Modeling," by H. G. Stefan, J. Gulliver, A. Y. Fu, and M. G. Hahn, SAFHL Project Report No. 193, June, 1980, 168 pp. and the price is $10.00. The memoranda costs are based on the reproduction charge which is currently 10¢ per page.

The following accomplishments are summarized:

1. Measurement of Hydraulic and Thermal Parameters

The field channels of the MERS represent a mesoscale ecosystem whose hydraulic characteristics have been measured and estimated.

a. The investigators intermittently collected data on flow velocity profiles, surface water slope, flow cross sections, bed material size, bed porosity and permeability, and water temperature stratification below the channel bed. These data have been used to derive a number of hydraulic parameters as follows.

The hydraulic characteristics of the experimental channels under study in 1975-1977 include:

Manning's roughness: $n = 0.06$ in the clear channels
$n = 0.3$ with extensive weed growth

Mean flow velocities: $U \simeq 0.1$ m/s in riffles
$U \simeq 0.02$ m/s in pools

depending on flow rate and downstream channel control. (U is based on fixed conditions of flow and channel dimension.) Velocity profiles are strongly affected by growth of filamentous algae in the rock sections and macrophytes in the pools.

b. The soil profile below pool beds is composed of four layers: a highly organic surface layer, water saturated sandy loam, water saturated bentonite clay layer, and a dry sandy loam, in downward order. The depth of the highly organic surface layer is variable and increases with time. The thermal diffusivity of each layer was determined by fitting soil temperature prediction to temperature measurements.

$D = 0.0017$ cm^2/s in the organic surface layer
$D = 0.013$ cm^2/s in the wet sandy loam below
$D = 0.0013$ cm^2/s in the dry sandy loam below the bentonite seal

c. The bed of the riffle is composed of coarse rock with mean size $d_{50} = 30$ mm. The rock porosity was estimated at $\varepsilon = 0.42$ and its Darcy permeability coefficient at $k = 0.18$ m/s. The thermal diffusivity of the riffle bed was estimated to be $D = 0.0031$ cm^2/s in the rock/water system without natural convection.

2. Water Temperature Instrumentation

Development and operation of instrumentation for continuous monitoring of flow rates and water temperatures in the channels from 1975 to 1977 was in the hands of MERS staff, in particular Charles F. Kleiner and Thomas Henry. The investigators participated in the selection of the temperature sampling sites.

Temperature sensors (thermocouples) were installed at the upstream and downstream ends and in the center pools and riffles of each of the experimental channels 1, 4, 5, and 8 analyzed in 1975-1977. The sensors provided continuous water temperature information which was recorded on strip charts. Three stations per channel were not sufficient, however, for the analysis of stratification, surface heat transfer, and mixing. Channel 1 was selected for in-depth study of temperature regimes, and 21 continuous recording sensors were installed in it. Ten of the sensors measured water temperature 12.5 cm (5 in.) to 25 cm (10 in.) below the water surface. There were two vertical arrays of four sensors each installed in Pools 6 and 12 which provided information on water temperature stratification and soil temperature. Three sensors were within 12.5 cm (5 in.) from the bottom of pools 4, 10, and 18, and one sensor 2 to 5 cm (1 to 2 in.) in the rocks of riffle 17. All temperature sensors were connected to Leads-Northrup multi-channel color-coded temperature chart recorders. Temperatures were recorded from November 1975 through December 1977.

3. Water Temperature Data Processing

Water temperature data processing had the following elements.

- Extraction of 3-hour data from strip charts
- Review and estimation of missing or faulty data
- Calibration
- Storage on magnetic tape

Water temperature data for Channel 1 (strongly heated), Channels 4 and 5 (unheated), and Channel 8 (intermediately heated) were processed for the period from December 1975 through September 1977.

4. Water Temperature Data Analysis and Results

The water temperature data analysis included

- Development of statistical analysis computer programs WTEMP1 and WTEMP2

- Computation of a number of statistical parameters from 3-hour data
- Determination of the seasonal water temperature cycle
- Determination of the diurnal water temperature cycle
- Analysis of longitudinal water temperature gradients
- Analysis of water temperature stratification in the pools

Development of computer programs

The computer program WTEMP1 is designed to extract from the 3-hour water temperature data statistical information including:

- Water temperatures at three probabilities of occurrence specified by the user
- Maximum and minimum water temperature in the period analyzed
- Mean, standard deviation, and dimensionless skewness coefficient of the water temperature

WTEMP1 can handle a series containing up to 19,200 individual water temperatures, equivalent to 400 days of data from six stations in a single channel. WTEMP1 can also handle sliding statistic calculations for sample periods of up to seven days. The output is in tabular form.

A second interactive program WTEMP2 for computing statistics on specified date-time intervals, composite station location, etc., from daily statistics was also developed.

Computations

Computations have been carried out for individual stations and channel composites using weekly sliding samples. The complete output comprises 151 pages for Channel 1 and 126 pages each for Channels 4, 5, and 8.

Seasonal water temperature cycle

The amplitude of the seasonal water temperature was of the order of $\pm$ 15^{o}C. The annual mean differed by channel and station depending on artificial heating. Channel 1 was artificially heated, and Channel 5 was not.

Water temperature fluctuations superimposed on the seasonal cycle were either due to irregularities in the artificial heating of the inflowing water or to weather.

Diurnal water temperature cycles

Inflowing water was taken from the Mississippi River. Because the field channels are shallower than the river, diurnal water temperature amplitudes at the downstream end of the channels were larger than upstream. Amplitudes of diurnal water temperature cycles varied strongly with season. Winter values were of the order of 1°C upstream and 2 to 3°C downstream. In the summer a 2°C amplitude upstream and a 5°C amplitude downstream were not uncommon.

Longitudinal water temperature gradients

Water temperature differentials between the upstream and the downstream ends of the channel were of interest for fish studies in the field channels. Such longitudinal water temperature gradients were dependent on several other hydrothermal parameters. The longitudinal ΔT can be expected to rise with the addition of artificial heat. A greater flow rate will decrease the longitudinal ΔT. Since the geometry of the MERS channels is fixed in terms of length and width, the two most important controllable parameters were flow rate and heat input. Actual values of longitudinal ΔT's depended on the amount of heat rejected to the atmosphere, which is a weather-dependent process.

The daily minimum and maximum temperature difference between the inflow and outflow of the artificially heated Channel 1 was recorded over a one-year period from December 1975 through November 1976. Table 1 summarizes the monthly mean and standard deviation of the longitudinal temperature differences of channel 1. Flow rates ranged from 0.015 to 0.039 m^3/s.

Daily diurnal water temperature variations at the outflow of Channel 1 were recorded over a one-year period and are also reported in Table 1. These characteristics are for a heated channel with inflow temperatures increased up to 15°C above the temperature of the Mississippi River water. Longitudinal temperature gradients and diurnal variations are not as large in a channel with ambient unheated inflow.

TABLE 1. MONTHLY MEAN AND STANDARD DEVIATION (σ) OF DAILY MINIMUM AND DAILY MAXIMUM LONGITUDINAL (SPATIAL) TEMPERATURE DIFFERENCE, AND OF DIURNAL (TEMPORAL) TEMPERATURE DIFFERENCE AT THE OUTFLOW FROM HEATED CHANNEL 1, DECEMBER 1975 - NOVEMBER 1976

Month	Minimum Longitudinal ΔT		Maximum Longitudinal ΔT		Diurnal ΔT at Outflow	
	Mean (°C)	σ (°C)	Mean (°C)	σ (°C)	Mean (°C)	σ (°C)
December (1975)	5.2	2.0	8.0	2.5	1.9	0.9
January (1976)	6.0	1.5	9.5	1.8	2.3	1.0
February	4.6	1.3	7.7	1.7	2.5	1.3
March	3.2	2.7	6.9	3.1	3.4	1.6
April	1.9	1.8	5.6	1.6	5.3	1.9
May	1.8	1.3	5.7	1.4	4.4	2.2
June	2.7	1.5	4.8	1.6	4.0	0.0
July	1.7	0.9	4.0	0.9	3.5	0.8
August	0.9	1.1	4.5	2.0	3.7	1.5
September	1.7	0.7	3.5	0.9	2.9	1.2
October	0.9	1.0	3.4	2.6	2.9	1.2
November (1976)	1.0	1.0	5.7	3.9	2.5	2.4

Temperature stratification in pools

Vertical stratification of the pool sections was studied in the artificially heated Channel 1 and was found to occur most frequently in August. The temperature gradient was found to occur primarily in the lowermost 20 cm of the pool below a 60 cm isothermal layer; the temperature difference was up to 5°C strong. Analyses of some 1975/76 data in pools 6 and 12 showed that a temperature differential of more than 1°C developed during 33 per cent of all hours in August and less frequently during other months. The more downstream pool showed a stronger tendency to stratify, presumably because the cumulative effect of atmospheric heating of the water in it is stronger.

5. Dynamic Soil Temperature Prediction Model, TSOIL

A dynamic soil temperature computer model TSOIL for the pool sections was developed, primarily to assist in invertebrate studies. The model solves the unsteady heat conduction equation and predicts the soil temperature profile for a specified time variation of the water temperature at the soil/water interface. It was verified that strongly transient soil temperatures may be accurately predicted with this model, as shown in Fig. 1.

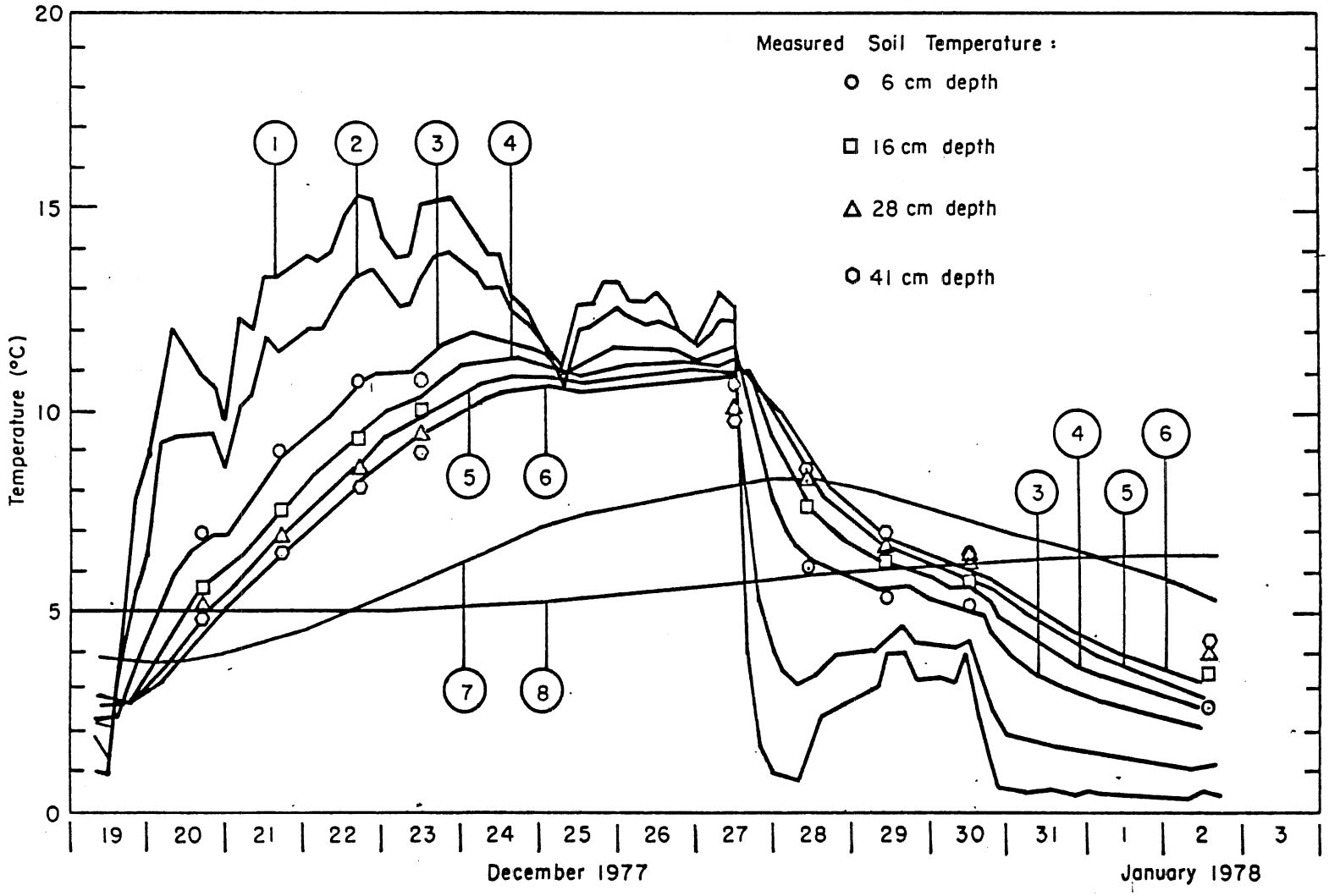

Fig. 1. Comparison of measured and predicted (solid lines) soil temperatures in Pool 12 during heat wave test. Notation for depth of predicted soil temperatures: (1) soil surface, (2) 2.5 cm, (3) 6 cm, (4) 15 cm, (5) 28 cm, (6) 41 cm, (7) 60 cm, (8) 1 m.

6. Longitudinal Dispersion Study

The flow field in the MERS channels is very non-uniform and mean flow velocities are small. Water moves through the MERS channels in a way far different from the novement of a piston in a cylinder (plug flow). Water may move faster in the center of a riffle or a pool than at its edges. Transverse and/or vertical mixing takes place between the faster and the slower water masses. Vegetation is present in pools and riffles in the summer. There is a weak jet effect at the transition from the riffles to the pools. In the pools water masses may be entrapped near the banks. There can be wind and there is intermittent stratification in the pool. As a result of all these interacting processes, heat or material contained in the water will spread out longitudinally along the channel. The effect of longitudinal spreading had to be incorporated in the channel water temperature model.

Since detailed study of the very complete low velocity channel hydrodynamics was not part of the research objective, the water temperature simulation was based on a uniform channel flow model with a longitudinal dispersion term. "Longitudinal dispersion coefficient" is used herein to describe a bulk coefficient which lumps the effects of all the processes mentioned above. It might also have been termed a "bulk or hydrodynamic longitudinal diffusion coefficient." To use separate coefficients for riffles and pools was considered, but the frequent transition and short lengths of these elements made it advisable not to use this approach.

The use of a diffusion equation to describe longitudinal mass transport in a channel is only justified after the initial convective period. The MERS channels begin with a pool into which water is discharged from a weir producing a very well mixed upstream condition. The mean residence time of the water in a pool was anywhere from 10 to 30 minutes depending on flow rate. The convective length of the first pool was estimated to be approximately 5 m, far less than its total length of 30 m. It was therefore considered that the convective length did not reach beyond the length of the first pool.

Longitudinal dispersion in the MERS field channels was studied using temperature fronts. The longitudinal dispersion coefficient was found to be best approximated by

$$D_L = 7.47 * \frac{Q}{B} ,$$

where Q is flow rate and B is mean surface width.

In the range of very low mean flow velocities investigated (0.04 m^3/s discharge and $U \simeq 0.02$ m/s in pool to 0.1 m/s in riffle) the typical wind and vegetation effects could not be distinguished separately. A typical value of D_L was 0.1 m^2/s.

7. Air-Water Interaction

Evaporative and convective surface heat exchange were found to be dependent on wind speeds and natural convection potential. A wind speed function similar to one previously investigated by Ryan and Harleman,

$$Wftn = 0.0096\ (\Delta\theta_v)^{1/3} + 0.0083\ W_2$$

was found to fit the experimental field data well. $\Delta\theta_v$ represents a virtual temperature differential and W_2 is the wind speed at 2 meters above the ground in m/s. The windspeed function is used to calculate evaporative surface heat transfer and convective surface heat transfer.

8. Finite Difference, Implicit Computer Model (MNSTREM)

A finite difference, implicit computer model (MNSTREM) for the simulation of the very dynamic channel water temperature regime was developed. It was shown capable of simulating 1 hr, 3 hr, or 6 hr water temperatures over periods up to one month with standard errors of 0.2 to 0.3°C between measurements and predictions. Weather data, specifically solar radiation, air temperature, dewpoint, and wind velocity, are required as input at least every six hours. Three-hour input data are standard for the model. If intervals of more than six hours are used, the accuracy of the prediction suffers. MNSTREM has unusually high time resolution (3 hrs normal Δt, 1 hr possible Δt), meaning that it can predict rapid water temperature changes in very shallow water (Fig. 2).

9. Concluding Remarks

In addition to providing information on some physical characteristics of the MERS experimental channels, this research produced material applicable to the study of temperature dynamics in thermally polluted streams in general, to the design of canals for cooling water disposal, and to the understanding and analysis of natural water temperature regimes of small streams. Some of the information may also be of use in studies of mass transport and ecosystem dynamics in shallow channels.

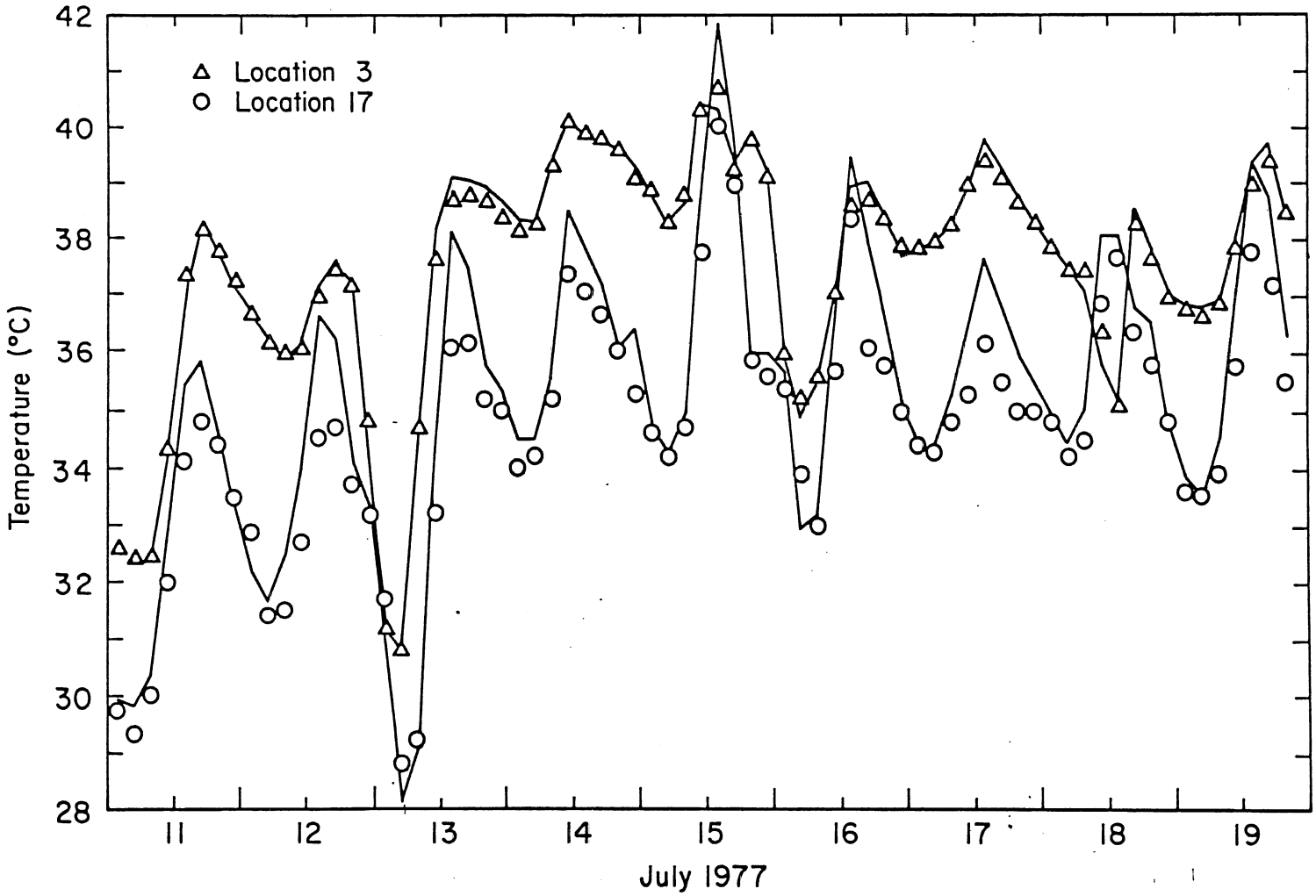

Fig. 2. Run C. Three-hour water temperatures at Station 3 (upstream) and Station 17 (downstream) in Channel 1. Symbols are recorded values; solid lines are values simulated with MNSTREM.